

**Development, Modelling and Control of a Continuous  
Pilot Scale Supercritical Fluid Extraction Process**

**by**

**Maedeh Roodpeyma**

**A thesis submitted in partial fulfillment of the requirements for the degree of**

**Doctor of Philosophy  
in  
Environmental Engineering**

**Department of Civil and Environmental Engineering  
University of Alberta**

**© Maedeh Roodpeyma, 2017**

# Abstract

In this thesis, the feasibility and operation of a continuous pilot scale supercritical fluid extraction (SFE) process for treatment of oil-contaminated solids, specifically drill cuttings, was investigated. For this purpose, a continuous pilot scale SFE process, the first of its kind, was designed, built, commissioned and operated. An important part in demonstrating operability of this process was controlling key variables, in particular pressure and slurry level in the extraction vessel. To conduct control studies, a hydrodynamic model based on first principle equations was developed, implemented, verified and validated for the continuous SFE process. The developed hydrodynamic model is capable of predicting pressure and slurry level inside the extraction vessel. The model was used towards designing model-based pressure controllers and comparing controller performances. The model was also used for exploring an approach (i.e. the pulse test approach) for measuring and controlling slurry level in the extraction vessel. Pressure control was successfully achieved in the extraction vessel of the pilot scale SFE process by applying a feedback loop with PI control. Both manually tuned and model-based PI controllers were tested and satisfactory pressure control was obtained for both cases. Promising results were also obtained for slurry level measurement and control in the extraction vessel in the modelling framework by applying the pulse test approach. Additional experiments are required to be conducted on the pilot scale SFE process to further evaluate the pulse test approach. Overall, the results of the thesis demonstrate the feasibility of this continuous process for the treatment of drill cuttings (i.e. extracting oil from the slurried solids). The obtained results are valuable for future upgrades towards commercializing this unique SFE process and for development of this process for the extraction of other compounds from contaminated solids.

# Preface

Chapter 3 of this thesis is a joint effort between Maedeh Roodpeyma and Christianne G. Street and it is available in both theses of the authors. This Chapter is associated with the continued design, build and commission/operation of the continuous pilot scale SFE process for treatment of drill cuttings. The three stated stages were conducted and completed as a collaboration between Maedeh Roodpeyma and Christianne G. Street. Department technicians (Civil/Environmental and Chemical/Materials Engineering) Perry Fedun, Todd Kinnee and Les Dean contributed to the build stage of the process.

In dedication to my parents and husband *Behzad*.

# Acknowledgements

I would like to start by thanking my supervisors Dr. Selma Guigard and Dr. Warren Stiver. Selma, thank you for providing a fun and stress-free environment for doing research and also for providing me with various teaching and research opportunities. I really enjoyed being in your research group i.e. the tea group! Warren, thank you for always being accessible, in spite of being kilometers away. Your patience and optimism in any condition, will always be inspirational to me. Special thanks must also go to my colleague and friend Christianne Street with whom I spent endless hours in the lab. Christianne, I will forever cherish the memories we shared in the lab. I could not have wished for a better teammate.

This thesis wouldn't be possible without the help of faculty technicians Les Dean, Perry Fedun and Todd Kinnee, whose support was instrumental in building the pilot scale process. The help of the SFE group technician, Eleisha Underwood is also greatly appreciated.

A big thank you to Cathy Taskey for her killer Muscular-Strength-Endurance classes at the University recreation center. Cathy, your awesome classes helped me completely forget my worries for an hour and helped me re-energize myself for what's to come. I will miss you and your classes.

I take this opportunity to express gratitude to my friends specially Leila Zargarzadeh and Saina Lajevardi. Leila, thank you for your friendship and for always being considerate. Your vibrant personality always gave me positive energy. Saina, thank you for introducing me to running! I will not forget your kindness and honesty and the enjoyable hours we spent running together. A special thanks must also go to Hoda SepehriRad and Majid Raghmi, our neighbour when my husband and I first came to Edmonton and close friends since. The wonderful memories we share will never be forgotten.

Last but not least, I am grateful for my wonderful *family*. I am deeply indebted to my mom and dad who have and always will be my role model in life. I would not be where I am without the help and support of my dad as well as the prayers and encouragement of my mom. Mom and dad, I appreciate all you have done for me, more than I can say. I am also thankful for my one and only brother, Mahdi. And, thank you to Behzad for his support, love and patience throughout these years. I thank *God*, each and every moment for having you all in my life.

# Table of Contents

1	Problem Definition .....	1
1.1	Introduction.....	2
1.2	Objectives .....	7
1.3	Context of this thesis in the overall project .....	8
1.4	Thesis structure .....	9
2	Literature Review .....	10
2.1	Overview of Supercritical Fluid Extraction (SFE) .....	11
2.2	The past, present and future of SFE for treatment of oil-contaminated solids .....	15
2.3	Modelling SFE processes.....	21
2.4	Process control and SFE applications .....	24
2.5	Summary .....	29
3	Design, Build, Commission and Experimental Runs .....	30
3.1	Introduction.....	31
3.2	SFE process overview.....	32
3.3	Design components.....	36
3.3.1	Flow through the process.....	37
3.3.2	Lab layout .....	38
3.3.3	Piping and Instrumentation (P&ID).....	41
3.3.4	Control philosophy.....	51
3.3.5	Operation manual.....	59
3.3.6	Hazard and Operability (HAZOP).....	63
3.4	Summary of runs.....	64
3.5	Summary .....	82

4	A Hydrodynamic Model for the Fully Continuous Pilot Scale SFE Process .....	84
4.1	Introduction.....	85
4.2	Hydrodynamic model.....	87
4.2.1	Model development .....	87
4.2.2	Model implementation.....	103
4.3	Results and discussion .....	107
4.3.1	Model verification.....	107
4.3.2	Model validation .....	121
4.4	Summary .....	134
5	Pressure Control in the continuous pilot scale SFE Process .....	136
5.1	Introduction.....	137
5.2	Background.....	138
5.2.1	Feedback control.....	138
5.2.2	Internal Model Control (IMC).....	140
5.3	Methodology .....	142
5.4	Results and discussion .....	144
5.4.1	Manual tuning of the controller .....	146
5.4.2	Model-based controller .....	152
5.4.3	Controller performance comparison (manually tuned vs. model-based).....	160
5.4.4	System identification via hydrodynamic model .....	166
5.5	Summary .....	177
6	Level Control in the continuous pilot scale SFE Process.....	180
6.1	Introduction.....	181
6.2	Methodology .....	183
6.2.1	Level measurement .....	183

6.2.2	Level control .....	185
6.3	Results and discussion .....	187
6.3.1	Case 1 .....	187
6.3.2	Case 2 .....	192
6.3.3	Case 3 .....	194
6.3.4	Case 4 .....	198
6.3.5	Case 5 .....	202
6.3.6	Case 6 .....	205
6.3.7	Case 7 .....	208
6.4	Application of the pulse test to the pilot scale SFE process .....	210
6.5	Summary .....	211
7	Conclusions and Recommendations .....	212
7.1	Conclusions .....	213
7.2	Recommendations .....	215
	References .....	218
	Appendices .....	226
	Appendix A1: Line specifications .....	227
	Appendix A2: Valve specifications .....	229
	Appendix A3: Instrumentation specifications .....	231
	Appendix A4: List of Priority 1, 2 ,3 and 4 alarms .....	233

# List of Tables

Table 2.1.	Comparing thermophysical properties of gases, SCFs and liquids .....	11
Table 3.1.	Specification of major equipment used in the SFE process .....	41
Table 3.2.	Summary of the modifications to the lines in the SFE process.....	44
Table 3.3.	Summary of the modifications in terms of valves used in the SFE process.....	46
Table 3.4.	Summary of modifications to the instrumentation used in the SFE process.....	48
Table 3.5.	Summary of modifications applied to the SFE alarm system .....	55
Table 3.6.	Summary of runs conducted on the pilot scale SFE process.....	65
Table 3.7.	Summary of runs, with operating conditions, that meet the functionality objectives.....	80
Table 4.1.	Quantities used in modelling equations.....	90
Table 4.2.	Values of constants and parameters in CO <sub>2</sub> continuity equation .....	94
Table 4.3.	Values of constants and parameters in slurry continuity equation.....	96
Table 4.4.	Values of constants and parameters in energy balance .....	101
Table 4.5.	Values of constants and parameters in CO <sub>2</sub> EOS.....	103
Table 4.6.	Values of constants and parameters in Density-Volume-Mass relationship.....	103
Table 4.7.	Degree of freedom analysis.....	104
Table 4.8.	Parameter values applied in simulation and obtained S.S. value of variables .....	109
Table 4.9.	Calculated values for Equations 4.45 to 4.49 .....	110
Table 4.10.	Calculated values for continuity equations when slurry flow is 12.8%.....	111
Table 4.11.	Inlet and outlet pressure of metering valve .....	112
Table 4.12.	Comparison of experimental and model responses for validation Tests V11 and V12 in terms of steady state pressure and settling time .....	128
Table 4.13.	Comparison of experimental and model responses for validation Tests V21 and V22 in terms of steady state pressure and settling time .....	130
Table 4.14.	SFE process data regarding level validation experiments.....	132
Table 4.15.	Summary of results for level validation experiments.....	133
Table 5.1.	SFE experiments related to implementation and demonstration of pressure control in the extraction vessel.....	143
Table 5.2.	IAE and TV values for Controller 1 (Run 7a) and Controller 2 (Run 7c) .....	150

Table 5.3.	PI controller settings based on different values of $\tau_c$ .....	156
Table 5.4.	IAE values for Controller 3, Controller 4 and Controller 5 .....	158
Table 5.5.	TV values for Controller 3, Controller 4 and Controller 5.....	159
Table 5.6.	Controller 2 and Controller 4 parameter comparison.....	160
Table 5.7.	IAE values for the manually tuned controller (Controller 2) and the model-based controller (Controller 4) .....	161
Table 5.8.	TV values for the manually tuned controller (Controller 2) and the model-based controller (Controller 4) .....	162
Table 5.9.	IAE values (based on actual SFE experiment) for the manually tuned controller (Controller 2) and the model-based controller (Controller 4) .....	164
Table 5.10.	TV values (based on actual SFE experiment) for the manually tuned controller (Controller 2) and the model-based controller (Controller 4) .....	166
Table 5.11.	Controller 4 and Controller 6 parameter comparison.....	168
Table 5.12.	Summary of IAE and TV values for Controller 4 and Controller 6.....	168
Table 5.13.	Model parameter comparison for system identification at a low operating pressure and a high operating pressure .....	170
Table 5.14.	Controller 6 and Controller 7 parameter comparison.....	170
Table 5.15.	IAE values for Controller 6 and Controller 7 at a low operating pressure.....	172
Table 5.16.	TV values for Controller 6 and Controller 7 at a low operating pressure .....	173
Table 5.17.	IAE values for Controller 6 and Controller 7 at a high operating pressure.....	174
Table 5.18.	TV values for Controller 6 and Controller 7 at a high operating pressure .....	175
Table 5.19.	Summary of IAE and TV values obtained for Controller 6 and Controller 7 .....	176
Table 6.1.	Defined Level states in the extraction vessel for Case 1 .....	185
Table 6.2.	Simulation cases for evaluating and exploring the pulse test approach for slurry level measurement and slurry level control.....	187
Table 6.3.	Slurry levels and corresponding pressure differences as a result of applying the pulse test in Case 1 .....	189
Table 6.4.	Defined Level states in the extraction vessel for Case 5.....	202

# List of Figures

Figure 1.1.	Circulation of drilling fluid during drilling operations.....	2
Figure 2.1.	Phase diagram of CO <sub>2</sub> .....	12
Figure 2.2.	Schematic of a lab scale batch SFE process .....	17
Figure 2.3.	Schematic of a continuous SFE process .....	19
Figure 3.1.	Schematic of the pilot scale SFE process .....	33
Figure 3.2.	The pilot scale SFE process for treatment of drill cuttings (1) CO <sub>2</sub> tank, (2a) rinse water tank, (2b) slurry feed tank, (2c) treated slurry tank, (3) separator and (4) extraction vessel .....	34
Figure 3.3.	The extraction vessel of the SFE process (Length: 2.45 m, Inner diameter: 0.0833 m).....	35
Figure 3.4.	The separator of the SFE process (Length: 1.52 m, Inner diameter: 0.0833 m).....	36
Figure 3.5.	Lab layout containing dimension of the main SFE process components: (1) CO <sub>2</sub> pump, (2) CO <sub>2</sub> feed tank, (3) fume hood, (4) slurry and rinse water tanks, (5) slurry pump, (6) separator frame and (7) extraction vessel frame (all dimensions in inches). .....	39
Figure 3.6.	Lab layout containing position of the main SFE process components: (1) CO <sub>2</sub> pump, (2) CO <sub>2</sub> feed tank, (3) fume hood, (4) slurry and rinse water tanks, (5) slurry pump, (6) separator frame and (7) extraction vessel frame (all dimensions in inches). .....	40
Figure 3.7.	CO <sub>2</sub> and slurry line configuration in current state of the SFE process (line colours indicate a change in tag number, which corresponds to a change in line size and/or material).....	45
Figure 3.8.	Valve configuration in current state of the SFE process.....	47
Figure 3.9.	Instrumentation configuration in current state of the SFE process.....	49
Figure 3.10.	P&ID of the continuous pilot scale SFE process .....	50
Figure 3.11.	Display of the SFE process GUI (top: monitor-1, bottom:monitor-2).....	52
Figure 3.12.	Pressure and temperature at top and bottom sensors over Run 38 .....	81
Figure 3.13.	Oil collected from the separator for Runs 39 and 41 .....	82
Figure 4.1.	Selected control volumes and streams for modelling .....	88

Figure 4.2.	Schematic of the slurry pump, slurry feed tank and extraction vessel.....	99
Figure 4.3.	Equation solving flowchart.....	106
Figure 4.4.	Response of main process variables .....	109
Figure 4.5.	SFE process pressure response for Case 1 and Case 2 .....	113
Figure 4.6.	SFE process pressure response comparison regarding slurry density and viscosity .....	114
Figure 4.7.	SFE process temperature response with and without heating tape.....	115
Figure 4.8.	SFE process pressure response with and without heating tape.....	115
Figure 4.9.	Pressure and level responses to a change in slurry flow.....	117
Figure 4.10.	Pressure and level responses to a change in CO <sub>2</sub> flow .....	118
Figure 4.11.	Pressure and level responses to a change in manifold length.....	119
Figure 4.12.	Pressure and level responses to a change in metering valve opening.....	120
Figure 4.13.	Temperature, pressure and level responses to a change in the slurry inlet temperature.....	121
Figure 4.14.	Pressure response comparison between process and modelling when applying different CO <sub>2</sub> flow equations (Equation 4.3 or Equation 4.4).....	123
Figure 4.15.	Pressure response comparison between process and modelling when applying Equation 4.20 or Equation 4.21 .....	124
Figure 4.16.	Pressure response comparison for Test V11.....	125
Figure 4.17.	Pressure response comparison of experimental responses and simulation responses .....	127
Figure 4.18.	Pressure response comparison between model, Test V21 and Test V22.....	129
Figure 4.19.	Experimental and simulated level response for Tests V11 and V12 .....	132
Figure 4.20.	Experimental and simulation results for level response for Tests V21 and V22.....	133
Figure 5.1.	Feedback control structure.....	138
Figure 5.2.	Schematic of IMC structure.....	141
Figure 5.3.	Pressure response at the top and bottom of the extraction vessel to a set point change in Run 7a.....	147
Figure 5.4.	Controller output as a result of a set point change in Run 7a.....	148

Figure 5.5.	Pressure response at the bottom of the extraction vessel to set point changes in Run 7c .....	149
Figure 5.6.	Controller output as a result of set point changes in Run 7c .....	150
Figure 5.7.	Pressure response to a set point change in Run 18 and Run 26 .....	151
Figure 5.8.	Controller output as a result of a set point change in Run 18 and Run 26.....	152
Figure 5.9.	Step test input (CO <sub>2</sub> flow) and output (pressure) time variation .....	154
Figure 5.10.	Pressure response to a set point change and disturbance for Controller 3, Controller 4 and Controller 5 .....	157
Figure 5.11.	Controller output as a result of a set point change and disturbance for Controller 3, Controller 4 and Controller 5 .....	158
Figure 5.12.	Pressure response to a set point change and disturbance for manually tuned controller (Controller 2) and model-based controller (Controller 4) .....	161
Figure 5.13.	Controller output as a result of a set point change and disturbance for the manually tuned controller (Controller 2) and the model-based controller (Controller 4) .....	162
Figure 5.14.	Pressure response in the SFE process to a set point change and disturbance for the manually tuned controller (Controller 2) and the model-based controller (Controller 4) .....	164
Figure 5.15.	Controller output in the SFE process as a result of a set point change and disturbance for the manually tuned controller (Controller 2) and the model-based controller (Controller 4) .....	165
Figure 5.16.	Step test output (pressure) time variation for identification via SFE process and identification via hydrodynamic model .....	167
Figure 5.17.	Step test output (pressure) time variation for identification via hydrodynamic model at a high operation pressure .....	169
Figure 5.18.	Pressure response to a set point change and disturbance for Controller 6 and Controller 7 at a low operating pressure .....	171
Figure 5.19.	Controller output as a result of a set point change and disturbance for Controller 6 and Controller 7 at a low operating pressure.....	173
Figure 5.20.	Pressure response to a set point change and disturbance for Controller 6 and Controller 7 at a high operating pressure .....	174

Figure 5.21.	Controller output as a result of a set point change and disturbance for Controller 6 and Controller 7 at a high operating pressure.....	175
Figure 6.1.	Applied pulses in slurry flow (pulse amplitude = 8%, width =10 s and frequency = 1/500 1/s) and obtained slurry level and pressure responses for Case 1.....	188
Figure 6.2.	Fitted polynomial to data obtained from the pulse test (pulse amplitude = 8%, pulse width = 10 s) in Case 1 .....	189
Figure 6.3.	Responses associated with slurry flow (controller action and pulse), slurry level, measured slurry level, Level state and pressure in Case 1.....	191
Figure 6.4.	Responses associated with slurry flow (controller action and pulse), slurry level, measured slurry level, Level state and pressure in Case 2.....	193
Figure 6.5.	Responses associated with slurry flow (controller action and pulse), slurry level, measured slurry level, Level state and pressure in Case 3.....	195
Figure 6.6.	Responses associated with slurry flow (controller action and pulse), slurry level, measured slurry level, Level state and pressure in Case 3 (with initial high slurry level).....	197
Figure 6.7.	Responses associated with slurry flow (controller action and pulse), slurry level, measured slurry level, Level state and pressure in Case 4.....	199
Figure 6.8.	Responses associated with slurry flow (controller action and pulse), slurry level, measured slurry level, Level state and pressure in Case 4 (initial high slurry level).....	201
Figure 6.9.	Responses associated with slurry flow (controller action and pulse), slurry level, measured slurry level, Level state and pressure for Case 5 .....	203
Figure 6.10.	Responses associated with slurry flow (controller action and pulse), slurry level, measured slurry level, Level state and pressure for Case 5 (initial high slurry level).....	204
Figure 6.11.	Applied pulses in slurry flow (pulse amplitude = 4%, width =10 s and frequency = 1/500 1/s) and obtained slurry level and pressure responses for Case 6 .....	206
Figure 6.12.	Comparison between the polynomial associated with Equation 6.1 and the polynomial associated with Equation 6.2.....	207
Figure 6.13.	Responses associated with slurry flow (controller action and pulse), slurry level, measured slurry level, Level state and pressure for Case 7 .....	209

# 1 Problem Definition

## 1.1 Introduction

The oil and gas extraction industry is generally categorized into four main sectors: (i) exploration, (ii) well development, (iii) production and (iv) site abandonment (EPA, 2000). The sector of interest to this thesis is well development, which mainly involves the construction of wells through drilling operations. Drilling operations are carried out onshore or offshore. Onshore operations relate to drilling under the earth surface while offshore drilling is associated with drilling wells under the seabed. One of the major differences between onshore and offshore drilling is the need for special equipment for offshore operations that can operate robustly in the marine environment as well as harsh weather conditions, Canada being the case (CCEI, 2004). Nevertheless, for both onshore and offshore sites, drilling operations are similar.

During rotary drilling, which is employed in most oil and gas wells, the drilling fluid is pumped down the drill string (CAPP, 2001). As the drill bit rotates, small broken pieces of rock are flushed out of the borehole by the drilling fluid, along the annulus between the drill string and borehole wall. The mixture of drilling fluid and rock fragments, known as drill cuttings or drilling waste, are forced up to the surface and are collected for treatment on the drilling platform (OGP, 2003). In other words, drill cuttings are solids that are produced during drilling into the subsurface geological formations and are carried to the surface, mixed with drilling fluids (NEB, 2010). Figure 1.1 provides a schematic diagram of the circulation of the drilling fluid during drilling operations.

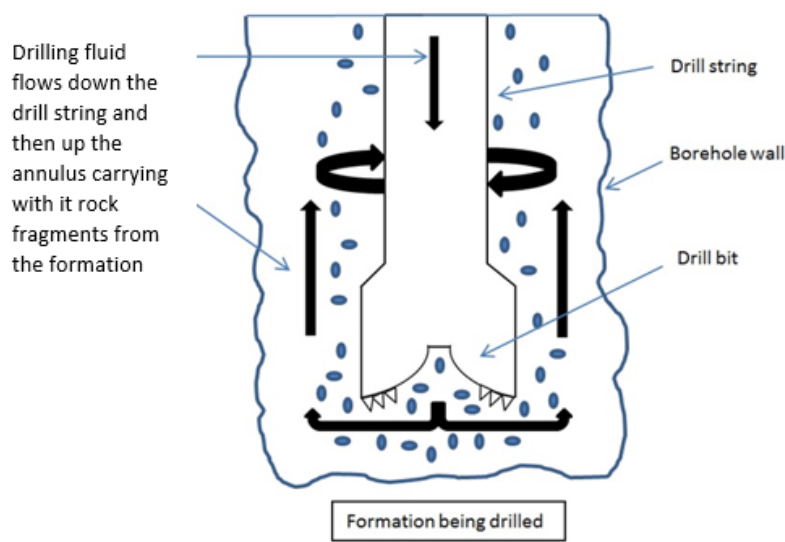


**Figure 1.1. Circulation of drilling fluid during drilling operations (adapted from OGP, 2003)**

Drilling fluids, also known as drilling muds, play a crucial role in drilling operations (EPA, 2000). They can be considered as fluids, that consist of a complex mixture of chemicals and solids, which serve to cool and lubricate the drill bit and drill pipe, clean and condition the bottom of the hole by transporting rock fragments to the surface and maintain hydrostatic pressure on the formation, thus stabilizing the borehole wall (EPA, 2000; OGP, 2003; Stantec, 2009; NEB, 2010;).

Drilling fluids are comprised of a continuous phase (which forms the base fluid) along with other components which are either dissolved or suspended in the base fluid (NEB, 2010). Drilling fluids can be categorized into two general types: water-based fluids (WBFs) and non-aqueous fluids (NAFs) (EPA, 2000; CAPP, 2001; OGP, 2003). NAFs can either be oil-based fluids (OBF) or synthetic-based fluids (SBF). The main reason for development of SBFs was to have drilling fluids with the same performance as OBFs but with lower toxicity i.e. lower aromatic and poly-aromatic hydrocarbon content, which in turn would result in improved worker safety as well as a lower environmental impact (CAPP, 2001).

Each type of drilling fluid has its own advantages and disadvantages. From a performance point of view, NAFs offer significant advantages over WBFs, especially in difficult drilling situations. From an environmental perspective, NAFs, especially OBFs, are the least desirable fluid to be used for drilling operations. In most cases however, both WBFs and NAFs are used for drilling wells. Due to the higher chemical stability and natural lubricity of NAFs, they are applied in deeper parts of the wells, while the WBFs are mostly applied for drilling in shallow parts (Melton *et al.*, 2000; CAPP, 2001).

The average rate of drilling a well is 200 m/day in which approximately 0.1 tonnes/m of waste is produced. As a result, approximately 20 tonnes of waste is generated per day. Assuming a well depth of 2500 m, 250 tonnes of waste is produced per well (EPA, 2000). This large amount of waste (consisting of used drilling mud and cuttings) needs to be managed appropriately. The Canadian Association of Petroleum Producers (CAPP, 2014) has estimated that from 1947 to 2013, a total of 148,602 exploratory wells, equivalent to 207,701,612 metres have been drilled in Western Canada alone. As reported by the Canadian Association of Oilwell Drilling Contractors (CAODC, 2016), 11,226 and 5,292 wells were drilled in 2014 and 2015, respectively. Assuming an average well depth of 2500 m and a waste production of 0.1 tonnes/m

of a well, this drilling activity translates into over 4,000,000 tonnes of waste produced in the years 2014 and 2015.

In the early years of the oil and gas industry, little attention was given to waste management from an environmental and public health perspective. Therefore, mostly convenient and inexpensive methods, such as discharge into the ocean (for offshore drilling) and disposal onto land (for onshore drilling) were applied (Argonne, 2002). During the 1970s and 1980s however, claims were made that these techniques had undesirable effects on the local ecology. An example of this “undesirable effect” is formation of a mud blanket on the seafloor as a result of discharging a large volume of drill cuttings in a short period of time, consequently impacting the benthic organisms (EPA, 2000). Environmental protection agencies then began placing restrictions and guidelines for discarding waste. In subsequent years and as a result of stricter environmental regulations, major amendments were made to drilling operation practices so that less waste was produced, wastes could be reused/recycled and wastes would be disposed appropriately (Argonne, 2002).

Currently, three general options exist for handling wastes after their collection on offshore drilling platforms (OGP, 2003; Stantec, 2009). These options include discharge to the marine environment, cuttings reinjection and onshore treatment and management.

Providing that the produced drill cuttings passes regulatory requirements, discharge of waste to the marine environment can be carried out. Discharge is very common for wastes produced as a result of using WBFs in drilling. Cuttings produced when using SBFs might also be allowed to be discharged; nevertheless, for cuttings containing OBFs, discharge to the marine environment is usually not an option (Argonne, 2002). The major advantages of discharge to the marine environment are that it is easy from an operational standpoint and it does not require any kind of pre-treatment or specialized equipment for discharging the waste. In addition, discharge to the marine environment is the least expensive method since there is no cost associated with storing the waste and/or transporting the waste to shore (CAPP, 2001; OGP, 2003).

For reinjection, and similar to waste discharge, there is no cost or labor associated with transporting the waste to shore. However, reinjection is considered an expensive and labour intensive process because it is complicated and requires complex design, specialized equipment and careful monitoring (CAPP, 2001; OGP, 2003). From an environmental standpoint, in

comparison to discharge, reinjection eliminates impacts on the seafloor but results in greater energy use and air emissions (Melton *et al.*, 2000; OGP, 2003).

Different techniques exist for treatment and management of drill cuttings onshore. These techniques can be grouped into three major categories: disposal, reuse and treatment. Based on economic considerations as well as waste characteristics, one or a combination of these options may be applied for cuttings generated onshore or after the drill cuttings has been transported to shore (OGP, 2003). Onshore treatment and management options require a considerable amount of equipment and effort, resulting in costly operations. In addition to the cost of the processes themselves, considerable cost is associated with storing the waste in containers and transporting the waste from the offshore drilling platform to the disposal and/or treatment facilities. Marine transport of waste to shore also results in increased air emissions (due to the fuel consumption) and increased safety and environmental risks (due to hazards associated with handling and transporting waste). However, the major benefit of marine transport for onshore disposal is that there will be considerably less environmental impact on the marine environment.

Depending on the type of drilling fluid used, the regional regulations, the location of the well and economic considerations, different treatment and waste management techniques are applied. As environmental regulations become more stringent, the cost of treatment also increases. Hence, newer methods and technologies are constantly being investigated for the treatment of drill cuttings.

A potential method for the treatment of drill cuttings is supercritical fluid extraction (SFE). SFE is the process of removing a compound of interest from a solid or liquid phase using a supercritical fluid (SCF). A SCF is a substance that exists at or above its critical point, defined by the critical pressure and critical temperature. For example, the critical pressure and critical temperature of carbon dioxide (CO<sub>2</sub>) are 7.4 MPa and 31°C, respectively (McHugh and Krukonis, 1994). Above this point, distinct liquid and gas phases do not exist and the fluid shows some characteristics of a liquid such as density and some characteristics of a gas such as viscosity. These characteristics make SCFs excellent solvents for extraction. Extraction by supercritical carbon dioxide (SC-CO<sub>2</sub>) has drawn much attention because SC-CO<sub>2</sub> is a strong solvent, yet it is not a toxic material if inadvertently released to the environment (Akgerman, 1993).

Application of SFE for treatment of drill cuttings involves removing hydrocarbons (oil) from the drill cuttings using a SCF. As a result of the SFE process (via SC-CO<sub>2</sub> as the solvent), drill cuttings with reduced hydrocarbon (oil) content is produced. One of the main advantages of SFE in comparison to current treatment methods is the recovery of the oil.

Studies on the treatment of drill cuttings by SFE dates back to the 1980's. Eppig *et al.* (1984) patented an apparatus for removing organic contaminants from inorganic rich mineral solids. Research has since been conducted on batch SFE processes for the treatment of drill cuttings (Saintpere and Morillon-Jeanmaire, 2000; Odusanya, 2003; Lopez Gomez, 2004; Tunnicliffe and Joy, 2007; Street, 2008; Jones, 2010). In these studies, different operating conditions and parameters have been tested and optimized for various drill cuttings. Treatment of drill cuttings using SC-CO<sub>2</sub> has resulted in treated cuttings containing less than 1 wt% oil.

In spite of the promising results achieved, SFE has not been commercialized for this application to date. The reason is that a batch operation coupled with high pressure requirements, results in an expensive and labor intensive process (Cocero *et al.*, 2000). One solution for overcoming these challenges is to move to a continuous process. A continuous SFE process is believed to be more efficient and economical than a batch SFE process (Phelps *et al.*, 1996). Hence, demonstrating operation and feasibility of a continuous SFE process for treatment of drill cuttings would be a big step towards commercializing this process.

All industrial processes involving SFE from solids are operated in batch or semi-continuous mode, in which the solid phase has to be loaded in the extractor (Machado *et al.*, 2013). For example, in the field of food sciences, specifically in the extraction of oil from seeds, Temelli (2009) has indicated that the commercial plants still work in semi-continuous mode in which the vessels need to be loaded and unloaded. Therefore, handling the large amount of oilseeds is still a challenge. However, a continuous system with countercurrent flow of the solids and SCFs would overcome this challenge. One method for achieving continuous flow is slurring the solids in order to have a free flowing phase. In the case of extracting from a liquid, the two phases i.e. the SCF and the liquid, move continuously and countercurrently through the extraction vessel. Yet, a continuous countercurrent SFE process for treatment of slurried solids, to the best of knowledge of the author of this thesis, has not been commercialized for any application to date.

## 1.2 Objectives

The overall objective of this thesis was to investigate the feasibility and operation of a continuous pilot scale SFE process for treatment of drill cuttings. For this purpose, a pilot scale fully continuous SFE process must first be built and commissioned. Process control is an important aspect regarding the reliable operation of a continuous process and thus control strategies must be developed and tested on the pilot scale SFE process. Such developments can be facilitated through a reliable dynamic model of the SFE process. This model in turn can be used for testing different control structures/controllers before applying them to the physical pilot scale SFE process. Dynamic modelling is especially important when a continuous extraction process is to be employed.

Based on the above, the objectives of this thesis are explicitly specified as follows:

1. Design, build, commission and operate a pilot scale continuous SFE process.
2. Characterize the continuous pilot scale SFE process with a hydrodynamic model.
3. Design and implement controllers for pressure and slurry level control in the extraction vessel and assess their performance.

The first objective involved completing the process design, building the pilot scale process, commissioning the pilot scale process and using the process to conduct experiments safely and reliably. An important outcome of the operational process is being able to extract oil.

The second objective involved developing mathematical equations for the SFE process based on fundamental principles, implementing the derived equations, verifying and finally validating the model with data obtained from the continuous SFE process. Based on the work of Fortin (2003) and Forsyth (2006), pressure and slurry level in the extraction vessel were selected as the main process variables to be controlled. To test and implement effective control strategies for the continuous pilot scale SFE process, a hydrodynamic model is required that could predict pressure and slurry level response at different operating conditions. Therefore, the primary goal for characterizing the continuous pilot scale SFE process with a hydrodynamic model was to predict states of the system, specifically pressure and slurry level in the extraction vessel, at different operating conditions.

The third objective was associated with process control i.e. controllers were independently tuned/ designed and implemented for pressure and slurry level control inside the extraction vessel. Regarding pressure control, both manually tuned and model-based controllers were applied (in a feedback control loop) to the pilot scale SFE process and their performances were compared. For slurry level control, pressure response in the extraction vessel from a pump pulse input was employed to measure slurry level. This approach (referred to as the pulse test) for measuring and controlling slurry level was explored by utilizing the hydrodynamic model of the SFE process.

### **1.3 Context of this thesis in the overall project**

This thesis is part of an overall project aimed at designing, building, commissioning and operating a continuous pilot scale supercritical fluid extraction (SFE) process for the treatment of drill cuttings. Results obtained will be used towards utilizing a full scale continuous SFE process for treatment of drill cuttings on an offshore drilling platform or in a fixed facility onshore. The overall project is a collaboration between the University of Alberta and the University of Guelph supported by an industrial partner and the Natural Sciences and Engineering Research Council (NSERC) of Canada.

Previous SFE group members have contributed towards designing this pilot scale SFE process under the supervision of Dr. Selma Guigard (from the University of Alberta) and Dr. Warren Stiver (from the University of Guelph). The process concept drawings and calculations were initiated in 2009 by Drs. Guigard and Stiver. Piping and instrumentation (P&ID) diagrams as well as process pipe and flow diagrams (PFD) were drafted and completed by Rosenthal (SFE group member, University of Guelph) and Street (SFE group member, University of Alberta). Part of these design materials were based on results obtained from the batch bench scale SFE process located at the University of Alberta (Odusanya, 2003; Lopez Gomez, 2004; Street, 2008; Jones, 2010). In 2012, safe design of the continuous SFE process was conducted by Rosenthal (2012). Part of Rosenthal's study was based on results obtained from Fortin (2003) and Forsyth (2006) which investigated a bench scale continuous SFE process (located at the University of Guelph) for the treatment of slurried contaminated soil.

Building of the SFE process was initiated in 2010 by Street. From 2011 to 2016, Street and Roodpeyma (author of this thesis) were involved in completing the design, building and

commissioning/operating the pilot scale SFE process. Building the pilot process consisted of purchasing and assembling equipment and instruments. Building the process took place in the Innovative Process Lab in the Department of Civil and Environmental Engineering at the University of Alberta by Roodpeyma and Street with the assistance of department technician Perry Fedun and Todd Kinnee. In addition, the control system of the SFE process was built and programmed based on the control philosophy as proposed by Rosenthal (2012) and with the assistance of Les Dean (technician from the Department of Chemical Engineering). After building of the process was completed, experimental runs were conducted by Roodpeyma and Street on the pilot scale SFE process. Based on the results obtained, trouble shooting was employed and as needed, modifications were made to the preliminary design of the SFE process.

An important aspect regarding reliable operation of this continuous process is control. The development of the control philosophy for the continuous SFE process was initiated by Rosenthal (2012) and continued, completed and implemented by Roodpeyma as described in this thesis. For this purpose, a model was developed and validated for the SFE process and utilized for designing controllers and exploring different control strategies.

## **1.4 Thesis structure**

This thesis consists of seven chapters. Chapter 1 defines the problem and the objectives of this thesis. Chapter 2 provides an overview of SFE followed by a literature review of the history of SFE for the treatment of drill cuttings as well as studies related to the modelling and control of SFE processes. Chapter 3 is associated with the first objective of this thesis, that is building, commissioning and conducting safe experiments on the pilot scale SFE process. Chapter 4 relates to the second objective of this thesis, that is developing, implementing, verifying and validating a hydrodynamic model capable of predicting slurry level and pressure response in the extraction vessel. Chapter 5 is associated with the first part of the third objective i.e. controlling the pressure in the extraction vessel. Chapter 6 is associated with the second part of the third objective, namely slurry level control in the extraction vessel. A summary of conclusions and recommendations of this thesis is provided in Chapter 7. The references used in developing this thesis and appendices are provided at the end of the thesis.

## 2 Literature Review

## 2.1 Overview of Supercritical Fluid Extraction (SFE)

Each compound has a critical point, defined by its critical pressure ( $P_c$ ) and critical temperature ( $T_c$ ). Above this critical point, distinct liquid and gas phases do not exist and some of the fluid characteristics, such as density, are close to those of liquids whereas other characteristics, such as viscosity, are close to those of a gas (Laitinen *et al.*, 1994). The diffusion coefficient of a SCF is intermediate to that of a liquid and a gas. Thermophysical properties of SCFs, gases and liquids are provided in Table 2.1 for comparison.

**Table 2.1. Comparing thermophysical properties of gases, SCFs and liquids (Vanwasen *et al.*, 1980; Bright *et al.*, 1992)**

Phase	Density (g/cm <sup>3</sup> )	Diffusion coefficient (cm <sup>2</sup> /s)	Viscosity (g/cm.s)
Gas	10 <sup>-3</sup>	10 <sup>-1</sup>	10 <sup>-4</sup>
SCF	0.1-1	10 <sup>-3</sup> -10 <sup>-4</sup>	10 <sup>-3</sup> -10 <sup>-4</sup>
Liquid	1	<10 <sup>-5</sup>	10 <sup>-2</sup>

In addition, SCFs have very low surface tensions, resulting in easier penetration into porous material (McHugh and Krukonis, 1994). A unique property of a SCF is that its solvating power can be adjusted by regulating the density. The fluid density itself is regulated by adjusting the temperature and pressure in the critical region (McHugh and Krukonis, 1994; Phelps *et al.*, 1996). This attribute makes SCFs excellent solvents for extraction because solvating power can be manipulated to have a strong solvent under certain conditions of pressure and temperature (e.g. the extraction phase) and a weak or non-solvent under other conditions of pressure and temperature (e.g. separation phase).

One of the most common SCFs utilized in supercritical fluid extraction (SFE) is carbon dioxide (CO<sub>2</sub>) (Phelps *et al.*, 1996). The main reasons for this choice is that CO<sub>2</sub> is readily available and inexpensive (Laitinen *et al.*, 1994), non-toxic, available in high purity (Madras *et al.*, 1994), non-flammable and non-reactive (Akgerman, 1993). In addition, it has a relatively low and attainable critical temperature of 31°C and critical pressure of 7.4 MPa (McHugh and Krukonis, 1994). Supercritical CO<sub>2</sub> (SC-CO<sub>2</sub>) is also considered as an excellent solvent for extracting non-polar organic compounds, specifically hydrocarbons and oils (Laitinen *et al.*, 1994). The P-T phase diagram of CO<sub>2</sub> is illustrated in Figure 2.1.

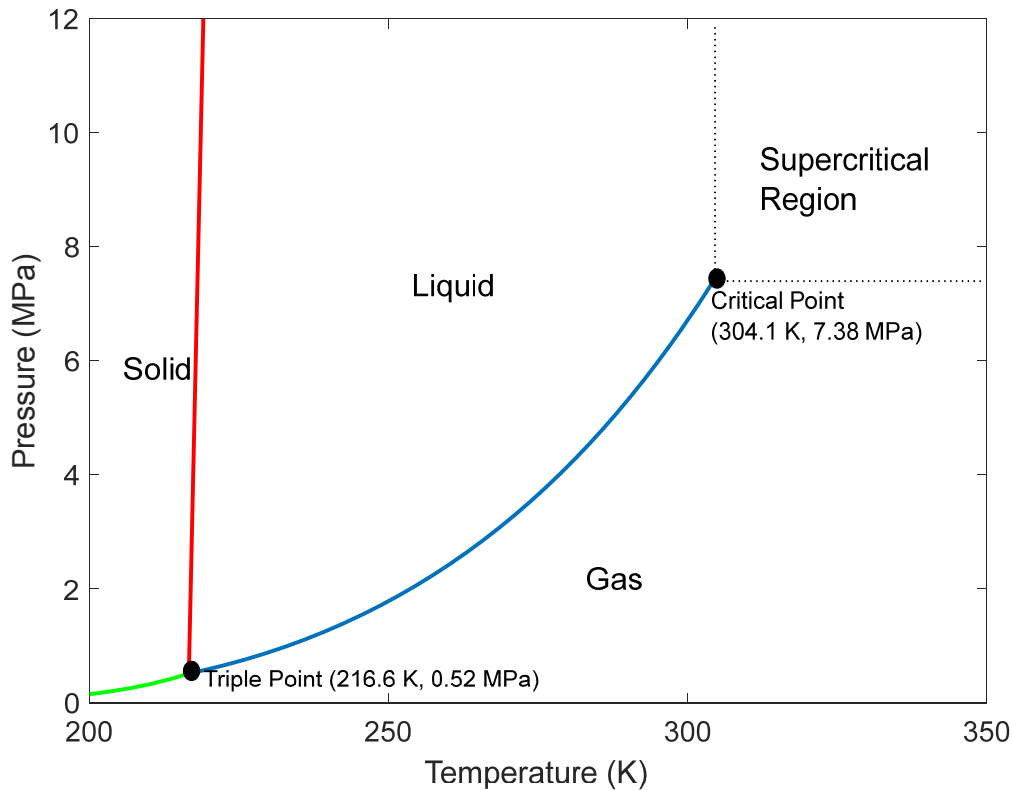


**Figure 2.1. Phase diagram of CO<sub>2</sub>**

There are many benefits associated with SCFs (specifically SC-CO<sub>2</sub>) in comparison to conventional solvents used in extraction processes. SFE processes are faster compared to extractions done using conventional solvents (Phelps *et al.*, 1996). With regards to solvent recovery, conventional extraction processes require a complex distillation system after the extraction process while in SFE, a simple pressure reduction is sufficient for the purpose of recovering the solvent. In industrial applications, extraction processes that use SCFs require lower energy consumption during operation in comparison to extraction processes which use conventional solvents (Knez *et al.*, 2014). Due to such environmental benefits, extractions with SCFs namely SC-CO<sub>2</sub>, are referred to as “green” chemistry (Camel, 2013). SC-CO<sub>2</sub> has also been referred to as “green solvents for the future” (Brunner, 2012; Knez *et al.*, 2014). The main drawback in using SCFs versus conventional solvents is associated with the high cost of equipment required for pressurizing the fluid, to obtain a SCF, and the pressure rated equipment needed to handle a high pressure fluid (Machado *et al.*, 2013).

Although the use of SCFs was initially presented in the literature in 1822, it was not until the second half of the twentieth century that these fluids started to be applied at an industrial

scale, specifically in the field of food sciences and pharmaceuticals (Phelps *et al.*, 1996; Machado *et al.*, 2013). One of the reasons for the delay in applying this technology was the difficulty in developing safe equipment to operate near and above supercritical temperatures and especially supercritical pressures (Machado *et al.*, 2013). In 1976, the Max Planck Institute began to build the first industrial scale coffee decaffeination plant in Germany using SCF technology (Phelps *et al.*, 1996). After start-up and successful production of the decaffeination plant in 1978, construction of a hops extraction plant was initiated in 1982 followed by a tea decaffeination plant a few years later.

Current well-known industrial applications of SFE in the field of food sciences are decaffeination of coffee and tea, defatting of cacao, production of extracts from hops, fruits, spices, nuts and other natural materials (Brunner, 2010). A more recent industrialized SFE application in the field of food sciences is the extraction of sesame oil from sesame seeds (Brunner, 2010). In 2004, a Korean company, UMAX Co., reported an oil extraction rate of approximately 8000 L/day in their industrialized SFE plant. In 2006, another Korean company (Ottogi) started an industrialized SFE plant for the same application. Three extractors with a volume of 2300 L have been reported for this SFE plant (Brunner, 2010). It should be noted that extraction of oil from seeds is carried out in semi-continuous mode in which the solids are usually loaded in a fixed bed extractor and the SCF flows through the vessel and extracts the oil from the solid substrate.

Another recent industrialized application of SFE in the field of food sciences is cleaning of rice using SFE (Brunner, 2010). The company associated with this process is located in Taiwan (named The Five King Cereal Industry Company Ltd.) and it uses three extractors, each with a volume of 5800 L. The company claims that the rice is cleaned from pesticides and heavy metals as well as waxes and fatty acids (which cause degradation of the rice if not removed).

Another wide spread industrial application of SFE is in the field of cosmetics and pharmaceuticals. One of the earliest applications in this field was developed in 1988 for the extraction of acetone residue from antibiotics and in 1993 for the extraction of pharmaceuticals from botanicals (Phelps *et al.*, 1996). Currently, many countries (e.g. United States, France, Italy, China, and South Korea) apply SFE for production of pharmaceutical products (Machado *et al.*, 2013).

Presently, the application of SFE is widely applied not only in the field of food sciences and pharmaceuticals, but also in the areas related to toxicology, environmental remediation, textile dyeing, petrochemical manufacturing, polymers manufacturing, etc. A comprehensive review of research conducted in these areas is presented by Machado *et al.* (2013). As seen, numerous studies have been reported in literature which apply SFE technology for various applications. A great deal of these studies have remained at the research scale i.e. they have not yet been commercialized. One of the main reasons is linked to a major drawback in employing SFE specifically with CO<sub>2</sub> i.e. the high capital cost associated with high pressure equipment required for turning CO<sub>2</sub> from a gas to a SCF (Cocero *et al.*, 2000; Camel, 2013). One application that is currently in the research scale but has the potential to be industrialized is SFE using SC-CO<sub>2</sub> for the treatment of oil-contaminated solids. A well-known example of oil-contaminated solids in the oil and gas industry is drill cuttings.

If an extraction process involves the removal of a certain component from a solid phase, then a solid-liquid extraction problem is posed and the related equipment are generally operated in a cyclic batch or semi-batch mode (Machado *et al.*, 2013). Alternatively, the feed may be in liquid form, either in the form of a solution or a slurry and the operation, called liquid-liquid extraction, is aimed at separating certain components from the liquid by bringing them into contact with a suitable liquid solvent. In this case, both batch and continuous operations are viable and may be selected as modes of operation. Clearly, operability and cost considerations are the key factors in choosing between the different operation modes.

In general, a batch operation is deemed to be less efficient than continuous operation and consideration should be given to the advantages of continuous over batch operations (Peters and Timmerhaus, 1991; Phelps *et al.*, 1996). However, regarding extraction from the solid phase, it is challenging to continuously feed the solid phase into a high pressure extractor. Therefore, commercial SFE plants for extraction from a solid phase are still operated in semi-continuous mode, in which the solid phase is cycled through multiple extraction vessels by filling and emptying them batch-wise (Temelli, 2009). This mode of operation leads to major challenges for handling large volume of solids. Laitinen *et al.* (1994) suggested making a solids slurry mixture and then feeding it to the extractor, allowing continuous flow of solids and SC-CO<sub>2</sub> through the SFE process. Based on the available literature, such a continuous system has not been commercialized yet.

## 2.2 The past, present and future of SFE for treatment of oil-contaminated solids

SFE for treatment of oil-contaminated solids encompasses a wide range of applications. This section is mostly focused on treatment of drill cuttings and some relevant studies in this area that led to the current study.

Studies on SFE for the treatment of drill cuttings dates back to the 1980's. Eppig *et al.* (1984) patented an apparatus for removing oil and other organic contaminants from inorganic rich mineral solids by SFE in semi-continuous mode. Dichlorodifluoromethane, propane and CO<sub>2</sub> were introduced as the preferred SCFs for this extraction process. The choice of SCF dictates process conditions i.e. temperature and pressure in the extraction vessel. Producing a pumpable slurry has been suggested in this patent by using an oil (such as diesel) or aqueous liquid (such as brine) as the slurry base to convey the solids to the extractor. However, the excess oil or aqueous liquid is drained before introducing the solvent (SCF) into the extraction vessel. In this patent, it has been stated that the proposed methods and apparatus are especially suitable for removing oil from contaminated drill cuttings. Eppig *et al.* (1984) concluded that treatment by SFE resulted in oil-free cuttings that could be disposed of by dumping into the ocean.

In 1996, Eldridge (1996) conducted a comprehensive study on treatment of drill cuttings using SFE. For this purpose, semi-continuous extractions were conducted using 1,1,1,2-tetrafluoroethane (HFC134a) and propane as the SCF. The extractor in this process was a 1 L stainless steel autoclave in which the cuttings were loaded. After process conditions were reached in the extractor (650 psi and 250 °F), the solvent flowed through. It was concluded that SFE is capable of reducing the contamination of drill cuttings to a level acceptable for offshore disposal. The experimental results and cost estimates obtained from this research indicated that this technology was very competitive with disposal technologies of that time, however further work was required for optimizing the system before actual installation.

Saintpere and Morillon-Jeanmaire (2000) investigated the efficiency of a pilot SFE unit for handling up to 500 g of cuttings per batch using SC-CO<sub>2</sub>. For this purpose, different extraction conditions were tested and optimized; hence, a pressure of 100 bars and temperature of 35 °C were selected as the optimal extraction conditions. As a result of applying these conditions, Residual Oil Contents (ROC) as low as 0.2 % by weight of dry cuttings were

reported. Extraction efficiency in two larger scale units i.e. a 6 kg static reactor and a 10 kg rotating autoclave was also investigated at the same extraction conditions. ROC below 1% by weight of dry cuttings was achieved for these units. Saintpere and Morillon-Jeanmaire (2000) concluded that SC-CO<sub>2</sub> has the potential to be a feasible alternative for the cleaning of cuttings.

A patent for the cleaning of hydrocarbon-containing solids and/or liquids such as drilling fluids, used oils and oil-contaminated soils with near critical and supercritical solvents was published by Tunnicliffe and Joy (2004). The solvent(s) were one or a combination of CO, CO<sub>2</sub>, H<sub>2</sub>O, lower alcohols, lower alkanes and/or lower alkenes. Depending on the choice of solvent, treatment conditions were reported as 1.0 to 1.4 for reduced temperature and 1.0 to 2.0 for reduced pressure. Different modes of operation (batch and semi-continuous) were considered. It has been stated that the patented invention provides a solid phase free of organic and/or non-organic water-soluble components.

The reviewed literature are among the key studies and developments conducted in the area of the application of SFE for the treatment of oil-contaminated solids. A comprehensive study in this field has also been conducted at the University of Alberta and the University of Guelph over the last 13 years. Bench scale SFE batch and continuous systems have been tested at different operating conditions and parameters have been optimized for obtaining high mass transfer coefficients and removal efficiencies (Odusanya, 2003; Fortin, 2003; Lopez Gomez, 2004; Forsyth, 2006; Street, 2008; Jones, 2010).

Studies at the University of Alberta (Odusanya, 2003; Lopez Gomez, 2004; Street, 2008; Jones, 2010) focused on bench scale batch SFE. A typical batch SFE system is illustrated in Figure 2.2.

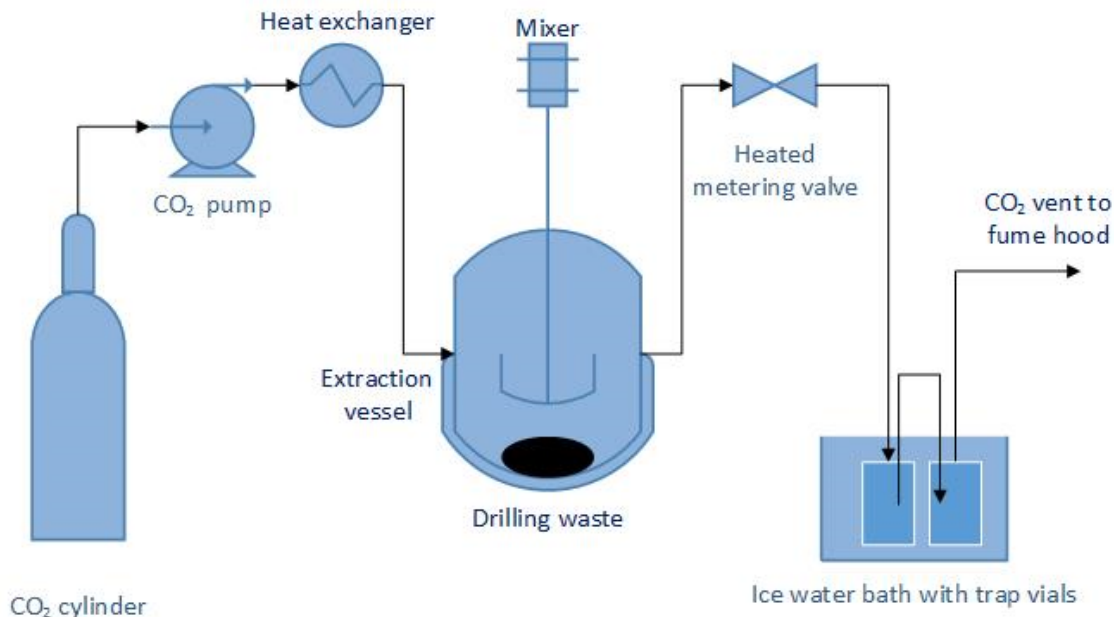


**Figure 2.2. Schematic of a lab scale batch SFE process**

In 2003, Odusanya (2003) was successful in reducing the hydrocarbon content of oil-contaminated drill cuttings from 17.19% to 1.76% (equivalent to an extraction efficiency of 90%) in a single cycle bench scale batch SFE system. A double cycle, resulted in an increase of extraction efficiency to 97%. The feed used in this study was OBM drill cuttings obtained from active drilling sites. Different operating conditions were tested ranging from 35 °C to 60 °C and 8.3 MPa to 17.2 MPa for temperature and pressure respectively. The highest extraction efficiency was achieved at 60 °C and 12.4 MPa. The extraction vessel used in this study was a 300 mL extraction vessel. Better mixing was recommended for obtaining higher extraction efficiencies.

Lopez Gomez (2004) continued the work of Odusanya (2003) on the same lab scale batch SFE process and was able to reduce the oil content of the drill cuttings (diesel-contaminated, centrifuge underflow drill cuttings) from 19.4% to below 0.5%. It has been stated that the use of a ribbon blender resulted in good mixing and consequently higher extraction efficiencies were obtained. Different operating conditions were tested ranging from 40 °C to 60 °C and 8.96 MPa to 15.2 MPa for temperature and pressure, respectively. The highest extraction efficiencies were obtained at 40 °C and 14.5 MPa.

In 2008, Street (2008) optimized the same batch SFE process (Odusanya, 2003; Lopez

Gomez, 2004) for the treatment of drill cuttings specifically with regards to mixing speed, initial waste mass and additives. The optimum conditions as determined by Lopez Gomez (2004) were applied. As a result, the hydrocarbon content of the drill cuttings was reduced to 0.4%. This result was achieved at a mixing speed of 50 rpm, 50 g of initial waste mass and 15 g of additive. It should be noted that the feed used in this study was synthetic-contaminated, centrifuge underflow drill cuttings.

As a continuation of the previous studies conducted at the University of Alberta, Jones (2010) investigated the treatment of slurried drill cuttings using the batch SFE system. The aim of this study was to explore extraction from a slurried feed which can potentially be used in a continuous SFE process. It was concluded that the slurry should be at least 1:1 (water to drill cuttings ratio) to be “free-flowing”. Initial experimental results revealed that slurring with water lead to lower extraction efficiencies in comparison to the case in which the cuttings were not slurried. However, Jones (2010) also concluded that by introducing the SC-CO<sub>2</sub> at the bottom of the extraction vessel and by applying effective mixing inside the vessel, treated slurries with less than 1% hydrocarbon content could be obtained.

At the University of Guelph, studies by Fortin (2003) and Forsyth (2006) focused on a fully continuous SFE process for the treatment of slurried solids. A schematic of a typical continuous SFE process, similar to the lab scale process designed and constructed by Fortin (2003) is presented in Figure 2.3.

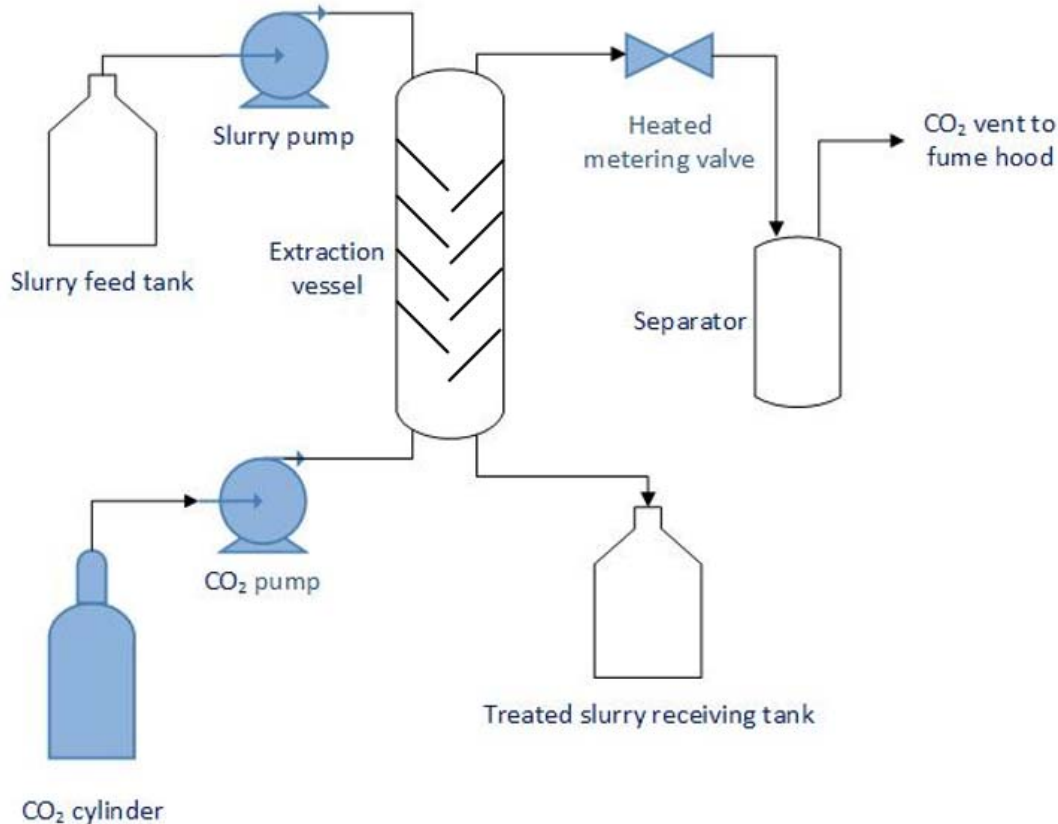


**Figure 2.3. Schematic of a continuous SFE process**

The objectives of Fortin’s research specifically consisted of designing, building and testing a lab scale SFE process to remove naphthalene from soil slurries. The main components of the continuous SFE process as designed by Fortin (2003) consisted of an extraction vessel (with an inner diameter of 4.2 cm and a height of 50 cm), a CO<sub>2</sub> pump, a slurry pump, a CO<sub>2</sub> cylinder, a slurry tank, a rinse tank and an acetone and CO<sub>2</sub> cooling bath. To promote mixing between the two phases inside the vessel, a structure with inclined baffles was designed and installed inside the extraction vessel.

An important outcome of Fortin’s research was demonstrating continuous flow of the two phases i.e. soil slurry (containing solids) and SC-CO<sub>2</sub>. The continuous system could be kept steady for as long as two hours, during which successful extraction of naphthalene from the slurried soil was achieved. Another outcome of the research was the necessity to automate the system specifically slurry level inside the extraction vessel. It was concluded that major process issues were related to uncertainties regarding slurry level in the vessel. In instances where the vessel was filled with water, mass transfer still occurred between the two phases as the CO<sub>2</sub>

bubbled up through the vessel. However, mass transfer is less effective in comparison to scenarios in which slurry is at lower levels inside the vessel.

Forsyth (2006) continued the work of Fortin (2003) on the same lab scale continuous SFE process. In the work of Forsyth (2006), the SFE process was applied to investigate the ability to extract PAHs from soil slurries using SC-CO<sub>2</sub>. Another important objective of this research aimed at implementing slurry level control in the extraction vessel due to the uncertainties that Fortin (2003) experienced regarding slurry level in the vessel. In countercurrent mass transfer operations, a common technique to control liquid level in the column is using a control valve on the liquid exit line. However, due to the abrasive nature of the slurried soil (due to solids content) it was concluded that one of the pumps i.e. one of the inlet flows (slurry/CO<sub>2</sub>) should be used for this purpose. It was also decided that the level should be kept between two elevations within the extractor (50 cm high). The level increasing above 13 cm would result in a decreased column height for countercurrent mass transfer, while a level decreasing to below 3 cm would promote CO<sub>2</sub> entrainment. In successful implementation of slurry level control in the continuous lab scale SFE system, Forsyth (2006) summarized its importance as follows:

- Increased mass transfer coefficients
- Capacity to run longer experiments
- Ability to have steady state operation, specifically in term of temperature and pressure, inside the extraction vessel

After successful operation of this continuous lab scale SFE process for treatment of contaminated solids, the subsequent step was designing and building the next scale (i.e. pilot scale) of this SFE process (for treatment of oil-contaminated solids) and testing its operability. In this direction, Rosenthal (2012) initiated the safe design of a continuous pilot scale SFE process for the treatment of drill cuttings. As a result, a process Piping and Instrumentation Diagram (P&ID), a control philosophy and an operations manual was developed and a Hazard and Operability (HAZOP) analysis was conducted. The aim of the control philosophy as defined by Rosenthal (2012) was to provide guidelines for controlling the continuous pilot scale SFE process from both a safety and process control perspective. The control philosophy specifically described a control system structure (data acquisition (DAQ) system, computer, sensors, etc.), control modes (manual mode, run mode, safe mode, emergency mode), control loops (pressure

control and slurry level control) and an alarm philosophy (alarm limits and prioritization). An important outcome regarding the control loops was that two main process variables must be controlled i.e. pressure and slurry level inside the extraction vessel. Pressure is controlled via the CO<sub>2</sub> inlet flow to the vessel while slurry level is controlled via the slurry inlet flow to the vessel. Rosenthal (2012) also indicated that the two stated loops are not completely isolated and interaction between the two loops is expected.

## **2.3 Modelling SFE processes**

Depending on the modelling aim, process models can be developed and utilized at different phases of setting up a process (Luyben, 1996). Modelling may be attempted before a physical system exists or it may be attempted during or after a physical system has been designed and developed. The intent for modelling a process may be to explore the impact of different operating conditions, to conduct optimization and control studies, to troubleshoot the process, to aid in scale-up calculations, etc. It is obvious that conducting these kinds of studies on the process representative model can be cheaper, safer and faster than conducting them on the actual process (Bruno and Ely, 1991; Luyben, 1996). However, no model is perfect and it will always be based on some simplifying assumptions, which in turn may lead to process-model mismatch.

Modelling SFE processes, similar to modelling any extraction process, can focus on thermodynamic, mass transfer and/or hydrodynamic behaviour. An important and widely investigated aspect of modelling SFE processes is thermodynamic modelling, which leads to the prediction of equilibrium stage compositions. The next important aspect of modelling concerns sizing of extraction equipment. Such models establish the desired relationships between the solute removal efficiency, feed flow rate and the size of the extractor. The third important aspect of modelling the SFE process is related to operability and control. Such studies are usually aimed at hydrodynamic modelling and are specifically relevant when continuous countercurrent liquid-liquid contact is to be employed. Based on the process under investigation and on the intent of the modelling, one or a combination of these three aspects might be taken into account when modelling a SFE process.

In designing and developing a SFE process, knowledge of phase behaviour is essential. For pure CO<sub>2</sub>, the Pressure-Volume-Temperature (PVT) behaviour can be calculated via available cubic equations of state (EOS) such as the van der Waals EOS, the Redlich-Kwong

EOS (RK-EOS), the Peng-Robinson EOS (PR-EOS), or modifications of these equations (Marr and Gamse, 2000). The other option is developing empirical equations/models based on the available database. Such equations have been developed over the years. Bender (1970) was one of the first to develop an empirical thermodynamic model for CO<sub>2</sub> for a temperature range of 216-1076 K and pressure range of 0-50 MPa. A comprehensive review of well-known empirical models developed for CO<sub>2</sub> is presented in Span and Wagner (1996). The Span and Wagner EOS (1996) is another well-known equation in this category, which is capable of relating CO<sub>2</sub> properties to pressures and temperatures up to 800 MPa and 1100 K, respectively. Additional material regarding the Span and Wagner EOS (1996) is presented in Chapter 4.

Another aspect of thermodynamic modelling for SFE processes is associated with describing the phase equilibrium of multi-component mixtures at high pressures. For describing phase behaviour of a mixture, cubic EOSs can be applied by calculating their parameters via mixing rules. Through this approach, interaction parameters have to be fit to experimental data (Marr and Gamse, 2000). The other option is applying empirical equations, Chrastil (1982) being a well-known equation. In developing or applying such equations, data have to be fit to the adjustable parameters of the equation. Either way (EOS vs. empirical), experiments must be conducted to produce the required data. A comprehensive review of phase equilibrium modelling in natural product mixtures has been presented by Diaz and Brignole (2009). Group contribution equations of state (GC-EOS) and empirical models such as Chrastil (1982) have been stated as being extensively used for predicting thermodynamic equilibrium in SFE processes.

Predicting the composition of the extract and raffinate (or predicting the extraction efficiency) in a SFE process is very valuable. Therefore, mass transfer modelling (by applying equilibrium stage relationships or mass transfer approaches) has been investigated in several studies (Cesari *et al.*, 1989; Ramchandran *et al.*, 1992b; Ruivo *et al.*, 2004; Fernandes *et al.*, 2007b, 2007a, 2011), including continuous or semi-continuous SFE processes. It should be noted that thermodynamic and hydrodynamic equations have also been employed in these studies however, the focus of the studies are predicting the composition of the extract and raffinate.

Cesari *et al.* (1989) developed a mathematical model for a semi-continuous SFE process. The model was applied to simulate two processes: fractionation of ethanol from water with SC-CO<sub>2</sub> and extraction of citral from lemon oil with SC-CO<sub>2</sub>. Material and energy balances as well

as equilibrium and hydrodynamic relationships were employed in modelling. As a result, the process outputs were predicted at different pressures, temperatures and CO<sub>2</sub> flowrates. Validation was only provided for the fractionation of ethanol from water. Good agreement (visually) was obtained between the model and process data (i.e. variation of moles of CO<sub>2</sub> and ethanol in the high density and low density phase) at various process conditions.

Ramchandran *et al.* (1992b) simulated a complete continuous SFE plant for the extraction of isopropyl alcohol from an aqueous solution using SC-CO<sub>2</sub>. Modelling of the extraction vessel was based on tray-to-tray equilibrium relationships. The main outputs of the modelling were the extract and raffinate compositions as a function of SC-CO<sub>2</sub> flowrate. The modelling outputs (i.e. composition of the extract and raffinate) were visually compared with experimental data measured from a pilot scale SFE process. In some tests, the model did not correctly represent the experimental data. Issues in maintaining level in the extractor was mentioned as one of the reasons for this inconsistency.

Ruivo *et al.* (2004) and Fernandes *et al.* (2007b, 2007a, 2011) conducted a comprehensive study of modelling a SFE process. The study was initiated by modelling a countercurrent packed column for the fractionation of a binary liquid mixture of squalene and methyl-oleate using SC-CO<sub>2</sub> (Ruivo *et al.*, 2004). The dynamic model consisted of equations describing thermodynamic phase equilibrium, mass transfer and hydrodynamics of the SC-CO<sub>2</sub> and liquid phases. The main outputs of the model were the composition of the extract and raffinate as well as the axial profile of liquid holdup at different extraction times. The model was validated with experimental data and good agreement between the model and experimental data was observed. Although Ruivo *et al.* (2004) assumed a constant temperature in their study, Fernandes *et al.* (2007b) continued the work by investigating non-isothermal dynamic modelling of the packed column. For this purpose, the model incorporated momentum and energy balances in the packed bed extraction column. Both temperature and composition profiles were provided as outputs of the model. Fernandes *et al.* (2007a) further extended the work to incorporate dynamic modelling of a complete SFE plant, which included not only the isothermal packed bed extraction column modelled by Ruivo *et al.* (2004) but also other main unit operations in the SFE plant namely the separation column and heat exchangers. In their most recent study, Fernandes *et al.* (2011) presented modelling and simulation of a complete SFE plant with non-isothermal conditions and other modelling upgrades.

## 2.4 Process control and SFE applications

Until the 1960's, control of most processes was based on analog controllers, normally designed for single-input single-output (SISO) linear systems. Due to fewer environmental regulations and lower product quality requirements, classical controllers served as satisfactory means of process control at the time (Ray, 1989). However, over the years, with the introduction of large scale continuous processes with high-performance specifications as well as intense environmental and safety regulations, more difficult control problems have been posed. These difficult control problems are mainly associated with process interactions, process non-linearities, operating constraints, time delays and uncertainties in the process. Nevertheless, at the same time, significant improvements were implemented in computer control and digital instrument systems that provided improved functionality and flexibility (Birchfield, 2002). Thus, modern control theory coupled with advanced process control through advanced computers became the solution to controlling modern processes and obtaining optimal system performance.

Kozak (2014) has categorized the time development of control engineering methods (applied in research and industry) into four phases. The first phase is associated with classical control i.e. the conventional Proportional-Integral-Derivative (PID) controller applied in different control structures such as feedback control, feedforward control, cascade control, ratio control or a combination of these structures. Classical control has been widely used in industry for several decades. The controllers in this category are either tuned manually or automatically. Implementation of this controller started from the early mechanical and pneumatic designs. Currently, it is implemented in microprocessor-based systems. Additional material on a PID controller and characteristics of its tuning parameters is provided in Chapter 5.

The second phase of control engineering development is associated with the initial advancements in the field of control engineering i.e. introduction of modern control namely multivariable control methods (state space models, transfer function models, decoupling), adaptive control, gain scheduling and nonlinear control methods. These control methods have been commercialized for more than 40 years. However, they are not as popular as the conventional control methods. The control methods in this category are mostly model-based, leading to better control in comparison to the conventional methods. However, for implementation, model accuracy becomes an important factor and time must be invested for

developing a model of the process. Generally, two types of models exist i.e. models based on first principles and models based on system identification. Additional material regarding process modelling is provided in Chapter 4. Brief specifications of the stated control methods in this phase follows.

Available control methods in the category of multivariable control are advantageous for processes in which (i) more than one controlled variable exists (i.e. more than one control loop is required) and (ii) considerable interaction exists between the control loops (Stephanopolous, 1984; Kozak, 2014). Multivariable control methods take into account the interaction between different manipulated-controlled variables in a process.

Due to the nonlinear and/or nonstationary characteristics of some processes, it is advantageous to have a control system which can adjust its parameters automatically to compensate for the variations of the process. In other words, an adaptive controller adapts itself to the needs of the process. Gain scheduling is a type of adaptive control in which the parameters of the controller can be programmed or scheduled (Shinskey, 1979; Stephanopolous, 1984).

Linearizing the behaviour of a process and applying linear control techniques is only valid at around the selected operating points. Far deviations from this operating point will usually not result in satisfactory control. Therefore, for cases in which a large range of operating conditions must be considered, nonlinear control is applied (Goodwin *et al.*, 2000).

The third phase is associated with next level of modern control methods such as Model Predictive Control (MPC), robust control, Internal Model Control (IMC) and decentralized control. Among the stated methods, MPC is the most famous and it is widely used in industrial processes such as distillation columns, furnaces, reactors, etc. It is specifically the method of choice in oil refineries and petrochemical plants and its application in this field has increased rapidly (Kozak, 2014). Kano and Ogawa (2009) have reported the first multivariable MPC controller in an industrialized continuous plant for olefin production as early as the 90s in Japan. Brief specifications of the stated control methods in this phase follows.

Model predictive control uses a dynamic model and available measurements of the process to predict future process behaviour (future value of output variables). For this purpose, the manipulated variables are calculated so that they minimize an objective function (Kozak, 2014). In other words, a predictive controller is capable of observing the current and also

predicting future process variables to compute control moves expected to optimize the future behavior of a plant. MPC is commonly applied to multivariable systems with nonlinear and/or difficult dynamic behaviour in which there are constraints on the inputs and/or outputs. It should be noted that the MPC approach is a computationally costly operation. Therefore, it is conventionally applied for processes with relatively slow dynamics such as thermal, chemical and biotechnological processes (Kozak, 2016). A disadvantage associated with MPC is that it is not suitable for integrating processes specifically level control (Kano and Ogawa, 2009).

In process modelling, there are always uncertainties in the developed model of the process. Source of this uncertainty is either the result of parametric uncertainty or unmodelled dynamics (Skogestad and Postlethwaite, 2005). Model uncertainty, also referred to as model/plant mismatch, affects controller design and controller performance. If a control system is insensitive to this uncertainty (i.e. differences between the actual process and the process model used to design the controller), it is referred to as a robust controller.

In processes with multiple controlled/manipulated variables i.e. multi-input multi-output (MIMO), it is usually advantageous to have decentralized control loops (multiple decoupled control loops) rather than a single multivariable controller. In the case of the former (known as decentralized control), controllers can be maintained easier and upgrade of the control system (in case of plant upgrade) is more straightforward (Goodwin *et al.*, 2000).

The fourth phase of control engineering development is associated with soft computing methods (SCM) such as fuzzy control and neural network control. These methods have been introduced as versatile and effective techniques to deal with process non-linearity and uncertainty. In the fuzzy logic method, human reasoning and decision making is systematically and mathematically emulated (Malhotra *et al.*, 2011). A fuzzy logic controller generally acts in three stages: fuzzification (converting a crisp input to a fuzzy value), fuzzy inference (drawing conclusions from the available database) and defuzzification (converting the fuzzy control action to a crisp control action). Industrial applications of this control method have begun in some countries, Japan being an example (Kozak, 2014).

Artificial neural network (ANN) is another method which has found wide spread application in process modelling and control. The concept of this method is inspired by biological neural networks in which a network of neurons can be trained for a specific

application. Two general approaches exist when applying ANN in process control: in the first approach control action is directly computed by the neural network; while in the second approach, controller parameters are generated by the ANN (Kozak, 2016).

Among all the control methods introduced, the PID controller has the longest history and it is currently the most common controller type applied in industry (87% - 90%) (Kozak; 2016). The main reason behind this fact is that PID controllers are versatile and robust. In addition, good performance and stability has been obtained in many real processes in the industry in which PID controllers are used (Kozak, 2016).

A basic classification of PID controllers is conventional vs. advanced. For the conventional PIDs, standard PID tuning methods are applied such as the Ziegler-Nichols method (1942), the Cohen-Coon method, minimum error integral methods, etc. For the advanced PIDs, advanced PID tuning methods such as IMC tuning rules (namely Skogestad-IMC tuning rules and Viteckova-IMC tuning rules), gain scheduling methods, robust PID tuning methods, supervisory fuzzy PID methods, neural PID tuning methods, etc. are applied.

Unfortunately, not many studies have been reported in literature regarding control of SFE processes. In the few studies that have been reported, both classic and modern control methods have been considered. These studies are reviewed in the following paragraphs.

Cygnarowicz and Seider (1990) conducted a SFE control study on the extraction of  $\beta$ -carotene from water with SC-CO<sub>2</sub> via simulation. The selected controlled and manipulated variables in this study were separator pressure and vapour flowrate, respectively. Both Proportional (P) and Proportional-Integral (PI) controllers were tuned using the Cohen-Coon method (1953). Set-point change (servo problem) and disturbance rejection (regulatory problem) were explored. Simulation results indicated that the set-point response of the PI controller is acceptable, but its response to disturbance rejection is oscillatory and sluggish. Proportional control, as expected, exhibits an offset in the pressure response. The authors concluded that advanced control strategies such as model predictive control (MPC) will lead to more satisfactory control in comparison to classical controllers (P and PI), specifically for disturbance rejection.

Another comprehensive study with regards to process control was conducted by Ramchandran *et al.* (1992a) on a SFE process using SC-CO<sub>2</sub>. The two main unit operations in

the process were an extractor (for extracting isopropyl-alcohol (iPA) from water) and a stripping column (for recovering the CO<sub>2</sub>). Modern control strategies, which use mathematical models of the system to perform a control action, were considered. The model obtained for the system was based on mass and energy balances, as well as on equilibrium relationships (Ramchandran *et al.* 1992b). As a result, nonlinear plant-wide control was applied to the SFE process in two different modes i.e. “stand-alone” mode and “integrated” mode. In “stand-alone” mode, each unit operation is controlled via an independent controller while in “integrated” mode, only one controller is applied to the entire process. The main controlled variable in this process is the composition of iPA in the raffinate in which the solvent flow rate is used as the manipulated variable. However, control of stripper overhead and bottom composition - via reflux rate and CO<sub>2</sub> flow rate through the reboiler, respectively - have also been considered. Both set-point tracking and disturbance rejection were explored in the control studies. It was concluded that the “integrated” mode of the nonlinear controller had better performance in rejecting disturbances in comparison to the “stand-alone” mode. Furthermore, Ramchandran *et al.* (1992b) stated that simple PI controllers were also tested on the process, but satisfactory control was not achieved i.e. the classical controllers were not able to maintain the controlled variables at their desired set-points.

Samyudia *et al.* (1996) also investigated different control strategies for the same SFE system that was introduced by Ramchandran *et al.* (1992b). For this purpose, different plant decompositions of the SFE process have been tested and the use of a decentralized controller in each plant decomposition has been investigated. It should be noted that the decomposition was applied via two methods: physical decomposition (PD) and decomposition across units (DAU). In the PD approach, the multi-unit plant is decomposed based on the physical unit operations. In the DAU approach, decomposition is applied based on the dynamics of the controlled variables. Samyudia *et al.* (1996) developed a modified version of Ramchandran’s model to be applied in the control studies.

Although the cited studies are of the earliest and most comprehensive works done in this field, as can be seen, they are generally based on simulation and not control of an actual SFE system. A study based on the control of an actual SFE system was reported by Riverol and Cooney (2005). The system under investigation was a semi-batch system used for the decaffeination of coffee in which CO<sub>2</sub> is continuously recycled. The main unit operations are the

extraction vessel and the gas washer used to separate the CO<sub>2</sub> from the extracted caffeine. Similar to the above studies, mathematical models have been obtained for the process and used in the control structure. Performance of the model-based controller is compared with that of decoupled PID controllers. It has been concluded that increasing the complexity of the controller i.e. applying model-based controllers instead of classical PID controllers, results in higher caffeine extraction.

While the stated studies are associated with different SFE systems, they have all concluded that applying modern control theory which utilizes a model of the process in the control structure, results in improved control.

## **2.5 Summary**

The above literature review demonstrates that, although SFE for treatment of drill cuttings has a long history and very good results (i.e. high extraction efficiency) have been obtained, an industrial process for applying this application of SFE has not been developed to date. The main challenge in industrializing this process is the operability and cost considerations associated with batch and semi-continuous SFE processes. A fully continuous SFE process is believed to overcome the challenges associated with batch and semi-continuous SFE processes. Therefore, the next important step towards industrialization of the SFE process for the treatment of drill cuttings is demonstrating operation and feasibility of a fully continuous pilot scale process.

In terms of modelling SFE processes, various studies have been reported in the literature and depending on the process and intent of modelling, the focus of these studies was on thermodynamic and/or mass transfer and/or hydrodynamic behaviour of the process. Regarding control of SFE processes, not many studies have been reported. From the few studies that have explored the control of SFE processes, the majority are based on simulation and not control of an actual SFE process.

### 3 Design, Build, Commission and Experimental Runs\*

---

\* Chapter 3 of this thesis is a joint effort between M. Roopdeyma and C.G. Street and it is available in both theses of the authors. This Chapter is associated with the continued design, build and commission/operation of the continuous pilot scale SFE process for treatment of drill cuttings. The three stated stages were conducted and completed as a collaboration between M. Roodpeyma and C.G. Street. The preliminary design of the process was provided by A. Rosenthal. Department technicians (Civil/Environmental and Chemical/Materials Engineering) P. Fedun, T. Kinnee and L. Dean contributed to the build stage of the process.

### 3.1 Introduction

If a continuous SFE process is the solution for the problem of drill cuttings treatment, then first the process must exist. Second, the process must function with the primary goal of removing oil from the cuttings. As mentioned previously, a bench scale continuous SFE process was developed to treat contaminated solids (Fortin, 2003; Forsyth, 2006), however a larger, pilot scale process, for the treatment of drill cuttings does not exist. Therefore, this chapter details the development of such a process in the Innovative Process Lab in the Department of Civil and Environmental Engineering at the University of Alberta. The process that is described in this chapter is unique - in both its size and function. To the authors' knowledge, it is the first pilot scale SFE process that can continuously provide countercurrent flow of both a supercritical solvent and slurried solids through the extraction vessel.

The aim of this chapter is to present this unique process and prove its functionality through experiments that demonstrate:

1. The process can operate at supercritical conditions of pressure and temperature (above 7.4 MPa and 31°C for CO<sub>2</sub>).
2. The process can operate in a continuous, countercurrent flow regime with both supercritical carbon dioxide (SC-CO<sub>2</sub>) and slurry (containing water and cuttings or cuttings-like solids at varying solids: water ratios).
3. The process can be operated for a period of time, not dictated by deviations from normal operations that require emergency shutdowns.

Additionally, in meeting the three objectives stated above, it will be shown that the process can operate safely and extract oil from the slurry.

The preliminary design for the process is documented in the thesis of Rosenthal (2012), and is based upon the bench scale process developed at the University of Guelph (Fortin, 2003; Forsyth 2006). This chapter lays out the steps that were undertaken to complete the process design, procure its parts, build it, commission it and conduct safe operation. The development of the continuous pilot scale SFE process is categorized into three main phases: design, build and commission/operation. Although the activities in each phase are distinct, implementation of the phases overlapped. The design of the SFE process was initiated in early 2009, and is available in

Rosenthal (2012). Improvements to the design of the process were continuous and triggered by troubleshooting required in the building and commissioning phases. But the majority of the process was built between late 2009 and mid-2014. The build phase specifically consisted of sourcing, purchasing and assembling the different components and programming the control system. Commissioning began in December 2012 as specific sub-systems were completed, and is also currently ongoing. The commission/operation phase includes both proving basic functionality and studying the impacts of process parameters on mass transfer and process control.

In this chapter, Section 3.2 provides an overview of the SFE process that was developed. Section 3.3 describes the changes made to the preliminary process design proposed by Rosenthal (2012). In Section 3.4, the completed commissioning experiments are summarized. Important modifications made to the process as a result of certain experimental runs are also provided. The summary outlining the claims of the chapter is presented in Section 3.5.

## **3.2 SFE process overview**

A schematic diagram of the pilot scale continuous SFE process under investigation in this thesis is presented in Figure 3.1.

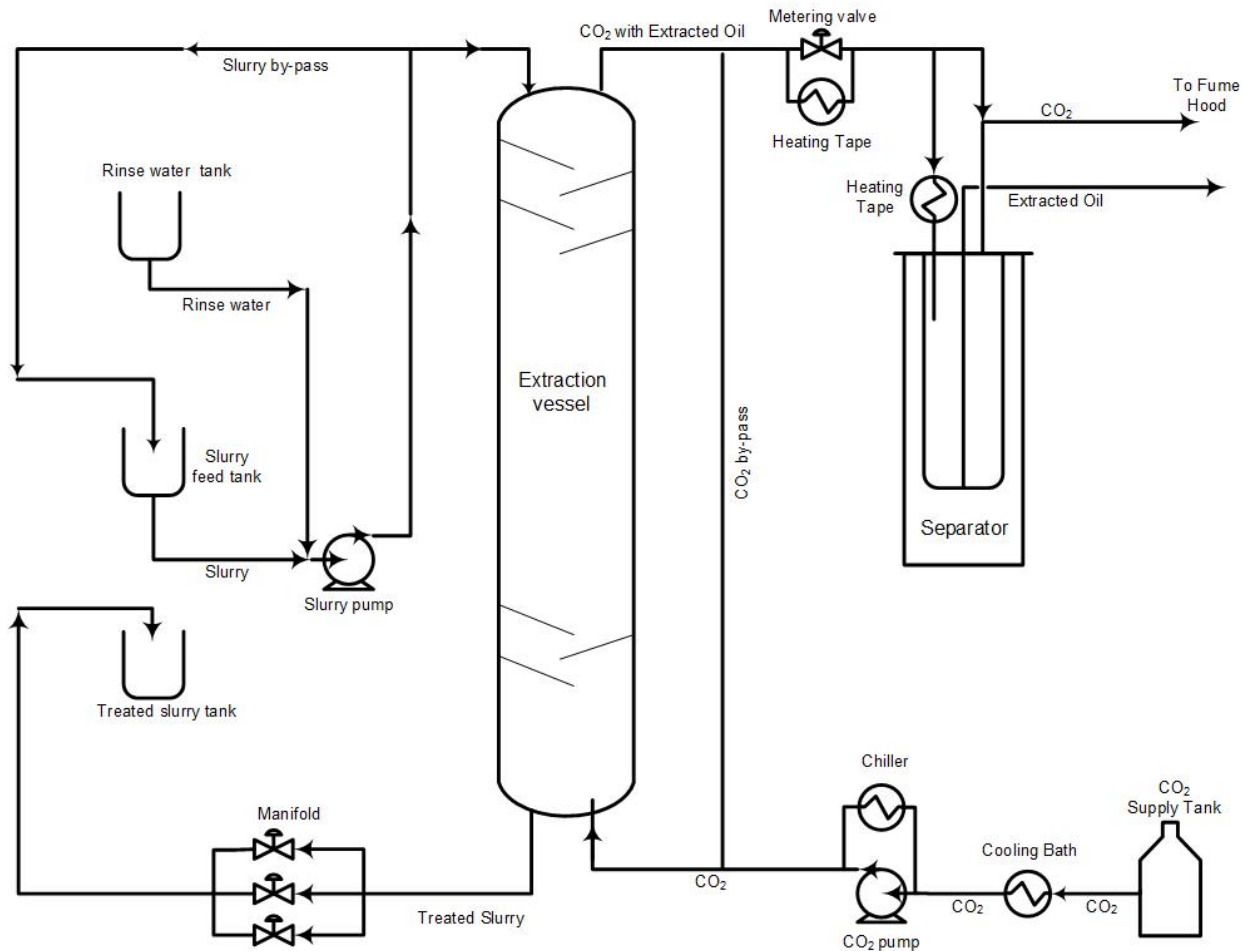


**Figure 3.1. Schematic of the pilot scale SFE process**

The main unit operation in this process is an extraction vessel with a height of approximately 2.5 m. The CO<sub>2</sub> is pumped via a positive displacement pump from the CO<sub>2</sub> supply tank into the bottom of the extraction vessel. The pump head is cooled with a chiller. During the CO<sub>2</sub> pressurization stage, SC-CO<sub>2</sub> is obtained. The slurry (drill cuttings mixed with water) is pumped via a positive displacement pump from the slurry feed tank to the top of the extraction vessel.

The slurry and CO<sub>2</sub> flows are brought into contact inside the extraction vessel countercurrently. The interior of the extraction vessel holds a structure consisting of 62 inclined baffles. The baffles provide mixing between the two phases. Upon entrance to the extraction vessel, the slurry feed cascades down the baffles, while the CO<sub>2</sub> moves from the bottom to the top. As a result of this continuous contact, the CO<sub>2</sub> extracts the hydrocarbons present in the slurry.

The treated slurry exits from the bottom of the vessel, where it goes through a manifold to depressurize before entering the treated slurry tank. The manifold consists of three branches, only one of which is used based on the operating pressure of the process. CO<sub>2</sub> along with the extracted hydrocarbons exits from the top of the extraction vessel and flows through a heated metering valve, where it is depressurized through a metering valve prior to entering the separator. The separator has a height of approximately 1.5 m and allows for the CO<sub>2</sub> and extracted hydrocarbons to be separated. The depressurized CO<sub>2</sub> exits the separator and is vented into the fume hood. The hydrocarbons are collected inside the separator and are removed from the separator after the process has been depressurized.

The built pilot scale SFE process is presented in Figure 3.2.



**Figure 3.2.** The pilot scale SFE process for treatment of drill cuttings (1) CO<sub>2</sub> tank, (2a) rinse water tank, (2b) slurry feed tank, (2c) treated slurry tank, (3) separator and (4) extraction vessel

As seen in Figure 3.2, the scale of the process is much larger than a bench scale extraction process.

Figure 3.3 and Figure 3.4 present a closer view of the extraction vessel and separator.



**Figure 3.3. The extraction vessel of the SFE process (Length: 2.45 m, Inner diameter: 0.0833 m)**



**Figure 3.4. The separator of the SFE process (Length: 1.52 m, Inner diameter: 0.0833 m)**

This process is the first of its kind to the best of the author's knowledge. The unique attributes of this process are two-fold:

- (1) A fully continuous SFE process designed to extract oil from slurried solids.
- (2) A pilot scale process that is beyond the size of a bench scale and a step closer to a commercial scale process.

Successful operation of this continuous pilot scale SFE process paves the way to industrializing it for this drill cuttings application and other applications in the oil and gas industry.

### **3.3 Design components**

In building and commissioning the process, major modifications were made to the preliminary design of the process described in Rosenthal (2012). The following sections will outline these changes and will demonstrate how the process was built and commissioned.

The important design components of the SFE process are broken down into six main

sections: (i) flow through the process, (ii) lab layout, (iii) P&ID (piping and instrumentation diagram), (iv) control philosophy, (v) operation manual and (vi) HAZOP (hazard and operability study). In each section, modifications to what was presented in Rosenthal (2012), are explained in detail. These details will include the stage in which the modification was made (build vs. commission) and the reason why the modification was made.

### **3.3.1 Flow through the process**

In this section, the flow of CO<sub>2</sub>, slurry and rinse water through the SFE process as built are described for a typical experiment.

#### **3.3.1.1 CO<sub>2</sub>**

Liquid CO<sub>2</sub> is supplied to the process from a CO<sub>2</sub> feed tank. It is supplied through a 3/4" insulated stainless steel pipe (consisting of flexible and rigid sections) at a pressure of approximately 400 – 450 psia. It should be noted that the CO<sub>2</sub> tank has a pressure building circuit which prevents large pressure drops in the CO<sub>2</sub> supply. Before entering the pump, the CO<sub>2</sub> supply line goes through a cauldron filled with a mixture of water and anti-freeze that is cooled to -15 °C with dry ice. The cauldron will maintain the cold temperature of the liquid CO<sub>2</sub> and prevent flashing in the lines. After going through the pump head (which is also cooled to -25 °C with the aid of a chiller), the pressurized CO<sub>2</sub> is pumped into the extraction vessel through a 1/4" stainless steel line. At the entry of the vessel, the line size changes to 1/8" (due to the size of the fittings on the extraction vessel) and the CO<sub>2</sub> is introduced into the extraction vessel just below the lowest baffle. Introducing the CO<sub>2</sub> at this point causes better distribution of CO<sub>2</sub> flow up through the vessel and reduces channelling. SC-CO<sub>2</sub> conditions of temperature and pressure are reached in the extraction vessel. As CO<sub>2</sub> flows upward in the vessel, it contacts the slurry, which is cascading down on the baffles, and the SC-CO<sub>2</sub> extracts the hydrocarbon from the slurry. The SC-CO<sub>2</sub> along with the dissolved hydrocarbons exit from the top of the extraction vessel through a 1/4" stainless steel line and enter a heated metering valve where it is depressurized. This multiphase stream enters the separator through a 1/4" stainless steel line where the CO<sub>2</sub> and hydrocarbons are separated. This line extends towards the wall of the separator (inside the separator) to promote deposition of the hydrocarbons onto the wall to minimize entrainment. CO<sub>2</sub> which is in a gaseous state at this stage exits through a 1/4" stainless steel line and goes to the fume hood.

### **3.3.1.2 Slurry**

Slurry feed is stored in the slurry feed tank. From the feed tank, slurry flows through a 2" stainless steel pipe, goes through a flow meter before entering the slurry pump. A heater is installed in the slurry feed tank and is turned on prior to a run to heat the slurry to 40 – 45 °C. Therefore, the slurry entering the pump will be at atmospheric pressure and approximately 40 °C. The slurry is then pumped by the slurry pump and through a ¾" stainless steel line to the top of the pressurized extraction vessel. The slurry cascades down the baffles and is exposed to the SC-CO<sub>2</sub> flowing upwards in the extraction vessel. As a result, mass transfer occurs between the two phases and hydrocarbon is transferred from the slurry to the SC-CO<sub>2</sub>. The pressure within the vessel, forces the slurry to exit through the ¼" slurry outlet line at the bottom of the extraction vessel. Soon after exiting the extraction vessel, the slurry flows through the manifold. The manifold to be used for a given experiment is chosen before the experiment, based on the operating pressure in the extraction vessel. The manifold is designed to provide resistance in the slurry outlet line and cause pressure drop after slurry exits the extraction vessel. Slurry then flows through a ¾" stainless steel line and is directed towards the slurry receiving tank.

### **3.3.1.3 Rinse water**

Rinse water is used to create a water plug at the bottom of the extraction vessel prior to process pressurization. It is also used to clean the slurry lines and extraction vessel at the end of an experiment. The rinse water follows the same path as the slurry but it is supplied from the rinse water tank which is for storing rinse water only.

## **3.3.2 Lab layout**

During the design process, major equipment (the extraction vessel and its frame, the separator and its frame, the CO<sub>2</sub> pump, the slurry pump and CO<sub>2</sub> tank) were purchased and placed in the lab based on the preliminary layout. However, due to the large components and their mass, Facilities and Operations at the University of Alberta requested an engineering analysis of the standard load that these components would place on the lab floor. The lab layout was independently evaluated by an engineering firm (DIALOG) in terms of structural load. The final approved lab layout is provided in Figure 3.5 and Figure 3.6. Figure 3.5 depicts dimension and Figure 3.6 depicts position of the main SFE process components.

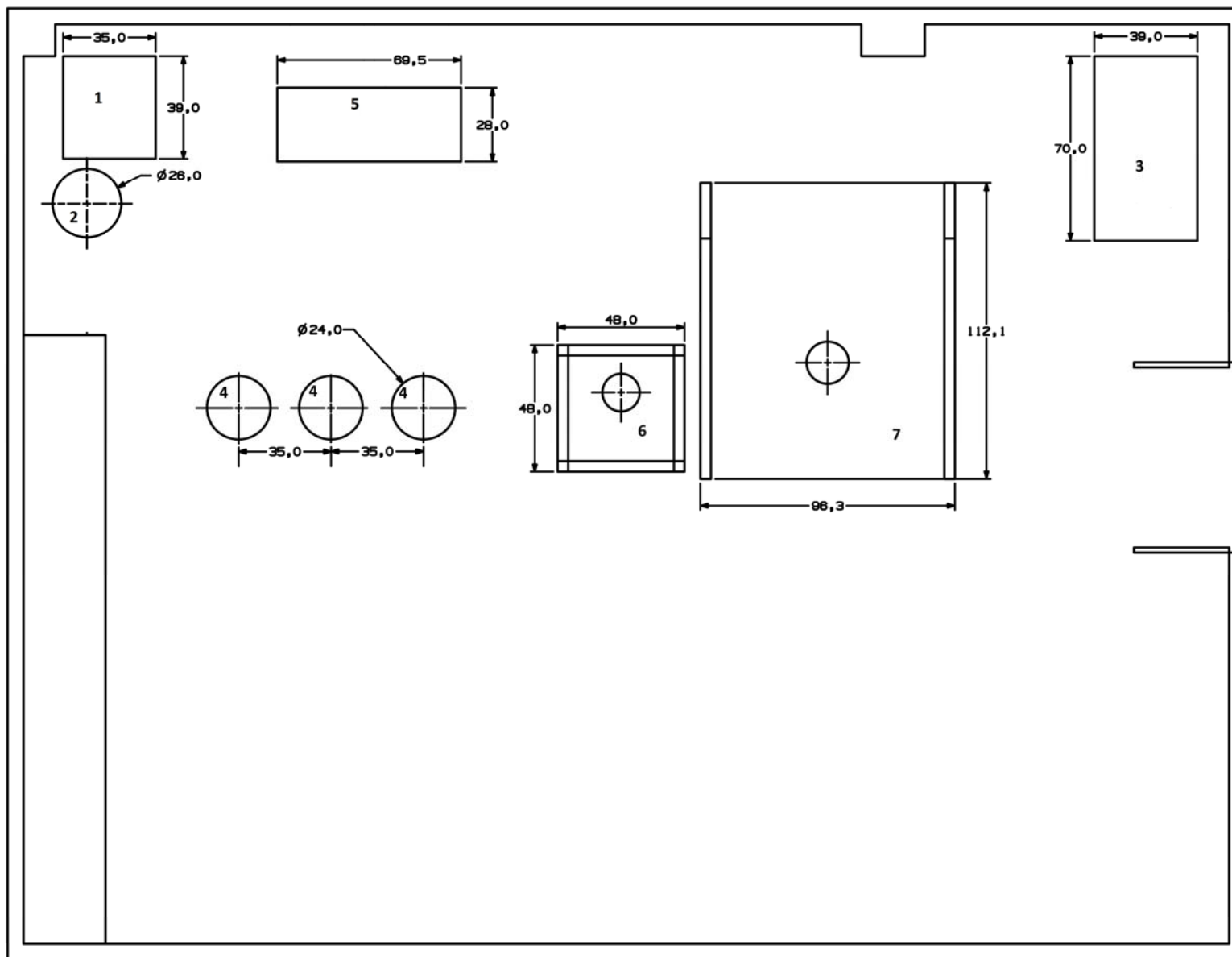


Figure 3.5. Lab layout containing dimension of the main SFE process components: (1) CO<sub>2</sub> pump, (2) CO<sub>2</sub> feed tank, (3) fume hood, (4) slurry and rinse water tanks, (5) slurry pump, (6) separator frame and (7) extraction vessel frame (all dimensions in inches).

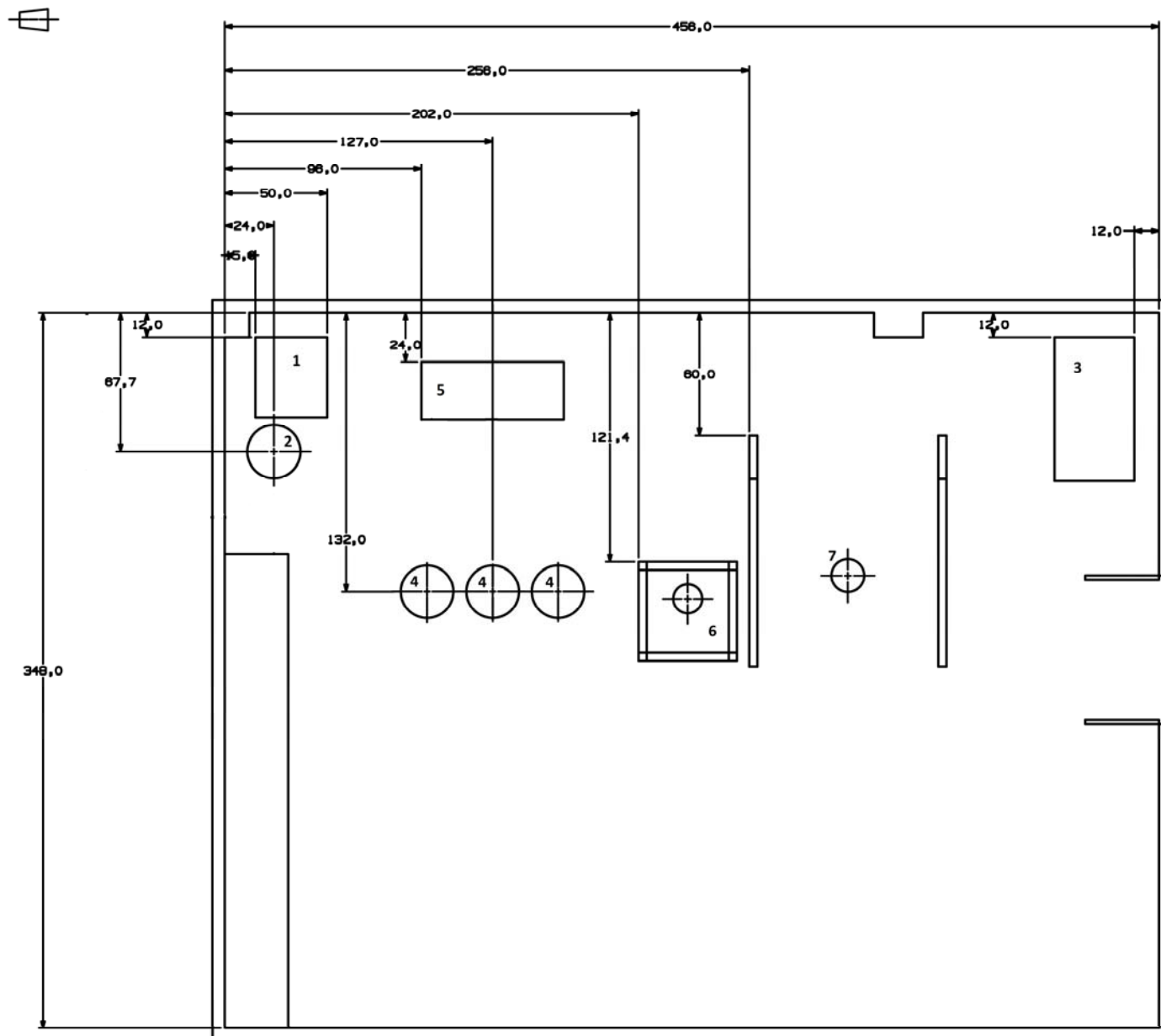


Figure 3.6. Lab layout containing position of the main SFE process components: (1) CO<sub>2</sub> pump, (2) CO<sub>2</sub> feed tank, (3) fume hood, (4) slurry and rinse water tanks, (5) slurry pump, (6) separator frame and (7) extraction vessel frame (all dimensions in inches).

### 3.3.3 P&ID

In this section, description of the major equipment, lines, valves and instrumentation in the SFE process are presented. Modifications to the preliminary design are also outlined.

#### 3.3.3.1 Major equipment

The major equipment currently in use in the pilot scale continuous SFE process includes the CO<sub>2</sub> tank, rinse water tank, slurry tanks, CO<sub>2</sub> pump, slurry pump, extraction vessel and separator. The specifications of the major equipment are listed in Table 3.1.

**Table 3.1. Specification of major equipment used in the SFE process**

Tanks							
ID	Description	Volume (m <sup>3</sup> )	Dimensions (m)	Material of Construction	Pressure Rating (MPa)	Temperature Rating (°C)	Supplier
N/A	CO <sub>2</sub> Supply Tank	0.42 (liquid)	0.762 (ID) 1.557 (h)	SS (grade not specified)	3.1	N/A	Praxair, Alberta, Canada
FT-3603, FT-3601 & FT-3602	Rinse Water and Slurry Tanks	0.227	0.61 (ID) 0.99 (h)	Seamless Polyethylene	N/A	N/A	Blaze Plastics Inc., Alberta, Canada
Pumps							
ID	Description	Type	Capacity (L/s)	Power Supply	Suction (S) + Discharge (D) Pressure (MPa)	Pumping Temperature (normal, max) (°C)	Supplier
P-2201	CO <sub>2</sub> Pump	Positive displacement	0.108	208 V, 3Ph, 8.4 A	2.758 (S) 34.474 (D)	20 & 71	Pelco, Ontario, Canada
P-3201	Slurry Pump	Positive displacement	0.282	208 V, 3Ph, 38 A	0.1 (S) 34.474 (D)	N/A	North Fringe, Alberta, Canada
Vessels							
ID	Description	Volume (m <sup>3</sup> )	Dimensions (m)	Material of Construction	Pressure Rating (MPa)	Temperature Rating (°C)	Supplier
EC-1101	Extraction Vessel with 62 baffles	0.0126 (empty bed)	0.0833 (ID) 2.45 (h)	316 SS	40	200	Price-Schonstrom, Ontario, Canada
SC-4101	Separator	0.0076 (empty bed)	0.0833 (ID) 1.52 (h)	316 SS	30	200	Price-Schonstrom, Ontario, Canada

ID=inner diameter; h=height  
N/A = not available

The CO<sub>2</sub> tank originally installed in the process was the Carbomax750. During the commissioning stage, however, it was not possible to consistently pressurize lines downstream of the CO<sub>2</sub> pump. Working with both the CO<sub>2</sub> pump supplier (Pelco) and CO<sub>2</sub> tank supplier (Praxair), a number of steps were taken to try to remedy this problem. These are as follows:

1. Initially, it was thought that the pump valves might be damaged so the pump was opened and its low pressure seals were replaced. The issue was not resolved.
2. It was believed that perhaps gaseous CO<sub>2</sub> and not liquid CO<sub>2</sub> was reaching the CO<sub>2</sub> pump, due to “flashing” in the pump head. A chiller was purchased to cool the pump head and ensure that any liquid CO<sub>2</sub> reaching the pump head remained as liquid CO<sub>2</sub> in the pump head. Improvements were observed but consistency was not obtained.
3. Because the chiller was set to very low temperatures (-45 °C), it was thought that perhaps the high pressure seals in the pump were damaged (because they were not rated to very low temperatures). So the pump was opened again to look for possible damages. No sign of damage was observed.
4. The maximum allowable pressure on the CO<sub>2</sub> tank was 300 psi but during operations it was even lower and normally around 285 psi. Based on the CO<sub>2</sub> phase diagram, there was a very small operating window to have liquid CO<sub>2</sub> enter the pump. The safest scenario was to be at 300 psi and -30 °C which was hard to achieve. Therefore, it was concluded that in addition to the pump head, the CO<sub>2</sub> line itself had to be cooled to low temperatures and that was when a cauldron was introduced into the process. The cauldron is a large bucket containing water and anti-freeze solution. Before starting a run, this solution has to be cooled to around -15 °C by adding dry ice to it. After this modification, a few consistent experimental runs were achieved.
5. After a long SFE run, the CO<sub>2</sub> tank pressure did not recover to 285 psi and the tank did not function anymore. Therefore, it was confirmed that this CO<sub>2</sub> tank would not work for the SFE process and that a tank is required with a higher pressure rating and also the capability of maintaining pressure inside it when being used. Therefore, the Carbomax750 CO<sub>2</sub> tank was replaced by a Permacyl

450 VHP CO<sub>2</sub> tank between August to October 2014. As a result, the pressure in the Permacyl450 CO<sub>2</sub> tank was maintained at approximately 450 psi in experimental runs. The Permacyl 450 VHP CO<sub>2</sub> tank resolved issues created when using the previous CO<sub>2</sub> tank i.e. the Carbomax750 tank.

### **3.3.3.2 Lines, valves and instrumentation**

In the following subsections, applied modifications with regards to lines, valves and instrumentation are summarized. The reason behind each modification is outlined.

#### *Lines*

Table 3.2 summarizes the modifications applied to the lines of the continuous SFE process. As a result of these modifications, the current state of the process in terms of lines is depicted in Figure 3.7. Line specifications are summarized in Appendix A1.

**Table 3.2. Summary of the modifications to the lines in the SFE process**

<b>Description/ID</b>	<b>Preliminary design</b>	<b>Final design</b>	<b>Reason for modification</b>	<b>Modification stage</b>
Inlet line to slurry pump (LN-3008)	2½" OD	2" OD	A 2" line size is more common for sourcing valves and instrumentation.	Build
Inlet line to CO <sub>2</sub> pump (LN-2002)	1" OD	¾" OD	A ¾" line size is more common for sourcing valves and instrumentation.	Build
CO <sub>2</sub> lines entering and exiting the extraction vessel and separator	1/8" OD	¼" OD	The fittings on the extraction vessel lid and separator lid are ¼" , so the line was upsized to match and to minimize pressure drops into and out of the extraction vessel and separator.	Build
Line exiting the separator (LN-4006)	½" OD	¼" OD	The fittings on the separator lid are ¼", so the line was downsized to match. ¼" lines are also less expensive and readily stocked with suppliers.	Build
Flexible line from CO <sub>2</sub> tank (LN-2001)	none	new	The line allowed for installation flexibility which was needed due to the layout of the CO <sub>2</sub> tank and pump.	Build
Brass cooling coil (LN-2003)	none	new	The coil was added to cool the CO <sub>2</sub> entering the pump to below the liquid-vapor equilibrium temperature at tank pressure (to ensure a liquid feed to the pump).	Commission
Separator bypass line (LN-4009)	none	new	The bypass was added to give operational flexibility during depressurization or in a scenario where it might be necessary to bypass the separator (e.g., freezing in the separator).	Build
Flexible slurry line (LN-3011)	none	new	The line provided installation flexibility and also acts as a pulsation dampener.	Build
¼" slurry line entering the extraction vessel (LN-3012)	none	new	Because the fittings on the extraction vessel lid are ¼", the slurry line had to be down sized to ¼" after the flexible hose to enter the extraction vessel.	Build
Extended CO <sub>2</sub> line into extraction vessel (LN-2006)	none	new	The line was extended to ensure the CO <sub>2</sub> entering the extraction vessel hits a baffle.	Commission

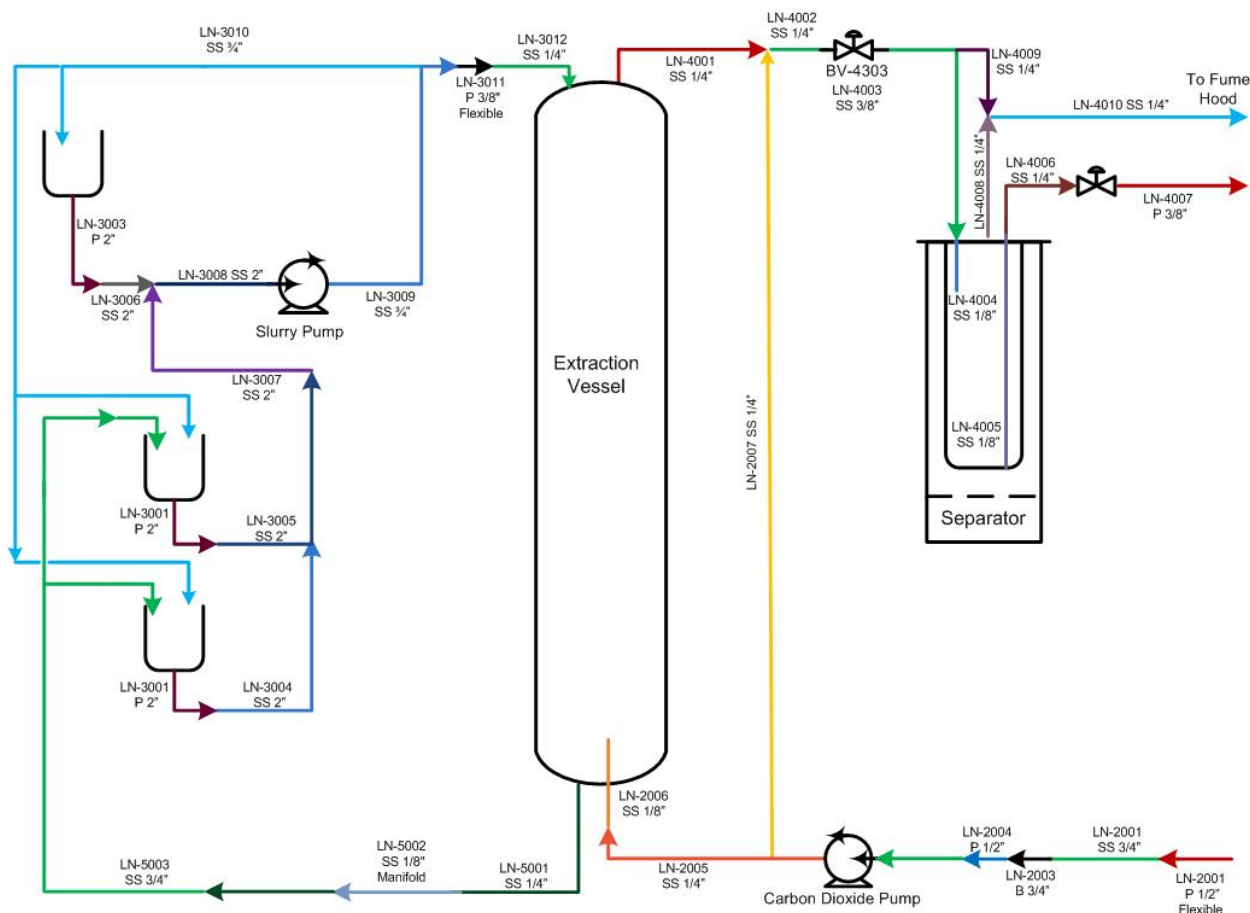


**Figure 3.7. CO<sub>2</sub> and slurry line configuration in current state of the SFE process (line colours indicate a change in tag number, which corresponds to a change in line size and/or material).**

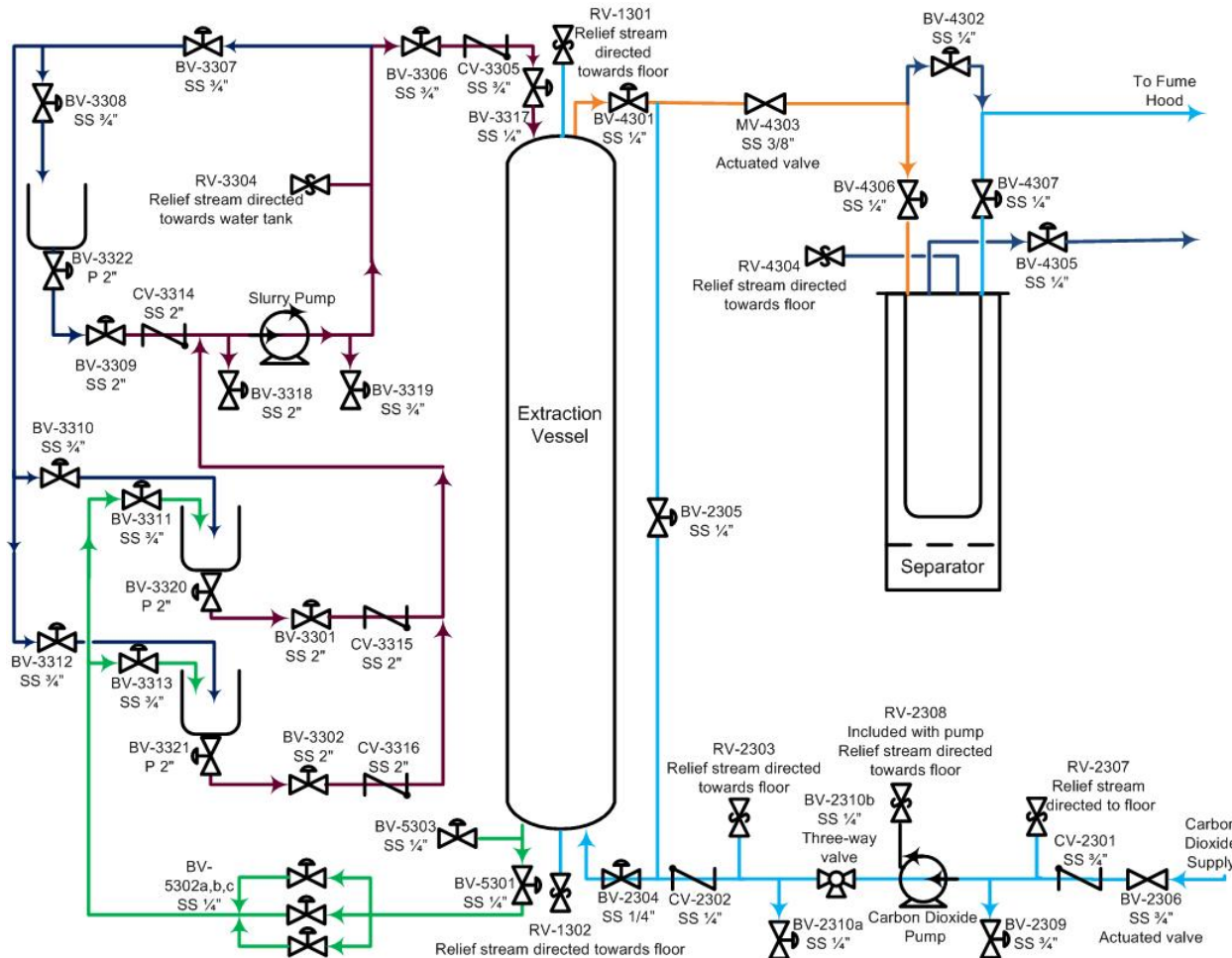
### Valves

Table 3.3 summarizes the modifications applied to the valves of the continuous SFE process. As a result of these modifications, the current state of the process in terms of valves is depicted in Figure 3.8. It should be noted that based on the modifications made to line sizes, related valves on those lines were accordingly upsized or downsized. These changes have not been reflected in Table 3.3. Valves specifications are summarized in Appendix A2.

Two general modifications were made in terms of valve IDs i.e. ID of relief valves are changed from BV-XXXX to RV-XXXX. Similarly, metering valve ID is changed from BV-XXXX to MV-XXXX.

**Table 3.3. Summary of the modifications in terms of valves used in the SFE process**

<b>Description/ID</b>	<b>Preliminary design</b>	<b>Final design</b>	<b>Reason for modification</b>	<b>Modification stage</b>
Check/Relief valve (CV-2301)	One valve that served both as a check valve and relief valve	Addition of RV-2307 to LN-2001	It was decided to separate the two functions of this valve. Hence, CV-2301 acts as a check valve only and RV-2307 acts as a relief valve on that line.	Build
Relief valve (BV-3303)	Existed in P&ID	deleted	The valve was needed for the slurry grinding loop which was not installed in the current build.	Build
2" plastic isolation valves (BV-3320, BV-3321, BV-3322)	none	new	The valves were added to isolate the slurry in the tanks from the 2" SS slurry supply lines.	Build
¼" isolation valves (BV-4302, BV-4306, BV-4307)	none	new	The valves were added on as a result of adding the separator bypass line.	Build
Manifold (BV-5302a, BV-5302b, BV-5302c)	none	new	The manifold was installed to restrict the slurry flow exiting the extraction vessel.	Build
Drain valve on CO <sub>2</sub> pump outlet line (BV-2310)	BV-2310	BV-2310a and BV-2310b	BV-2310b is a three-way valve which was installed as an alternative to BV-2310a which would allow the pump to be turned off and drained without depressurizing the extraction vessel.	Commission
Isolation valve (BV-3317)	none	new	The isolation valve on the slurry line before going in to extraction vessel (BV-3306) was located too far from the extraction vessel. It was decided that it would be useful to add another isolation valve closer to the vessel.	Commission



**Figure 3.8. Valve configuration in current state of the SFE process**

### *Instrumentation*

Table 3.4 summarizes the modifications applied to the instrumentation of the continuous SFE process. As a result of these modifications, the current state of the process in terms of instrumentation is depicted in Figure 3.9. Instrumentation specifications are summarized in Appendix A3.

**Table 3.4. Summary of modifications to the instrumentation used in the SFE process**

<b>Description/ID</b>	<b>Preliminary design</b>	<b>Final design</b>	<b>Reason for modification</b>	<b>Modification stage</b>
Pressure indicator (PI-1404)	In field display only	Data collection and control	The pressure sensor was added to allow for logging the data and controlling the CO <sub>2</sub> pump.	Build
Temperature sensor (TI-1410)	none	new	Adding a temperature sensor at the bottom of the extraction vessel allowed for better understanding of the temperature profile in the extraction vessel.	Commission
Heating tape (HX-1411)	none	new	In order to have SC CO <sub>2</sub> , its temperature should be above 32 °C. Therefore, it was decided to heat the extraction vessel bottom, where CO <sub>2</sub> is expanding inside the vessel.	Commission
Temperature sensor (TI-2404)	Initially clamp-on and eventually an adhesive type	Inline temperature sensor	It is important to know the exact temperature of CO <sub>2</sub> entering the pump to ensure that the CO <sub>2</sub> is cooled adequately to provide a liquid feed to the pump.	Commission
Chiller (HX-2409)	none	new	In order to avoid flashing of the CO <sub>2</sub> in the pump, the pump head should be kept below the liquid-vapor equilibrium temperature at CO <sub>2</sub> tank pressure.	Commission
Cauldron-dry ice (HX-2410)	none	new	The cauldron cools the CO <sub>2</sub> supply to ensure a liquid feed to the pump.	Commission
Pressure indicator (PI-4406)	none	new	The indicator was installed to show pressure between extraction vessel and separator.	Commission
Heating tape (HX-4407)	none	new	The heating tape was installed to prevent CO <sub>2</sub> freezing in the automated metering valve due to CO <sub>2</sub> expansion.	Commission
Heating tape (HX-4408)	none	new	The heating tape was installed to prevent freezing of the ¼" line going into the separator due to CO <sub>2</sub> expansion.	Commission
Pressure indicator (PI-5404)	none	new	The indicator was installed to monitor the pressure of the slurry outlet line from the manifold. The indicator helps with manually controlling the liquid level inside the extraction vessel.	Commission

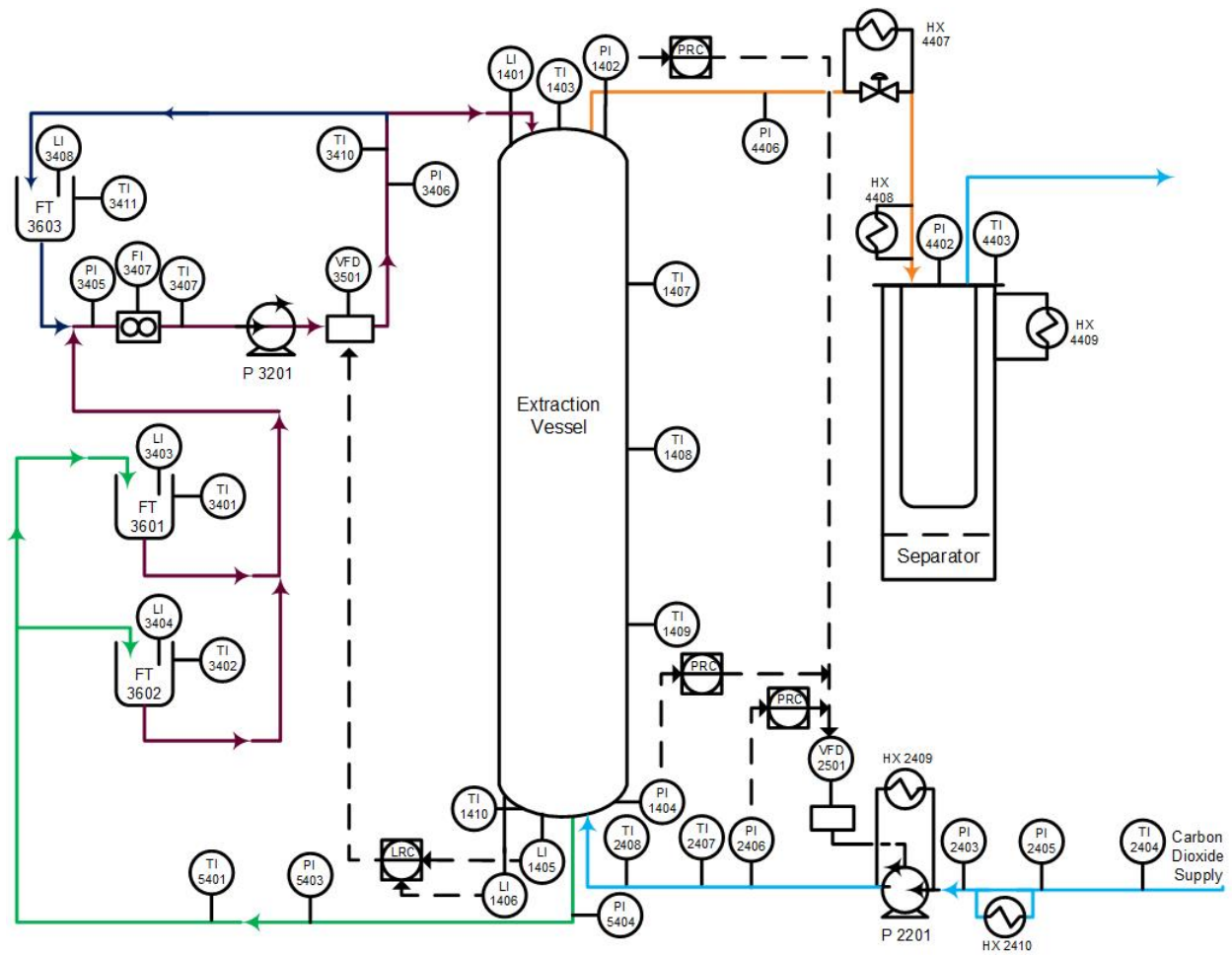


**Figure 3.9. Instrumentation configuration in current state of the SFE process**

As a result of the modifications applied to lines, valves and instrumentation, the final P&ID of the continuous pilot scale SFE process is as shown in Figure 3.10.

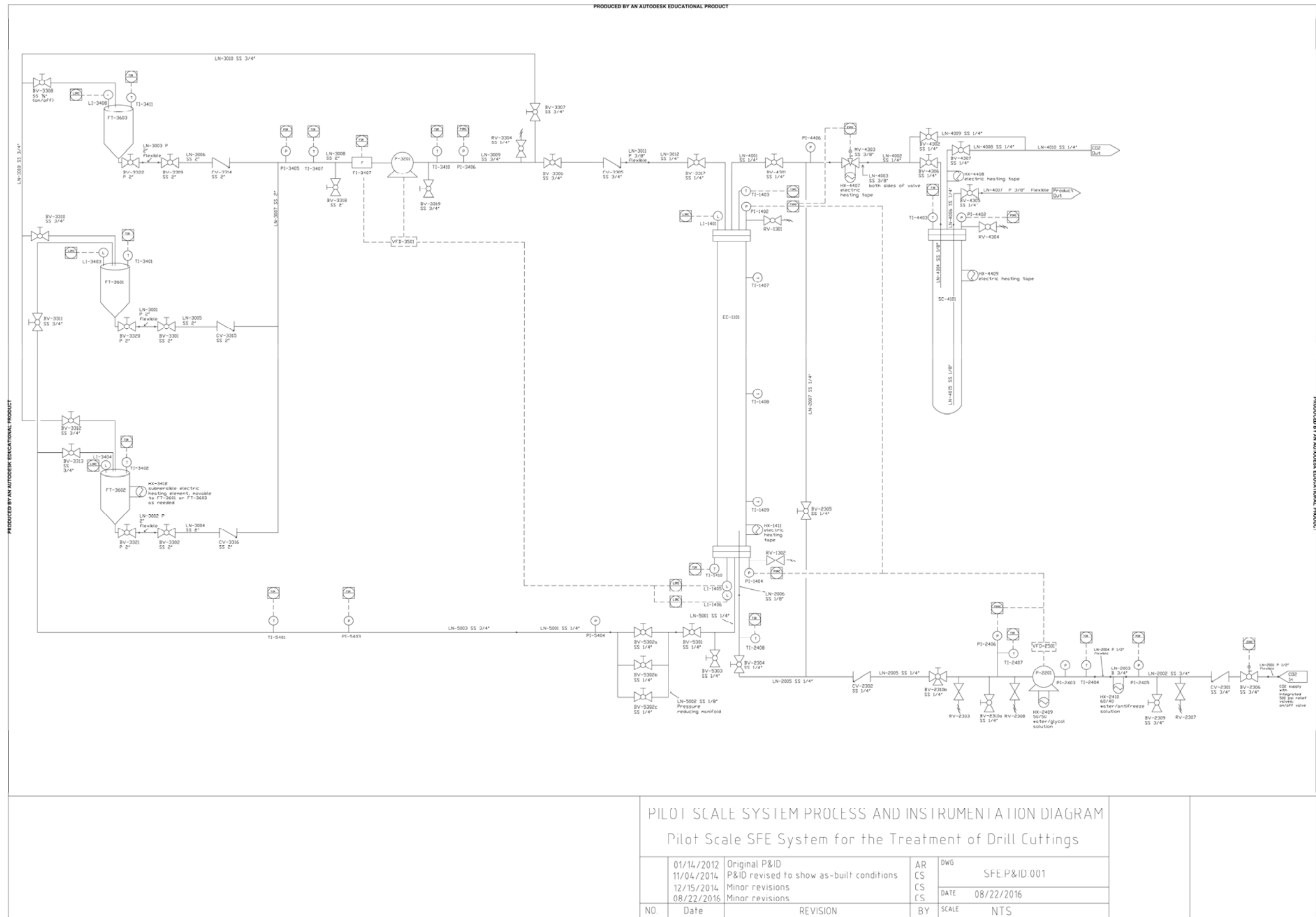


Figure 3.10. P&ID of the continuous pilot scale SFE process

### 3.3.4 Control philosophy

A control philosophy for the pilot scale continuous SFE process was proposed by Rosenthal (2012). Based on this control philosophy, the control system was built. For this purpose, National Instrument's CompactRIO, a programmable automation controller (PAC), has been chosen to provide communication between the system elements (i.e. instrumentation, automated valves, VFDs and computer). This real-time controller provides high performance control as well as reliability and serves as a bridge between the data coming from instruments/valves/VFDs and the computer. The programming software applied is National Instrument's LabVIEW™. LabVIEW™ also provides a graphical user interface (GUI) for controlling the SFE process from the computer. It should be noted that LabVIEW™ files have the extension .vi; therefore, files created in LabVIEW™ are also referred to as VI's.

The control program generally consists of two main VI's. One is the RT (Real Time) VI which is considered as the core program for control and it is loaded into the CompactRIO. The RT VI should be considered as a piece of hardware because it is the source of actions in the CompactRIO. The HMI (Human Machine Interface) VI on the other hand basically provides the interface for running the process but operational-wise is controlled by the RT. In other words, if for any reason the HMI VI is closed or if the computer crashes, after re-opening the HMI file, it will continue from the state it was closed and it will not restart from its initial mode.

Two monitors are connected to the computer in the SFE lab. When the HMI file is opened, monitor-1 displays the P&ID of the SFE process and the control panel, while monitor-2 displays SFE process modes, the alarms and interlocks. A view of the GUI is presented in Figure 3.11.

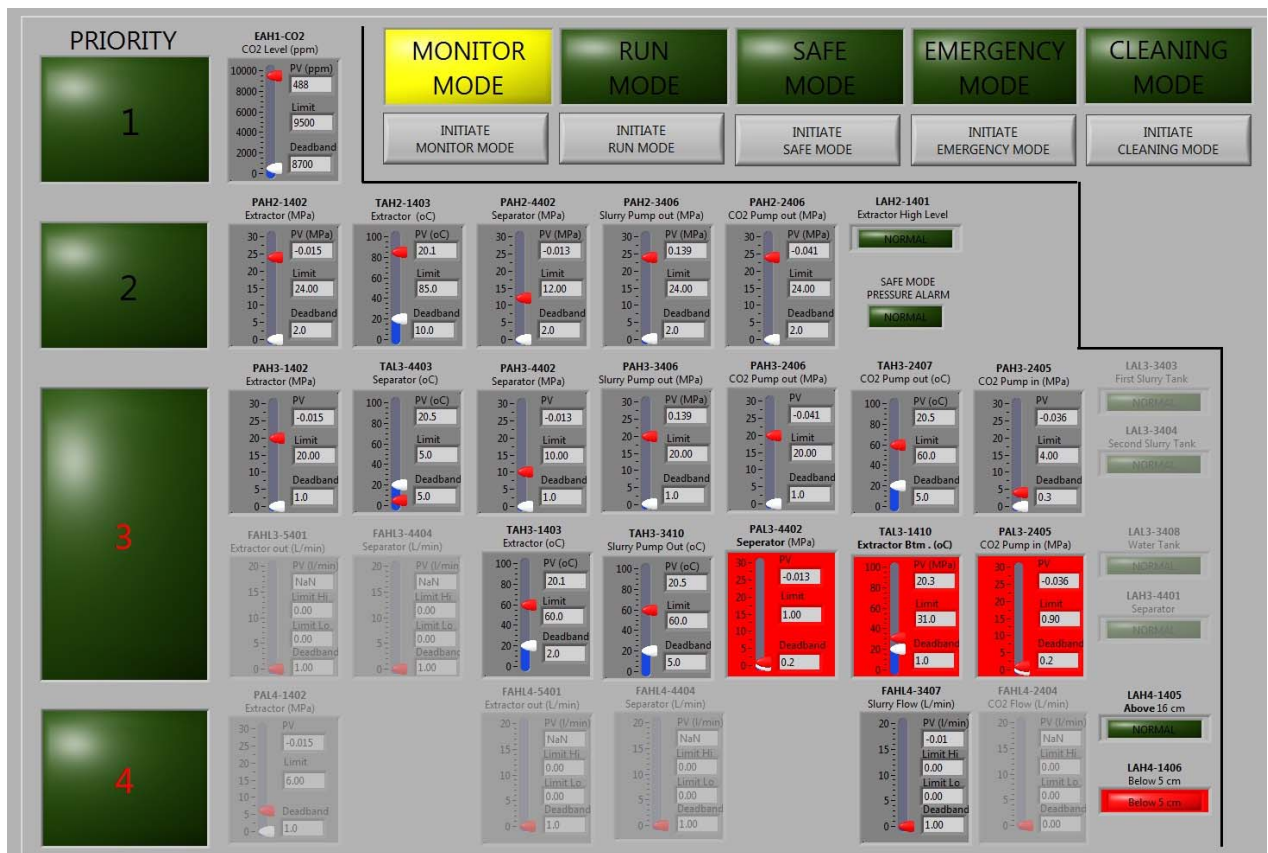
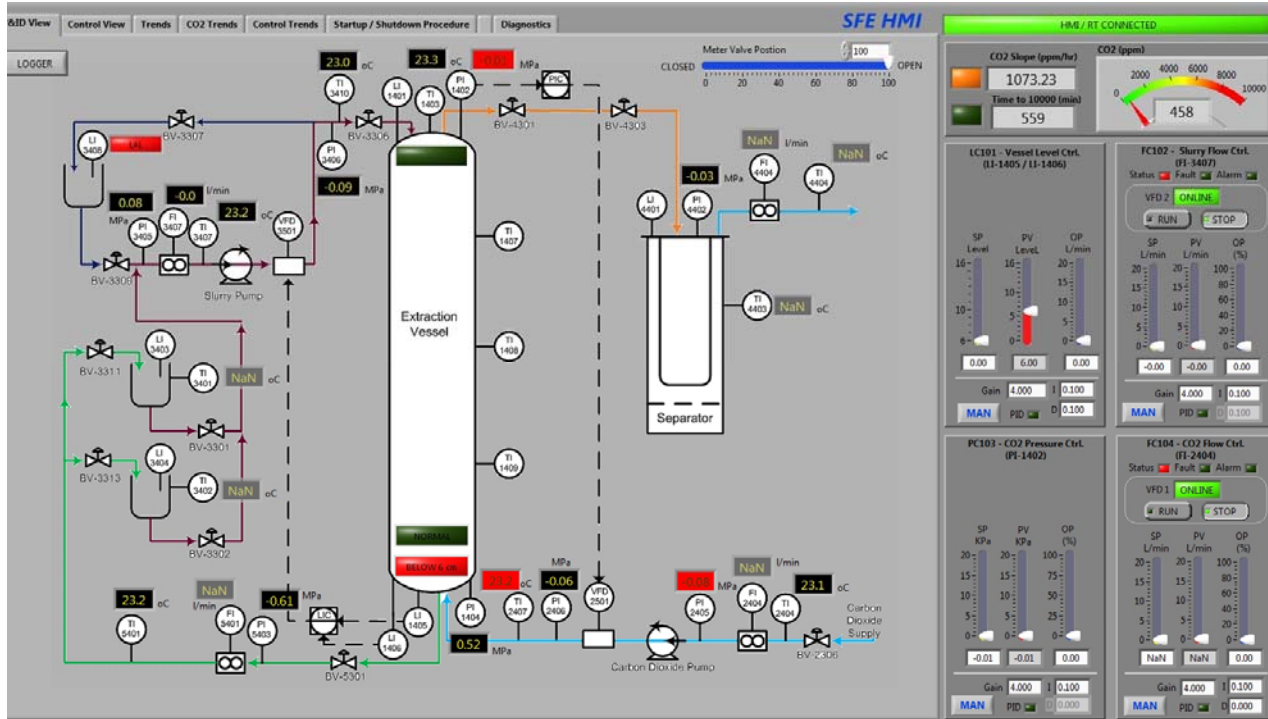


Figure 3.11. Display of the SFE process GUI (top: monitor-1, bottom: monitor-2)

A manual has been prepared to explain how the control system/GUI of the SFE process works. It is the responsibility of future operators to read and fully understand this document before conducting any runs on the process.

The following sections describe process modes, alarms and process control.

#### **3.3.4.1 Process modes**

The SFE process can operate in five different modes. These modes are as follows:

1. *Monitor Mode*: This mode is mainly for testing and troubleshooting. Process control can be done manually or automatically when in this mode. The process automatically enters *Monitor Mode* when the HMI VI is started.
2. *Run Mode*: The main application of this mode is operating the process in an automated approach. In other words, when process enters this mode, process control is done automatically. This mode is to be used after testing and troubleshooting of the process is completed and all controllers have been designed and tested on the process. As built, the system has not been operated in *Run Mode*.
3. *Emergency Mode*: The process can enter this mode either automatically through the safety interlocks defined for the process or by manually clicking the *Emergency Mode* button on the interface. When the process enters this mode, the pumps are automatically stopped, the automated metering valve (MV-4303) is fully opened and the CO<sub>2</sub> feed tank actuated valve (BV-2306) is fully closed.
4. *Safe Mode*: This mode acts as an intermediate mode between *Emergency Mode* and *Monitor Mode*. A safety checklist should be completed before entering *Safe Mode* from *Emergency Mode*. Similarly, an emergency shutdown checklist should be completed before entering *Monitor Mode* from *Safe Mode*. Some operational restrictions apply when process is in *Safe Mode*. These restrictions are as follows:
  - System pressure limited to 3 MPa.
  - CO<sub>2</sub> pump flowrate limited to 1 L/min (equivalent to 15% CO<sub>2</sub> pump speed).

- Slurry pump flowrate limited to 3 L/min (equivalent to 18% slurry pump speed).
5. *Cleaning Mode*: This mode is designed specifically for cleaning and rinsing the extraction vessel. Because activation of the level sensor located at the top of the vessel (LI-1401) is an indication of a full vessel, this level sensor (LI-1401) is applied for stopping the slurry pump when filling the extraction vessel for cleaning purposes. However, activation of this sensor initiates emergency mode. To prevent confusion, *Cleaning Mode* was programmed to use when rinsing the extraction vessel and prevent any unnecessary false alarms.

Modifications made with regards to process modes are as follows:

- *Cleaning Mode* was added to process modes.
- Only *Emergency Mode* was programmed into the process modes. The preliminary design identified both an *Emergency Shutdown* and an *Emergency Mode*. It could not be understood whether the *Emergency Mode* was a result of an *Emergency Shutdown* or if they are two independent modes. However, it seemed that both modes perform the same actions. Thus, only an *Emergency Mode* has been programmed which can be activated by alarms or interlocks or by pressing the corresponding button.
- *Safe Mode* is a required mode before entering *Monitor Mode* from *Emergency Mode*, for both priority 1 and 2 alarms. The preliminary design required only priority 1 alarms to use *Safe Mode* (with the associated emergency shutdown checklist and supervisor authorization), but it is safer to also have priority 2 alarms, which are mostly related to high pressures in the process, go through *Safe Mode* also. Having both priority 1 and 2 alarms go through *Safe Mode* makes the procedure safer and less complicated.
- To enter *Safe Mode* from *Emergency Mode* a supervisor authorization password has been added as one of the requirements of the safety checklist.

#### **3.3.4.2 Process alarms**

Alarms are prioritized into four groups:

- Priority 1 alarms: These alarms are a critical safety alarm because the alarmed conditions pose an immediate health threat to the operators and lab occupants. The process is interlocked to shut down. As a result, the process enters *Emergency Mode*.
- Priority 2 alarms: These alarms specify process instability due to a failure in the process itself or in the process control system. Similar to priority 1 alarms, the process is interlocked to shut down when a priority 2 alarm is activated and the process will enter *Emergency Mode*.
- Priority 3 alarms: These alarms indicate abnormal process conditions which might lead to process instability if not handled properly. Therefore, troubleshooting the process is required when a priority 3 alarm is activated. There is no change in mode associated with Priority 3 alarms.
- Priority 4 alarms: These alarms inform the operator of abnormal process conditions, which should be monitored. There is no change in mode associated with Priority 4 alarms.

A complete list of the alarms available in the process is provided in Appendix A4. After initial testing of the process, some modifications were made to the alarms. These changes are summarized in Table 3.5.

**Table 3.5. Summary of modifications applied to the SFE alarm system**

Alarm ID	Alarm Priority	Preliminary design	Final design	Logic
PAH2-2406 PAH2-3406 PAH2-4402	2	none	Added to Priority 2 alarms	These high alarms were added for extra safety regarding process pressure. The system will shut down if alarm is activated.
LAH2-1401	2	Had not been specifically prioritized	Added to Priority 2 alarms	Because we do not have continuous reading of the slurry level inside the extraction vessel, this alarm will shut down the process if the extraction vessel fills with slurry.
PAH3-1402 PAH3-2406 PAH3-3406	3	$22 < P < 27$ MPa	$22$ MPa < P	The ranges of the alarms were changed because pressure exceeding 27 MPa will automatically result in a Priority 2 alarm.
PAH3-2405	3	$2.1 < P < 2.4$ MPa	$2.75$ MPa < P	The original alarm range is redundant and was modified based on the maximum allowable inlet pressure of the CO <sub>2</sub> pump.
PAL3-2405	3	$0.9 > P > 1.0$ MPa	$P < 3.1$ MPa	The original alarm values were mathematically incorrect. The modified value is based on the specifications of the CO <sub>2</sub> tank.
TAH3-2407	3	$T > 85$ °C	$T > 60$ °C	It was decided to decrease the limit of this alarm. The alarm relates to the temperature

Alarm ID	Alarm Priority	Preliminary design	Final design	Logic
				in LN-2005 (CO <sub>2</sub> line exiting the pump). This line is typically very cold and an increase in temperature represents a system upset that would need to be investigated quickly.
TAH3-3410	3	T > 85 °C	T > 60 °C	This alarm relates to the temperature of the slurry leaving the slurry pump (in LN-3009). As the slurry is not actively heated during the extraction phase, an increase in slurry temperature is an indication of a system upset that would need to be investigated quickly.
PAH3-4402	3	4 < P < 4.5 MPa	8 MPa < P	Based on initial testing, it was decided that the separator pressure should not exceed 8 MPa during normal operation.
LAL3-3408	3	none	Added to Priority 3 alarms	The alarm is triggered when the water level is low in water tank to prevent the slurry pump from running dry or to indicate a leak in the tank.
TAL3-1410	3	none	Added to Priority 3 alarms	A thermocouple, TI-1410, was installed at the bottom of the extraction vessel. The alarm alerts the Operator when the temperature drops below supercritical (32° C).
PAL3-4402	3	none	Added to Priority 3 alarms	During normal operation, the separator pressure is above 1 MPa. If the pressure drops to below 1 MPa, it is an indication of freezing.
TAL3-4403	3	T < 16 °C	T < 0 °C	This temperature should be closely monitored. If the temperature in the separator drops below 0 °C, freezing might occur.
TAH3-1403	3	Priority 4 alarm	Changed to Priority 3	It was decided that the increase of this temperature could cause problems in the vessel and so it should be a Priority 3 alarm.
TAH3-1403	4	60 < T < 85 °C	60 °C < T	There is no need to have upper limit. Going over 85°C will automatically trigger a Priority 2 alarm.
PAL4-1402	4	4 < P < 6 MPa	P < 6 MPa	Because this is a low level alarm, the upper limit is sufficient.

### 3.3.4.3 Process control

Two main control objectives for the pilot scale continuous SFE process are (i) controlling the pressure and (ii) controlling the slurry level inside the extraction vessel. These two process variables must be controlled during a run to have efficient and safe operation of the process. Based on these objectives, three control loops have been programmed and exist on the control panel of the GUI. These control loops are as follows:

1. Control of slurry level inside the extraction vessel via slurry pump VFD: In this control structure, the slurry level in the extraction vessel is controlled by the speed of the slurry pump through a feedback control loop. Two modes exist for controlling slurry level: “man” and “auto”. In “man” mode, the slurry pump speed can be changed manually. In “auto” mode, control logic applies and the slurry level will be controlled via a feedback control loop. It should be noted that currently, due to lack of continuous level sensors in the extraction vessel, automatic level control is not fully functional and this control loop is mostly operated in manual mode (i.e. “man” mode). The manual approach that is conducted is based on visual observations of the system and adjusting slurry flow based on these observations. A pressure gauge located on the slurry outlet line from the extraction vessel is the main indicator used during manual mode. During normal operation i.e. when only slurry is flowing through this line, the pressure gauge on the slurry outlet line typically reads 100 psia. However, as the slurry level decreases, CO<sub>2</sub> starts exiting the slurry outlet line along with the slurry. The pressure gauge readings start to fluctuate and the slurry outlet line which becomes cold (as a result of CO<sub>2</sub> flowing through it). In some cases, the CO<sub>2</sub> exiting with the slurry goes into the receiving tank and into the lab, triggering an increase in the CO<sub>2</sub> levels in the lab as measured by the CO<sub>2</sub> sensors. To counteract this scenario, the slurry level inside the extraction vessel is increased by increasing the slurry pump flow in increments of 0.5% until conditions are back to normal i.e. pressure gauge fluctuation stops and CO<sub>2</sub> sensors measurements are back to normal. Normal conditions indicate that slurry level is high enough to prevent CO<sub>2</sub> from exiting the slurry outlet line. Overfilling of the vessel is also not desirable and level should be kept as low as possible. For this purpose, the slurry flow is decreased in increments of 0.5% until CO<sub>2</sub> is again observed in the slurry outlet line. This procedure is repeated throughout an experiment in order to manually maintain level within an acceptable range near the bottom of the extraction vessel.
2. Control of pressure inside the extraction vessel via CO<sub>2</sub> pump VFD: In this control structure, the extraction vessel pressure is controlled by the CO<sub>2</sub> pump speed through a feedback control loop. One of three pressure sensors (PI-2406, PI-1404 or PI-1402) can be chosen as the process variable for this purpose (i.e. to provide feedback in the control

loop). Based on the desired set-point and the pressure readings recorded from the chosen pressure sensor, the CO<sub>2</sub> pump speed is manipulated. This control structure can also be set to “man” and “auto” mode. In “man” mode, the pressure can be adjusted by manually changing the CO<sub>2</sub> pump speed. In “auto” mode, the control logic applies. In using this feedback loop for controlling the extraction vessel pressure during the pressurization stage for a typical run, PI-2406 (the pressure sensor located on the CO<sub>2</sub> inlet line (¼”) to the extraction vessel) is chosen as the desired process variable. The reason for this selection is that, during testing, it was observed that this pressure sensor responds much faster to changes in CO<sub>2</sub> flow in comparison to PI-1402 or PI-1404 pressure sensors, which are located at the top and bottom of the extraction vessel, respectively. But, the pressure measured at PI-2406 is slightly higher than the extraction vessel pressure and it is not an accurate representation of the pressure inside the extraction vessel. Hence, when the desired pressure set-point is reached at PI-2406 (e.g. 14 MPa), the control system then uses PI-1404, the pressure sensor at the bottom of the extraction vessel, for the rest of the operation of the SFE process.

3. Control of pressure inside the extraction vessel via the metering valve: In this control structure, the extraction vessel pressure is controlled by the metering valve (MV-4303) located on the CO<sub>2</sub> outlet line from the extraction vessel. This control loop gets feedback from pressure sensor PI-1402, which is located at the top of the extraction vessel and close to the metering valve. During initial testing of the process, it was observed that the pressure sensor at the top of the extraction vessel (PI-1402) did not respond as quickly as the sensor at the bottom (PI-1404). It was also observed that the opening of the metering valve quickly effects the pressure reading at this pressure sensor (PI-1402). Therefore, it was decided to program a feedback loop to control the pressure at the top of the vessel (PI-1402) by manipulating the metering valve opening. In later stages, it was decided that the metering valve opening should stay unchanged during a run (excluding pressurization and depressurization stages). Hence, this loop is no longer used.

### **3.3.5 Operation manual**

During this research, the preliminary operation manual was modified during the commissioning and troubleshooting of the SFE process. In this section, major changes made to the operation manual and the reasons behind each change is explained in detail.

#### **3.3.5.1 Environmental monitoring**

Preliminary environmental monitoring included two CO<sub>2</sub> sensors and one O<sub>2</sub> sensor. Rosenthal (2012) proposed connecting one of the CO<sub>2</sub> sensors to the University of Alberta Central Control and connecting the other CO<sub>2</sub> sensor to the control system to trigger in-lab alarms and initiate emergency shutdown of the process. Connecting the O<sub>2</sub> sensor to the control system to trigger in-lab alarms and initiate emergency shutdown of the process had also been proposed.

The final environmental monitoring of the SFE process lab, which was designed during the “build” phase, consists of two O<sub>2</sub> monitors and two CO<sub>2</sub> monitors. The O<sub>2</sub> monitors are portable and are attached to a belt or lab coat pockets, to be worn by two operators as soon as they enter the lab and throughout their time spent in the lab. The two O<sub>2</sub> monitors have a low alarm setting of 19.50% (volume) and a high alarm setting of 23.50% (volume). If these levels are reached, the monitor will start beeping and vibrating to notify the user of the state of the O<sub>2</sub> concentration in the lab. It should be noted that these monitors are not connected to the DAQ system and their data is not being logged.

The CO<sub>2</sub> monitors, CO<sub>2</sub>(1) and CO<sub>2</sub>(2), are stationary and both probes are located inside the lab at a height of approximately 50 cm on the east wall of the lab. The display of CO<sub>2</sub>(1) is located inside the lab, near the DAQ box and also connected to the DAQ system. Hence, the CO<sub>2</sub> concentration in the lab can be seen on the computer as well as on the CO<sub>2</sub>(1) monitor display at all times. Data from the CO<sub>2</sub>(1) monitor is being logged 24 hours a day and saved on the computer. The operating range of the CO<sub>2</sub>(1) monitor is 0 -10,000 ppmv. When 5,000 ppmv is reached through this monitor, the orange light of a stack light, located above the monitor and connected to the monitor, will start to flash along with a beeping sound. When 10,000 ppmv is reached, the red light of the stack light will start flashing with a constant beep. The audible alarm and stack light serve to notify occupants to leave the lab. Also, if the system is in use and running, the emergency shutdown is activated through the programmed interlocks of the process.

The display of CO<sub>2</sub>(2) is located just outside the lab (in the hallway) and its operating range is 0 - 5%. This CO<sub>2</sub> sensor is connected to University's Central Control. As a result, if a CO<sub>2</sub> level of 1% (equivalent to 10,000 ppmv) is recorded by this monitor, a critical alarm is activated in Central Control, which requires them to move building ventilation to 100% fresh air, increase the air exchange rate of the lab, dispatch trades people and start calling the people on the emergency contact list, starting with the lab itself. It should be noted that the CO<sub>2</sub>(2) monitor is connected to two stack lights: one inside the lab (above the computer) and the other outside the lab (above the CO<sub>2</sub> monitor in the hallway). The purpose of the stack lights is to inform the lab occupants or others in the hallway of potentially unsafe conditions in the lab.

### **3.3.5.2 Start-up and controlled shutdown procedures**

After commissioning runs and troubleshooting the process, start-up and controlled shutdown procedures for the process were upgraded. These upgrades are outlined in the following subsections.

#### *Start-up procedure*

The major changes made to the start-up procedure are as follows:

- In the preliminary procedure, the plan was to pressurize the vessel with CO<sub>2</sub> and then introduce the slurry. However, based on initial runs, it was difficult to create an initial plug of slurry at the bottom of the extraction vessel while the vessel was pressurized. As a result, it was decided to create a plug of water before the vessel was pressurized. This procedure also helped prevent fast temperature drops at the bottom of the vessel when initially introducing CO<sub>2</sub> into the empty extraction vessel. With the extraction vessel containing an initial volume of water at approximately 45 °C, the CO<sub>2</sub> is warmed as it enters the extraction vessel.
- Based on experiments, it was concluded that having the level slightly above 16 cm is a good level for the initial water plug inside the extraction vessel. In creating the water plug, due to splashing, the 16 cm level sensor is immediately activated and the actual level of water inside the vessel could not be determined. Since the level sensor could not be used to determine the level of slurry, the slurry pump has to be stopped once to stop splashing in the vessel and determine the approximate level of water (i.e. level above vs.

below 16 cm). However, based on calculations, it was concluded that running the slurry pump for approximately 20 seconds at 15% of maximum pump rpm would provide a 16 cm of water level inside the extraction vessel. Therefore, this approach was applied for creating a 16 cm plug of water in the extraction vessel at the beginning of an experiment.

- After initial testing, it was concluded that the slurry temperature has a dominant effect on the temperature inside the extraction vessel. Therefore, to reach a higher temperature inside the extraction vessel, the slurry feed needs to be heated.
- After initial testing, the procedure that ultimately worked best for introducing countercurrent flow of slurry and CO<sub>2</sub> (after creating a plug of water) was to first bring the extraction vessel to CO<sub>2</sub> tank pressure (~3 MPa) by opening the valve on the CO<sub>2</sub> feed tank. After the extraction vessel reached CO<sub>2</sub> tank pressure, the slurry pump and CO<sub>2</sub> pump are turned on simultaneously to initiate countercurrent flow. The starting flowrates for the two pumps are typically 13.8% and 12.5% respectively. When the pressure inside the extraction vessel reaches approximately 10 MPa, the pressure control loop is set to “auto” and the set point is increased step wise to reach the desired pressure inside the extraction vessel. In the presence of level sensor (or an alternative approach for measuring level inside the extraction vessel), the level control loop is set to “auto” after reaching the desired pressure in the extraction vessel.
- An “Operation Log” was prepared and placed in the lab. As part of the start-up procedure, operators are required to fill out this log at the beginning of each run.

### *Controlled shutdown procedure*

The major change made to the controlled shutdown procedure is as follows:

- For cleaning the vessel at the end of an experiment, rinse water is used (slurry flow is switched to rinse water flow). Therefore, water and SC-CO<sub>2</sub> are countercurrently flowing through the extraction vessel and the process is still pressurized. At this stage, samples will be taken from the receiving slurry tank to make sure that solids have mostly exited the process and then the pumps will be stopped. In addition, after the depressurization stage, the extraction vessel is completely filled and then rinsed from the drain valve at the bottom of the vessel to clean the extraction vessel from any remaining solids.

### **3.3.5.3 Checklists**

The checklists proposed in the preliminary design (i.e. start-up checklist, shutdown checklist, operation checklist, safety checklist and emergency shutdown checklist) were developed before the process had been set up. As a result, these checklists were very general. Completing the process set up and conducting several experiments allowed more detailed checklists to be developed. These checklists are available on the computer in the lab (in the GUI).

Important modifications are as follows:

- A complete valve checklist was prepared to be placed in lab and checked as part of the start-up procedure.

### **3.3.5.4 Slurry level in extraction vessel**

Three single point type level sensors exist in the extraction vessel (LI-1401, LI-1405 and LI-1406). LI-1401 is located at the top of the extraction vessel. LI-1405 and LI-1406 are located at the bottom of the extraction vessel. LI-1405 has a length of approximately 16 cm and LI-1406 has a length of approximately 5 cm.

The two level sensors located at the bottom of the extraction vessel are not giving reliable readings especially LI-1405 which is the 16 cm level sensor. The reason is that when the slurry pump is turned on and slurry flows through the vessel, splashing of water/slurry in the vessel causes this level sensor to activate even though the level is below 16 cm. Better solutions should be considered for this purpose. Hence, an automated response for level control does not exist at the moment and level control is done manually. The slurry pump speed is adjusted based on physical observations of the slurry outlet line and the pressure gauge located on that line. With regards to automating slurry level control, an approach (referred to as the pulse test approach) has been explored and presented in Chapter 6.

### **3.3.5.5 Extraction vessel and separator temperature**

Temperature control in the extraction vessel and separator is not automated. However, the temperature can be kept within a certain range if the heating equipment is turned on, functioning correctly and adjusted to the correct set-point. Regarding the extraction vessel temperature, the slurry temperature plays a dominant role in controlling the temperature in the extraction vessel;

therefore, the slurry tank heater (HX-3412) is turned on before initiating a run. As a result, the slurry enters the extraction vessel at approximately 45°C.

Regarding the separator temperature, heating tape on the CO<sub>2</sub> line entering the separator (HX-4408), heating tape located on MV-4303 (HX-4407) and heating tape on the separator itself (HX-4409) are turned on during normal operations and set to their maximum value i.e. 204.4 °C (equivalent to 400 °F). These three heating devices play a significant role in determining the temperature inside the separator and preventing the lines from freezing and preventing the temperature in the separator to drop below 0 °C.

### **3.3.6 HAZOP**

A HAZOP study was completed in November 2010 by some members of the SFE design team (A. Rosenthal and C. Street) and team members from M-I SWACO (industrial partner). Those HAZOP results are provided in Rosenthal (2012), and have been updated for this thesis. The primary changes are as follows:

- Equipment tag numbers were updated in the HAZOP document to reflect any system design changes (provided in Tables 3.3, 3.4 and 3.5).
- The original HAZOP (Rosenthal 2012) assumed that spill containment (“drip trays”) would be installed; however, these have not been installed. Some slurries are dilute enough to be disposed of directly. For those slurries that cannot be disposed of directly, spills are contained, collected and disposed of according to protocols outlined by Environmental Services of the University of Alberta.
- Flow meters have not been installed on CO<sub>2</sub> lines upstream or downstream of the CO<sub>2</sub> pump or downstream of the extraction vessel. Originally, the justification for installing these flow meters was to avoid pump damage or process upsets that would be caused by low or high flows in these locations. Due to issues of specifications and cost, the flowmeters were not installed. To prevent pump damage, the CO<sub>2</sub> pump cannot be started until the CO<sub>2</sub> supply valve is open (by both an automated valve programmed into the control system and a manual valve integrated on CO<sub>2</sub> tank). Process upsets in the vessel caused by CO<sub>2</sub> primarily affect pressure. Increases or decreases in pressure are monitored by pressure sensors at the top and bottom of the extraction vessel.

- The original HAZOP specified the installation of a flow switch prior to the slurry pump to prevent cavitation in the slurry pump. There were issues in sourcing adequate flow switches. Operators currently ensure the feed tanks are full and valves are in the correct position to avoid running the pump dry.
- The grinding loop is not installed. Instead, a procedure regarding slurry preparation has been completed and added to the Operations Manual.

### **3.4 Summary of runs**

Table 3.6 summarizes the experimental runs conducted on the continuous pilot scale SFE process. The summary includes the date of run, the component/fluid(s) that were used for conducting the SFE experimental runs, the objective of the run, and the main outcomes and observations of the run. Runs are presented in chronological order. Each experiment is identified with a run number which is used in following chapters for referencing purposes.

Experimental Runs 1 to 11 are associated with pressurizing the extraction vessel with CO<sub>2</sub> (via the CO<sub>2</sub> pump). Pressure control loops were also implemented, tested and modified in these runs. Experimental Runs 12 to 18 were aimed at establishing countercurrent flow of CO<sub>2</sub> and slurry (as water) inside the vessel for as long as possible. Experimental Runs 13 to 26 were also aimed at establishing countercurrent flow. However, from Run 13, the original CO<sub>2</sub> feed tank was replaced with the current CO<sub>2</sub> feed tank and troubleshooting was again required for pressurizing the extraction vessel. Experimental Runs 27 to 30 were conducted to obtain data for system identification (developing a model of the process based on data from the continuous pilot scale process).

From Run 31, slurry was used in the countercurrent SFE process, instead of only water, as in previous runs. Experimental Runs 31 to 40 were mainly associated with adding solids to the slurry and troubleshooting to maintain continuous flow of slurry through the process. Experimental Runs 41 to 61 were associated with collecting data from the process for model validation purposes and performing mass transfer calculations. Experimental Runs 62 to 82 were conducted for various purposes, for example testing different operating conditions and different control strategies.

**Table 3.6. Summary of runs conducted on the pilot scale SFE process**

Run	Date	Component(s)	Objective	Outcomes	Observations
<i>Experiments to test system pressurization</i>					
1	30/05/2014	CO <sub>2</sub> only	Have the CO <sub>2</sub> pump produce pressure.	The CO <sub>2</sub> pump produces pressure, as long as it is provided with a liquid CO <sub>2</sub> feed. This can be accomplished by venting CO <sub>2</sub> through the pump until the line temperature reaches -21°C, and maintaining the cauldron and chiller at approximately -25 °C.	None.
2	2/06/2014	CO <sub>2</sub> only	Pressurize vessel to 10 MPa and hold the pressure.	The vessel was successfully pressurized.	Re-pressurization of the system after a shutdown is achievable if cauldron temperature is maintained at around -20°C.  A temperature gradient exists along the vessel. The bottom of the vessel (where the CO <sub>2</sub> enters) is much colder than the top where the thermocouple is placed. Thus, the CO <sub>2</sub> may exist in several states throughout the vessel.
3	3/06/2014	CO <sub>2</sub> /water	Attempt to introduce water into the vessel when vessel is pressurized with CO <sub>2</sub> at 4 MPa.	Slurry was successfully introduced into the pressurized vessel.	The level sensors did not give reliable results. The reason might be that water froze on them because it is very cold at the bottom of the vessel where CO <sub>2</sub> enters.
4	4/06/2014	CO <sub>2</sub> only	Repeat Run 2	The vessel was successfully pressurized to 10 MPa.	A large temperature gradient exists along the vessel which should be resolved.
5	11/06/2014	CO <sub>2</sub> only	Introduce CO <sub>2</sub> first from top and then bottom to see if the temperature gradient along the vessel can be reduced.	The temperature gradient was not improved by this vessel pressurization method.	A pressure spike happens at around 8 MPa. The reason could be that we are entirely in the liquid region and a few additional grams of CO <sub>2</sub> increases pressure significantly.
6	13/06/2014	CO <sub>2</sub> only	Observe the effect of pump speed on pressure response.	The pressure did respond to changes in pump speed as expected.	A steady state pressure was not achieved. The reason could be that the temperature is changing inside the vessel which affects the pressure.

<b>Run</b>	<b>Date</b>	<b>Component(s)</b>	<b>Objective</b>	<b>Outcomes</b>	<b>Observations</b>
7	4/07/2014	CO <sub>2</sub> only	Test the pressure control loop (the pump speed is varied according to the pressure at the top of the vessel).	Steady state pressure was achieved, especially when the pump controller parameters were optimized.	<p>There was a distinct pressure difference between the line, vessel bottom, and vessel top readings.</p> <p>The CO<sub>2</sub> line before the pump warms up if pump RPM decreases.</p> <p>A 5% to 60% limit should be put on CO<sub>2</sub> pump RPM (do not allow the pump to stop or to jump to high speed).</p>
8	14/07/2014	CO <sub>2</sub> only	Test the effect of having a heating tape at the bottom of the vessel.	The heating tape did not have a large effect on the temperature at the bottom of the vessel. (Prior to this test, a thermocouple was installed in the bottom of the vessel). Overall, a 10 °C temperature profile exists along the vessel length.	When the pump speed increases, vessel bottom temperature starts to decrease.
9	17/07/2014 (a)	CO <sub>2</sub> only	Test the effect of slowly increasing the pressure to operating conditions to try to minimize the temperature gradient in the vessel.	Slowly increasing the pressure to operating conditions results in the same temperature gradient in the vessel.	Slowly increasing the pressure reduces rapid changes in temperature (which was previously observed).
10	17/07/2014 (b)	CO <sub>2</sub> only	Limit the pressure gradient in the vessel by testing a new control structure where the vessel bottom pressure is controlled with pump rpm and the vessel top pressure is controlled with metering valve position.	A smaller pressure gradient was observed in the vessel.	Controlling the pump RPM with the bottom pressure can result in very high pressures in the inlet line (as a result of flow restrictions and pump controller settings).

<b>Run</b>	<b>Date</b>	<b>Component(s)</b>	<b>Objective</b>	<b>Outcomes</b>	<b>Observations</b>
11	18/07/2014	CO <sub>2</sub> only	Limit the pressure gradient in the vessel by testing a new control structure where the CO <sub>2</sub> inlet line pressure is controlled with pump rpm and the vessel top pressure is controlled with metering valve position (limit on metering valve between 5% and 50%).	Uniform pressure between the inlet line and the vessel top can be observed; however, it takes some time to reach steady state.	None.
<i>Experiments to establish countercurrent flow of CO<sub>2</sub> and slurry (as water) inside the extraction vessel as long as possible</i>					
12	23/07/2014	CO <sub>2</sub> /water	Attempt to pump slurry into a pressurized vessel at 10 MPa by first pressurizing with CO <sub>2</sub> while water is between 5 and 16 cm. Then, when the pressure is steady, turn the CO <sub>2</sub> pump off and turn slurry pump on.	Successfully introduced slurry into pressurized vessel of 10 MPa.	After turning on the slurry pump, the bottom temperature is the same and even more than the top temperature. So, the slurry brings in heat to the process.  The level sensors not giving consistent results.
13	24/07/2014	CO <sub>2</sub> /water	Attempt countercurrent flow.	Countercurrent flow achieved.	The manifold was set to 1 meter of 1/8" tubing. This seems to be able to hold the pressure inside the vessel.
14	29/07/2014	CO <sub>2</sub> /water	Attempt countercurrent flow.	Countercurrent flow achieved but run aborted due to freezing in the metering valve.	The separator was drained after this run and quite a lot of water came out.

Run	Date	Component(s)	Objective	Outcomes	Observations
15	31/07/2014	CO <sub>2</sub> /water	Attempt countercurrent flow with new heating tape on the metering valve to prevent freezing.	The CO <sub>2</sub> tank was recently filled and the pressure wasn't high enough for a run (it was at 280 psi). And it even dropped to 260 psi when we started the run. Countercurrent flow could not be achieved because CO <sub>2</sub> pump failed to pressurize; however, continuous flow of water was achieved through the vessel for quite some time with the pressure at around 5-6 MPa.	7 to 10 days is required to pressurize the CO <sub>2</sub> tank from fill pressure before a run.  For the water flow part of the test, the manifold was set to the second most restricted line (1/8" ID and 0.5 m length), which seemed to be enough for the pressure the vessel was at.
16	7/08/2014	CO <sub>2</sub> /water	Countercurrent run for as long as possible.	Ran for 23 min until the slurry receiving tank was overfilled and the run had to be terminated.	Restart of the CO <sub>2</sub> pump was not possible because CO <sub>2</sub> line had warmed up.
17	8/08/2014	CO <sub>2</sub> /water	Repeat Run 16.	Ran for 22 min. The run was terminated because it sounded like freezing was happening somewhere in the lines and/or near the separator.	
18	20/08/2014	CO <sub>2</sub> /water	Repeat Run 16.	Countercurrent run was achieved for one hour. No reason was observed to terminate run.	The CO <sub>2</sub> tank pressure had dropped significantly over the run and was far away from the necessary 290 psi. It was decided to change the CO <sub>2</sub> tank. This was the last run done with this CO <sub>2</sub> tank.
19	2/10/2014	CO <sub>2</sub> only	Test the new CO <sub>2</sub> tank.	Successfully pressurized the system to 8 MPa.	This run was initiated without venting to pre-cool the system to liquid CO <sub>2</sub> temperature (at tank pressure). Venting requirement removed from operation manual.  A leak was observed on the pressure building circuit on the tank which has to be fixed.

Run	Date	Component(s)	Objective	Outcomes	Observations
20	7/10/2014	CO <sub>2</sub> only	Test the new CO <sub>2</sub> tank after the tank leak was fixed.	Successfully pressurized the system to 7 MPa.	The CO <sub>2</sub> pump stopped at the middle of the run and was successfully restarted (previously not possible due to venting requirement).  The tank was able to maintain its pressure at around 3 MPa.
21	9/10/2014	CO <sub>2</sub> /water	Run system countercurrently with the new CO <sub>2</sub> tank.	Countercurrent run was achieved for around 20 minutes before CO <sub>2</sub> pump stopped pressurizing.	None.
22	17/10/2014 (a)	CO <sub>2</sub> /water (first part of the run)	Obtain data for system identification.	Unsuccessful due to CO <sub>2</sub> pump stopped pressurizing after 20 minutes of running.	None.
23	17/10/2014 (b)	CO <sub>2</sub> (second part of the run)	Solve issue in previous part of the run i.e., will the pump stop again with CO <sub>2</sub> only?	Unsuccessful at achieving pressure with CO <sub>2</sub> pump after 45 minutes of running.	None.
24	21/10/2014 (a)	CO <sub>2</sub> only	Test CO <sub>2</sub> pump with the pump head chiller at -25 °C.	CO <sub>2</sub> pump did not pressurize.	None.
25	21/10/2014 (b)	CO <sub>2</sub> only	Retry Run 24 with line cooling cauldron back into the process and cooling it to -15 °C.	Ran successfully for 1 hour, indicating that the cauldron is required and needs to be cooled to around -15 °C.	None.
26	23/10/2014	CO <sub>2</sub> /water	Replicate Run 16.	Successfully ran for 1 hour.	Could not run beyond 1 hour because of freezing in the CO <sub>2</sub> line going to fume hood, likely because of water carry over. For next run, consider extending the separator inlet line to prevent carry over.
<i>Experiments to obtain data for system identification</i>					
27	30/10/2014	CO <sub>2</sub> /water	Obtain system identification data at around 8 MPa.	Successfully obtained system identification data.	Process will stay relatively stable during "Manual Mode" at a constant CO <sub>2</sub> and slurry rpm.
28	4/11/2014	CO <sub>2</sub> /water	Replicate of Run 27.	Successfully obtained system identification data.	None.

<b>Run</b>	<b>Date</b>	<b>Component(s)</b>	<b>Objective</b>	<b>Outcomes</b>	<b>Observations</b>
29	6/11/2014	CO <sub>2</sub> /water	Obtain system identification data at around 12 MPa.	Successfully obtained system identification data.	Temperatures inside vessel slowly decreases over the run. Consider a heater for slurry tanks (as the slurry controls the system temperature).  A lot of CO <sub>2</sub> is used. Consider closing metering valve to conserve CO <sub>2</sub> .
30	12/11/2014	CO <sub>2</sub> /water	Replicate of Run 29.	Successfully obtained system identification data.	None.
<i>Experiments with slurry (both control system and mass transfer tests)</i>					
31	18/11/2014	CO <sub>2</sub> /slurry	Test the system with actual slurry (solids in the water).	Successfully ran countercurrently with solids in the water (actual slurry).	Solids separate out of the slurry in the tank. Consider a mixer for the tank.  Separator shows signs of freezing. Consider another heating tape for around the separator body.
32	16/12/2014	CO <sub>2</sub> /water	Test the new designed pressure controller to 14 MPa and observe the response of RBS signal to be used to identify the system again.	Test completed successfully but the new controller seemed to be very sluggish.	There was a high atmospheric CO <sub>2</sub> concentration during run (mainly around 14 MPa).
33	18/12/2014	CO <sub>2</sub> /slurry	Test a countercurrent run with slurry, mixed with a hockey stick. Run includes new composition of solids in slurry. Tested sending the slurry to a receiving tank to prevent the temperature from dropping.	The test was completed successfully. The mixing allowed more solids to flow to the vessel. The longer manifold prevented the CO <sub>2</sub> concentration in the atmosphere from increasing.  Because the feed tank was different from receiving tank this time, slurry temperature didn't drop as fast as before.	None.

Run	Date	Component(s)	Objective	Outcomes	Observations
34	20/01/2015	CO <sub>2</sub> /slurry	Replicate of Run 33 but tested switching from pressure control on CO <sub>2</sub> inlet line to vessel bottom.	Successful run. After the pressure stabilized, the pressure sensor on the control loop was changed from the line pressure to vessel bottom pressure. This change keeps the vessel closer to the pressure set point.	None.
35	26/01/2015	CO <sub>2</sub> /slurry	Replicate of previous Runs 33 and 34. However this run included a longer manifold, a heater, and a mixer.	Successful run. The longer manifold (1/8" ID and 2m length) worked well with the higher pressure in vessel (14 MPa) to prevent CO <sub>2</sub> "burps". The heater was effective, increasing the vessel bottom temperature to 40 °C.	None.
36	13/02/2015	CO <sub>2</sub> /slurry	Replicate of Run 35, but the heating tape was moved from the bottom of the extraction vessel to the CO <sub>2</sub> inlet line.	Successful run. The heating tape on the CO <sub>2</sub> inlet line did not seem to have any impact on the vessel temperature.	None.
37	18/02/2015	CO <sub>2</sub> /slurry	Replicate of Run 36 but with increased solids content of the slurry.	Successful run. Increased solids did not cause any operational difficulties.	A blender was used to successfully create slurry. Took a long time just to create one pale of slurry.
38	24/02/2015	CO <sub>2</sub> /slurry	Replicate of Run 37 but with additional solids mixed in using the tank mixer.	The tank mixer worked well to incorporate the additional solids and the increase in solids content did not cause operational difficulties.	Freezing occurred in the separator near the end of the run.  The vessel seemed quite full.
39	3/03/2015	CO <sub>2</sub> /slurry	This run was a flow test to make sure the vessel is not filling during the run by minimizing the slurry flow as much as possible (create burps).	Modestly successful run but complete burps could not be created because the CO <sub>2</sub> level would increase inside the lab. However, the run had a lower slurry pump rpm in comparison to previous runs.	At the end, only 125 mL of rinse water was collected from the vessel.

Run	Date	Component(s)	Objective	Outcomes	Observations
40	13/03/2015	CO <sub>2</sub> /slurry	Replicate of Run 38 but with high solids concentration (approximately 5%).	Unsuccessful run as the slurry pump could not be operated at low speeds (15 rpm).	None.
<i>Experiments to validate hydrodynamic model and to determine mass transfer</i>					
41	26/03/2015	CO <sub>2</sub> /slurry	Get validation data at 10 MPa and 14 MPa but dilute the slurry because of Run 40 outcome.	Successfully obtained system data.	None.
42	1/04/2015	CO <sub>2</sub> /slurry/water	Replicate Run 41 and test the new CO <sub>2</sub> coil (coil of tubing wrapped in heating tape).	Unsuccessful run because of the increased flow resistance of the CO <sub>2</sub> coil and also freezing occurring in the slurry outlet line when attempting to start countercurrent phase.	None.
43	8/04/2015	CO <sub>2</sub> /water	Troubleshoot the CO <sub>2</sub> coil and decide whether to keep it.	The run start-up was very slow because of the coil. As configured, the coil does not seem to provide any temperature benefit at the bottom of the vessel.	Freezing occurred in the slurry line when attempting to start countercurrent, but was successful when slurry pump was started at 20%.
44	15/04/2015	CO <sub>2</sub> /water	Conduct a pulse test at 14 MPa without the CO <sub>2</sub> coil (based on Run 43).	Unsuccessful run because there was a blockage at the slurry outlet line. Blockage was not due to freezing as in Runs 42 and 43. There was a solid blockage at the exit of the vessel (of unknown origin).	None.
45	22/04/2015	CO <sub>2</sub> /water	Do an hour uncontrolled CC run and compare results with modelling results. Burps of CO <sub>2</sub> were expected at certain times (based on modelling prediction).	First attempt was unsuccessful due to freezing and the incorrect manifold was used. Second attempt was successful as the same steady state pressure was reached as the model predicted (10 MPa). However, no burp was observed.	None.
	24/04/2015 (a)	CO <sub>2</sub> /water		The run was successful as the same steady state pressure was reached as the model predicted (10 MPa). However, no burp was observed.	Mid-run pressure slightly increased.

Run	Date	Component(s)	Objective	Outcomes	Observations
46	24/04/2015 (b)	CO <sub>2</sub> /water		The run was successful as the same steady state pressure was reached as the model predicted (14 MPa). However, no burp was observed.	Mid-run pressure slightly increased.
47	29/04/2015	CO <sub>2</sub> /water	Replicate Runs 45 and 46 but include a heating tape on the slurry outlet and fume hood lines to prevent freezing (that may be the cause of the mid-run pressure increase and no burps).	The same steady state pressure reached as the model predicted (10 MPa) with no pressure increase. However, still no burp was observed.	Noticed vessel filling procedure not the same between Runs 45, 46, 47. Need a consistent filling procedure in order to compare better between runs.
48	5/05/2015	CO <sub>2</sub> /water	Measure the amount of time it takes to empty the vessel at 10 MPa.	Unsuccessful test as once the slurry outlet valve was opened a burp was observed which typically indicates that the vessel is empty. It was later realized that the CO <sub>2</sub> may be short circuiting because its density is quite high at the vessel conditions.	None.
49	7/05/2015 (a)	CO <sub>2</sub> /water	Test the model prediction of the vessel emptying (observed as a CO <sub>2</sub> burp) after 10 minutes of an uncontrolled run.	The run was not successful as no burps were observed after 10 minutes.	None.
50	7/05/2015 (b)	CO <sub>2</sub> /water	Replicate of Run 48 but with the CO <sub>2</sub> pump turned off after pressurizing to 10 MPa, and isolate the vessel before draining it.	The run was not successful because of an emergency alarm on the CO <sub>2</sub> line pressure between the pump and the vessel after isolating. The pressure reached 20 MPa.	It took approximately 4 minutes to drain the vessel.
51	7/05/2015 (c)	CO <sub>2</sub> /water	Replicate of Run 50, but draining the CO <sub>2</sub> inlet line before isolating the vessel to avoid the emergency alarm.	Draining the line helped with the alarm initially but as soon as the drain valve was closed, the pressure increased again.	There were freezing issues of unknown origin at the beginning of the run.

Run	Date	Component(s)	Objective	Outcomes	Observations
52	12/05/2015 (a)	CO <sub>2</sub> /water	Validate the model with an uncontrolled run to get to approximately 14 MPa.	Successfully reached 14 MPa and obtained validation data.	Towards the end of the run, the separator began to freeze even though the heating tapes were at their maximum.
53	12/05/2015 (b)	CO <sub>2</sub> /water	Replicate of Run 50 but this time the CO <sub>2</sub> inlet valve was left open to prevent that line from pressurizing and activating the alarm.	Successfully emptied the vessel as expected. At approximately 3 min and 50 s CO <sub>2</sub> was observed to be leaving with the slurry. At 4 min and 10 s full CO <sub>2</sub> flow through the slurry line and into the receiving tank was observed (a “burp”).	None.
54	15/05/2015 (a)	CO <sub>2</sub> /slurry	Get model validation and mass transfer data at 10 MPa and 14 MPa.	Unsuccessful run because the slurry flow was too high for the pressure and manifold settings (10MPa and longest manifold).	None.
55	15/05/2015 (b)	CO <sub>2</sub> /slurry	Replicate of Run 54.	Successful run.	None.
56	20/05/2015	CO <sub>2</sub> /slurry	Replicate of Run 54.	Successful run.	None.
57	26/05/2015	CO <sub>2</sub> /water	Get model validation and mass transfer data at 18 MPa.	Unsuccessful run as atmospheric CO <sub>2</sub> concentration kept going up and down. There was a leak in the pressure relief on the CO <sub>2</sub> pump.	None.
58	2/06/2015	CO <sub>2</sub> /water/slurry	Replicate of Run 57 but used a bucket in the fume hood to catch any oil leaving with the CO <sub>2</sub> .	Successful run, but the atmospheric CO <sub>2</sub> was going up and because of the bucket we put in the fume hood.	None.
59	15/06/2015	CO <sub>2</sub> /water/slurry	Replicate of Run 57 with no bucket.	Successful run.	The atmospheric CO <sub>2</sub> concentration was consistent with movement of gauge slurry outlet pressure gauge.  When depressurizing, the separator was isolated to try to prevent oil from being pushed out into the fume hood.

<b>Run</b>	<b>Date</b>	<b>Component(s)</b>	<b>Objective</b>	<b>Outcomes</b>	<b>Observations</b>
60	17/06/2015	CO <sub>2</sub> /water/slurry	Replicate of Run 57 but with the shorter manifold until 10 MPa is reached.	Unsuccessful run because as soon as the system was switched from water to slurry at 18 MPa the slurry outlet line froze. The reason could be that the shorter manifold was used while pressurizing to 10 MPa and so the vessel slurry level was quite low (not as high as when we used the longer manifold) causing more CO <sub>2</sub> to exit that line.	None.
61	24/06/2015	CO <sub>2</sub> /water/slurry	Replicate of Run 57.	Successful, however towards the end of the run, the vessel started to lose pressure and seemed like the CO <sub>2</sub> pump was not pressurizing perhaps as a result of the pump head chiller leaking.	None.
<i>Experiments for miscellaneous purposes</i>					
62	30/06/2015	CO <sub>2</sub> /water	Uncontrolled CO <sub>2</sub> run for model validation.	Unsuccessful run because there was a problem with pressurizing the system which could be a result of the pump, tank, or a line blockage. Eventually the system was depressurized and it was confirmed not to be a line blockage.	None.
63	6/07/2015 (a)	CO <sub>2</sub> /water	Conduct a flow test to see how high we can go in terms of slurry flow and CO <sub>2</sub> flow.	Unsuccessful test because of a high atmospheric CO <sub>2</sub> alarm.	Pressurizing still seemed to be a bit slow and was using more CO <sub>2</sub> than usual to maintain pressure.
64	6/07/2015 (b)	CO <sub>2</sub> /water	Do an uncontrolled CO <sub>2</sub> flow for model validation.	Successful test as 10.3 MPa steady state was reached.	None.
65	9/07/2015 (a)	water only	Test pressure drop in slurry line by running slurry pump at 50% going into the vessel.	Successful test as 10 MPa is observed on the pressure sensor of the slurry inlet line. This pressure is because of the restriction caused by the line change from 1/4" to 1/8" going into the vessel.	None.
66	9/07/2015 (b)	CO <sub>2</sub> only	Do an uncontrolled run of CO <sub>2</sub> for model validation.	Successful run.	It was determined that when only CO <sub>2</sub> is going in and out of the vessel, the vessel is a bit slow in pressurizing.

<b>Run</b>	<b>Date</b>	<b>Component(s)</b>	<b>Objective</b>	<b>Outcomes</b>	<b>Observations</b>
67	15/07/2015	CO <sub>2</sub> /water/slurry	Do a second pass of the slurry from Run 61 at 14 MPa	Successful run.	The CO <sub>2</sub> pump rpm was observed to be higher than usual.
N/A	07/2015	CO <sub>2</sub> /REAL slurry	Attempt a run with real cuttings made into slurry.	Unsuccessful run because the slurry pump began pulsing (not providing flow) as a result of solids settling in the 2" SS pump supply line.	None.
68	10/08/2015	CO <sub>2</sub> only	Check to make sure that the slurry pump can withstand the back pressure from the CO <sub>2</sub> .	Successful run.	None.
69	12/08/2015	Real slurry	Test the slurry pump on bypass with the real slurry to see if the pulsation problem can be replicated. We also removed the support ring from the top of the vessel baffle structure and removed the 1/8" slurry extension line into the vessel.	When using the real slurry, the slurry pump started pulsating if the pump was left running at low flows. However, when the pump speed was increased it recovered from the pulsating. It was concluded that higher flows should be used for this slurry type to make sure the solids in the slurry don't settle out and restrict supply to the pump.	None.
70	13/08/2015 (a)	CO <sub>2</sub> /water	To test shorter manifolds and higher water flows to see how high we can go before switching from water to slurry.	Successful as up to 27% slurry flow was shown with the medium length manifold. However, as soon as the flow was switched to slurry, there was a high level emergency shutdown because of slurry splashing.	None.
71	13/08/2015 (b)	CO <sub>2</sub> /water	Replicate of Run 70 to observe if splashing incident is repeatable.	Successful run as the same thing happened as in Run 70.	It was decided to extend the 1/4" into the vessel until it touches a baffle.
72	19/08/2015	CO <sub>2</sub> /water	Conduct a pulse test with the slurry flow as a method to sense level.	Due to clogging issues, run was unsuccessful.	None.

Run	Date	Component(s)	Objective	Outcomes	Observations
73	20/08/2015	CO <sub>2</sub> /water	Replicate of Run 72.	Pulse test program worked but there was a small programming issue. Also, there was an emergency shutdown because workers had disconnected our CO <sub>2</sub> sensor power in the hallway.	None.
74	25/08/2015	CO <sub>2</sub> /water/slurry	Replicate of Run 72 with a new slurry.	The pulse test seemed to be calculating, but the results did not seem to be reliable. The system went on emergency shutdown when the flow was switched to slurry as a result of splashing (as in Run 71).	None.
75	31/08/2015	CO <sub>2</sub> /water/slurry	Replicate of Run 74 with increased time between pulses and the angle of the slurry inlet line towards vessel wall to help with splashing issue.	The pulse test worked better by increasing time between pulses. Successfully switched the system to slurry without splashing and emergency shutdown. Unfortunately, there was an emergency shutdown for splashing when the flow was switched back to water.	None.
76	9/09/2015	CO <sub>2</sub> /water/slurry	Conduct a controlled pulse test with the position of the level sensor at the top of the vessel opposite the slurry inlet (instead of being at the centre). The sensitivity of the level sensor at the top was also slightly changed. Take mass transfer samples.	Controlled pulse test did not work and it suddenly decreased slurry pump speed from 20% to 1%. After the pulse test was terminated, the system was switched to slurry (controlling level manually) to get mass transfer samples. However, after 10 min there was freezing in the separator and run had to be terminated.	Less than 1L of slurry was drained from the bottom of the vessel.
77	16/09/2015	CO <sub>2</sub> /water/slurry	Conduct a controlled pulse test with a new separator inlet line was switched from 1/8" to 1/4" to prevent freezing issues. Take mass transfer samples.	Controlled pulse test is still not working due to a programming bug. Run was terminated in the end because CO <sub>2</sub> pump could not pressurize due to the CO <sub>2</sub> tank getting near empty.	None.

<b>Run</b>	<b>Date</b>	<b>Component(s)</b>	<b>Objective</b>	<b>Outcomes</b>	<b>Observations</b>
78	3/11/2015	CO <sub>2</sub> /water/slurry	Take mass transfer samples new slurry (with soap + heavy solids removed to prevent pulsing of pump).	The vessel high level alarm was activated due to splashing in first attempt, therefore run was terminated. The second attempt was good.	None.
79	10/11/2015	CO <sub>2</sub> /water	Test level control with pulsing water flow.	The pulse level control is still not working, this time because of an issue with a controller parameter.	None.
80	17/11/2015	CO <sub>2</sub> /water	Replicate Run 79.	Good run as the level measurements are consistent. However, the pump control part is still not working as expected.	None.
81	26/01/2016	CO <sub>2</sub> /water	Test the model-based controller on the process and compare its performance with the previous manual based controller.	Successful run. Run had to be terminated at the end because of freezing near the separator.	None.
82	24/08/2016	CO <sub>2</sub> /water	Test the level controller and compare the experimental result to the model prediction.	Unsuccessful run. The level controller was not calculating realistic levels and the pump control would shut off the slurry pump instead of lowering the speed in set increments.	None.

Based on Table 3.6, it can be seen that the general phased development of the process occurred from pressure testing with CO<sub>2</sub> only, to CO<sub>2</sub> with water, then to CO<sub>2</sub> with slurry. By Run 35, the process was operating as it is currently. That is, no major changes were made to the equipment or experimental procedures beyond Run 35.

From the 82 total runs completed on the process, the 12 runs summarized in Table 3.7 are the runs that meet the functionality objectives presented in Section 3.1, that is runs in which slurry (not water) was processed and they were not aborted due to process issues (e.g., emergency shutdowns, lines or valves freezing, major equipment malfunction, running out of CO<sub>2</sub>).

From the remaining 70 runs, only 5 runs (i.e. Runs 15, 24, 40, 42 and 44) completely failed to initialize. The problem in Runs 15 and 24 was associated with the CO<sub>2</sub> feed tank - CO<sub>2</sub> pump incompatibility. The problem in Run 40 was associated with pumping a high solids concentration slurry. Because of the configuration of the slurry pump upstream line and also the incapability of the mixer to provide a completely homogeneous mixture, a very thick slurry was delivered to the slurry pump. The thick slurry resulted in the slurry pump output pulsing, and therefore malfunctioning of the slurry pump. The problem in Runs 42 and 44 was associated with freezing/blockage (in the slurry outlet line from the extraction vessel) of unknown origin.

From the remaining 66 runs, 55 runs were partially or completely successful in reaching their proposed objective. The remaining 11 runs (i.e. Runs 48, 49, 50, 51, 54, 57, 60, 62, 63, 72 and 82) failed in reaching their objectives (as outlined in Table 3.6). The failures were due to different reasons such as activation of an emergency alarm, freezing in lines, CO<sub>2</sub> leak in the process, etc. The design evolved to address these factors.

**Table 3.7. Summary of runs, with operating conditions, that meet the functionality objectives**

Run	Pressure (MPa)	Temperature (°C)	CO <sub>2</sub> flow (L/min)	Slurry flow (L/min)	Slurry solids (% wt.)	Duration (s)	Duration (min)
35	13.5	41.3	0.96	2.7	0.24	2030	34
36	13.9	44.9	0.97	2.5	0.16	2493	42
37	13.8	41.0	1.0	2.5	1.1	2395	40
38	13.9	44.1	0.86	2.7	3.0	1923	32
39	13.3	37.7	1.5	2.0	2.8	414	7
41	10.3	38.8	1.1	2.5	2.5	2557	43
	14.0	45.4	0.64	2.1			
55	10.0	42.7	0.70	2.3	2.6	1700	28
	14.0	41.1	1.3	2.6			
56	14.0	32.6	1.5	2.4	2.5	428	7
58	17.9	42.2	1.9	3.1	2.3	1331	22
59	17.9	43.2	1.7	3.4	2.1	1755	29
67	13.9	40.6	2.0	2.6	1.7	1355	23
78	13.9	34.1	1.4	3.3	0.5	1530	26

The pressures and temperatures listed in Table 3.7 are the averages of measured values from both sensors (one of each located at the top and bottom of the extraction vessel) over the duration of the run. The flow rates are the average value of each pump speed, converted to L/min, also over the duration of the run. The duration is calculated as the time during the run where:

- the vessel has reached at least 7.4 MPa at the pressure sensors on the top and the bottom of the extraction vessel;
- the temperature is at least 31°C at the temperature sensors on the top and bottom of the extraction vessel; and
- the extraction vessel is being operated countercurrently with CO<sub>2</sub> and slurry.

For all the runs in Table 3.7, the duration start point occurred once the bottom

temperature sensor reached 31°C. The duration end point was when the slurry feed was switched to the rinse water feed. As an example of the duration of a typical run, Figure 3.12 shows the pressure and temperature in the vessel at both the top and bottom sensors over the length of Run 38. In this case, the bottom temperature sensor reads 31°C at 2100 s. The feed was switched to rinse water at 4023 s, for a total duration of 1923 s.

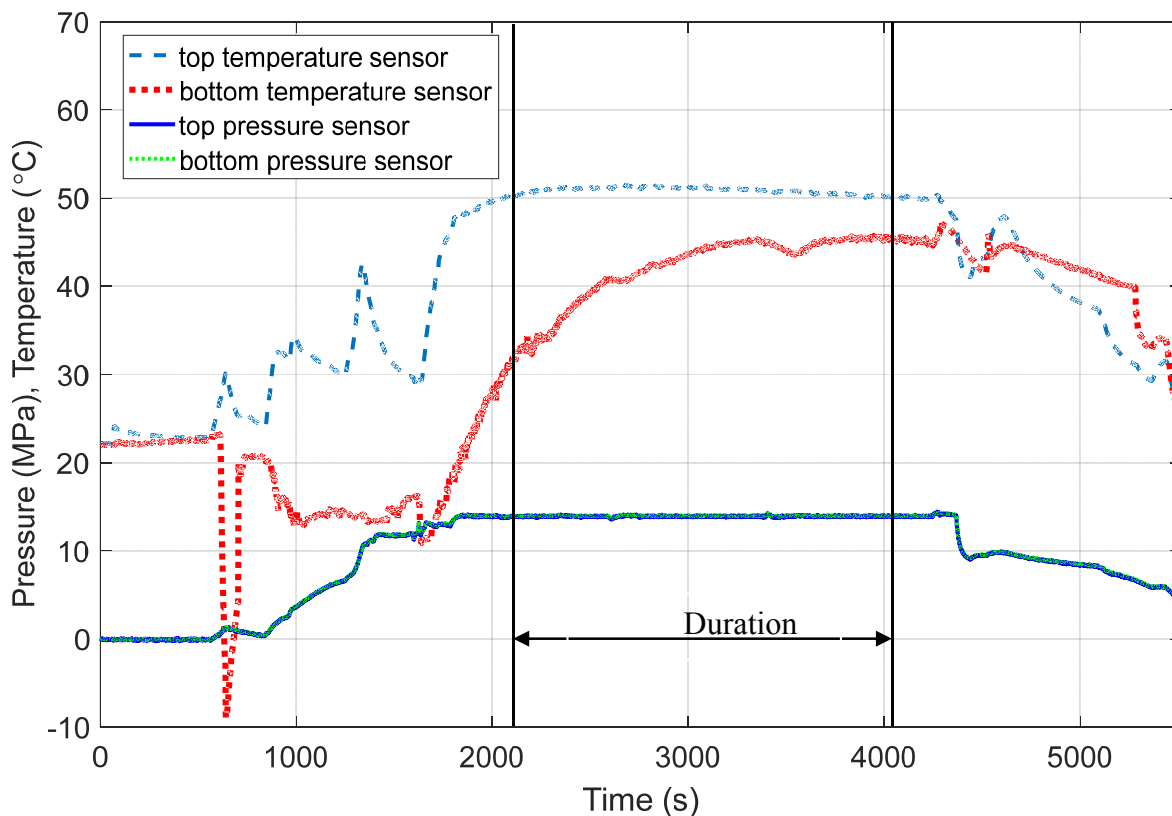


**Figure 3.12. Pressure and temperature at top and bottom sensors over Run 38**

Figure 3.12 also shows that the total typical run time was longer than the duration listed in Table 3.7, and as a matter of functionality, most of the extra time in a given run was also under SC-CO<sub>2</sub> and countercurrent flow conditions using water instead of slurry (bringing the process up to pressure and rinsing under pressure at the end of the run). Although there has to be boundaries set to determine functionality of the process, the duration listed in Table 3.7 is shortened by considering both temperature sensors instead of an average. Because of its location near the incoming CO<sub>2</sub>, which tends to be cold, the bottom sensor always dictated the start of the run duration. However, by that point in time, supercritical conditions would prevail in a majority of the extraction vessel length.

For Runs 41 and 55, where two pressure set points were tested without stopping and re-starting the process, the transition period was also counted in the duration. However, average pressure, temperature and flow rates (not including the transition period) were determined for each segment of the run.

Finally, for experiments in which oil-contaminated slurry was processed, SC-CO<sub>2</sub> successfully extracted oil from the slurry phase. After select runs, once the process was depressurized, the accumulated oil in the separator was pumped out. A sample of the collected oil is presented in Figure 3.13.

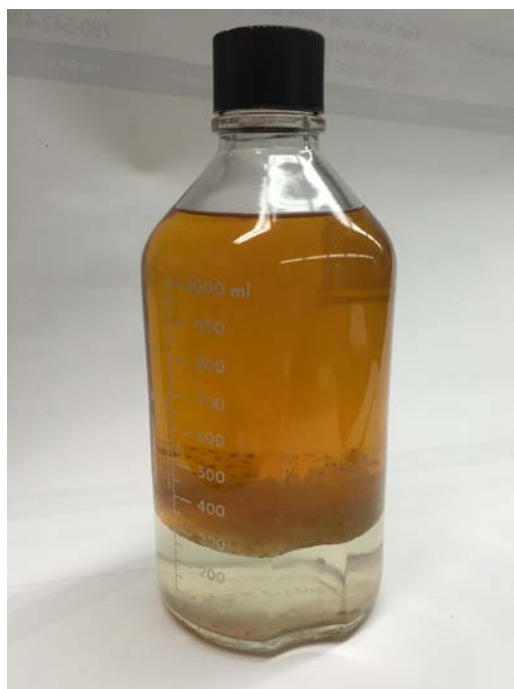


**Figure 3.13. Oil collected from the separator for Runs 39 and 41**

### **3.5 Summary**

To solve the problem of oil-contaminated drill cuttings, a continuous pilot scale SFE process, including both the physical equipment and a control system capable of maintaining process variables, has been successfully developed. This chapter has detailed the development from design, to construction, to commissioning and operation. The objective of the chapter is to demonstrate that the process can extract oil from water-slurried cuttings under supercritical conditions (above 7.4 MPa and 31°C) using continuous, countercurrent flow.

From the basis of a previous preliminary design, modifications to flow specifications, lab layout, P&ID, control philosophy, operation manual and HAZOP were completed. Construction of the process was also successful, despite the challenges in procuring equipment for a novel SFE process of this scale.

For commissioning the process, 82 experimental runs were completed. The initial runs were mostly aimed at troubleshooting the process to ensure it was operating as expected. As necessary, equipment and procedural changes were made. The majority of the remaining runs were aimed at gathering data for mass transfer and control studies.

Of the 82 experimental runs, 12 directly demonstrated the functionality of the process as solution to the drill cuttings problem. That is, the process extracted oil from slurried cuttings while maintaining supercritical conditions in the extraction vessel (above 7.4 MPa and 31°C for CO<sub>2</sub>); operating in a countercurrent, continuous flow scheme; and running for duration of time without process upsets or emergency shut downs. Over the course of these runs, the process operated at pressures from 10.0 to 17.9 MPa; temperatures from 31.6 to 45.4°C; slurry flow rates from 2.0 to 3.4 L/min; CO<sub>2</sub> flow rates from 0.64 to 2.0 L/min and slurry solids concentration varied between 0.16 to 3 wt%. The experimental run durations, varied from 7 to 43 minutes.

Safe process operation was integrated into all phases of the process development. The evidence is documented throughout this chapter, including: an updated HAZOP on the as-built design; integration of the CO<sub>2</sub> alarms into Central Control of the University of Alberta; and updating the system process alarms/modes. The environmental monitoring and process alarm safety features activated appropriately in a number of the 82 runs completed.

The novel SFE process built for this project, which is the first of its kind, has been shown to be functional over a range of pressures, temperatures, solids concentrations, and flow rates. The process operates safely, and can extract oil from a slurried solid phase. As a solution to the drill cuttings problem, this is a major step towards a commercial process. Future work would expand the range of the process variables studied i.e. temperature, pressure, CO<sub>2</sub> flowrate, slurry flowrate, slurry solids concentration and it would include investigating the extraction of oil from other types of solid slurries.

## 4 A Hydrodynamic Model for the Fully Continuous Pilot Scale SFE Process

## 4.1 Introduction

This chapter focuses on dynamic (unsteady state) modelling of the continuous pilot scale SFE process under investigation in this thesis. Dynamic modelling of a process is associated with describing changes of independent variables as a function of time, that is, describing the transient behaviour of the process (Roffel and Betlem, 2003). Generally, three main approaches exist for modelling chemical processes (Huang *et al.*, 2013). The first approach is mathematical modelling, also known as first principle modelling, because it is an analytic method based on fundamental laws of physics and chemistry such as the laws of conservation of mass, energy and momentum. The second approach is based on experimental data and is known as process or system identification. In this method, a model is fitted to the data obtained from the real process. The third approach is a combination of the first two approaches in which the model is based on fundamental laws but it also contains empirical parameters due to lack of understanding of the process or lack of information (Soderstrom and Stoica, 2001). These empirical parameters can be estimated from data obtained from the actual process if available.

In comparing mathematical modelling and process identification, mathematical modelling has advantages from the standpoint that it gives physical insight to the process and is not restricted to certain operating conditions. Parameters of a model obtained through process identification do not have a physical meaning and the model is valid around the operating conditions at which measurements were taken from the process (Roffel and Betlem, 2003). However, there are scenarios in which limited time is available and/or the process is too complex to be explained by first principle equations. In this case, if the actual process is available, a model based on process identification is superior in comparison to the first approach i.e. mathematical modelling.

One important objective of the dynamic modelling of a chemical process is to better understand the dynamic (or transient) behaviour of the process. This understanding can serve various purposes (Luyben, 1996; Schmal, 2013). Some examples include scenario testing at various operating conditions of the process, conducting control tests and optimization, simulating start-up and shutdown procedures and troubleshooting the process. It is quite obvious that conducting these kinds of experiments with a representative model can be cheaper, safer and faster than conducting them on the actual process (Luyben, 1996).

The SFE process in this study deals with high pressures, specifically pressures over 7.4 MPa, the critical pressure of CO<sub>2</sub> (Span and Wagner, 1996). Therefore, maintaining pressure at a desired set point is necessary to ensure safe operation of the chemical process. Pressure control also contributes to consistent extractions (resulting in uniform product quality) due to the direct relationship between mass transfer and pressure throughout an SFE process. Hence, effective control of pressure in this process will specifically lead to uniform product quality as well as increased process safety.

Also, in liquid-liquid (liquid-fluid) extraction processes such as the SFE process in this study, level control of the dispersed phase is also important in order to have a reliable operation (Weinstein *et al.*, 1997). Otherwise overflowing of the vessel (flooding) or emptying the vessel might occur in the extraction vessel leading to operational complications.

Hence, pressure and liquid level in the extraction vessel of the continuous SFE process are the two main variables of interest and it is of primary importance to explore the dynamic behaviour of these two variables. Therefore, a hydrodynamic model is constructed for the SFE process and its main purpose is to predict pressure and level response in the extraction vessel at different operating conditions. This model will be applied for different purposes including controller design. Application of the model for control is the focus of Chapter 5 and Chapter 6. To summarize, the objective of this study is to characterize the continuous pilot scale SFE process with a hydrodynamic model. The capability of the model to predict pressure and slurry level at different operating conditions is tested by comparing with responses obtained from the pilot scale SFE process.

Characterizing the SFE process with a hydrodynamic model is broken down into four steps: (i) model development, (ii) implementation, (iii) verification and (iv) validation (Kleijnen, 1995; Schmal, 2013). Model development is associated with generating a mathematical model that is a translation of the physical process under study (Schmal, 2013). Model implementation is concerned with transition from the mathematical world to the numerical world. For this purpose, an appropriate numerical solver should be selected and initial conditions should be defined. Model verification is associated with determining whether the implemented model works as expected. Model validation focuses on determining how precisely the model represents the actual process (Kleijnen, 1995; Luyben, 1996).

In the following sections of this chapter each of these phases are explored in detail. In Section 4.2, model development and model implementation are presented. The results and discussion section of model verification and model validation are given in Section 4.3. The summary is presented in Section 4.4.

## **4.2 Hydrodynamic model**

This section is broken down into two parts: model development and model implementation. For consistency throughout subsequent sections, the “process” refers to the physical reality that provides the experimental data while the “system” represents a mathematical description of the process. These definitions have been adopted from Soderstrom and Stoica (2001).

### **4.2.1 Model development**

The model development phase is associated with transforming the physical domain into mathematical equations (Schmal, 2013). As stated earlier, pressure and level in the extraction vessel are the two important variables of the SFE process. Therefore, mathematical equations are selected to develop a hydrodynamic model of the process that will describe the transient response (behaviour) of pressure and slurry level inside the extraction vessel.

A simple schematic diagram of the process used for modelling is presented in Figure 4.1. For modelling purposes, streams are numbered. Control volumes are also indicated by dashed lines. The extraction vessel and two inlet pumps comprise Control Volume A. Control Volume B surrounds the metering valve for the CO<sub>2</sub> outlet while Control Volume C surrounds the manifold for the slurry outlet.

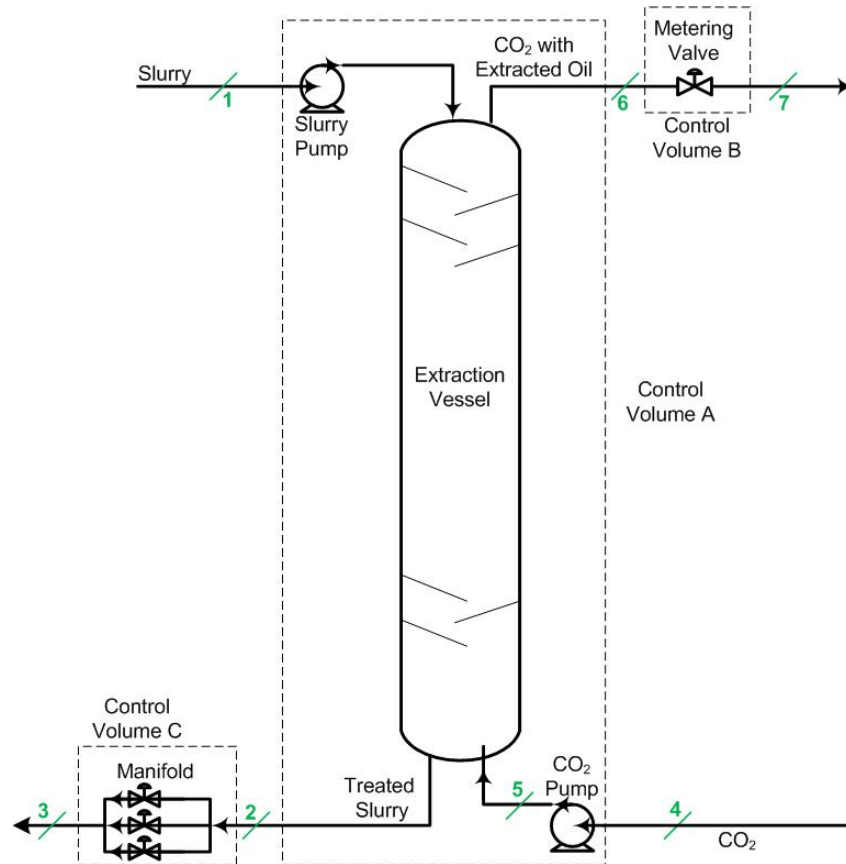


**Figure 4.1. Selected control volumes and streams for modelling**

First principle mathematical equations were selected which would lead to a hydrodynamic model of the process demonstrating transient behaviour of pressure and slurry level. The derived equations are based on the following first principles:

1. Continuity equation for CO<sub>2</sub>
2. Continuity equation for slurry
3. Energy balance
4. An equation of state (EOS) for CO<sub>2</sub>
5. Density-Volume-Mass relationship for CO<sub>2</sub>

In the following subsections, derivations of the above equations are presented.

In mathematical modelling of a process, modelling assumptions form an important section of the modelling procedure. No model is perfect because it will always be based on some assumptions. As a matter of fact, the perfect model would be the real process itself. And by

definition, any other model will always be a *simplification* of the real process (Kleijnen, 1995). However, the level of model accuracy depends on the level of detail and on the assumptions selected by the modeller, which in turn will depend on the purpose of the modelling (Schmal, 2013).

In the model development stage, assumptions with regard to each of the above equations are stated in the corresponding section and an explanation is given to why a certain assumption is made at this stage. Most of the assumptions are based on observations from the SFE process. In the model verification section, the effect of assumptions on process response is discussed and modifications are made to assumptions if deemed necessary.

The first, and potentially most important, assumption regarding all five equations is that the extraction vessel is ideally mixed and intensive thermodynamic properties such as temperature and pressure are lumped to an overall average and not distributed.

In order to better classify quantities that appear in the modelling, the following definitions are adopted from Pajonk (2009):

1. Variables: quantities whose value change with time.
2. Parameters: quantities whose value can be changed but a change will result in a new problem.
3. Constants: quantities whose value can never be changed and are physically fixed.

In this process, quantities such as pressure, temperature, CO<sub>2</sub> density in the vessel, etc. are “variables” because for a fixed set of conditions, their value changes with time. These variables depend on and are determined by the parameters selected for the process and the nature of the process/system itself. Quantities such as CO<sub>2</sub> flow, slurry flow, etc. are defined as “parameters” since they may have different values but a new value will result in a new problem, or in other words, a different state/condition of the process. Therefore, for each simulation, it is necessary to state the values used for these quantities. Quantities such as vessel surface area, vessel volume, manifold tube diameter, etc. are considered as “constants” (within the scope of this thesis) because each has a fixed value in this process and this fixed value is applied in all simulations.

Quantities used in the modelling equations are provided in Table 4.1. It should be noted that the numerical subscripts used for the quantities in Table 4.1 refer to the stream numbers presented in Figure 4.1.

**Table 4.1. Quantities used in modelling equations**

Quantity	Description	Unit	Type
<i>CO<sub>2</sub> continuity equation</i>			
$\dot{m}_4$	Mass flowrate of CO <sub>2</sub> entering	kg/s	parameter
$\dot{m}_6$	Mass flowrate of CO <sub>2</sub> exiting	kg/s	variable
$m$	Mass of CO <sub>2</sub> inside the vessel	kg	variable
$t$	time	s	variable
$Q_4$	Volumetric flowrate of CO <sub>2</sub> entering	m <sup>3</sup> /s	parameter
$\rho_4$	Density of CO <sub>2</sub> entering	kg/m <sup>3</sup>	parameter
<i>Metering valve equation*</i>			
$Q_6$	CO <sub>2</sub> volumetric flowrate	ft <sup>3</sup> /h	variable
$C_V$	Valve coefficient of flow	unitless	constant
$f_V$	Metering valve fractional opening	fractional	parameter
$P_6$	Inlet pressure to valve	psia	variable
$P_7$	Outlet pressure from valve	psia	variable
$S_G$	Gas specific gravity	unitless	variable
$S_{GF}$	Liquid specific gravity	unitless	variable
$T_6$	Stream temperature	°R	variable
$\rho_6$	Density of CO <sub>2</sub> exiting	kg/m <sup>3</sup>	variable
<i>Slurry continuity equation</i>			
$Q_1$	Volumetric flowrate of slurry entering	m <sup>3</sup> /s	parameter
$Q_2$	Volumetric flowrate of slurry exiting	m <sup>3</sup> /s	variable
$z$	Slurry level inside the vessel	m	variable
$A_v$	Cross sectional area of extraction vessel	m <sup>2</sup>	constant

Quantity	Description	Unit	Type
<i>Manifold equation</i>			
$f$	Darcy friction factor	unitless	variable
$\varepsilon$	Average wall roughness	unitless	constant
$d$	Inner diameter of manifold tube	m	parameter
$A_t$	Cross sectional area of manifold tube	m <sup>2</sup>	parameter
$\mu_s$	Slurry viscosity	Pa.s	parameter
$\Delta P$	Pressure difference between two sides of the manifold	Pa	variable
$l$	Length of manifold	m	parameter
$\rho_s$	Slurry density	kg/m <sup>3</sup>	parameter
$v$	Linear velocity of slurry flow through manifold	m/s	variable
<i>Energy balance</i>			
$U_s$	Total slurry internal energy	J	variable
$U_{CD}$	Total CO <sub>2</sub> internal energy	J	variable
$U_v$	Total vessel internal energy	J	variable
$h_1$	Slurry specific enthalpy entering	J/kg	parameter
$h_2$	Slurry specific enthalpy exiting	J/kg	variable
$h_4$	CO <sub>2</sub> specific enthalpy entering	J/kg	parameter
$h_6$	CO <sub>2</sub> specific enthalpy exiting	J/kg	variable
$C_s$	Slurry heat capacity	J/kg.K	parameter
$C_{VCD}$	CO <sub>2</sub> constant volume heat capacity	J/kg.K	variable
$C_{ve}$	Vessel heat capacity	J/kg.K	constant
$m_{ve}$	Mass of extraction vessel	kg	constant
$\dot{m}_1$	Mass flowrate of slurry entering	kg/s	parameter
$\dot{m}_2$	Mass flowrate of slurry exiting	kg/s	variable
$\dot{m}_4$	Mass flowrate of CO <sub>2</sub> entering	kg/s	parameter
$\dot{m}_6$	Mass flowrate of CO <sub>2</sub> exiting	kg/s	variable
$m_s$	Mass of slurry in the vessel	kg	variable
$h_s$	Slurry specific enthalpy in the vessel	J/kg	variable
$P$	Pressure in the vessel	Pa	variable
$\rho$	CO <sub>2</sub> density in the vessel	kg/m <sup>3</sup>	variable
$T$	Temperature in the vessel	K	variable
$\dot{Q}$	Heating tape heating rate	J/s	parameter
$\dot{W}_{pump}$	Power input of slurry and CO <sub>2</sub> pumps	J/s	variable
<i>CO<sub>2</sub> equation of state</i>			

Quantity	Description	Unit	Type
$A$	Molar Helmholtz energy	J/mol	variable
$R$	Specific gas constant	kJ/kg.K	constant
$\phi$	Dimensionless Helmholtz energy	unitless	variable
$\phi^o$	Ideal gas part of the dimensionless Helmholtz energy	unitless	variable
$\phi^r$	Residual part of the dimensionless Helmholtz energy	unitless	variable
$\rho_c$	CO <sub>2</sub> critical density	kg/m <sup>3</sup>	constant
$T_c$	CO <sub>2</sub> critical temperature	K	constant
$\tau$	Reduced temperature	unitless	variable
$\delta$	Reduced density	unitless	variable
<i>Density-Volume-Mass relationship</i>			
$V$	Volume of the extraction vessel	m <sup>3</sup>	constant

\*Units presented in Imperial as provided in the valve literature (Autoclave Engineers, 2012)

As will be explained in succeeding sections, the four important parameters that are expected to have an effect on pressure and slurry level inside the extraction vessel, are slurry flowrate (calculated based on slurry pump speed), CO<sub>2</sub> flowrate (calculated based on CO<sub>2</sub> pump speed), metering valve opening and manifold length. These are considered as the inputs of the process. Values chosen for these parameters are discussed in related sections. Values applied in modelling for the remaining parameters and constants of each equation are summarized at the end of corresponding subsections of each equation.

#### 4.2.1.1 Continuity equation for CO<sub>2</sub>

As illustrated in Figure 4.1, a CO<sub>2</sub> stream (Stream 4) enters the CO<sub>2</sub> pump and exits from the top of the extraction vessel (Stream 6). Hence, the continuity equation for the mass of CO<sub>2</sub> in Control Volume A (denoted as  $m$ ) is defined as:

$$\frac{dm}{dt} = \dot{m}_4 - \dot{m}_6 \quad (4.1)$$

In Equation 4.1, the mass flowrate of the stream entering Control Volume A ( $\dot{m}_4$ ) is a set parameter and is calculated as:

$$\dot{m}_4 = \rho_4 Q_4 \quad (4.2)$$

In Equation 4.2, the density of CO<sub>2</sub> is based on the pressure and temperature of Stream 4. In the SFE process, CO<sub>2</sub> is directly supplied from a CO<sub>2</sub> tank that is maintained at a pressure of

approximately 2.5 MPa. The temperature of the liquid CO<sub>2</sub> leaving the tank however is not known and as the CO<sub>2</sub> flows from the storage tank to the CO<sub>2</sub> pump, it slightly absorbs heat from the surrounding atmosphere and warms up. In order to keep the CO<sub>2</sub> at a liquid state for the pump, a cooling cauldron has been placed between the CO<sub>2</sub> feed tank and the pump. The cauldron temperature is maintained at approximately -15 °C. Based on this information, the density of CO<sub>2</sub> in Stream 4 is calculated based on a pressure and temperature of 2.5 MPa and -15 °C, respectively.

Calculating the mass flowrate of CO<sub>2</sub> exiting Control Volume A is a bit more complicated because it goes through an automated metering valve (i.e. Control Volume B) upon exiting the vessel. The automated metering valve that exists in the process is a Parker Autoclave Engineers Electronic Flow Control valve (Autoclave Engineers, 2012). The valve coefficient of flow ( $C_V$ ) and the various flow formulas are provided in the valve literature depending on the state of the fluid going through the valve i.e. liquid, gas, superheated steam or saturated steam. In the extraction vessel, CO<sub>2</sub> will be changing state from gas to liquid and finally to supercritical depending on the pressure and temperature of the process. And as the CO<sub>2</sub> goes through the automated metering valve, CO<sub>2</sub> changes phase from supercritical to liquid or gas. A flow formula for SCFs is not provided in the valve literature. Hence, the liquid mass flowrate and gas volumetric flowrate are chosen as the two applicable choices for the metering valve in the SFE process. The liquid mass flowrate equation provided in the valve literature is:

$$\dot{m}_6 = \frac{500 C_V f_V \sqrt{(P_6 - P_7)}}{\sqrt{S_{GF}}} \quad (4.3)$$

In Equation 4.3, the specific gravity ( $S_{GF}$ ) is calculated relative to the density of water at 20 °C and atmospheric pressure, that is 998.21 kg/m<sup>3</sup> (Linstrom and Mallard, 2015).

The gas volumetric flowrate (temperature corrected) provided in the valve literature is:

$$Q_6 = \frac{963 C_V f_V \sqrt{(P_6 - P_7)(P_6 + P_7)}}{\sqrt{S_G T_6}} \quad (4.4)$$

In Equation 4.4, the specific gravity ( $S_G$ ) is calculated relative to the density of dry air at 20 °C and 101.325 kPa, that is 1.205 kg /m<sup>3</sup>.

The  $f_V$  factor in Equations 4.3 and 4.4 is added to represent the fractional opening of the

automated metering valve. It should be noted that the inlet pressure ( $P_6$ ) and inlet stream temperature ( $T_6$ ) are equal to the pressure and temperature inside the extraction vessel. The density for Stream 6 ( $\rho_6$ ), which is required to calculate  $S_G$  and  $S_{GF}$ , is also equal to the density of CO<sub>2</sub> inside the vessel.

The pressure after the metering valve ( $P_7$ ) in Equations 4.3 and 4.4 is a function of the pressure before the metering valve ( $P_6$ ). The pressure before the metering valve itself is equal to the pressure inside the extraction vessel. For simplicity in this stage of modelling, the following assumption is made:

*Assumption 1:*  $P_7$  assumed to be constant (i.e. a set parameter) and equal to 2.5 MPa. This pressure (2.5 MPa) is the approximate pressure observed after the metering valve in the SFE process when the pressure in the extraction vessel is at 14 MPa.

By applying Equation 4.3 and a unit conversion, the mass flowrate of CO<sub>2</sub> is calculated in kg/s. By applying Equation 4.4 and a unit conversion, the volumetric flowrate of CO<sub>2</sub> is calculated in m<sup>3</sup>/s. In this case, the mass flowrate of CO<sub>2</sub> exiting process boundaries is calculated as:

$$\dot{m}_6 = \rho_6 Q_6 \quad (4.5)$$

Both Equations 4.3 and 4.4 can be used to calculate the flowrate of CO<sub>2</sub> through the metering valve. The use of both of these equations and their results are compared and discussed in Section 4.3.2.

Table 4.2 summarizes the applied values of constants and parameters in the equations related to the continuity equation.

**Table 4.2. Values of constants and parameters in CO<sub>2</sub> continuity equation**

Quantity	Unit	Value	Reference
$\rho_4$	kg/m <sup>3</sup>	1.009 x10 <sup>3</sup>	Based on -15 °C and 2.5 MPa (Span and Wagner, 1996)
$C_V$	unitless	4.000 x10 <sup>-3</sup>	Valve literature (Autoclave Engineers, 2012)

#### 4.2.1.2 Continuity equation for slurry

As shown in Figure 4.1, in Control Volume A, a slurry stream enters the top of the extraction vessel (Stream 1) and exits from the bottom of the extraction vessel (Stream 2). The

change of slurry level ( $z$ ) inside the vessel is determined by converting the mass flow into a volumetric flow in the slurry continuity equation by applying the assumption of incompressible flow. The resulting continuity equation for slurry is:

$$A_v \frac{dz}{dt} = Q_1 - Q_2 \quad (4.6)$$

The slurry volumetric flow rate entering Control Volume A ( $Q_1$ ) is calculated based on the slurry pump speed. The slurry exiting the vessel however goes through a manifold (Control Volume C) and its flowrate ( $Q_2$ ) is calculated by applying the Darcy-Weisbach equation for the pressure drop in a circular pipe:

$$\Delta P = f \frac{l \rho_s v^2}{d} \quad (4.7)$$

and the Swamee-Jain equation to calculate the Darcy friction factor for turbulent flow:

$$f = \frac{0.25}{\left[ \log_{10} \left[ \frac{\varepsilon}{3.7d} + \frac{5.74}{Re^{0.9}} \right] \right]^2} \quad (4.8)$$

where  $Re$  is the Reynolds number defined as:

$$Re = \frac{\rho_s v d}{\mu_s} \quad (4.9)$$

in which  $Re > 4000$  i.e. flow in the pipe is turbulent.

The Darcy-Weisbach equation is valid for fully developed and steady flows in a circular pipe (Potter and Wiggert, 2002). The Swamee-Jain equation is one of the explicit equations in terms of  $f$  that was proposed for calculating  $f$  in the Darcy-Weisbach equation (Swamee and Jain, 1976).

After calculating slurry velocity ( $v$ ) from Equations 4.7, 4.8, and 4.9, volumetric flow of slurry exiting the process boundaries is calculated as:

$$Q_2 = v A_t \quad (4.10)$$

In Equation 4.7,  $\Delta P$  is the pressure difference on two sides of the manifold. The pressure before the manifold is affected by the pressure generated by the  $CO_2$  and the head of slurry inside the extraction vessel. The maximum pressure generated as a result of slurry level

(equivalent to 2.5 m) is 0.0245 MPa. This small portion is safely neglected.

An important aim when designing the manifold was to drop the pressure of the slurry coming from the extraction vessel to around atmospheric pressure. Hence, the pressure after the manifold is assumed to be 0.6895 MPa (equivalent to 100 psia), which is the pressure observed in the SFE process via a pressure gauge located after the manifold.

The following assumption is made for extracting properties of slurry:

*Assumption 2:* Slurry dynamic viscosity and density is assumed to be those of water at 45 °C and 10 MPa.

The reason for this assumption is that slurries treated via the pilot scale process for this project, specifically at the early stages of experimentation were dilute and hence it is safe to assume the properties of water instead of slurry. In addition, although the pressure changes in the process, it will not have a significant effect on water density and viscosity. Therefore, a constant pressure of 10 MPa is assumed for extracting water properties. The temperature of 45 °C is the approximate temperature of the slurry in the slurry feed tank as a result of a heating element installed in the tank.

Table 4.3 summarizes the applied values of constants and parameters in the equations related to the continuity equation.

**Table 4.3. Values of constants and parameters in slurry continuity equation**

Quantity	Unit	Value	Reference
$A_v$	m <sup>2</sup>	5.45 x10 <sup>-3</sup>	(Price-Schonstrom, 2009)
$\varepsilon$	m	1.50 x10 <sup>-5</sup>	(Moody, 1944)
$d$	m	1.753 x10 <sup>-3</sup>	(Swagelok, 2015)
$A_t$	m <sup>2</sup>	2.41 x10 <sup>-6</sup>	N/A
$\rho_s$	kg/m <sup>3</sup>	9.94 x10 <sup>2</sup>	(NIST,2015)
$\mu_s$	Pa.s	5.97 x10 <sup>-4</sup>	(NIST,2015)

#### 4.2.1.3 Energy balance

The conservation of energy for Control Volume A is expressed as:

$$\frac{dU_s}{dt} + \frac{dU_{CD}}{dt} + \frac{dU_v}{dt} = (h_1\dot{m}_1 - h_2\dot{m}_2) + (h_4\dot{m}_4 - h_6\dot{m}_6) + \dot{Q} + \dot{W}_{pump} \quad (4.11)$$

The left side of the equation represents the rates of internal energy change for the slurry, CO<sub>2</sub> and

vessel itself. The right side of the equation characterizes the energy entering and exiting the process boundaries (Control Volume A) by means of the CO<sub>2</sub> and slurry streams. The rate of work done as well as the net rate of heat transfer on the process are also on the right side of the energy balance equation. The rate of work done is associated with slurry and CO<sub>2</sub> pumps. The net rate of heat transfer is related to heat from heating tape located on the vessel and heat transfer between the vessel and the surrounding environment.

To derive the temperature change inside the vessel, Equation 4.11 needs to be modified. The following relationship exists between the internal energy and the specific internal energy:

$$U = mu \quad (4.12)$$

An exact differentiation of Equation 4.12 yields:

$$\frac{d(mu)}{dt} = m \frac{du}{dt} + u \frac{dm}{dt} \quad (4.13)$$

The time derivative of the specific internal energy is stated as:

$$\frac{du}{dt} = \frac{du}{dT} \frac{dT}{dt} \quad (4.14)$$

where  $du/dT$  is recognized as the constant volume heat capacity:

$$C_v = \left( \frac{du}{dT} \right)_{v=const.} \quad (4.15)$$

Substituting Equations 4.14 and 4.15 into Equation 4.13 results in:

$$\frac{d(mu)}{dt} = mC_v \frac{dT}{dt} + u \frac{dm}{dt} \quad (4.16)$$

The following relationship exists between the specific internal energy and the specific enthalpy:

$$u = h - Pv = h - \frac{P}{\rho} \quad (4.17)$$

Therefore, the specific internal energy on the right side of Equation 4.16 is substituted to give:

$$\frac{d(mu)}{dt} = mC_v \frac{dT}{dt} + \left( h - \frac{P}{\rho} \right) \frac{dm}{dt} \quad (4.18)$$

Inserting Equation 4.18 for the CO<sub>2</sub>, slurry and vessel internal energies into Equation 4.11 results in:

$$m_s C_s \frac{dT}{dt} + \left( h_s - \frac{P}{\rho_s} \right) \frac{dm_s}{dt} + m C_{vCD} \frac{dT}{dt} + \left( h - \frac{P}{\rho} \right) \frac{dm}{dt} + m_{ve} C_{ve} \frac{dT}{dt} = (4.19)$$

$$(h_1 \dot{m}_1 - h_2 \dot{m}_2) + (h_4 \dot{m}_4 - h_6 \dot{m}_6) + \dot{Q} + \dot{W}_{pump}$$

In this form of the energy balance (Equation 4.19), dT/dt exists and is solved to depict the change of temperature in the process. It should be noted that the enthalpies present in Equation 4.19 are specific enthalpies (J/kg).

For determining the required CO<sub>2</sub> pump power (in horsepower), Equation 4.20 is proposed in the CO<sub>2</sub> pump literature (Cat Pumps, 2008):

$$\dot{W}_{CO_2 pump} = \frac{GPM \times PSI}{1460} \quad (4.20)$$

In Equation 4.20, GPM is the volumetric flowrate of liquid through the pump (in gallons per minute) and PSI is the pump downstream pressure (in psi). In order to apply Equation 4.20 and calculate the pump work done on fluids at different pump speeds and process pressures, the pump downstream pressure is required. Based on observations from the SFE process, this pressure is slightly more than the pressure inside the extraction vessel (*P*). Hence, the pressure inside the vessel is used when applying Equation 4.20.

Another approach for calculating the work done by the CO<sub>2</sub> pump is applying the following equation:

$$\dot{W}_{CO_2 pump} = m_4 \Delta h \quad (4.21)$$

In Equation 4.21, Δ*h* is the enthalpy difference between the upstream CO<sub>2</sub> and downstream of the CO<sub>2</sub> pump. The upstream enthalpy is calculated based on the CO<sub>2</sub> inlet conditions i.e. 2.5 MPa and -15 °C and using the Span and Wagner EOS for CO<sub>2</sub> (Span and Wagner, 1996). The downstream enthalpy is calculated based on the pressure and temperature inside the extraction vessel.

The results using either Equation 4.20 or 4.21 for calculating the CO<sub>2</sub> pump work are compared and discussed in Section 4.3.2.

The Bernoulli equation is applied for calculating delivered work by the pump to the fluid.

A schematic of the slurry pump, slurry feed tank and extraction vessel for the pump work calculation is provided in Figure 4.2.

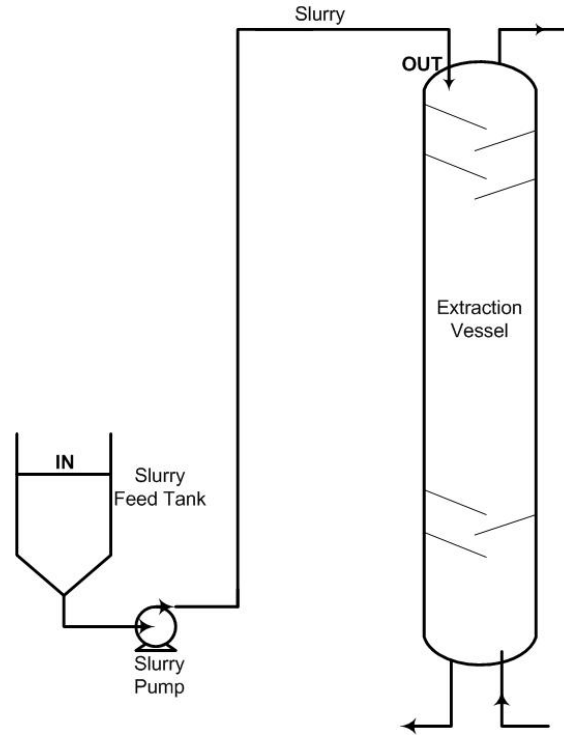


**Figure 4.2. Schematic of the slurry pump, slurry feed tank and extraction vessel**

The energy form of the Bernoulli equation is described as:

$$\frac{P_{out}}{\rho} + \frac{V_{out}^2}{2} + gz_{out} = \frac{P_{in}}{\rho} + \frac{V_{in}^2}{2} + gz_{in} - loss - w_s \quad (4.22)$$

By rearranging Equation 4.22, the work delivered by the pump is calculated as:

$$-w_s = \frac{P_{out} - P_{in}}{\rho} + \frac{V_{out}^2 - V_{in}^2}{2} + g(z_{out} - z_{in}) + loss \quad (4.23)$$

Because the SFE process is associated with high pressures, terms associated with kinetic energy, potential energy and loss are negligible compared to the energy required for pressurizing the fluid. Hence, by simplifying Equation 4.23 and applying a unit conversion, the power supplied to the fluid by the pump is calculated as:

$$-\dot{W}_{slurry\ pump} = Q(P_{out} - P_{in}) \quad (4.24)$$

where  $Q$  is the slurry volumetric flowrate (calculated based on the slurry pump speed),  $P_{in}$  is the

pressure in the slurry tank and  $P_{out}$  is the pressure of slurry entering the extraction vessel, which is equal to the pressure inside the extraction vessel.

As mentioned earlier, the net heat transfer to the process is associated with two sources. A 360 Watt, silicone rubber heating tape with adjustable thermostat control (Omega, 2015) and heat transfer between vessel and the surrounding environment. The heating tape was initially installed at the bottom of the extraction vessel for heating the contents of the vessel. However, no substantial temperature rise was observed inside the extraction vessel. Hence the following assumption is made with regards to process net heat transfer:

*Assumption 3:* Process assumed to be adiabatic i.e. negligible heat transfer to and from the system.

For calculating the enthalpy of the slurry entering the vessel ( $h_1$ ), the enthalpy of water is calculated at 45 °C and atmospheric pressure. The temperature of 45 °C is the approximate temperature of the slurry entering the extraction vessel. As stated earlier, this temperature is a result of a heating element installed in the slurry feed tank.

For calculating the slurry enthalpy exiting the vessel ( $h_2$ ), a linear equation is developed based on slurry at 10 MPa and 20 °C:

$$h_2 = C_s (T - 20) + 93.32 \times 10^3 \quad (4.25)$$

In Equation 4.25,  $T$  is in °C and  $h_2$  is in J/kg. Therefore, the slurry enthalpy is calculated at different temperatures of the extraction vessel. In other words, the slurry enthalpy is only dependent on temperature i.e. the effect of pressure is neglected when calculating the slurry enthalpy. It should be noted that the enthalpy of the slurry in the vessel (i.e.  $h_s$  in Equation 4.19) is equal to  $h_2$ , which is the enthalpy of the slurry exiting the vessel. The same analogy is applied to the enthalpy of CO<sub>2</sub> inside the vessel ( $h$ ) and the enthalpy of CO<sub>2</sub> exiting the vessel ( $h_6$ ).

Some properties of CO<sub>2</sub> appear in the energy balance equation and previous equations i.e. pressure, enthalpy and CO<sub>2</sub> constant volume heat capacity, which are calculated via an Equation of State (EOS) for CO<sub>2</sub>. More details are provided in Section 0.

Table 4.4 summarizes the applied values of constants and parameters in the equations related to the energy balance.

**Table 4.4. Values of constants and parameters in energy balance**

Quantity	Unit	Value	Reference
$C_s$	J/kg.K	$4.16 \times 10^3$	Based on 45 °C and 10 MPa (NIST,2015)
$C_{ve}$	J/kg.K	$4.50 \times 10^2$	(Alloy Digest, 2012)
$m_{ve}$	kg	$1.69 \times 10^2$	(Price-Schonstrom, 2009)
$h_l$	J/kg	$1.88 \times 10^2$	Based on 45 °C and atmospheric pressure (NIST,2015)
$h_4$	J/kg	$-3.41 \times 10^2$	Based on -15 °C and 2.5 MPa (Span and Wagner, 1996)

#### 4.2.1.4 CO<sub>2</sub> equation of state

Many equations exist for calculating properties of CO<sub>2</sub> in various regions of the phase diagram. The Span and Wagner equation of state (Span and Wagner, 1996) is employed for calculating properties of CO<sub>2</sub> in this thesis. This equation of state is accurate to within  $\pm 0.02\%$  -  $\pm 0.05\%$  in density for operating conditions within the region of this study. The Span and Wagner equation of state, which is accepted and used in the NIST Chemistry WebBook (NIST, 2015), is capable of relating CO<sub>2</sub> properties to pressures and temperatures up to 800 MPa and 1100 K, respectively.

The fitting procedure as applied by Span and Wagner (1996) is based on thermal properties of the single-phase region, the liquid-vapour saturation curve, speed of sound, specific isobaric heat capacity, specific isochoric heat capacity, specific enthalpy, specific internal energy and Joule-Thomson coefficient.

The Span and Wagner equation of state is expressed as a fundamental equation in the form of the Helmholtz free energy as a function of density and temperature:

$$\frac{A(\rho, T)}{(RT)} = \phi(\delta, \tau) = \phi^0(\delta, \tau) + \phi^r(\delta, \tau) \quad (4.26)$$

In this equation, the dimensionless Helmholtz energy,  $\phi$ , comes from two contributions. The first ( $\phi^0$ ) depends on ideal gas behaviour while the second ( $\phi^r$ ) accounts for residual fluid behaviour. Each contribution is a function of  $\delta$  and  $\tau$ , where  $\delta$  is the reduced density:

$$\delta = \frac{\rho}{\rho_c} \quad (4.27)$$

and  $\tau$  is the inverse reduced temperature:

$$\tau = \frac{T_c}{T} \quad (4.28)$$

The expressions for calculating the ideal gas part and residual part of the Helmholtz energy are as follows:

$$\phi^0(\delta, \tau) = \ln(\delta) + a_1^0 + a_2^0 \tau + a_3^0 \ln(\tau) + \sum_{i=4}^8 a_i^0 \ln[1 - \exp(-\tau \theta_i^0)] \quad (4.29)$$

$$\begin{aligned} \phi^r(\delta, \tau) = & \sum_{i=1}^7 n_i \delta^{d_i} \tau^{t_i} + \sum_{i=8}^{34} n_i \delta^{d_i} \tau^{t_i} \exp(-\delta^{c_i}) \\ & + \sum_{i=35}^{39} n_i \delta^{d_i} \tau^{t_i} \exp(-\alpha_i (\delta - \varepsilon_i)^2 - \beta_i (\tau - \gamma_i)^2) \\ & + \sum_{i=40}^{42} n_i \Delta^{b_i} \delta \exp(-C_i (\delta - 1)^2 - D_i (\tau - 1)^2) \end{aligned} \quad (4.30)$$

where

$$\Delta = \{(1 - \tau) + A_i [(\delta - 1)^2]^{1/2B_i}\}^2 + B_i [(\delta - 1)^2]^{a_i} \quad (4.31)$$

The coefficients  $a_i^0, \theta_i^0, n_i, a_i, b_i, c_i, d_i, t_i, \alpha_i, \beta_i, \varepsilon_i, \gamma_i, A_i, B_i, C_i, D_i$  are provided in Span and Wagner (1996).

The thermodynamic properties of pure CO<sub>2</sub> are calculated by combining the derivatives of Equation 4.26. The three main properties of CO<sub>2</sub> required for modelling the SFE process as stated previously are pressure, enthalpy and constant volume heat capacity. These three properties are calculated from the dimensionless Helmholtz energy based on the following equations:

$$\frac{P(\tau, \delta)}{\rho RT} = 1 + \delta \frac{\partial \phi^r}{\partial \delta} \quad (4.32)$$

$$\frac{H(\tau, \delta)}{RT} = 1 + \tau \frac{\partial \phi}{\partial \tau} + \delta \frac{\partial \phi^r}{\partial \delta} \quad (4.33)$$

$$\frac{C_v(\tau, \delta)}{R} = -\tau^2 \left( \frac{\partial^2 \phi^0}{\partial \tau^2} + \frac{\partial^2 \phi^r}{\partial \tau^2} \right) \quad (4.34)$$

Table 4.5 summarizes the applied values of constants and parameters in the equations related to the CO<sub>2</sub> EOS.

**Table 4.5. Values of constants and parameters in CO<sub>2</sub> EOS**

Quantity	Unit	Value	Reference
$R$	kJ/kg.K	$1.88924 \times 10^{-1}$	(Span and Wagner, 1996)
$\rho_c$	kg/m <sup>3</sup>	$4.676 \times 10^2$	(Span and Wagner, 1996)
$T_c$	K	$3.041282 \times 10^2$	(Span and Wagner, 1996)

#### 4.2.1.5 Density-Volume-Mass relationship

The CO<sub>2</sub> density within the vessel is linked to the total mass of CO<sub>2</sub> in the vessel and the volume space for CO<sub>2</sub> within the vessel:

$$\rho = \frac{m}{V - A_v z} \quad (4.35)$$

In Equation 4.35, the denominator is the volume of the vessel minus the volume occupied by the slurry. The slurry volume is the cross-sectional area of the vessel times the level of liquid at the bottom of the vessel. In this case, any liquid holdup in the extraction vessel is neglected. Table 4.6 summarizes the applied values of constants and parameters in Equation 4.35.

**Table 4.6. Values of constants and parameters in Density-Volume-Mass relationship**

Quantity	Unit	Value	Reference
$V$	m <sup>3</sup>	$1.34 \times 10^{-2}$	(Price-Schonstrom, 2009)
$A_v$	m <sup>2</sup>	$5.45 \times 10^{-3}$	(Price-Schonstrom, 2009)

#### 4.2.2 Model implementation

The mathematical relations representing the physical process have been developed in Section 4.2.1. The next step is model implementation, which is concerned with the transition of these equations from the mathematical world to the numerical world. For this purpose, an appropriate numerical solver should be selected and initial conditions should be defined (Schmal, 2013).

An important step before solving these equations is conducting a “degree of freedom” analysis. The degree of freedom is a number representing the total number of quantities involved minus the total number of governing equations. Therefore, any properly specified problem can be set up when the number of selected known quantities equals the degrees of freedom resulting in a set of equations where the number of unknowns is equal to the number of equations.

Table 4.7 lists the unknown variables along with the equations applied to solve them. As can be seen, the number of both unknown variables and equations is equal to 5.

**Table 4.7. Degree of freedom analysis**

Description	Unknown variable	Equation used for solving
CO <sub>2</sub> density	$\rho$	Density-Volume-Mass relationship (Equation 4.35)
Slurry level	$z$	Slurry mass balance (Equation 4.6)
System pressure	$P$	CO <sub>2</sub> EOS (Equation 4.26)
System temperature	$T$	Energy balance (Equation 4.19)
CO <sub>2</sub> mass	$m$	CO <sub>2</sub> mass balance (Equation 4.1)
Total	5	5

The mass and energy balances i.e. Equations 4.1, 4.6 and 4.19 are ordinary differential equations (ODEs) and solving them requires numerical integration. Euler's forward integration algorithm, commonly known as Euler's Method, is chosen for this purpose. This algorithm is one of the most useful techniques for solving ordinary differential equations as well as the simplest for programming (Luyben, 1996).

An ODE has the general form:

$$\frac{dy}{dt} = f(t, y) \quad (4.36)$$

Euler's forward explicit method suggests replacing the derivative with:

$$\frac{dy}{dt} \approx \frac{y(t + \Delta t) - y(t)}{\Delta t} \quad (4.37)$$

Substituting Equation 4.37 in Equation 4.36 yields:

$$y(t + \Delta t) \approx y(t) + \frac{dy(t)}{dt} \Delta t = y(t) + f(t, y) \Delta t \quad (4.38)$$

Therefore, for each time step ( $i$ ):

$$y_{i+1} = y_i + f(t_i, y_i) \Delta t, \quad t_i = t_0 + i \Delta t \quad (4.39)$$

The set of Equations 4.1, 4.6 and 4.19 as described, form an initial value problem. Therefore, initial conditions are required to start solving the equations. Based on our knowledge of the SFE process and operating conditions, the following set of initial conditions are selected:

1. An initial slurry level of 16 cm was selected. This slurry level is typical in the vessel

when countercurrent flow of slurry and CO<sub>2</sub> is initiated.

2. The CO<sub>2</sub> stream entering and initially filling the vessel leads to an initial pressure of 2.5 MPa in the vessel. Thus, 2.5 MPa was taken as the initial value of pressure.
3. In a typical countercurrent run, the initial temperature of the vessel itself ( $T_{ve}$ ) is approximately at 25 °C. The entering CO<sub>2</sub> stream temperature ( $T_{CD}$ ) is -3 °C because it warms up on its way from the CO<sub>2</sub> tank to the vessel. In other words, it is assumed that its temperature increases from -15 °C to -3 °C. The entering slurry stream ( $T_s$ ) is 45 °C. The temperatures of the vessel, CO<sub>2</sub> and slurry come to equilibrium within a relatively short time and the resulting equilibrium temperature ( $T_{eq}$ ) must satisfy the following equation:

$$m_s C_s (T_s - T_{eq}) + m C_{vCD} (T_{CD} - T_{eq}) + m_{ve} C_{ve} (T_{ve} - T_{eq}) = 0 \quad (4.40)$$

The initial slurry mass is determined by the initial slurry level as:

$$m_s = z_s A_v \rho_s \quad (4.41)$$

Average values for  $C_s$ ,  $C_{ve}$  and  $C_{vCD}$  can be estimated and employed in Equation 4.40. As a result, the remaining unknowns are  $T_{eq}$  and the initial mass of CO<sub>2</sub> i.e.  $m$ . In order to develop a second relation between  $m$  and  $T_{eq}$ , the following mass-density-volume relationship can be applied:

$$\rho = \frac{m}{V - A_v z} \quad (4.42)$$

in which the vessel volume ( $V$ ), vessel cross-sectional area ( $A_v$ ) and initial level ( $z$ ) are known. Inserting  $T_{eq}$  and Equation 4.42 (i.e. density as a function of mass in the CO<sub>2</sub> equation of state at a known pressure i.e. 2.5 MPa) will result in another relation between  $T_{eq}$  and  $m$ . Therefore, simultaneous solution of the two equations results in  $T_{eq}$  and  $m$  as 27.3 °C and 0.599 kg CO<sub>2</sub> respectively. The initial value for density can then be calculated through Equation 4.42. To summarize, calculations based on the initial values of 16 cm and 2.5 MPa for  $z$  and  $P$  respectively leads to the initial values for  $m$ ,  $T_{eq}$  and  $\rho$ .

After defining the initial conditions, numerical integration is initiated to solve the system of equations as described in Sections 4.2.1.1 to 4.2.1.5 in MATLAB<sup>®</sup>. The step size that was initially selected to solve the equations was 0.01 s. It was observed that decreasing the step size made no difference in the obtained responses from the model. Increasing the step size however

did not provide smooth responses compared to the responses of a 0.01 step size or smaller.

It should be noted that the Span and Wagner equation of state for CO<sub>2</sub> has been the basis of a computer program in C by Dr. Warren Stiver and the program is employed in the present work. The inputs of the program are CO<sub>2</sub> density ( $\rho$ ) and temperature ( $T$ ). The program then uses these values to calculate properties of CO<sub>2</sub> i.e. pressure (Equation 4.32), enthalpy (Equation 4.33) and constant volume heat capacity (Equation 4.34). The compiled file of the EOS program is linked to MATLAB<sup>®</sup> and required values are used in conjunction with other parts of the MATLAB<sup>®</sup> program.

Starting from density, Figure 4.3 demonstrates the sequence in which the equations are solved. It should be noted that the number of loop iterations, which is equivalent to simulation time, would be set by user beforehand.

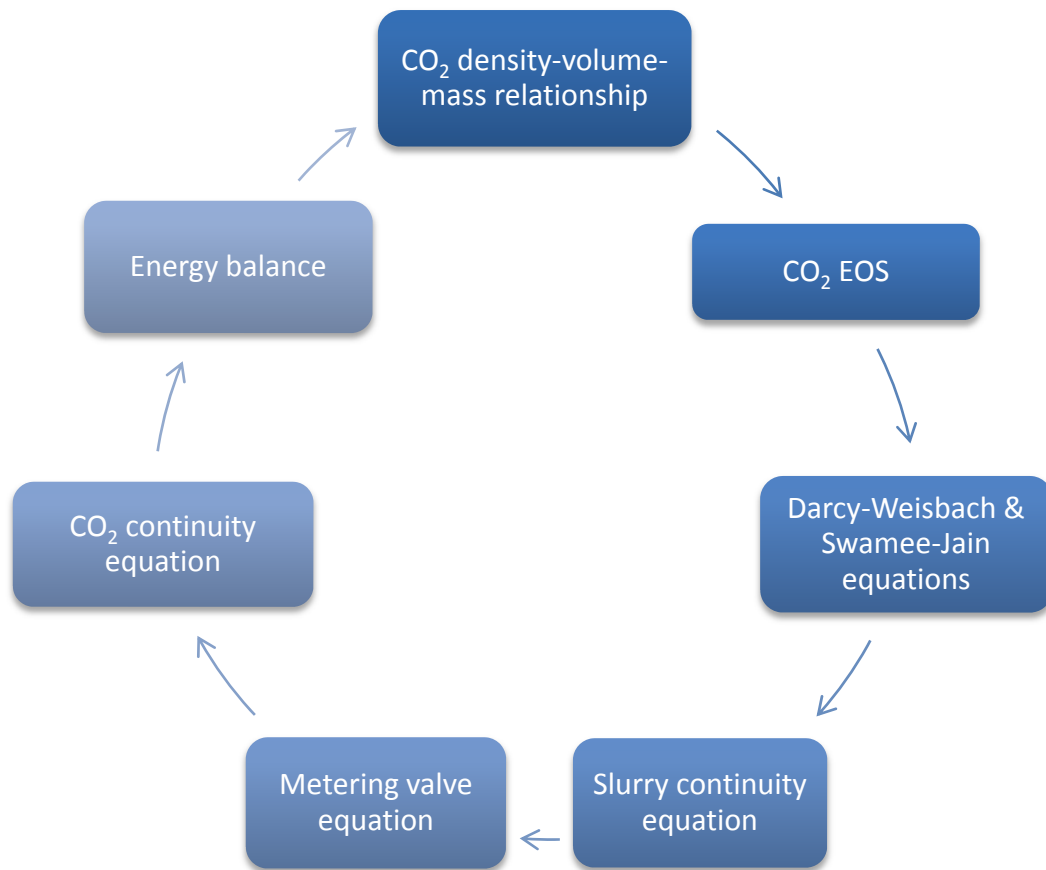


**Figure 4.3. Equation solving flowchart**

Equations were also solved in Simulink<sup>®</sup>. The reason for this is that Simulink<sup>®</sup> has a block diagram environment, which makes it easier to manage modelling especially when

different parts/equations exist in the model. It also provides various solvers for modelling dynamic systems resulting in faster simulations based on the selected solver and its parameters. The “ode45” solver with a variable step was applied in Simulink<sup>®</sup> to solve equations. The “ode45” solver is the default solver in Simulink<sup>®</sup> and is based on an explicit Runge-Kutta formula, which uses variable step time for solving differential equations (Mathworks, 2015). This solver (applied for non-stiff problem types) is a one-step solver in computing  $y_{i+1}$  i.e. it needs only the solution at the preceding time point  $y_i$ . At same conditions, the same results were obtained when using MATLAB<sup>®</sup> and Simulink<sup>®</sup> indicating that numerical errors are minor. It should be noted that the results as presented in subsequent sections, are an outcome of using Simulink<sup>®</sup>.

## **4.3 Results and discussion**

This section is broken down into two parts: model verification and model validation.

### **4.3.1 Model verification**

The model verification step is associated with confirming that the implemented model characterizes the conceptual description of the process (Schmal, 2013). In other words, by performing initial runs of the model, troubleshooting is done to make sure that results are in line with the nature/physics of the SFE process.

The implemented model needs to be verified from different perspectives. Therefore, after defining the equations for modelling the pilot scale continuous SFE process and solving them in Simulink<sup>®</sup>, verification of the model is categorized into three sections. The first category is associated with verifying the numerical solver applied for solving the equations. The second category deals with verifying assumptions as stated in the model development stage. The third category investigates effect of main process parameters on system response. It should be noted that at this point the model has not yet been validated, but results obtained from these analyses were considered as preliminary steps towards validating the model and designing experiments for model validation.

During the model verification process, the pump flows are expressed in %. For each pump, a certain % corresponds to a certain volumetric flow. Based on pump specification, for the slurry pump this conversion is applied as:

$$SlurryFlow \left( in \frac{L}{min} \right) = \left( \frac{16.9}{100} \right) \times PumpFlow(in \%) \quad (4.43)$$

and for the CO<sub>2</sub> pump as:

$$CO_2Flow \left( in \frac{L}{min} \right) = \left( \frac{6.46}{100} \right) \times PumpFlow(in \%) \quad (4.44)$$

where, 16.9 and 6.46 are the maximum volumetric flow capacities (in L/min) of the slurry and CO<sub>2</sub> pumps respectively. Therefore, in the following subsections, for simplicity, pump flows are specified in % rather than in L/min.

#### 4.3.1.1 Numerical solver verification

An important aspect of model verification is determining that the computer program performs as intended (Kleijnen, 1995). For the SFE process model, this translates into verifying responses obtained from the program that solves the SFE model equations via the selected solver. For this purpose, equations are solved in MATLAB<sup>®</sup>/Simulink<sup>®</sup> at certain process conditions. Figure 4.4 depicts changes of the main process variables with time as a result of the selected parameter values as listed in Table 4.8. Among the listed parameters, values for CO<sub>2</sub> flow, slurry flow and slurry temperature were selected based on the typical values applied in the actual SFE process. Values for metering valve opening and manifold length were adjusted to obtain steady state response. Further discussion regarding adjustable parameters is provided in Section 4.3.2.2

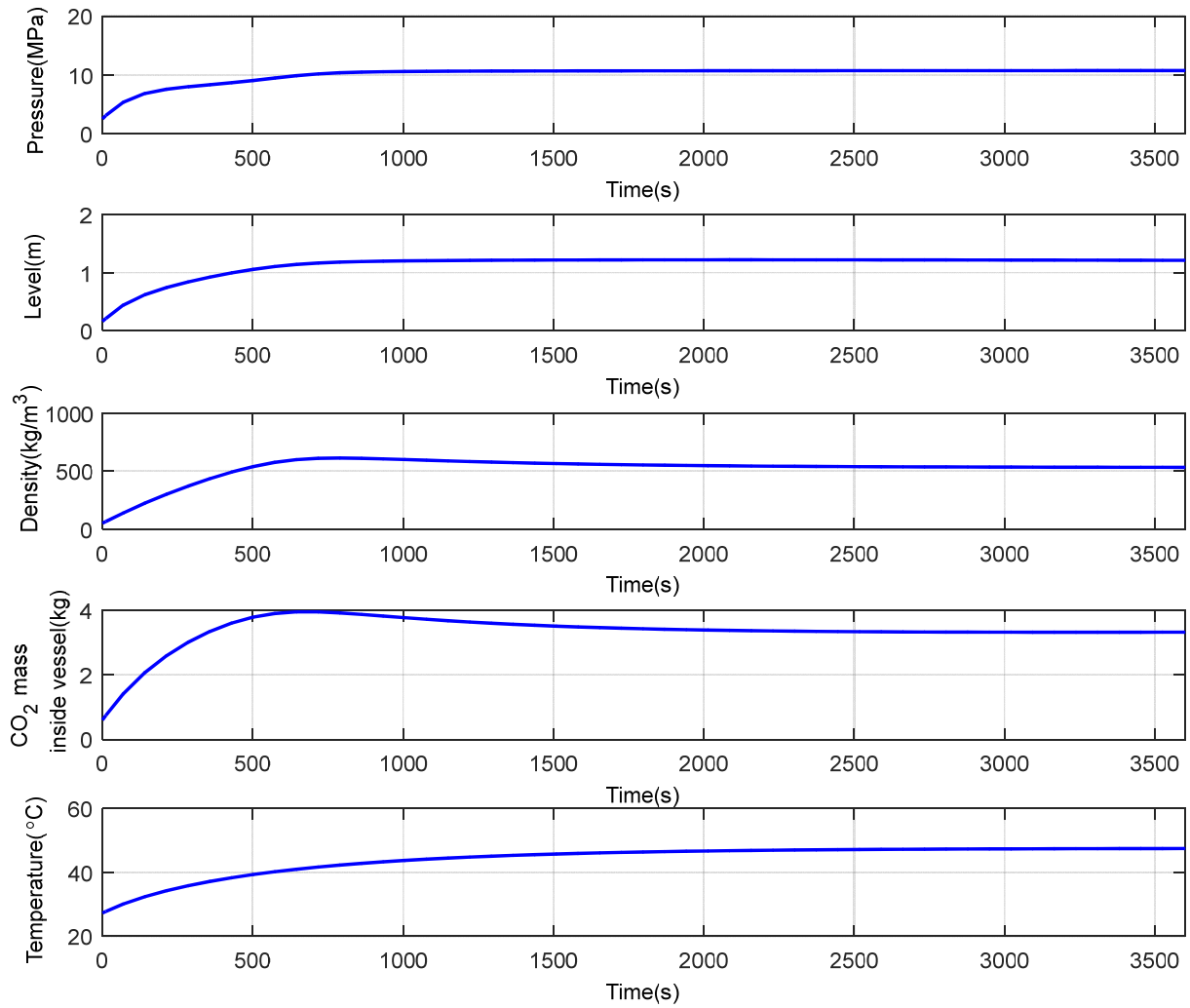


**Figure 4.4. Response of main process variables**

**Table 4.8. Parameter values applied in simulation and obtained S.S. value of variables**

Parameters			Variables		
Description	Value	Unit	Description	S.S. value	Unit
Slurry flow	13.8	%	Slurry level ( $z_{ss}$ )	1.21	m
CO <sub>2</sub> flow	12.5	%	Pressure ( $P_{ss}$ )	10.75	MPa
Metering valve opening	28	%	CO <sub>2</sub> density ( $\rho_{ss}$ )	533	kg/m <sup>3</sup>
Manifold length	3.605	m	CO <sub>2</sub> mass ( $m_{ss}$ )	3.33	kg
Slurry temperature	45	°C	Temperature ( $T_{ss}$ )	47.4	°C

As shown in Figure 4.4, based on the selected parameter values, a steady state response is obtained for all the variables of interest. Obtained steady state values for each variable are also presented in Table 4.8.

One technique for verifying the programmed numeric solver is to insert the obtained steady state values in the steady state form of the three main ordinary differential equations (Equations 4.1, 4.6, and 4.19) as well as the two main algebraic equations (Equations 4.32 and 4.35) to assess numerical error. The steady state forms of the main five equations are as follows:

$$\dot{m}_4 = \dot{m}_6 \quad (4.45)$$

$$\frac{Q_1}{A_v} = \frac{Q_2}{A_v} \quad (4.46)$$

$$h_1\dot{m}_1 + h_4\dot{m}_4 + \dot{Q} + \dot{W}_{pump} = h_2\dot{m}_2 + h_6\dot{m}_6 \quad (4.47)$$

$$P_{EOS}(T_{ss}, \rho_{ss}) = P_{ss} \quad (4.48)$$

$$\rho_{ss} = \frac{m_{ss}}{V - A_v z_{ss}} \quad (4.49)$$

By inserting the steady state values of the five main variables  $z_{ss}$ ,  $P_{ss}$ ,  $\rho_{ss}$ ,  $m_{ss}$  and  $T_{ss}$  into the above equations, the left side of each equation should equal the right side. Table 4.9 presents calculated values for each side of the equations as well as the absolute relative error (ARE).

**Table 4.9. Calculated values for Equations 4.45 to 4.49**

Equation #	Equation Description	Left Side of Equation	Right Side of Equation	ARE (%)
4.45	CO <sub>2</sub> continuity equation	1.3581 x10 <sup>-2</sup>	1.3556 x10 <sup>-2</sup>	0.18
4.46	Slurry continuity equation	7.7368 x10 <sup>-3</sup>	7.7469 x10 <sup>-3</sup>	0.13
4.47	Energy balance	5.8397 x10 <sup>3</sup>	5.8405 x10 <sup>3</sup>	0.01
4.48	CO <sub>2</sub> equation of state	1.0779 x10	1.0747 x10	0.30
4.49	Density-Volume-Mass relationship	5.3331 x10 <sup>2</sup>	5.3318 x10 <sup>2</sup>	0.02

As can be seen from the ARE values reported in Table 4.9, all of the calculated discrepancies between the left and right side of the five equations are less than 1%. Based on these results, the numerical error generated by the solver is small and the model results are well within the confidence of the input data. In other words, the performance of the programmed solver applied for solving the equations of the continuous SFE system is evaluated. It can be safely concluded that the solver is working as expected. Hence, the programmed solver is verified.

An interesting observation regarding the response of the continuous SFE system is that if any of the system inputs is slightly altered, the pressure response, as well as temperature and CO<sub>2</sub> density responses, will find their new balance point and a new steady state value is reached for

these variables. However, this is not the case for slurry level and, as a consequence, not the case for mass of CO<sub>2</sub> in the extraction vessel. In other words, by applying a new input in modelling, the slurry level response and CO<sub>2</sub> mass do not go towards a new steady state value. On the contrary, they tend to increase or decrease in the form of a ramp. This is due to the non-self regulating (or integrating) nature of these process variables (Rice and Cooper, 2008; Smith, 2009). Due to a lack of balance point, the integrating process variable i.e. slurry level tends to naturally increase or decrease if left uncontrolled.

This non-self regulating characteristic of slurry level in the extraction vessel is also proven from a numerical standpoint. For this purpose, a similar approach (as described earlier) is applied for calculating steady state response of the main five equations (Equations 4.45 to 4.49). However, in this scenario a value of 12.8% is applied for slurry flow. All other parameters are as listed in Table 4.8. Obtained results for the steady state calculation of the slurry and CO<sub>2</sub> continuity equations are presented in Table 4.10.

**Table 4.10. Calculated values for continuity equations when slurry flow is 12.8%**

Equation #	Equation Description	Left Side of Equations	Right Side of Equations	ARE (%)
4.45	CO <sub>2</sub> continuity equation	1.3581 x10 <sup>-2</sup>	1.2574 x10 <sup>-2</sup>	7.41
4.46	Slurry continuity equation	7.1762 x10 <sup>-3</sup>	7.6081 x10 <sup>-3</sup>	6.02

As seen from the ARE values reported in Table 4.10, relatively high ARE values are calculated for Equations 4.45 and 4.46 indicating that the right side of the continuity equations do not equal their left side. In other words, dh/dt and dm/dt are not equal to zero i.e. the CO<sub>2</sub> mass inside the vessel is increasing while the slurry level inside the extraction vessel is decreasing. Further results regarding this subject are presented in Section 4.3.1.3 where the effect of process parameters on main responses is explored.

Due to this non-self regulating characteristic of slurry level, only pressure response is presented in the following section related to verification of assumptions. Hence, decisions regarding assumptions are made solely based on pressure behaviour, but the actual choice of the assumption was based on a broader consideration.

### 4.3.1.2 Verification of assumptions

*Assumption 1:*  $P_7$  is assumed to be constant (i.e. a set parameter) and equal to 2.5 MPa.

Assumption 1 assumed that the pressure after the metering valve is constant and equal to 2.5 MPa. In reality however, this pressure is not constant and at a fixed position of the metering valve is dependent on the pressure inside the extraction vessel. In order to estimate a relationship between the pressure before and after the metering valve, experimental data from the actual SFE process is employed. Table 4.11 provides the pressures observed before and after the metering valve during a typical experiment conducted on the continuous SFE process.

**Table 4.11. Inlet and outlet pressure of metering valve**

$P_6$ - Inlet pressure (MPa)	$P_7$ - Outlet pressure (MPa)
2.5	0.5
10	1.3
14	2.2
18	2.9

These data points are applied to develop a relationship between the inlet and outlet pressure of the metering valve.

$$P_7 = 0.0048P_6^2 + 0.0604P_6 + 0.3036 \quad (4.50)$$

In order to verify or discredit *Assumption 1*, the vessel pressure response is compared between two cases. In Case 1, a constant pressure of 2.5 MPa is applied for pressure after the metering valve, while in Case 2, Equation 4.50 is applied. Result of this comparison is illustrated in Figure 4.5.

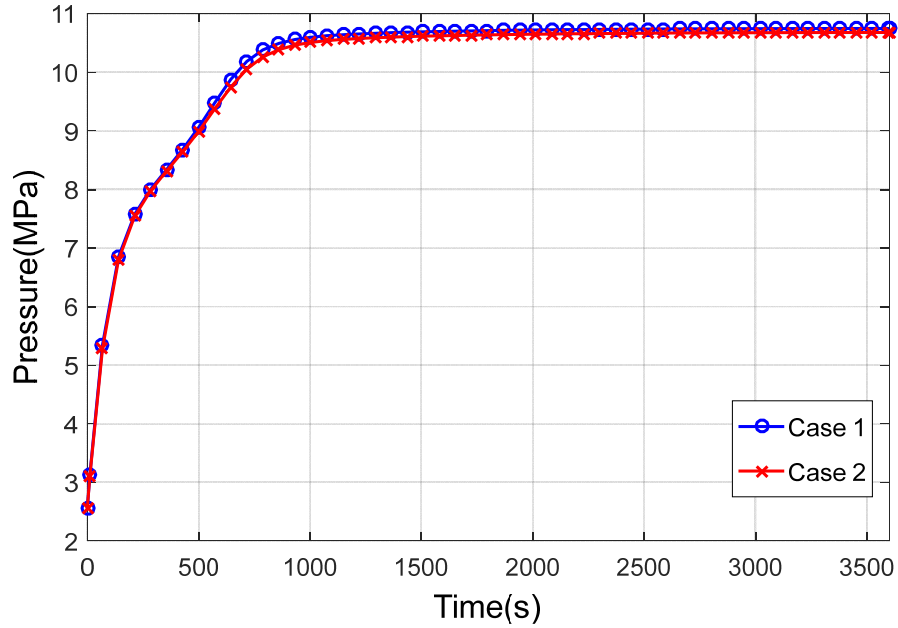


**Figure 4.5. SFE process pressure response for Case 1 and Case 2**

As can be seen from Figure 4.5, a steady state pressure of 10.75 MPa and 10.68 MPa is reached for Case 1 and Case 2, respectively. Based on this observation, it is concluded that applying Equation 4.50 does not significantly shift pressure response. Therefore *Assumption 1* is verified and applying Equation 4.50 is not deemed necessary.

*Assumption 2:* Slurry dynamic viscosity and density is assumed to be those of water at 45 °C and 10 MPa.

Assumption 2 assumes that the slurry dynamic viscosity and density are those of water at 45 °C and 10 MPa. In reality however, depending on the amount of solids present in the slurry, the density and viscosity will be higher than those of water. In order to investigate the effect of density and viscosity on pressure response inside the vessel, a slurry density of 1050 kg/m<sup>3</sup> and a dynamic viscosity of  $9.97 \times 10^{-4}$  Pa.s are applied in modelling. The selected values are approximate and they were chosen based on physical observation of the available slurry present in the lab. The result of this comparison are illustrated in Figure 4.6.

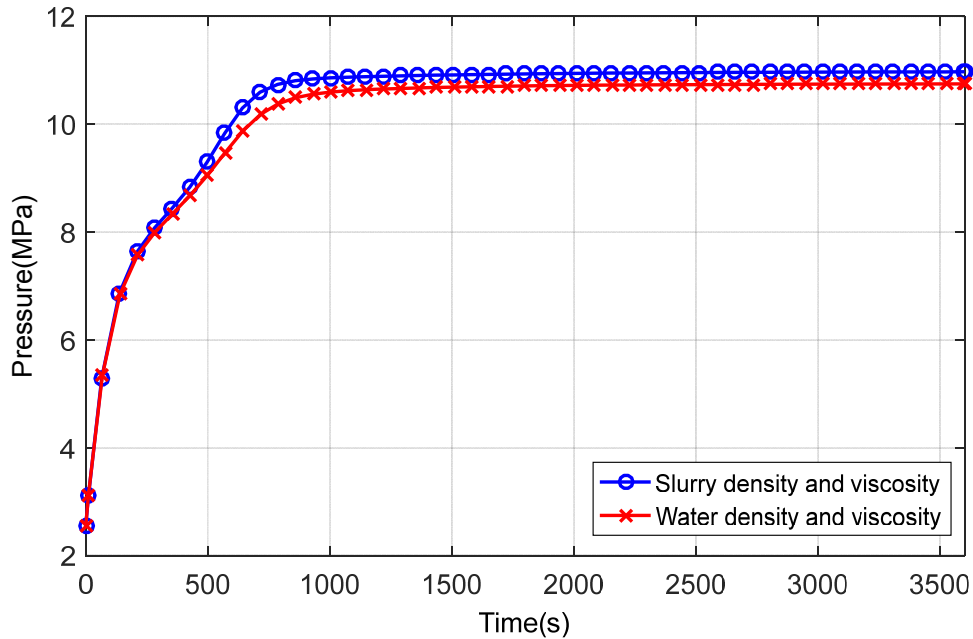


**Figure 4.6. SFE process pressure response comparison regarding slurry density and viscosity**

As can be seen from Figure 4.6, by applying a higher viscosity and density, the steady state pressure increases slightly from 10.75 MPa to 10.97 MPa. Similar to the previous assumption, because the assumption does not cause a significant shift in pressure, it can be concluded that applying the viscosity and density of water in modelling is reasonable and *Assumption 2* is verified.

*Assumption 3*: Process is assumed to be adiabatic i.e. negligible heat transfer to and from the process.

Assumption 3 states that the heat transfer to and from the process can be neglected. In other words, the extraction vessel is assumed to be adiabatic. In order to verify or discredit *Assumption 3*, the vessel pressure and temperature responses are compared between two cases in which the 360 Watt heating tape is and is not utilized to heat the extraction vessel. The result of this comparison are illustrated in Figure 4.7 and Figure 4.8.

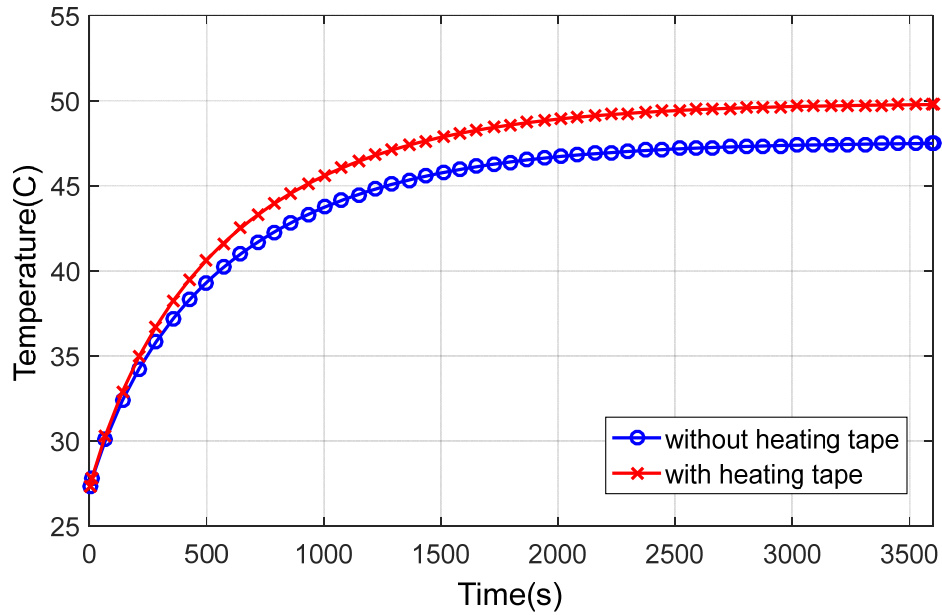


**Figure 4.7. SFE process temperature response with and without heating tape**

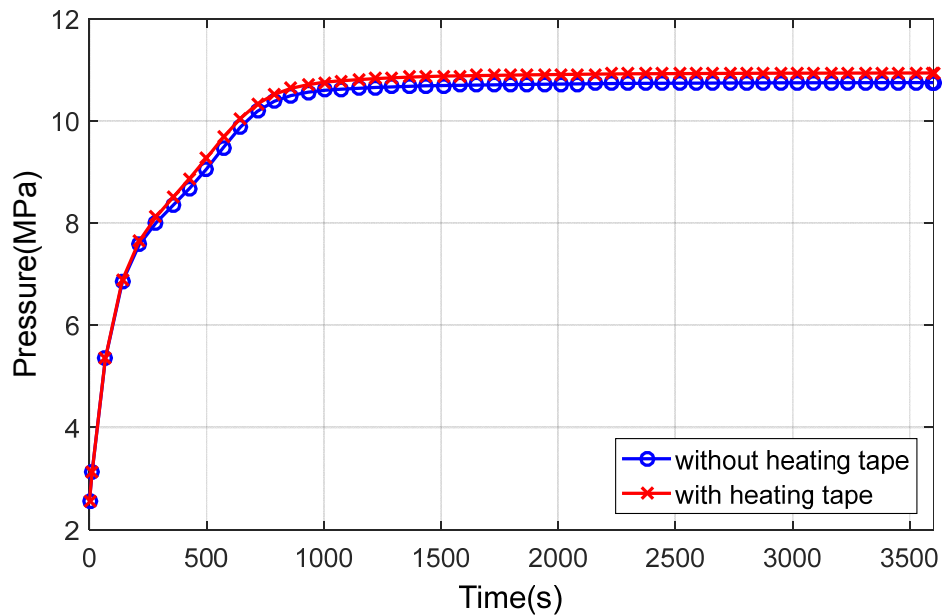


**Figure 4.8. SFE process pressure response with and without heating tape**

As can be seen from Figure 4.7, when utilizing the heating tape, the temperature inside the extraction vessel increases by approximately 2.5 °C compared to the case in which no heating tape is applied. This temperature increase however, does not significantly affect the pressure response as observed in Figure 4.8. Therefore, it is safe to neglect the net heat transfer term in the energy balance and hence *Assumption 3* is verified.

### 4.3.1.3 Verification of system response to main process parameters

The main parameters of interest that are expected to have significant effects on the process variables (i.e. extraction vessel pressure and slurry level) are slurry flow, CO<sub>2</sub> flow, manifold length, metering valve opening and inlet slurry temperature. Therefore, the effect of setting a parameter at two different values and observing the result on pressure and level transient response is valuable. Now that the model is at hand, these responses can be observed by solving the model equations. Furthermore, a visual examination of the pressure and level responses and a comparison of the results with our expectations based on the physics of the process is an important aspect of verifying the model.

In the following subsections, effect of changing each of the listed parameters in Table 4.8 on the variables is presented. For comparison purposes, Figure 4.4 and related parameter values are considered as the “base simulation”. In other words, in each subsection, the change of only one parameter will be explored and the value used for the unchanged parameters are as listed in Table 4.8. It should be noted that in the subsequent subsections, the focus is on pressure and slurry level responses in the extraction vessel, with the exception of the last subsection, in which the temperature response is also explored.

#### *Slurry flow*

Figure 4.9 provides the pressure and slurry level response to changes in the input slurry flow. The base case is 13.8% of the maximum slurry pump capacity, with the verification testing an increase to 14.8% and a decrease to 12.8% of the maximum slurry pump capacity.

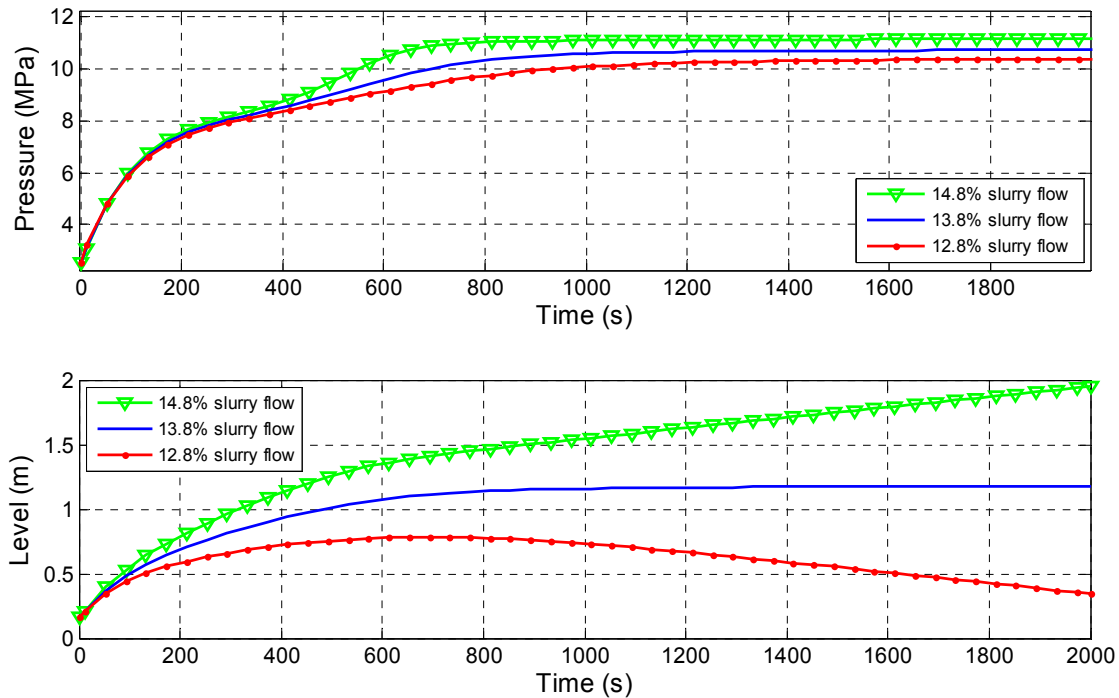


**Figure 4.9. Pressure and level responses to a change in slurry flow**

Increasing slurry flow into the system is expected to result in an increase in slurry level inside the vessel and an increase in system pressure. It is expected that a decrease in slurry flow would have the opposite impact. Figure 4.9 is consistent with these expectations.

Figure 4.9 also illustrates the different response of a self regulating property (pressure) and a non-self regulating property (slurry level). The system pressure reaches a new steady state position as a result of the change in input conditions, as is expected for all self regulating properties of a system. However, the slurry level does not proceed to a new steady state position as a result of the input change.

### *CO<sub>2</sub> flow*

Figure 4.10 provides the pressure and slurry level response to changes in the input CO<sub>2</sub> flow. The base case is 12.5% of the maximum CO<sub>2</sub> pump capacity, with the verification testing an increase to 13.5% and a decrease to 11.5% of the maximum CO<sub>2</sub> pump capacity.

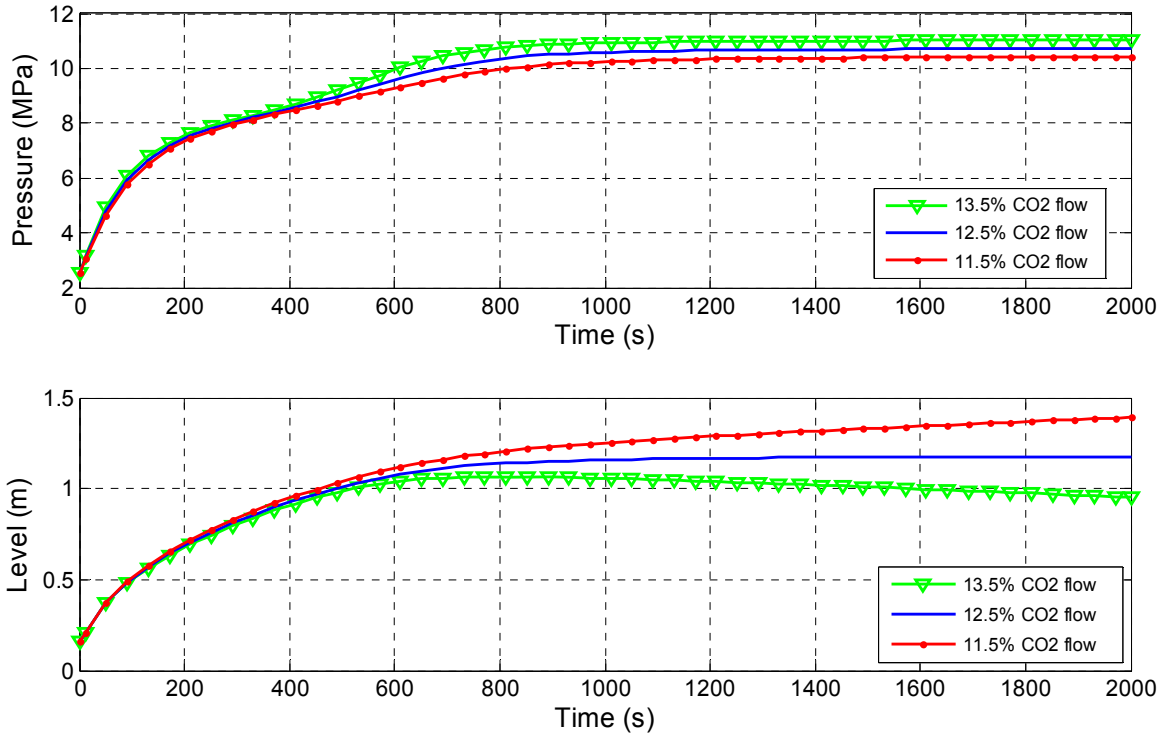


**Figure 4.10. Pressure and level responses to a change in CO<sub>2</sub> flow**

Figure 4.10 illustrates the expected results. Increasing CO<sub>2</sub> flow is expected to increase pressure inside the vessel. Consequently, liquid will be pushed out of the extraction vessel, resulting in a lower slurry level. The opposite is also expected to hold true i.e. with decreased CO<sub>2</sub> flow, the pressure inside the vessel will decrease and the slurry level will consequently increase. The slurry level once again displays the non-self regulating behaviour.

#### *Manifold length*

Figure 4.11 provides the pressure and slurry response to changes in the input manifold length. The base case is 3.605 m, with the verification testing an increase to 3.905 m and a decrease to 3.305 m.

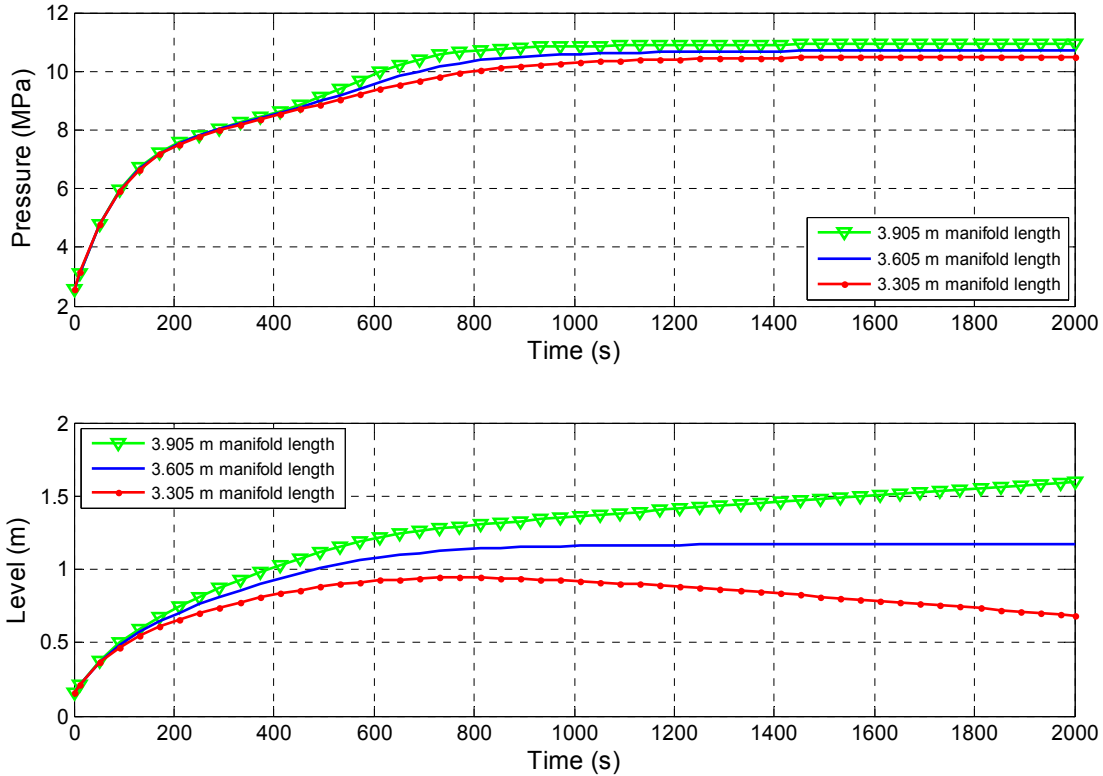


**Figure 4.11. Pressure and level responses to a change in manifold length**

Figure 4.11 illustrates the expected results. Increasing manifold length will result in more resistance to flow exiting the vessel; hence it is expected to increase the slurry level inside the vessel. Consequently, pressure inside the vessel also increases. On the other hand, decreasing the manifold length will result in less resistance to flow exiting the vessel; hence it is expected to decrease the slurry level and consequently pressure inside the vessel. The non-self regulating behaviour of slurry level is also observed in this scenario.

#### *Metering valve opening*

Figure 4.12 provides the pressure and slurry level response to changes in the input metering valve opening. The base case is 28% with the verification testing an increase to 33% and a decrease to 23%.

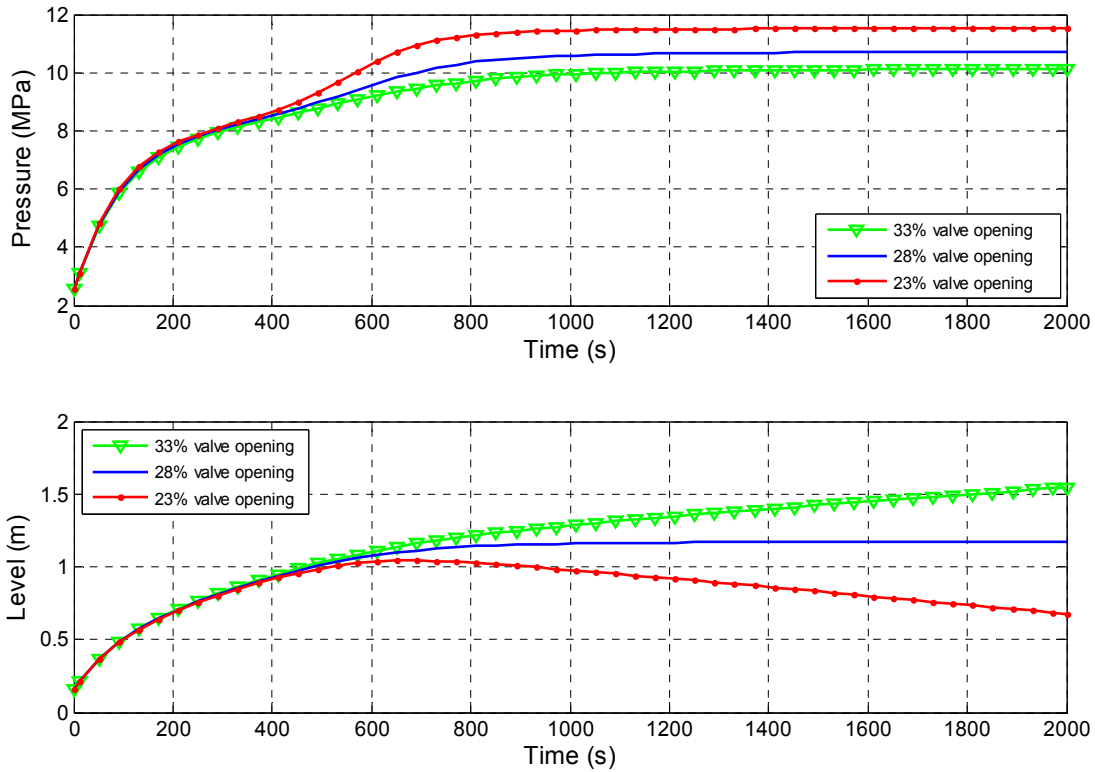


**Figure 4.12. Pressure and level responses to a change in metering valve opening**

Figure 4.12 illustrates the expected results. Increasing the percent opening of the metering valve translates into more CO<sub>2</sub> exiting the vessel. Consequently, pressure inside the vessel decreases and the slurry level is expected to increase. The opposite is also expected to hold true i.e. decreasing the percent opening of the metering valve will increase pressure inside the vessel and decrease slurry level. The slurry level again displays the non-self regulating behaviour.

### *Slurry temperature*

Figure 4.13 provides the pressure, slurry and temperature responses to changes in the input slurry inlet temperature. The base case is 45 °C with the verification testing an increase to 50 °C and a decrease to 40 °C.

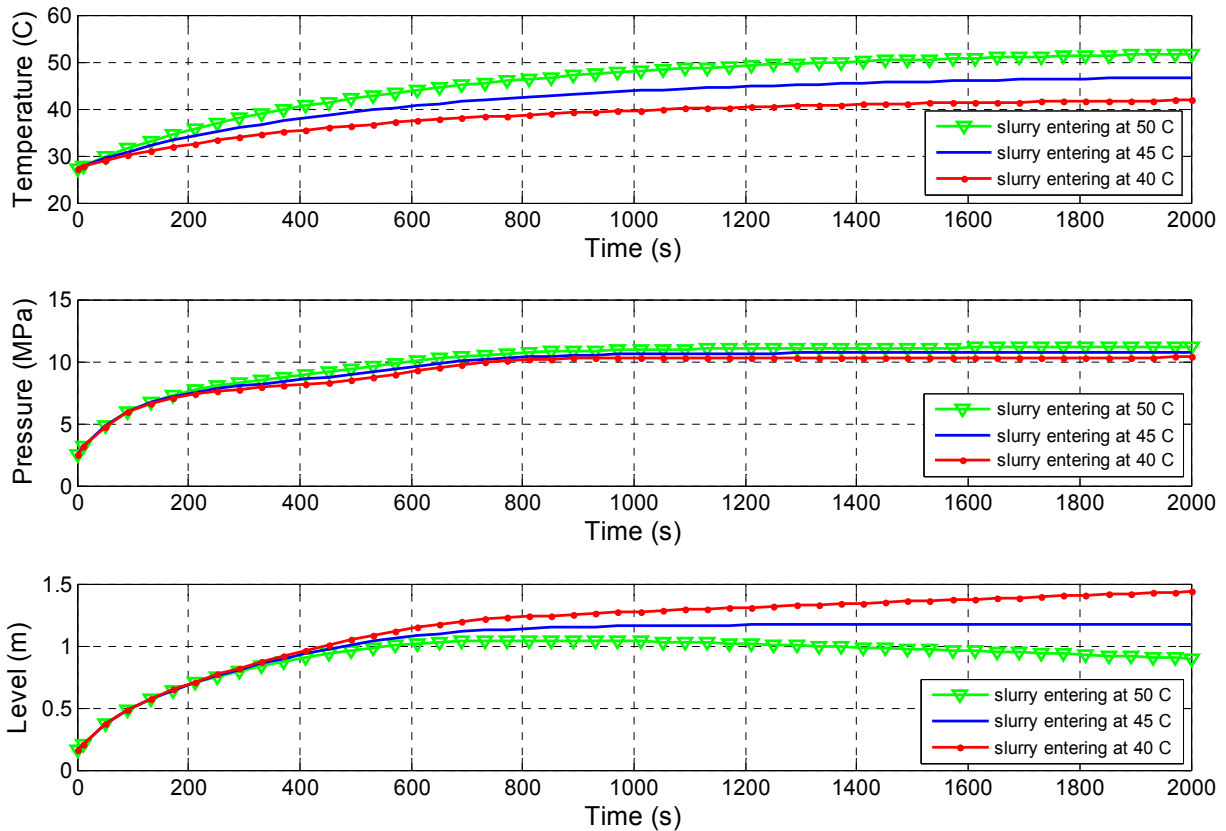


**Figure 4.13. Temperature, pressure and level responses to a change in the slurry inlet temperature**

Figure 4.13 illustrates the expected results. Increasing the slurry inlet temperature is expected to increase the temperature inside the vessel which in turn would cause an increase in pressure and a decrease in slurry level. The opposite is also expected to hold true i.e. decreasing the slurry inlet temperature will result in a decrease in vessel temperature and as a result pressure will decrease and slurry level will increase. The non-self regulating behaviour of slurry level is also observed in this scenario. It is also seen that the steady state temperature inside the vessel in each case is approximately equal to the temperature in which slurry enters the vessel i.e. 40 °C, 45 °C and 50 °C.

As expected, an important outcome of these verification simulations is that slurry level response/behaviour is highly dependent on process conditions because of its non-self regulating property. This fact emphasizes the need to control slurry level inside the extraction vessel.

### 4.3.2 Model validation

An important step in the process of mathematical modelling is model validation (Hvala *et*

*al.*, 2005). This step is associated with determining whether the model is a precise representation of the real process or not and to see how well it describes it (Kleijnen, 1995; Luyben, 1996). For this purpose, dynamic plant tests, also known as validation tests are vital to conduct in order to confirm the predictions of the mathematical model and assess the model's accuracy.

To validate the constructed model for the pilot scale continuous SFE process, experimental runs were designed and carried out by the actual process and experimental responses were measured and recorded. At similar conditions, parameter values and model responses were also calculated by using the hydrodynamic model. Then, experimental and model responses were compared to demonstrate how well the model represents the SFE process. In the following discussion, the model validation is divided into two subsections: verification of equations and adjustable parameters.

#### **4.3.2.1 Verification of equations**

Two scenarios were presented in the model development stage in which uncertainty existed in applying the correct equation. The first scenario was associated with an equation for calculating flow of CO<sub>2</sub> through the metering valve. The second scenario was related to an equation for calculating work done by the CO<sub>2</sub> pump. These two scenarios are explored in this section.

It should be noted that verification as explained in this section is only based on the pressure response. A continuous level sensor in the extraction vessel did not exist to be utilized for model verification purposes.

##### *Metering valve equation*

As stated earlier, the CO<sub>2</sub> exiting the extraction vessel and entering the metering valve will be changing phase between gas, liquid and supercritical, depending on the pressure and temperature inside the vessel, and changing to gas or liquid as it flows through the metering valve. An equation for calculating supercritical CO<sub>2</sub> flow is not provided in the metering valve literature. Therefore, only two options exist for calculating the flow of CO<sub>2</sub>: (i) assuming CO<sub>2</sub> is in the liquid phase (Equation 4.3) or (ii) assuming CO<sub>2</sub> is in the gas phase (Equation 4.4). In this section, these two equations are independently applied in modelling and the pressure response is compared for the two equations with the SFE process pressure response. All other model

parameters are identical between the two modelling attempts. Figure 4.14 depicts this comparison.

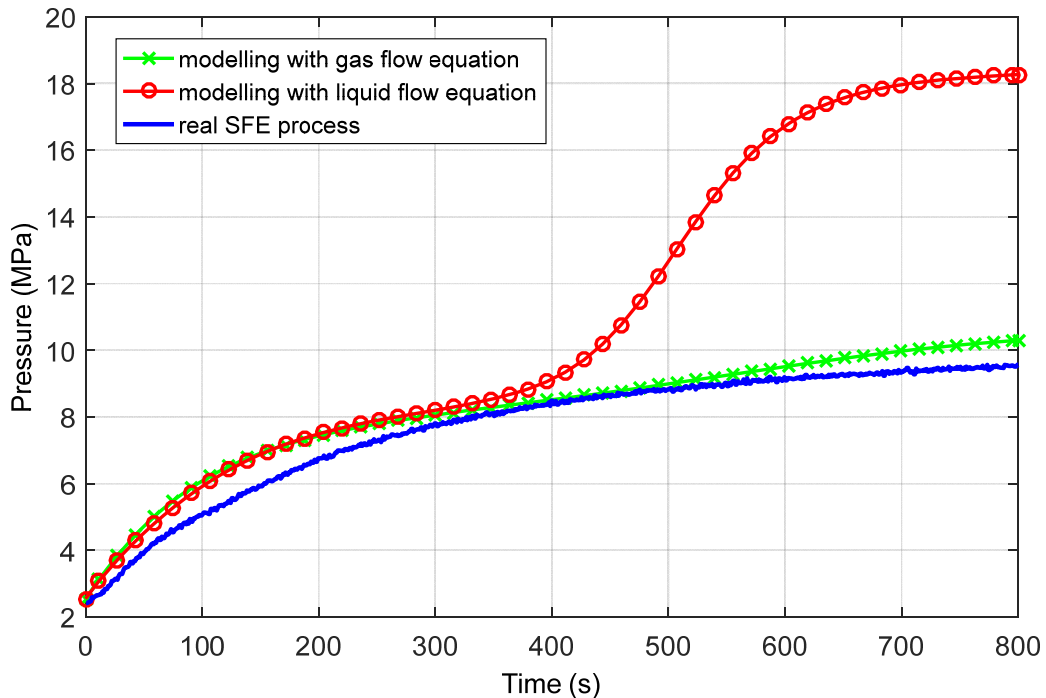


**Figure 4.14. Pressure response comparison between process and modelling when applying different CO<sub>2</sub> flow equations (Equation 4.3 or Equation 4.4)**

As seen in Figure 4.14, a sharp pressure jump is observed when applying the liquid flow equation. This sharp increase in pressure is not observed in the SFE process response. Conclusively, although the SCF density is closer to that of a liquid, it is observed that when applying the gas flow equation, a pressure response that more closely resembles the real SFE process (in terms of shape) is obtained in comparison to the case in which the liquid flow equation is applied. Hence, the temperature corrected gas flow equation (Equation 4.4) is applied in the model.

#### *CO<sub>2</sub> pump work equation*

As stated earlier, two equations were proposed in the model development section for calculating work done by CO<sub>2</sub> pump (Equations 4.20 and 4.21). In this section, these two equations are independently applied in modelling and compared with the process pressure response. All other model parameters are identical between the two modelling attempts. Figure 4.15 depicts this comparison.

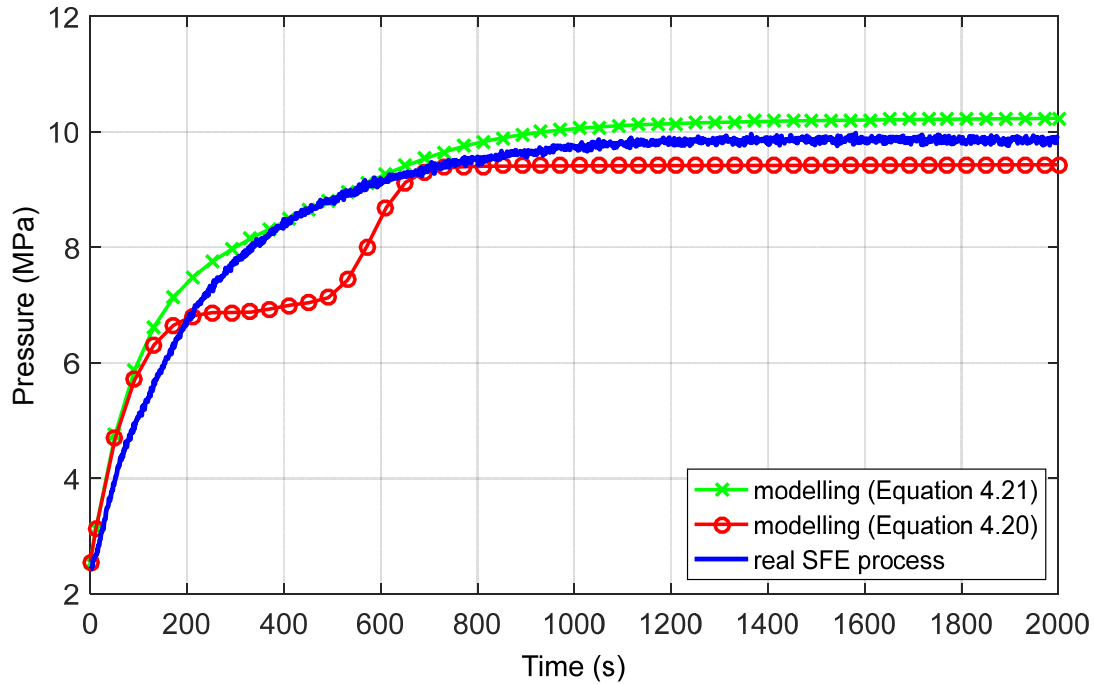


**Figure 4.15. Pressure response comparison between process and modelling when applying Equation 4.20 or Equation 4.21**

As seen from Figure 4.15, the modelling response by applying Equation 4.21 is similar to the SFE process response. A different response curve is observed when applying Equation 4.20 in modelling. In other words, a pressure response that more closely resembles the real SFE process (in terms of shape) is obtained by applying Equation 4.21 in comparison to the equation proposed in the CO<sub>2</sub> pump literature (Equation 4.20). Hence, Equation 4.21 is chosen for calculating work done by the CO<sub>2</sub> pump.

#### 4.3.2.2 Adjustable parameters

As stated earlier, the pressure and slurry level in the extraction vessel are chosen as the two key variables for control in the SFE process. Therefore, for model validation purposes it is important to design experiments that demonstrate the responses of these two variables so that the experimental responses can be compared to modelling responses at similar process conditions.

It should be noted that experiments conducted at this stage were with CO<sub>2</sub> and water and not slurry. In the following subsections, experiments designed for validating pressure response and level response are explained in detail and the results are compared with that of the model.

### Pressure response

To validate the pressure response of the model, similar inputs used in modelling were applied to the continuous pilot scale SFE process i.e. countercurrent and constant flow of slurry and CO<sub>2</sub> through the extraction vessel. The pressure response in the extraction vessel was recorded to observe how the vessel pressure changes over time i.e. the vessel pressure was subject to uncontrolled variation. In modelling industrial processes, validation by this method is a standard approach (Hvala *et al.*, 2005). This comparison can either be qualitative (for example, by visual inspection of the outputs) or quantitative using measures such as RMSE (Root Mean Square Error), RE (Relative Error) and OE (Output Error).

The first model validation test (Test V11) was conducted with a CO<sub>2</sub> flow rate of 12.5% and a slurry flow rate of 13.8%. The metering valve opening in this test was 10% and the chosen manifold length was 2.64 m. The pressure response in the extraction vessel of the SFE process was recorded to observe how the vessel pressure changed over time. The same inputs were applied to the mathematical model and a pressure response was obtained. Figure 4.16 depicts the pressure responses obtained from both the mathematical model (denoted as simulation response) and the SFE process (denoted as experimental response) for Test V11.

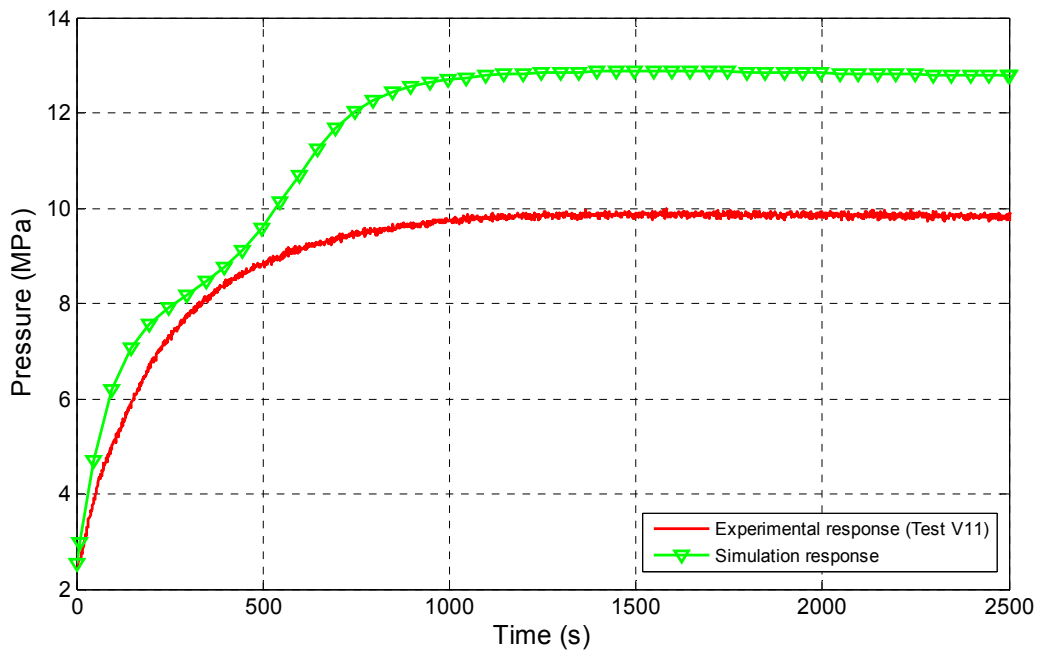


**Figure 4.16. Pressure response comparison for Test V11**

As can be seen in Figure 4.16, there is a discrepancy between the pressure response of the SFE process and that of the mathematical model. The two responses differ in shape and in steady state end point. The experimental response leads to a smooth asymptotic approach to steady state while the model provides an almost sigmoid shape in the approach to steady state. The model has a steady state pressure that is about 30% higher than that observed in the SFE process.

In developing mathematical models for predicting the transient behaviour of processes such as the continuous process under study, it is not unusual to encounter discrepancies between model and experimental responses. This discrepancy is usually attributed to the fact that the mathematical model is based on a number of simplifications and therefore it does not provide an exact account of the actual process behaviour. In addition, in conducting experiments on the SFE process, disturbances exist that impact responses in the process. However, these disturbances have not been, and for the most part, can not be accounted for in the mathematical model. A common example of such conditions/disturbances in the continuous SFE process is the occurrence of freezing in the lines, particularly in the CO<sub>2</sub> outlet line and slurry outlet line from the extraction vessel. Although the freezing might clear up after sometime and operators might not even recognize the event, it will impact the pressure and slurry level inside the extraction vessel. Experimental error in the measurements in the process could also contribute to discrepancies between model and actual process responses.

For the reasons cited, parameters are selected in the model and are looked upon as “adjustable parameters” to be used in reconciling the model responses with the real process responses. These parameters are usually associated with parts of the process in which uncertainties exist regarding the actual value of that parameter. In other words, due to existence of uncertainties in the process, empirical elements i.e. “adjustable parameters” may be selected in practical models, which can be estimated from experimental data by comparing responses of the model and the process (Schmal, 2013). For this purpose, the chosen “adjustable parameters” are given values not necessarily equal to their actual values in the process. In other words, data measured from the SFE process is used for constructing the model and also validating it.

As stated earlier, in the hydrodynamic model, the main inputs are CO<sub>2</sub> flow, slurry flow, manifold length and metering valve opening. CO<sub>2</sub> flow and slurry flow are calculated based on pump speed (revolutions per minute or rpm) and are considered as accurate. The most uncertain

aspects of the hydrodynamic model are the flow components through the manifold and the metering valve.

Regarding the metering valve, the CO<sub>2</sub> enters as a supercritical phase and transitions to a liquid or gas phase within the valve. However, Equation 4.3, which relates the volumetric flow rate of CO<sub>2</sub> to the pressure drop through the metering valve, is based on single-phase flow behaviour. Similarly, for the manifold, the slurry enters as a liquid phase saturated with dissolved CO<sub>2</sub>. As the slurry moves through the manifold, some of the CO<sub>2</sub> degasses leading to two phase flow. However, Equation 4.7 is based on single phase flow behaviour. Thus, the metering valve opening and the manifold length are chosen as the “adjustable parameters” and will be adjusted to attempt to reconcile the model responses with the SFE process responses.

The reconciliation process tested different values of the two parameters (manifold length and metering valve opening) to improve model versus experimental agreement. The agreement considered both system pressure and system slurry level, with an emphasis on the steady state system pressure result. This process was limited to a single experimental case, Test V11 (and its replicate Test V12). Figure 4.17 illustrates the comparison of responses. The adjusted model uses a manifold length of 3.1 m and a metering valve opening of 32%. It should be noted that the pressure inside the vessel is based on readings from the pressure sensor installed at the bottom of the extraction vessel.

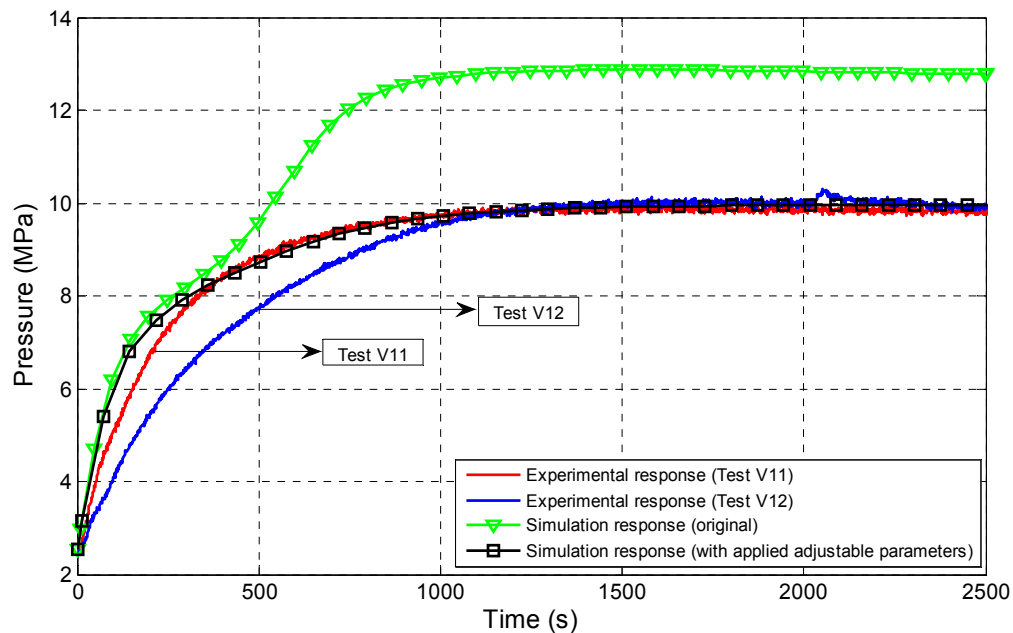


Figure 4.17. Pressure response comparison of experimental responses and simulation responses

Figure 4.17 illustrates that the adjusted model (with two empirically developed adjusted parameters) is substantially better than the original (purely predictive) model in terms of the pressure response to experimental Test V11. The agreement is evident in both the steady state value as well as fairly good agreement to the dynamic pressure response. It is evident that there is experimental variability in the dynamic pressure response. It should be emphasized that all *controllable* process conditions were similar between the two experiments; however, there are *uncontrollable* process conditions i.e. disturbances, which might have occurred during start-up and during the pressurization stage of the process, resulting in different pressure curves. Nevertheless, both the experimental and model responses reach the same steady state pressure.

A small bump is also observed in the pressure response of Test V12 at approximately 2100 s. This pressure increase was the result of freezing happening in the slurry outlet line. Consequently, the pressure started to increase in the vessel. However, after a few seconds, the freezing was eliminated and the pressure returned to its steady state value.

Table 4.12 summarizes the quantified performance of the adjusted models relative to the two experimental runs, Test V11 and Test V12. The performance comparison is based on both the steady state pressure and settling time. The settling time is defined as the time in which the response reaches within 5% of its steady state value and remains there. Based on these values, the absolute value of output errors (OE) is individually calculated between responses.

**Table 4.12. Comparison of experimental and model responses for validation Tests V11 and V12 in terms of steady state pressure and settling time**

	Adjusted model	Test V11	Test V12
<i>Results</i>			
SS Pressure (MPa)	9.96	9.85	10.01
Settling time (s)	800	790	970
<i>Performance Comparison (OE) based on SS pressure (OE in MPa) and settling time (OE in s)</i>			
Adjusted model	NA	0.11 MPa / 10 s	0.05 MPa / 170 s
Test V11	0.11 MPa / 10 s	NA	0.16 MPa / 180 s
Test V12	0.05 MPa / 170 s	0.16 MPa / 180 s	NA

NA – not applicable

As can be seen from the OE values reported in Table 4.12, regarding steady state pressure, the calculated errors between Test V11-Adjusted model (OE of 0.11 MPa) and Test V12-Adjusted model (OE of 0.05 MPa) are less than the error calculated for Test V11-Test V12 (OE of 0.16 MPa). These results show that the pressure response obtained from the model is within the range of the pressure response obtained from the physical process. For the settling time, the adjusted model agrees well with Test V11 but not with Test V12. The adjusted model does not capture the experimental settling time variability seen in the two tests.

Another validation test (Test V21) and its replicate (Test V22) were conducted on the physical process using a CO<sub>2</sub> pump flow of 23.5% and a slurry pump flow of 16.6%. Similarly, in simulating this validation test via the mathematical model, the adjusted values (from Test V11) for metering valve opening and manifold length were applied i.e. 32% and 3.1 m respectively. Figure 4.18 depicts pressure responses obtained from the mathematical model (with and without adjusted parameters) and the SFE process. Similar to the previous validation test, the adjusted model uses a manifold length of 3.1 m and a metering valve opening of 32%.

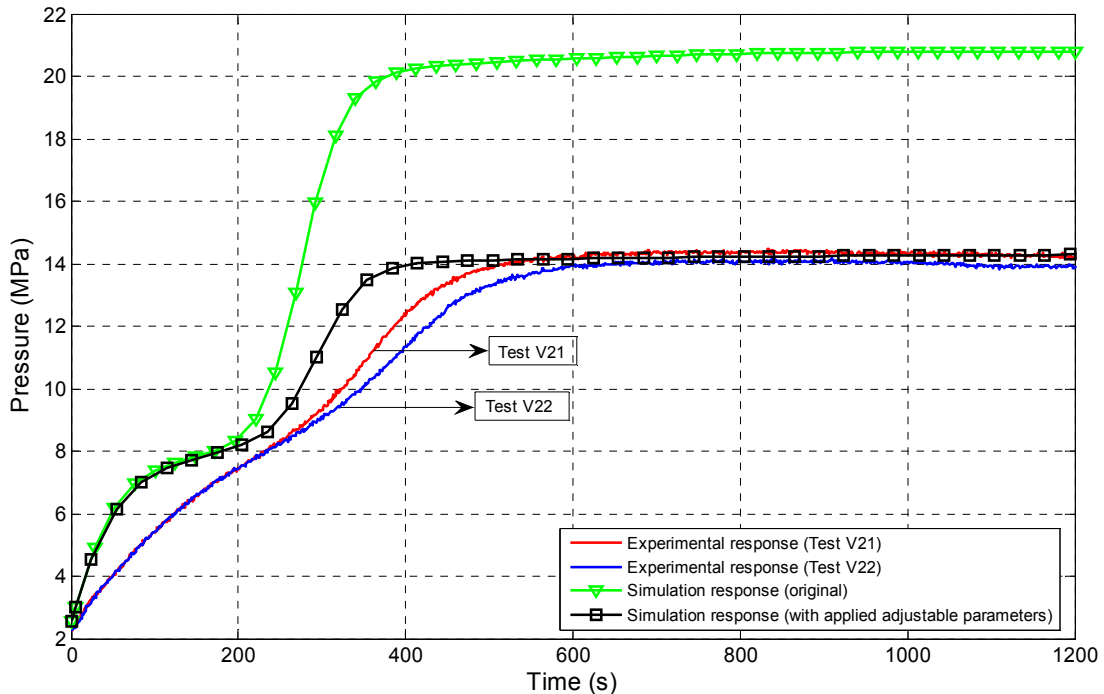


**Figure 4.18. Pressure response comparison between model, Test V21 and Test V22**

As can be seen in Figure 4.18, the responses of the adjusted model and the experimental runs (Test V21 and Test V22) reach approximately the same steady state pressure. It is also

observed that the adjusted model response is faster in reaching steady state pressure but it follows the same trend as the SFE process responses i.e. it changes slope at the pressure of approximately 8.5 MPa. It is again evident that that the adjusted model (with two empirically developed adjusted parameters) is substantially better than the original (purely predictive) model response.

To quantify the experimental results obtained from Test V21, Test V22 and the results obtained from the adjusted model, steady state pressure and settling time is calculated for all responses. Based on these values, the absolute value of output errors (OE) is individually calculated between each two responses. Table 4.13 summarizes these results.

**Table 4.13. Comparison of experimental and model responses for validation Tests V21 and V22 in terms of steady state pressure and settling time**

	Adjusted model	Test V21	Test V22
<i>Results</i>			
SS Pressure (MPa)	14.28	14.3	14.05
Settling time (s)	350	470	500
<i>Performance Comparison (OE) based on SS pressure (OE in MPa) and settling time (OE in s)</i>			
Adjusted model	NA	0.02 MPa / 120 s	0.23 MPa / 150 s
Test V21	0.02 MPa / 120 s	NA	0.25 MPa / 30 s
Test V22	0.23 MPa / 150 s	0.25 MPa / 30 s	NA
NA – not applicable			

As can be seen from the OE values reported in Table 4.13, regarding the steady state pressure, the calculated OE values for Test V21-Adjusted Model and Test V22-Adjusted Model are less than the error calculated for Test V21-Test V22. Therefore, with respect to steady state pressure, the adjusted model error is within an acceptable range.

Regarding settling time, the calculated OE value for Test V21-Test V22 is less than that of Test V21-Adjusted Model and Test V22-Adjusted Model. The adjusted model error indicates a bias towards a faster speed of response than is observed in either experimental case. This trend is also evident in Figure 4.18.

Overall, the adjusted model better represents the steady state pressures obtained experimentally under two different operating conditions. In terms of settling time, the adjusted

model provides a faster response for three of the four experimental trials.

The required degree of accuracy for a mathematical model is dependent on the intended use of the model. In this thesis, the primary objective for modelling the continuous SFE process is to predict pressure response in the extraction vessel for control studies. Based on this intent and the quantitative results as summarized in Table 4.12 and Table 4.13, it is concluded that the mathematical model is capable of successfully predicting pressure in the continuous SFE extraction vessel and it can be applied for the stated intent of control studies at different operating conditions.

### *Slurry level response*

Validating level response in the extraction vessel is not as simple as validating the pressure. Pressure is a regulating variable i.e. at steady conditions, it remains constant and with a slight change in conditions, it will find a new steady state value but it does not become unstable. On the contrary and as mentioned earlier, liquid level inside a vessel is a non-self regulating variable and tends to easily lose its balance point based on the surrounding conditions. Due to existence of unknown and uncontrollable disturbances in real processes, level trajectories can be very different in “similar runs” in which controllable parameters such as pump flows, manifold length and metering valve position, are the same between the different runs. In addition to this inherent characteristic of liquid level inside a vessel, in the current set-up of the pilot scale SFE process, due to technical difficulties, a continuous level sensor does not exist inside the extraction vessel to track changes of slurry level at different time instants therefore making it harder to validate level response. Consequently, the SFE process and mathematical model data for slurry level could not be continuously compared.

One technique for partially validating level is to compare the final level of slurry in the vessel i.e. slurry level at the end of an experimental run with the final slurry level as calculated by the mathematical model. The final slurry level in the extraction vessel is measured by draining the vessel, after the vessel has been depressurized. This remaining volume of slurry corresponds to a certain level inside the vessel based on the inner diameter of the extraction vessel, which is 0.08335 meters (Price-Schonstrom, 2009). It should be noted that a baffle structure also exists inside the extraction vessel, which partially occupies internal vessel volume. The largest part of the baffle structure in terms of volume is a cone located at the bottom of the

vessel. The existence of this cone and the baffle structure in general, introduces some error (i.e. a few centimeters) when calculating the slurry level based on only ID and length of the extraction vessel.

A summary of experimental data regarding level validation is provided in Table 4.14. Data presented are associated with the same validation tests introduced in the previous section. Test V11 and Test V12 were conducted with a CO<sub>2</sub> flow rate of 12.5% and a slurry flow rate of 13.8%. Test V21 and Test V22 were conducted with a CO<sub>2</sub> flow rate of 23.5% and a slurry flow rate of 16.6%.

**Table 4.14. SFE process data regarding level validation experiments**

Validation test ID	Volume of slurry drained (mL)	Equivalent slurry level (m)	Length of run (s)
Test V12	750	0.14	3600
Test V11	2100	0.39	3120
Test V22	1250	0.23	2220
Test V21	1250	0.23	1560

Figure 4.19 and Figure 4.20 present the level response as determined by the original and adjusted models for Tests V11 and V12 (Figure 4.19) and for Tests V21 and V22 (Figure 4.20). Figure 4.19 and Figure 4.20 also include the final experimentally measured slurry levels.

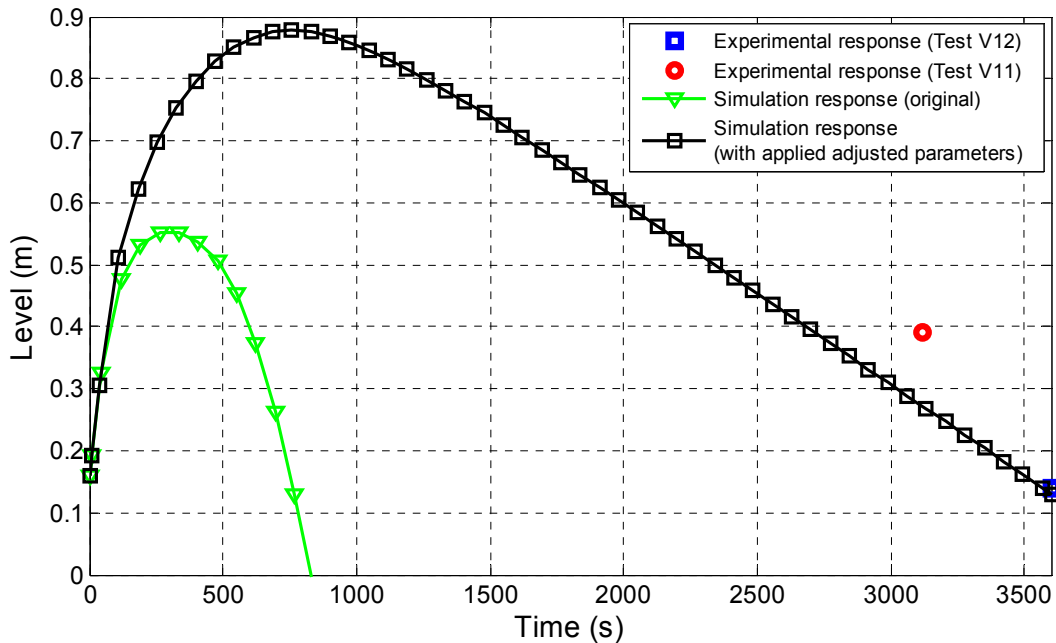


**Figure 4.19. Experimental and simulated level response for Tests V11 and V12**

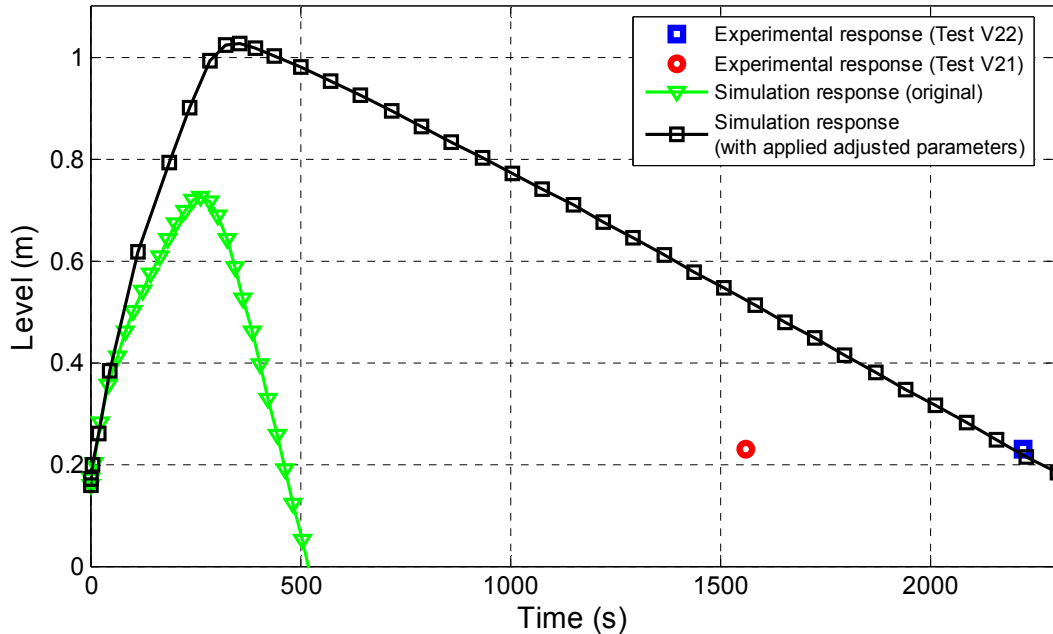


**Figure 4.20. Experimental and simulation results for level response for Tests V21 and V22**

As seen from Figure 4.19 and Figure 4.20, the original model level response results in the vessel becoming empty very early in the run (before 1000 s) i.e. the original model is completely inconsistent with experimental observations. However, the adjusted model response significantly improves and is very close to the experimental end point level data. The adjusted model responses are quantitatively compared with the experimental data. Results of this comparison are provided in Table 4.15.

**Table 4.15. Summary of results for level validation experiments**

	Test V11	Test V12	Test V21	Test V22
<i>Experimental Results</i>				
Level (m)	0.39	0.14	0.23	0.23
<i>Simulation Results with adjusted model</i>				
Simulation time (s)	3120	3600	1560	2220
Level (m)	0.29	0.14	0.52	0.23
OE (m)	0.10	0.00	0.29	0.00

Based on the results presented in Table 4.15, for Tests V11 and V12, the adjusted model is capable of predicting the trends observed in the experimental system, that is, as the length of the run increases from 3120 s to 3600 s, the final level inside the extraction vessel decreases. For Tests V21 and V22, the same trend was observed in the simulation results. However, experimentally, the same slurry level was measured for both Test V21 and Test V22, despite the

different run times. It was expected that a different slurry level should have been measured between Tests V21 and V22. As mentioned previously, this inconsistency may be related to the non-self regulating characteristic of slurry level inside the vessel and due to disturbances in the process. Therefore, it is challenging to precisely predict level response due to the high sensitivity of the level to process conditions. Nevertheless, the model is capable of predicting the trend of slurry level inside the vessel, as observed by the results presented in Figure 4.19 and Figure 4.20 for Tests V11, V12 and V22.

#### **4.4 Summary**

A hydrodynamic model characterizing the pilot scale continuous SFE process is developed. The model is capable of predicting the variables of the process i.e. pressure, slurry level, temperature, CO<sub>2</sub> mass and CO<sub>2</sub> density in the extraction vessel. This model is developed based on first principle equations i.e. continuity equation for CO<sub>2</sub>, continuity equation for slurry, energy balance, CO<sub>2</sub> equation of state and Density-Volume-Mass relationship for CO<sub>2</sub>. The model is implemented in MATLAB<sup>®</sup>/Simulink<sup>®</sup>. The model is verified and validated with regards to the two most important variables in the extraction vessel i.e. pressure and slurry level.

In the verification stage, the performance of the numerical solver, the main assumptions stated in the model development stage and the response of the system to the main process input parameters (i.e. slurry flow, CO<sub>2</sub> flow, manifold length, metering valve opening and slurry inlet temperature) are verified. With regards to the numerical solver, the generated numerical error for the main five equations is less than 1% and well within the confidence of the input data. With regards to the stated assumptions and based on the conducted simulations, it is concluded that none of the assumptions significantly impact pressure response in the extraction vessel, hence the stated assumptions are verified. With regards to the impact of the main process inputs (i.e. slurry flow, CO<sub>2</sub> flow, manifold length, metering valve opening and slurry temperature), obtained responses characterize the conceptual description of the SFE process.

In the validation stage, modelled pressure and level responses are compared with experimentally obtained data. In the first set of validation tests (i.e. Test V11 and its replicate Test V12), the metering valve opening and manifold length values originally used in the model were adjusted to reconcile model responses with physical process responses. In another set of validation tests (i.e. Test V21 and its replicate Test V22), the adjusted model responses are

compared with that of the validation tests. The adjusted model proved capable of accurately predicting the steady state pressure for the process (output error ranged from 0.02 to 0.23 MPa) and appears to predict a slightly faster response time (output error ranged from 120 s to 150 s for settling time). The adjusted model also provided consistency with the final slurry level in the extraction vessel (output error ranged from 0 to 0.29 m). The resulting adjusted model will prove valuable in process operation, development, and control. Future work would expand the hydrodynamic model to the separator.

## 5 Pressure Control in the Continuous Pilot Scale SFE Process

## 5.1 Introduction

During the operation of a chemical plant, many requirements must be fulfilled. Safety and production specifications are among such requirements and both are of critical importance (Stephanopoulos, 1984). Safe operation directly impacts the wellbeing of the people working in the plant as well as the chemical plant itself. For this purpose, process variables must be controlled and kept within allowable limits throughout the operation of the plant. It is also important for the chemical plant to be capable of meeting its production specifications. In other words, control systems are required to ensure that high quality and consistent products are produced. Therefore, consistent product quality, productivity and process safety are all increased as a result of effective control of key variables in a chemical plant (Shinskey, 1979; Goodwin *et al.*, 2000).

The SFE process under investigation in this thesis is no exception. This SFE process deals with high pressures and maintaining the pressure at a desired set point is necessary to ensure safe operation of the process. Pressure control also contributes to consistent extractions due to the direct relationship between mass transfer and pressure throughout an extraction process. Therefore, an important step in demonstrating successful operation of the continuous pilot scale SFE process is achieving effective pressure control in the process, specifically in the extraction vessel.

The main objectives of this chapter are twofold. The first objective is to implement and demonstrate successful pressure control in the extraction vessel of the continuous pilot scale SFE process. The second objective is to formulate a systematic approach for designing a model-based controller for the SFE process. As part of the second objective, the application and validity of the hydrodynamic model (developed in Chapter 4) for control studies is further explored.

As previously stated, the pressure and slurry level in the extraction vessel were selected as the two key variables that should be controlled during the SFE process. Pressure control in the extraction vessel is the focus of this chapter while level control is explored and implemented in Chapter 6. In Chapter 5, Section 5.2 gives background regarding feedback control and the Internal Model Control (IMC) framework for designing model-based controllers. Section 5.3 describes the methodology. Section 5.4 presents the results and a discussion related to tuning, testing and comparing controllers. In Section 5.4.1, the first objective is discussed i.e.

implementing and demonstrating pressure control in the SFE process by manual tuning of the PI controller. In Section 5.4.2, the second objective is discussed i.e. introducing a systematic approach for designing model-based controllers. The performance of the manually tuned and model-based controllers is compared in Section 5.4.3. In Section 5.4.4, as a continuation of the second objective, system identification is explored (via the hydrodynamic model) at different process conditions and the developed models are evaluated and compared. A summary is presented in Section 5.5.

## 5.2 Background

In this section, first the feedback control structure is briefly described. Next, the Internal Model Control (IMC) framework for designing model-based controllers is introduced.

### 5.2.1 Feedback control

The concept of feedback has a long history in process control and it is one of the most common and efficient structures for controlling variables such as pressure, temperature and level in chemical plants (Stephanopoulos, 1984; Astrom and Murray, 2010). In a feedback control structure, the variable of the process that needs to be controlled (controlled variable) is measured and compared to its desired value (set point). Based on the calculated difference (error), the controller,  $C(s)$ , adjusts the manipulated variable in order to reduce the error (Stephanopoulos, 1984). A typical feedback control structure is presented in Figure 5.1. The process is represented by  $G(s)$ . It should be noted that  $G(s)$  and  $C(s)$  are defined in the Laplace domain.

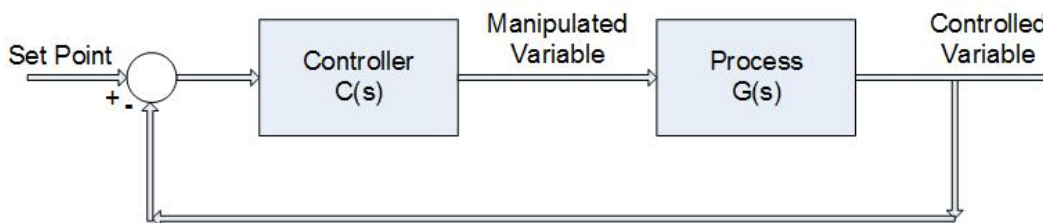


**Figure 5.1. Feedback control structure**

The most common type of controller applied in a feedback loop structure is from the Proportional-Integral-Derivative (PID) class of controllers (Astrom and Murray, 2010). These types of controllers are capable of solving extensive control problems and are recognized to be simple yet robust in the control of numerous industrial applications (Goodwin *et al.*, 2000; Astrom and Murray, 2010). The PID class of controllers have the following algorithm in time

domain (Astrom and Hagglund, 1995):

$$u(t) = K_c \left( e(t) + \frac{1}{\tau_I} \int_0^t e(\tau) d\tau + \tau_D \frac{de(t)}{dt} \right) \quad ( 5.1 )$$

In Equation 5.1, also known as the ideal PID controller,  $u(t)$  is the controlled variable and  $e(t)$  is the control error. The Laplace domain representation of Equation 5.1 is as follows:

$$C(s) = K_c \left( 1 + \frac{1}{\tau_I s} + \tau_D s \right) \quad ( 5.2 )$$

Depending on the values chosen for proportional gain ( $K_c$ ), integral time ( $\tau_I$ ) and derivative time ( $\tau_D$ ), different actions are obtained from the controller. Setting both  $\tau_D$  and  $1/\tau_I$  to zero results in a Proportional (P) controller with only one tuning parameter i.e.  $K_c$ . A proportional controller changes the manipulated variable by an amount that is proportional to the error. A limitation of proportional control is that it results in a steady state error (offset) (Coughanowr, 1991).

Setting only  $\tau_D$  to zero results in a Proportional-Integral (PI) controller with two tuning parameters i.e.  $K_c$  and  $\tau_I$ . Integral action results in a controller output proportional to the accumulation of error (Goodwin *et al.*, 2000). Responses obtained from a PI controller have the advantage of being offset-free. However, due to the integral action, an oscillatory response may be obtained (Coughanowr, 1991). A challenge associated with PI control is appropriately adjusting the two tuning parameters that interact with each other.

Applying a value to all the three parameters in Equation 5.1 i.e.  $K_c$ ,  $\tau_I$  and  $\tau_D$  results in a Proportional-Integral-Derivative (PID) controller with three tuning parameters. Adding derivative action results in a controller output proportional to the derivative of the error. In theory, a PID controller results in a less oscillatory and more damped response in comparison to a PI controller (Coughanowr, 1991; Astrom and Murray, 2010). However, adding the derivative action will also result in increased noise sensitivity and input usage (Skogestad and Grimholt, 2012). Due to these disadvantages and due to the fact that a PID controller requires additional tuning parameters in comparison to a PI controller, derivative action is not common in industrial applications, leading the way to a PI controller which is the most common controller applied in industry (Astrom and Murray, 2010). Hence, PI control is also the preferred controller, explored and employed in this chapter for pressure control.

## 5.2.2 Internal Model Control (IMC)

Many approaches exist for tuning a controller. PID class controller tuning methods can be categorized into two main groups: (i) closed loop methods and (ii) open loop methods. As indicated by their name, closed loop tuning methods take place when the process is in automatic mode (i.e. closed loop) while open loop tuning methods take place when the process is in manual mode (i.e. open loop).

Well known closed loop methods are the Ziegler-Nichols method (Ziegler and Nichols, 1942) and the Tyreus-Luyben method (Luyben and Luyben, 1997). The major disadvantage of closed loop methods is that they are based on trial and error and lead to time consuming operations.

Well known open loop methods are the open loop Ziegler-Nichols method (Ziegler and Nichols, 1942), the Cohen-Coon method (Cohen and Coon, 1953) and the Internal Model Control (IMC) method (Garcia and Morari, 1982). In these methods, process dynamics should first be approximated by a simple model, typically a first order plus dead time (FOPDT) model with the following equation:

$$G(s) = \frac{ke^{-\theta s}}{\tau_1 s + 1} \quad ( 5.3 )$$

In Equation 5.3,  $k$  is the process gain. This parameter is the steady state change of the controlled variable divided by the change in the manipulated variable.  $\tau_1$  is the dominant time constant of the process and represents the time it takes for the process variable (i.e. pressure) to reach 63.2% of its ultimate value.  $\theta$  is the process dead time and represents transportation and/or instrumentation lag in the process.

Among the stated open loop methods, the IMC method has achieved widespread industrial acceptance for tuning PID class controllers (Skogestad, 2003; Skogestad, 2004; Skogestad and Grimholt, 2011). The main advantage of the IMC method is that it explicitly takes into account model mismatch (i.e. the difference between process model and actual process). In addition, it allows a trade-off between system performance and robustness. The IMC method has been applied in this chapter for designing model-based controllers.

The IMC method, initially introduced by Garcia and Morari (1982), is a modern control

technique that utilizes a model of the process to compute the controller action (Roffel and Betlem, 2003). The basic IMC structure is illustrated in Figure 5.2.

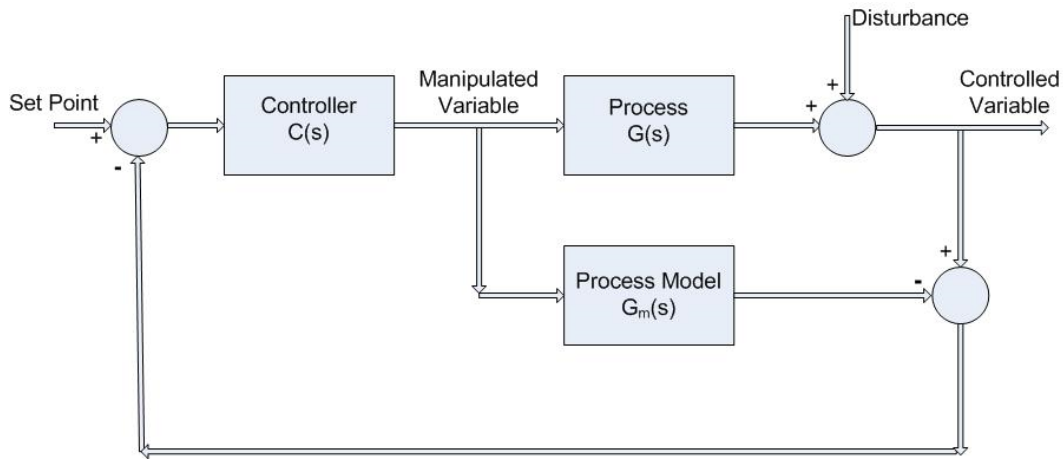


**Figure 5.2. Schematic of IMC structure**

As observed in Figure 5.2, a model of the process,  $G_m(s)$ , exists in this structure. The manipulated variable is introduced to both the process,  $G(s)$ , and the model of the process  $G_m(s)$ . The controlled variable is first compared with the output of the model. The result of this comparison is then compared with the feedback loop set point. Based on this control structure, if there is no model mismatch (i.e. process model is an exact representation of the process AND if the controller is chosen as the inverse of the model), perfect set point tracking and disturbance rejection is achieved. In reality however, discrepancies between the actual process and the model always exist. Therefore, the controller is designed in series with a filter to reduce the effect of process-model mismatch (Garcia and Morari, 1982).

The block diagram as presented in Figure 5.2 can be converted into a conventional feedback loop structure with a PI or PID controller as presented in Figure 5.1. In this structure, the parameters of the PID class controller are calculated from information obtained from simple models of the process. This approach was initiated by Rivera *et al.* (1986). The main goal of the work by Rivera *et al.* (1986) was to present simple rules (i.e. rules which can be easily applied in a process) to relate the process model (obtained from experimental data) to controller parameters. Rivera *et al.* (1986) concluded that the IMC structure naturally leads to PID class controllers based on simple models common to chemical processes (such as first or second order linear models obtained from system identification techniques). This framework is applied in this chapter to design the PI controller in the extraction vessel pressure control loop.

### 5.3 Methodology

Based on the discussion in Section 5.2.1, the feedback loop structure with PI control was chosen as the preferred structure for controlling pressure in the extraction vessel. To implement the feedback structure, reliable data of the controlled variable is required to compare with the set point and apply the correcting action. Direct digital control (DDC) is utilized in the continuous pilot scale SFE process for data acquisition and control. In other words, a central computer exists that directly receives measurements from the process. Based on the control law, already programmed via control software on the computer, a control action is calculated and applied. The selected control software for the SFE process is National Instrument's LabVIEW™. LabVIEW™ has data acquisition capabilities and also provides the user with an interface for controlling the SFE process from the computer.

In the current setup of the pilot scale SFE process, pressure at the top and bottom of the extraction vessel is measured and recorded. Therefore, data is available for the feedback loop structure to control the extraction vessel pressure. Either the pressure at the top or at the bottom of the extraction vessel can be selected for this purpose. The manipulated variable in the feedback loop is CO<sub>2</sub> flow from the pump, which is calculated based on the speed of the CO<sub>2</sub> pump.

Many experimental runs have been conducted on the continuous pilot scale SFE process. Each of these experiments followed a different aim e.g. control studies, mass transfer studies, process troubleshooting, etc. In some instances, one experiment contributed to two or more aims. A complete list of these experiments was presented in Chapter 3. However, only experimental runs and data regarding pressure control in the extraction vessel and controller design for the pressure control loop are presented and discussed in this chapter. Table 5.1 lists these experiments and summarizes main outcomes. Results regarding these experiments are presented and discussed in Section 5.4. It should be noted that Table 5.1 is a subset of Table 3.6 presented in Chapter 3.

**Table 5.1. SFE experiments related to implementation and demonstration of pressure control in the extraction vessel**

<b>Run</b>	<b>Component</b>	<b>Objective</b>	<b>Outcomes</b>	<b>Pressure range</b>
7a	CO <sub>2</sub>	Test the pressure control loop	Steady state pressure was achieved at 5.3 MPa.	Below supercritical pressure (around 5 MPa)
7b	CO <sub>2</sub>	Test the pressure control loop	Emergency shutdown happened.	Below supercritical pressure (around 5 MPa)
7c	CO <sub>2</sub>	Test the pressure control loop	Steady state pressure was achieved (at three different set points).	Below supercritical pressure (around 5 MPa)
18	CO <sub>2</sub> /water	Countercurrent run for as long as possible	Countercurrent run was achieved for one hour. No reason was observed to terminate run.	Around supercritical pressure (7-8 MPa)
26	CO <sub>2</sub> /water	Countercurrent run for as long as possible	Successful countercurrent run achieved for one hour.	In the vicinity of 10 MPa
29	CO <sub>2</sub> /water	Obtain system identification data at around 12 MPa	Successfully obtained system identification data.	In the vicinity of 12 MPa.
81	CO <sub>2</sub> /water	Test the model-based controller on the process and compare its performance with the previous manual-based controller.	Successful run achieved with model-based controller.	In the vicinity of 12 MPa

Before designing controllers, the aim of control should be defined for the SFE process. In the first phase of SFE experimental runs (Runs 7a, 7b and 7c), attempts were made to control the pressure. The aim of pressure control in this phase was to first achieve basic pressure control and next to pressurize extraction vessel at different pressures by increasing the pressure set point in consecutive steps. In other words, the aim of control at this point of time was focused on set point tracking. In the second phase of SFE experimental runs (Run 18 and 26), the aim of control was twofold: pressurize the extraction vessel in consecutive steps and maintain the pressure at the desired set point for as long as possible. During this long period, there is a high chance of disturbances occurring in the process. Therefore, the aim of control is both set point tracking and disturbance rejection.

The aim of control will affect the controller design. Therefore, it is important to define the main aim of control at this stage as being for set point tracking (servo problem) or disturbance rejection (regulator problem) or both. The regulator problem is more common in the chemical industry, while the majority of problems described as the servo type are from areas other than the chemical industry (Coughanowr, 1991). Well known examples of the regulator problem in the chemical industry are composition control, pressure control and temperature

control in unit operations such as heat exchangers, distillations columns, reactors, etc. A well-known example for set point tracking is tracking of missiles and aircraft. However, there are processes in which both the servo problem and the regulator problem are considered when defining the aim of control.

In the process under investigation in this research, disturbance rejection is important because during the extraction period of an experiment, the set point will not be changed but disturbances may occur during this long period (clogging and freezing in the lines, for example). Therefore, it is important for the designed controller to be effective in rejecting the effect of these disturbances on the extraction vessel pressure. However, during pressurization of the SFE process, the extraction vessel is brought up to the desired pressure in steps for safety reasons. Increasing the set point in consecutive steps until the final pressure set point is reached is to some extent set point tracking and it would be desirable to reach the set points faster in order to have a faster pressurization period. Therefore, set point tracking is also valuable. Based on this fact, both set point tracking and disturbance rejection are explored in comparing the performance of the designed controllers.

## 5.4 Results and discussion

In this section, different approaches are explored for tuning and designing the PI controller in the feedback loop structure. Results of manual tuning of the PI controller are presented in Section 5.4.1. In Section 5.4.2, a more systematic approach based on a model of the process is presented for designing the PI pressure controller. The IMC framework is applied in this section. In Section 5.4.3, the performance of both controller types (i.e. manually tuned and model-based) is compared. In Section 5.4.4, designing a model-based controller (via the hydrodynamic model) at different operating conditions is explored.

To quantitatively compare performance of the tuned controllers in each stage, both output performance and input performance are considered. Output performance is associated with the pressure change inside the extraction vessel and input performance is associated with CO<sub>2</sub> usage. To evaluate the output performance, the integral of the absolute error (IAE) is calculated based on the following equation:

$$IAE = \int |e| dt \quad ( 5.4 )$$

IAE is one of the most accepted performance criteria measurements (Shinskey, 1979) and, in this chapter, IAE represents the measure of total area under the pressure response curve on both sides of zero error. Unit time spacing (i.e. time interval of 1 s) is considered for calculating IAE. IAE should be as small as possible.

In addition to the pressure response, the CO<sub>2</sub> usage (i.e. CO<sub>2</sub> flowrate) is also important for the SFE process, especially from a safety stand point. The stainless steel feed line from the CO<sub>2</sub> pump to the extraction vessel is small (1/4" outer diameter). Therefore, aggressive use of CO<sub>2</sub> in a short time will result in high pressures in this line. As previously explained in Chapter 3, emergency alarms are defined for different components of the SFE process such as the CO<sub>2</sub> feed line to the extraction vessel. Over pressurization of this line will result in an emergency shutdown of the process. Therefore, a controller output that results in aggressive CO<sub>2</sub> usage and therefore rapid increase of pressure in the CO<sub>2</sub> feed line, must be avoided. To evaluate input performance, the total variation (TV) of the input (CO<sub>2</sub> usage) is calculated based on the following equation:

$$TV = \sum_{i=1}^{\infty} |u_{i+1} - u_i| \quad ( 5.5 )$$

where TV represents the sum of the change of the input i.e. CO<sub>2</sub> flowrate. TV is a good measure of the smoothness of a response (Skogestad, 2003) and it should be as small as possible. Unit time spacing is considered for calculating TV.

Qualitative criteria are also considered in comparing responses of controllers. These are overshoot, oscillation and response time. Overshoot and oscillation are associated with the quality of response, while response time is a measure of response speed (Coughanowr, 1991; Skogestad and Postlethwaite, 2005). Overshoot is defined as a measure of how far the response deviates from its set point. Large overshoots and oscillations are not desirable and should be minimized. Response time is defined as the time taken by the process variable to reach within a defined percent (%) of its set point and remain there. A short response time is preferred.

### 5.4.1 Manual tuning of the controller

A first attempt to control pressure in the extraction vessel is associated with experimental Runs 7a, 7b and 7c. As presented in Table 5.1, the component in the process for these experiments was CO<sub>2</sub> and the operating pressure was below SC-CO<sub>2</sub> pressure i.e. 7.4 MPa. The reason for this low pressure was that these experiments were the first experiments in which the feedback control loop was being tested. It was therefore decided that testing only with CO<sub>2</sub> and at relatively low pressures was a safe experimental strategy at this stage.

Before applying the feedback control loop, values had to be chosen for the parameters of the PI controller ( $K_c$  and  $\tau_I$ ). In the first experimental run (Run 7a),  $K_c$  and  $\tau_I$  were arbitrarily chosen as  $4 \frac{\%}{\text{MPa}}$  and 0.1 min (i.e. 6 s), respectively. In general, a higher  $K_c$  value and lower  $\tau_I$  value result in faster control. However, the aim of this experiment was to only test the feedback loop and make sure it was working as expected. Hence, the chosen controller parameter values were thought to be a good starting point for this experiment.

In Run 7a, the feedback control loop was based on the pressure as measured at the top of the extraction vessel. The controller setting was set to “auto” when the pressure reached 5 MPa. The selected set point was 5.3 MPa. Figure 5.3 depicts the pressure response at the top and bottom of the extraction vessel for Run 7a. It should be noted that time=0 in Figure 5.3 and all figures related to experimental runs in this chapter, represent the start of an event and not the start of an experiment.

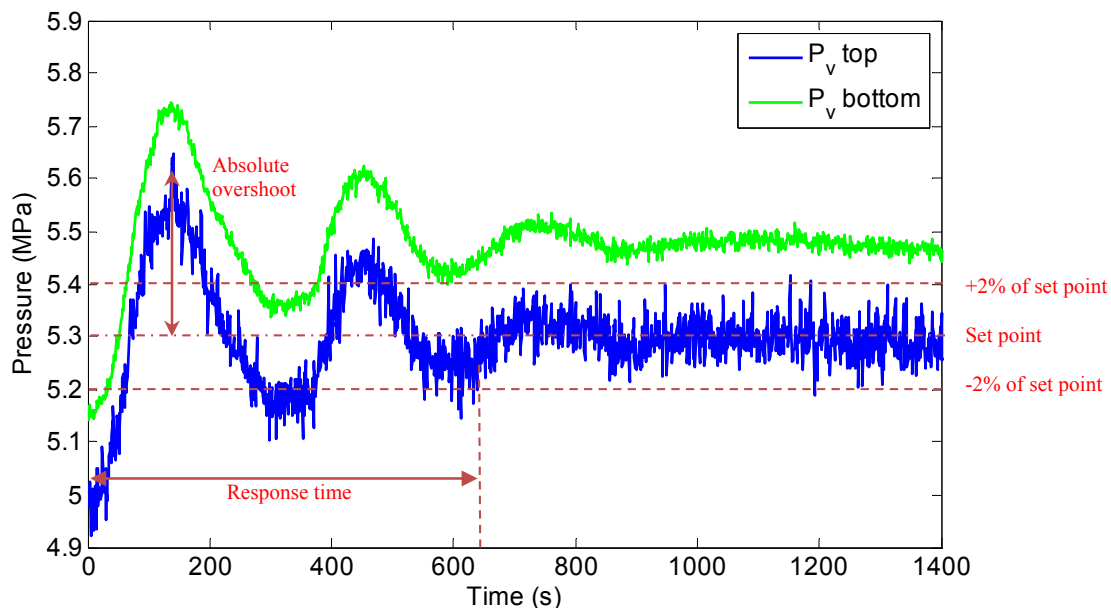


**Figure 5.3. Pressure response at the top and bottom of the extraction vessel to a set point change in Run 7a**

As seen in Figure 5.3, pressure control is achieved (i.e. the pressure converges to the selected set point) as a result of the applied PI controller parameters and it is concluded that the feedback control loop works as expected. An overshoot of approximately 0.3 MPa is observed. It is easily seen that the response is oscillatory and its response time (within  $\pm 2\%$  of set point) is approximately 650 s. These measures are approximate because of the noisy pressure response.

Another observation is that the pressure at the bottom of the extraction vessel is less noisy in comparison to the pressure at the top of the extraction vessel. Therefore, in subsequent experiments it was decided to set the feedback control loop based on the pressure at the bottom of the extraction vessel rather than at the top of the extraction vessel. Therefore, subsequent figures in this chapter only depict pressure as measured at the bottom of the extraction vessel. A slight pressure difference (approximately 0.15 MPa) between top and bottom pressures is also observed. This difference is assumed to be mostly associated with instrument offset.

Figure 5.4 depicts the CO<sub>2</sub> usage as a result of the applied controller in Run 7a. It should be noted that CO<sub>2</sub> flow is reported as the percentage of the maximum flow of the CO<sub>2</sub> pump (i.e. 6.46 L/min).

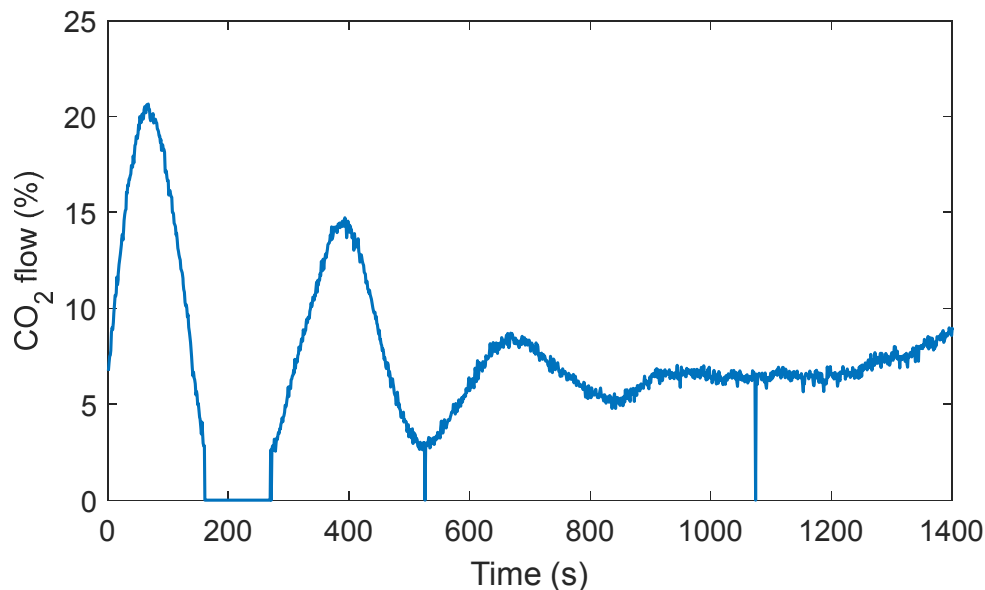


**Figure 5.4. Controller output as a result of a set point change in Run 7a**

As seen in Figure 5.4, the CO<sub>2</sub> usage has an oscillatory response as a result of the applied controller. This response is as expected based on the pressure response presented in Figure 5.3.

In Run 7b, in order to achieve a faster response, it was decided to increase  $K_c$  to 6  $\frac{\%}{MPa}$  and decrease  $\tau_I$  to 0.01 min (i.e. 0.6 s). In general, increasing the controller gain ( $K_c$ ) and decreasing the integral time ( $\tau_I$ ) will result in increased proportional action and integral action, respectively. As a result, faster control is achieved. By applying these settings and initiating the experiment, the CO<sub>2</sub> pump speed immediately jumped to 100%, resulting in an emergency shutdown because of a high pressure alarm in the CO<sub>2</sub> feed line. As a reminder, the CO<sub>2</sub> enters the extraction vessel through a 1/4" OD stainless steel line. Therefore, this line pressurizes much faster than the extraction vessel, especially at higher CO<sub>2</sub> pump speeds. There are several aspects to this event that are worthy of discussion:

- A possible reason for the emergency shutdown in Run 7b could be that the alarm limits for this CO<sub>2</sub> line were set low (as a safety precaution). If set higher, this emergency alarm might not have triggered and satisfactory pressure control may have been achieved.
- Another possible and most likely reason for the emergency shutdown could be associated with the selected PI controller parameters, which resulted in aggressive

CO<sub>2</sub> usage. Aggressive CO<sub>2</sub> usage in turn, resulted in rapid increase of pressure in the CO<sub>2</sub> feed line.

Run 7c therefore involved increasing the gain from 6 to  $8 \frac{\%}{MPa}$  in order to increase the speed of response and, at the same time, increasing the integral time from 0.01 min (i.e. 0.6 s) to 0.3 min (i.e. 18 s) to prevent rapid increase of pressure. Figure 5.5 depicts the pressure response as a result of these changes. In Run 7c, the set point was changed three times from 4.5 to 4.9 and finally to 5.7 MPa.

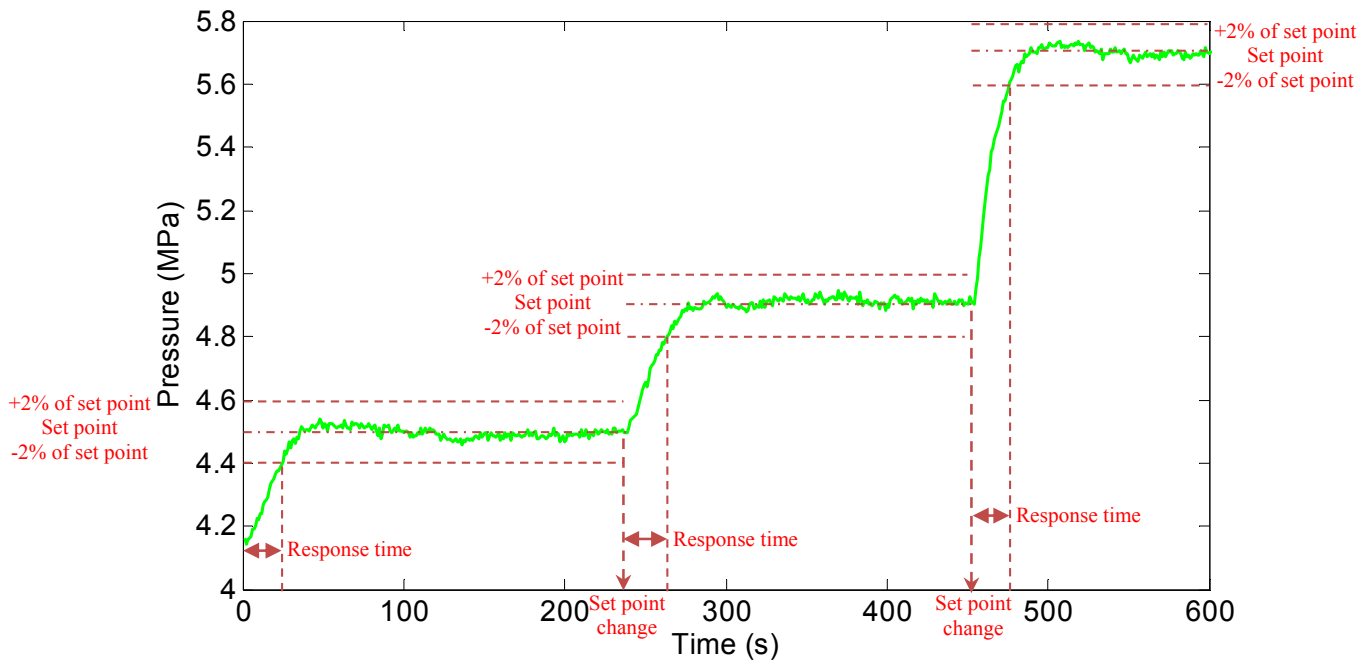


**Figure 5.5. Pressure response at the bottom of the extraction vessel to set point changes in Run 7c**

As seen from Figure 5.5, overshoot and oscillation are consistently less than  $\pm 2\%$  of set point. Response time (within  $\pm 2\%$  of set point) is less than 50 s. In qualitatively comparing responses obtained from Run 7c (Figure 5.5) with that of Run 7a (Figure 5.3), it is obvious that the responses obtained from the tuned controller in Run 7c are faster and have a better quality (i.e. oscillations are damped).

Figure 5.6 depicts the CO<sub>2</sub> usage as a result of the applied controller in Run 7c.

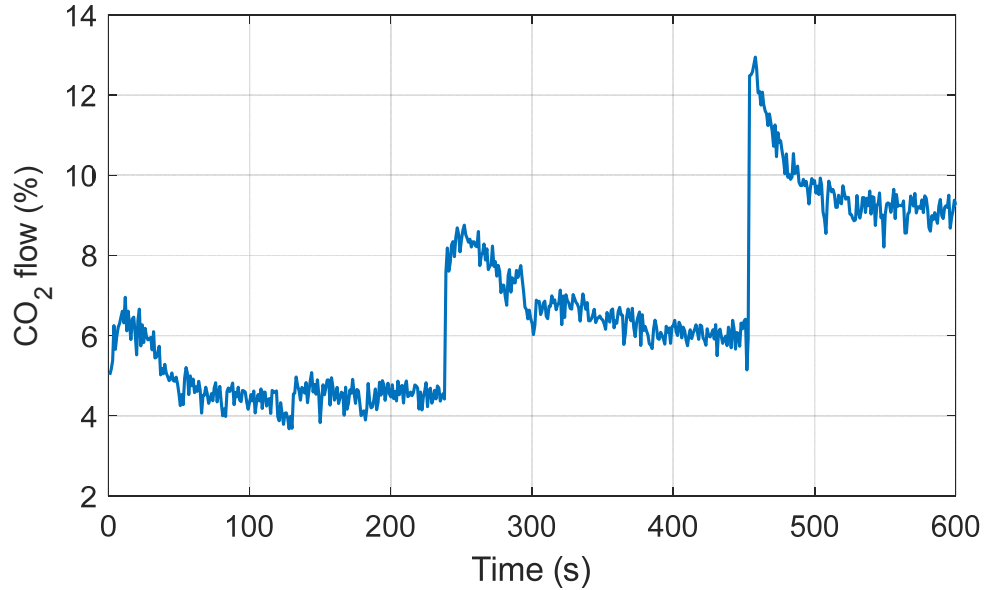


**Figure 5.6. Controller output as a result of set point changes in Run 7c**

As seen in Figure 5.6, no oscillation is observed in the CO<sub>2</sub> flow response for any of the set point changes.

To quantitatively compare the output performance and input performance of the two controllers of experimental Run 7a and Run 7c, the integral of the absolute error (IAE) and the total variation (TV) is calculated for the obtained pressure responses and CO<sub>2</sub> flows, respectively. IAE and TV values for Run 7a are calculated over the time span of 0 to 1400 s. For Run 7c IAE and TV values are calculated separately for each step change i.e. 0 to 240 s, 241 to 454 s and 455 to 600 s. Results of this comparison are presented in Table 5.2.

**Table 5.2. IAE and TV values for Controller 1 (Run 7a) and Controller 2 (Run 7c)**

	$K_c$ ( $\frac{\%}{MPa}$ )	$\tau_i$ (s)	Initial pressure (MPa)	Set point pressure (MPa)	IAE (MPa.s)	TV (%)
Controller 1	4	6	5	5.3	92.9	320.4
			4.2	4.5	8.8	68.5
Controller 2	8	18	4.5	4.9	8.3	55.4
			4.9	5.7	9.5	44.8

As seen from Table 5.2, lower IAE and TV values are calculated for the controller settings of Run 7c i.e. Controller 2. Because the time span in Run 7c is shorter than that of Run 7a, comparing values might not be the best way to compare the performance of the two controllers. However, based on the qualitative comparisons, it can safely be concluded that

Controller 2 has a better performance in comparison to Controller 1. Hence, the parameters of Controller 2 were applied in all subsequent experiments of the continuous SFE process.

To demonstrate the success of Controller 2 in controlling the pressure at other operational conditions, Runs 18 and 26 were performed. Both of these experimental runs were aimed at achieving countercurrent flow of SC-CO<sub>2</sub> and water through the extraction vessel for as long as possible and at higher pressures. The operational pressure of Run 18 is in the vicinity of the supercritical pressure of CO<sub>2</sub> (i.e. 7.4 MPa), while that of Run 26 is above supercritical pressure.

Figure 5.7 demonstrates the pressure response in Runs 18 and 26.

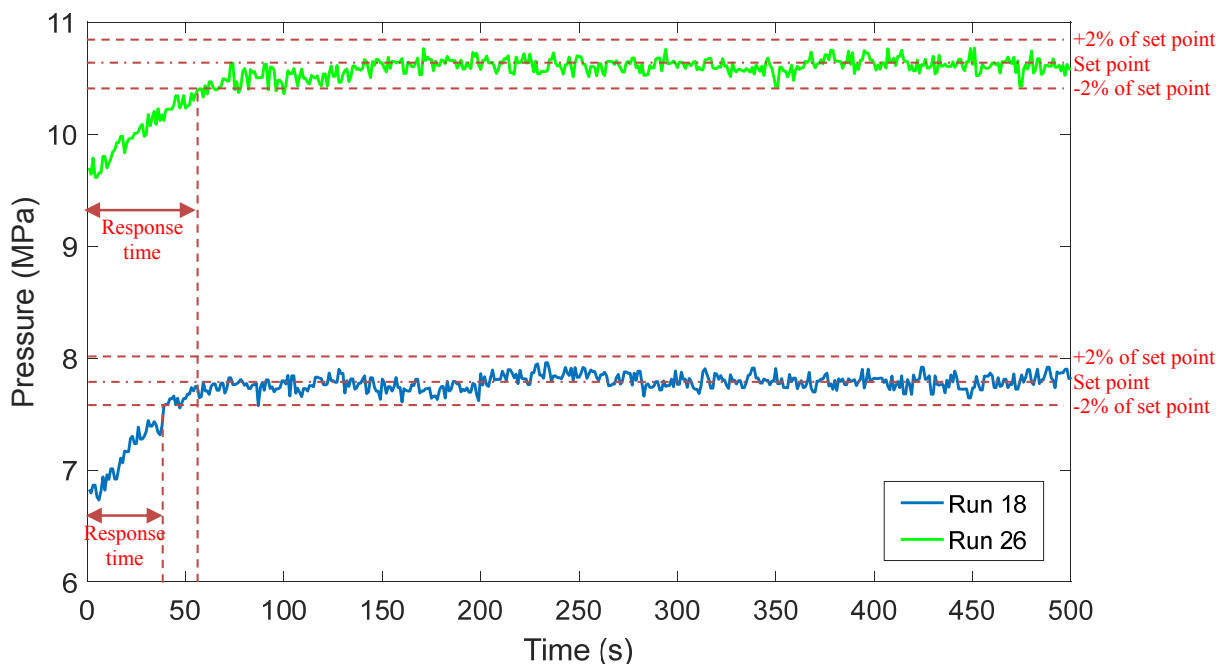


**Figure 5.7. Pressure response to a set point change in Run 18 and Run 26**

As seen in Figure 5.7, the response times (within  $\pm 2\%$  of set point) for Run 18 and Run 26 are 50 s and 65 s, respectively. The response times for Runs 18 and 26 are slightly higher in comparison to Run 7c (less than 50 s for Run 7c). However, in terms of quality, these pressure responses depict a similar behaviour i.e. oscillation and overshoot are less than 2% of set point.

As presented earlier in Table 5.1, in Runs 7a, 7b and 7c, only CO<sub>2</sub> was flowing in the process and the slurry pump was not turned on during these experiments. On the other hand, in Run 18 and Run 26, both CO<sub>2</sub> and water were flowing through the extraction vessel

countercurrently. However, by qualitatively comparing the pressure responses obtained from these runs as seen in Figure 5.5 and Figure 5.7, similar responses, or in other words, similar controller output performance is observed.

Figure 5.8 depicts the CO<sub>2</sub> usage in Run 18 and Run 26.

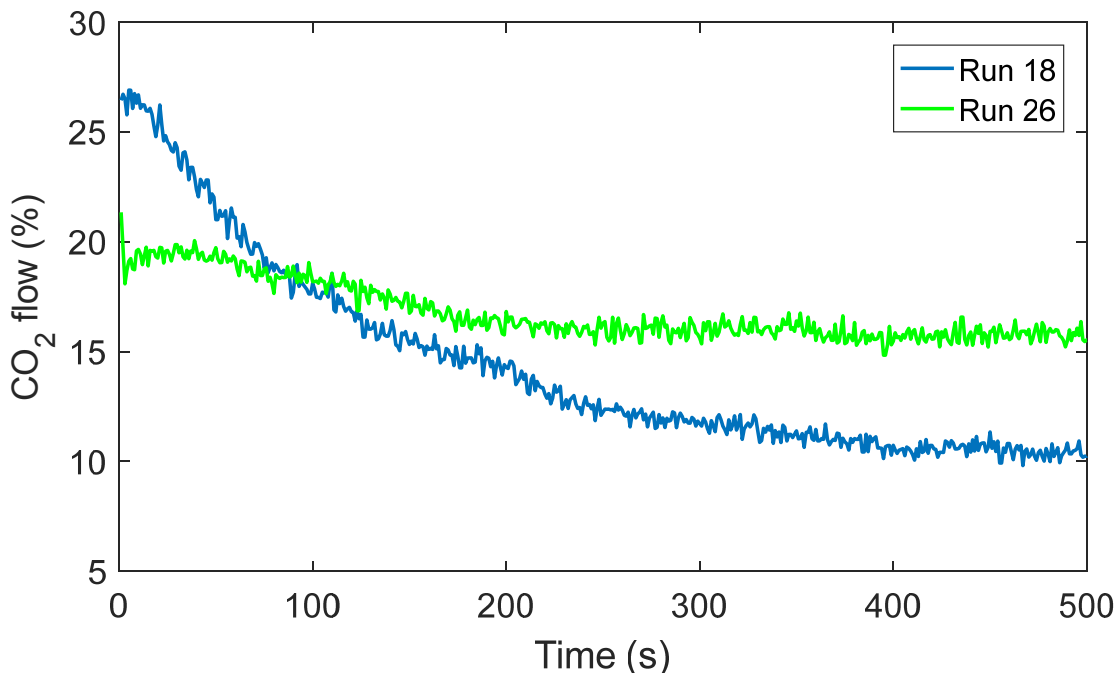


**Figure 5.8. Controller output as a result of a set point change in Run 18 and Run 26**

As seen in Figure 5.8 and as expected, smooth CO<sub>2</sub> flow responses are obtained for both Run 18 and Run 26.

In summary, a PI controller has been manually tuned and applied to the feedback control loop. As a result, pressure control is achieved in the extraction vessel of the SFE process. The manually tuned PI controller is applied for both the pressurization of the extraction vessel and during extraction.

#### **5.4.2 Model-based controller**

Although successful countercurrent SFE experiments were conducted with the manually tuned PI controller, the selected parameters of this controller are most likely not optimal because they were chosen based on trial and error, and have only been tested for a range of conditions. Other tuning parameters might lead to faster control of pressure while ensuring stability of the

SFE process and smooth usage of CO<sub>2</sub>. Hence, it is worthy to provide a systematic controller design procedure (vs. a trial and error approach) that can be applied in future stages of this research and to similar processes. Availability of a systematic approach for controller design is especially important for the pilot scale SFE process under investigation in this thesis. The reason being, successful operation of this process will lead the way to development of an industrial scale SFE process. Hence, presenting a systematic approach for designing an effective controller which can be applied to this industrial process is valuable for future development and upgrades.

In this section, a systematic approach is presented for designing a simple yet effective controller for the pilot scale SFE process. As introduced in Section 5.2.2, the IMC structure is a well-known approach for providing a framework for designing model-based controllers, especially for the PI and PID controller type.

The IMC-PID tuning rules and guidelines as presented by Skogestad (2003, 2004 and 2006) and Skogestad and Grimholt (2012) are applied to design a model-based controller for the extraction vessel of the SFE process with CO<sub>2</sub> flow as the manipulated variable and pressure as the controlled variable.

To design a model-based controller using the IMC framework, a simple linear model is required. One of the easiest methods for deriving a simple model of the process is by applying an open loop step test (Skogestad, 2003). This method was applied to the pilot scale SFE process and sufficient data for this purpose was acquired in Run 29. The aim of Run 29 was to obtain data in the vicinity of 12 MPa. Prior to Run 29, most SFE runs were conducted at a pressure between 10 to 14 MPa. Hence, conducting an open loop step test at an operating pressure in the range of 10 to 14 MPa was reasonable. Therefore, a step change was applied to the CO<sub>2</sub> flow from 21.5% to 25%. The time variation of the input variable (CO<sub>2</sub> flow) and the output variable (pressure) of the step test is presented in Figure 5.9.

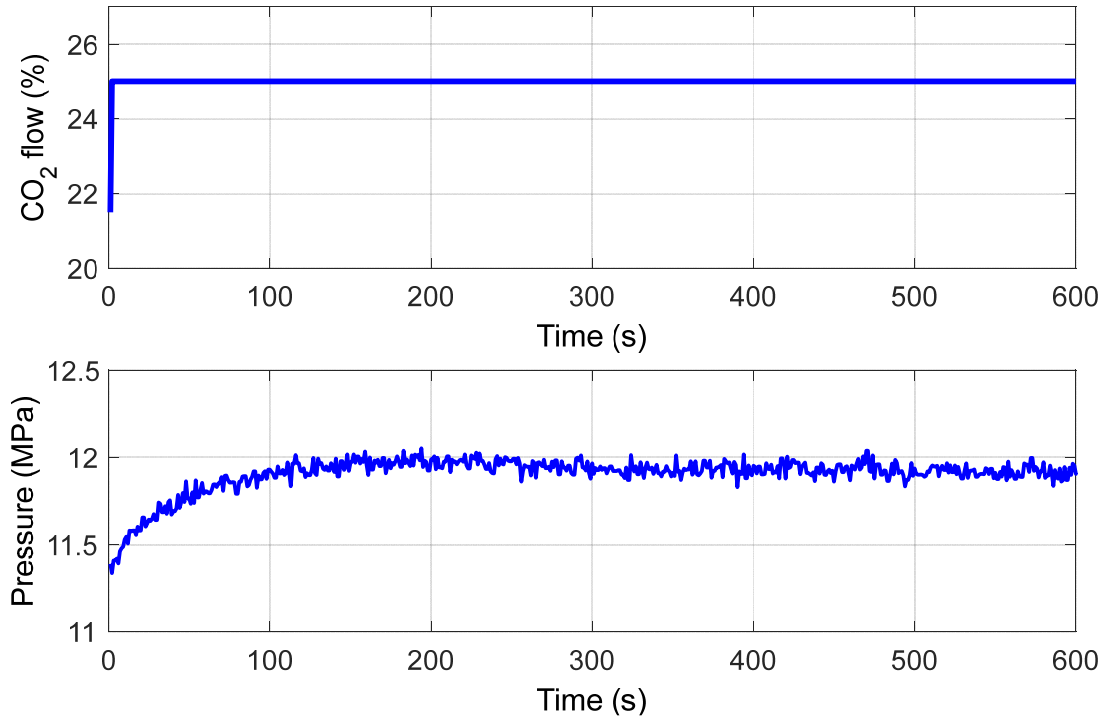


**Figure 5.9. Step test input (CO<sub>2</sub> flow) and output (pressure) time variation**

As seen in Figure 5.9, as a result of increasing the CO<sub>2</sub> flow, the extraction vessel pressure increases from 11.39 MPa to 11.95 MPa. During this period, the slurry flow was kept constant at 15.5%. The manifold length and metering valve opening were also kept constant.

The Input-Output data (i.e. measured values for the input and output variables) obtained from this step test were applied to develop a first order plus dead time (FOPDT) model. Model development was applied by importing the Input-Output data into the system identification toolbox in MATLAB<sup>®</sup>. As a result, the following first order model was estimated:

$$G(s) = \frac{0.16e^{-0.4s}}{36.8s + 1} \quad ( 5.6 )$$

Based on Equation 5.6, the process gain ( $k$ ) and the dominant time constant ( $\tau_1$ ) are calculated as  $0.16 \frac{MPa}{\%}$  and 36.8 s, respectively. The process dead time ( $\theta$ ) has a very small value of 0.4 s. A value of this order of magnitude is typical for fast loops such as pressure in which the dominant time constant is much larger than the dead time. This small value of  $\theta$  is also seen in Figure 5.9 i.e. pressure change takes place almost as soon as the step change in CO<sub>2</sub> flow is applied, resulting in a very small delay time.

Following the simple analytical rules for PID control tuning in the IMC structure as presented by Skogestad (2003, 2004 and 2006) and Skogestad and Grimholt (2012), the PI controller parameters recommended for a process represented by a first order linear model are:

$$K_c = \frac{1}{k} \frac{\tau_1}{\tau_c + \theta} \quad (5.7)$$

$$\tau_I = \min\{\tau_1, 4(\tau_c + \theta)\} \quad (5.8)$$

where  $K_c$  and  $\tau_I$  are the PI controller parameters and  $\tau_c$  is the time constant of the closed loop response.

Based on the estimated process model parameters ( $k$ ,  $\tau_1$  and  $\theta$ ), Equation 5.7 and Equation 5.8 are simplified as follows:

$$K_c = \frac{230}{\tau_c + 0.4} \quad (5.9)$$

$$\tau_I = \min\{36.8, 4(\tau_c + 0.4)\} \quad (5.10)$$

From Equation 5.9 and Equation 5.10, it is seen that only one parameter (i.e.  $\tau_c$ ) is required for tuning the PI controller which normally requires two parameters i.e. controller gain ( $K_c$ ) and integral time ( $\tau_I$ ). An ideal value for  $\tau_c$  is determined by a trade-off between output performance (tight control) and robustness (smooth control) (Skogestad, 2003, 2006; Skogestad and Grimholt, 2012). A small value of  $\tau_c$  results in a faster response and better disturbance rejection whereas a large value of  $\tau_c$  results in small input changes and smooth responses. Conclusively, an optimal value for  $\tau_c$ , that would result in optimal input and output performance of the controller, does not exist. In other words, selecting  $\tau_c$  is an engineering decision that should be made based on the process, governing conditions and the aim of control.

To design a model-based controller for the pressure control loop of the SFE process, three different values are chosen for  $\tau_c$  based on its acceptable range as explained by Skogestad (2006) and Skogestad and Grimholt (2012). A value of  $\tau_c$  which is much faster than the open loop time constant ( $\tau_l$ ) was chosen for Controller 3. A value of  $\tau_c$  which is close to the open loop time constant ( $\tau_l$ ) was chosen for Controller 4. A value of  $\tau_c$  which is much slower than the open loop time constant ( $\tau_l$ ) was chosen for Controller 5. In each case, controller parameters are calculated based on the selected  $\tau_c$  and each controller is individually applied to the system and responses

are compared. Table 5.3 lists the chosen values for  $\tau_c$  and the resulting PI controller parameters calculated from Equation 5.9 and Equation 5.10.

**Table 5.3. PI controller settings based on different values of  $\tau_c$**

	$\tau_c$ (s)	$K_c(\frac{\%}{MPa})$	$\tau_I$ (s)	$\tau_I$ (min)
Controller 3	$\tau_1/6 = 6.13$	35.2	26.1	0.44
Controller 4	$2\tau_1/3 = 24.5$	9.24	36.8	0.61
Controller 5	$2\tau_1 = 73.6$	3.11	36.8	0.61

As seen in Table 5.3, Controller 3 has a significantly higher gain ( $K_c$ ) in comparison to that of Controller 4 and Controller 5. Controllers 4 and 5 have the same time constant ( $\tau_I$ ), while the time constant of Controller 3 is approximately 10 s smaller.

Conducting control experiments and optimization tests on the process representative model can be much cheaper, safer and faster in comparison to conducting the tests on the actual process itself (Luyben, 1996). Hence, the validated hydrodynamic model based on fundamental laws as presented in Chapter 4 is applied in this section for testing the three designed model-based controllers and comparing their performances.

In order to compare the performance of the three tuned controllers as presented in Table 5.3, each controller is applied to the SFE process via the hydrodynamic model individually. The initial pressure of the system is assumed to be at 10 MPa. At time zero, a step change is applied to the pressure set point from 10 MPa to 12 MPa. Next, to simulate the occurrence of a disturbance in the system, the metering valve opening is decreased from 32% to 5% at 500 seconds. This disturbance is similar to a typical scenario that occurs in the SFE process when the separator temperature decreases because of the high volume of CO<sub>2</sub> passing through it and as a result, partial freezing occurs in the CO<sub>2</sub> line exiting the metering valve and entering the separator.

Figure 5.10 demonstrates the output performance (pressure response inside the extraction vessel) for the three tuned controllers as a result of the applied set point change and disturbance.

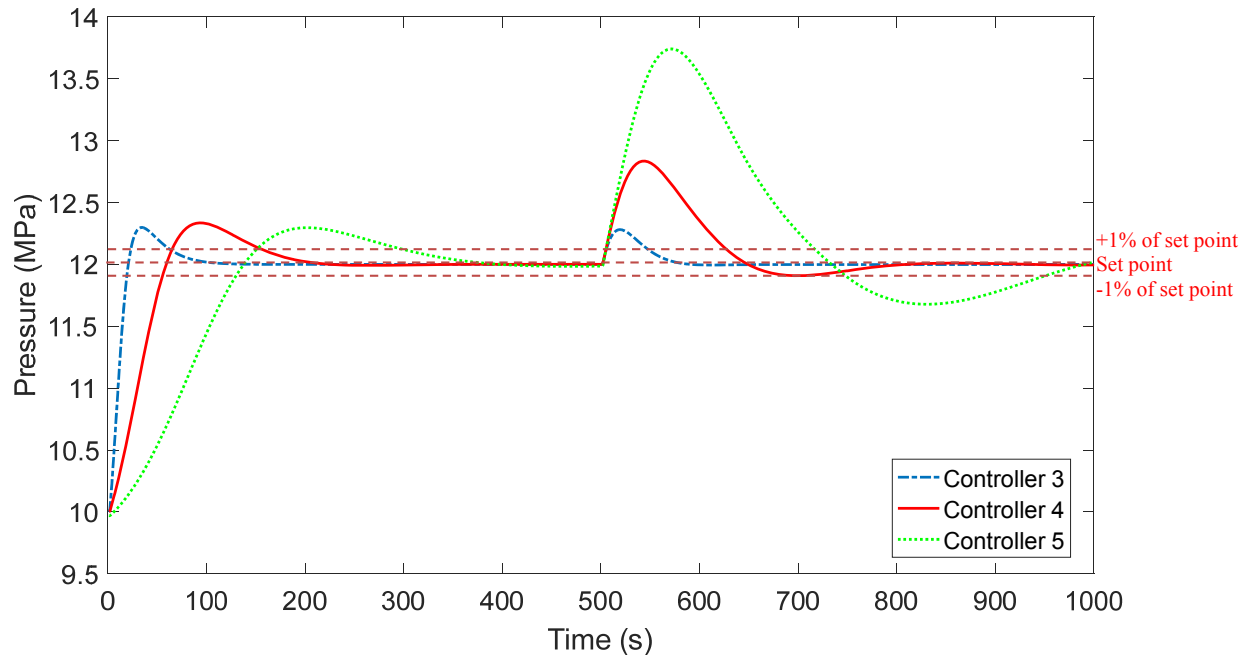


**Figure 5.10. Pressure response to a set point change and disturbance for Controller 3, Controller 4 and Controller 5**

As seen in Figure 5.10, in the time period of 0 to 500 seconds (associated with the step change), Controller 3 has the fastest response time (within  $\pm 1\%$  of set point), while Controller 5 has the slowest response time (within  $\pm 1\%$  of set point). Controller 4 has an intermediate performance in terms of response time. Approximately the same overshoot (0.5 MPa) is observed for all three responses.

In the time period of 500 to 1000 seconds (associated with disturbance rejection), Controller 3 has the smallest overshoot as well as the fastest response time. On the contrary, Controller 5 has the largest overshoot and slowest response time. Controller 4 has an intermediate performance in terms of overshoot and response time.

Based on the results gained from the qualitative comparison of the pressure responses, it is concluded that for set point tracking and disturbance rejection, Controller 3 is superior. The faster response time and the smaller overshoot are expected based on the higher gain (i.e.  $35.2 \frac{MPa}{\%}$ ) and lower time constant (i.e. 26.1 s) of this controller. Controller 4 has an intermediate performance and Controller 5 is the least preferred due to its sluggishness (i.e. slow response).

To quantitatively compare the output performance of the controllers, IAE is calculated based on the pressure responses as presented in Figure 5.10, for both set point tracking and

disturbance rejection. The calculated values are summarized in Table 5.4.

**Table 5.4. IAE values for Controller 3, Controller 4 and Controller 5**

	IAE		
	Overall	Set point tracking	Disturbance rejection
Controller 3	41.3	29.7	11.6
Controller 4	160	83.9	75.9
Controller 5	454	188	266

IAE results as summarized in Table 5.4 are in line with the qualitative comparison of the pressure responses. That is, Controller 3 and Controller 5 result in the lowest and highest IAE values respectively (for both set point tracking and disturbance rejection).

As stated earlier, another factor to consider when comparing controllers is the input performance i.e. how the CO<sub>2</sub> flow changes as a result of the chosen controller parameters. This comparison is provided for the three controllers in Figure 5.11.

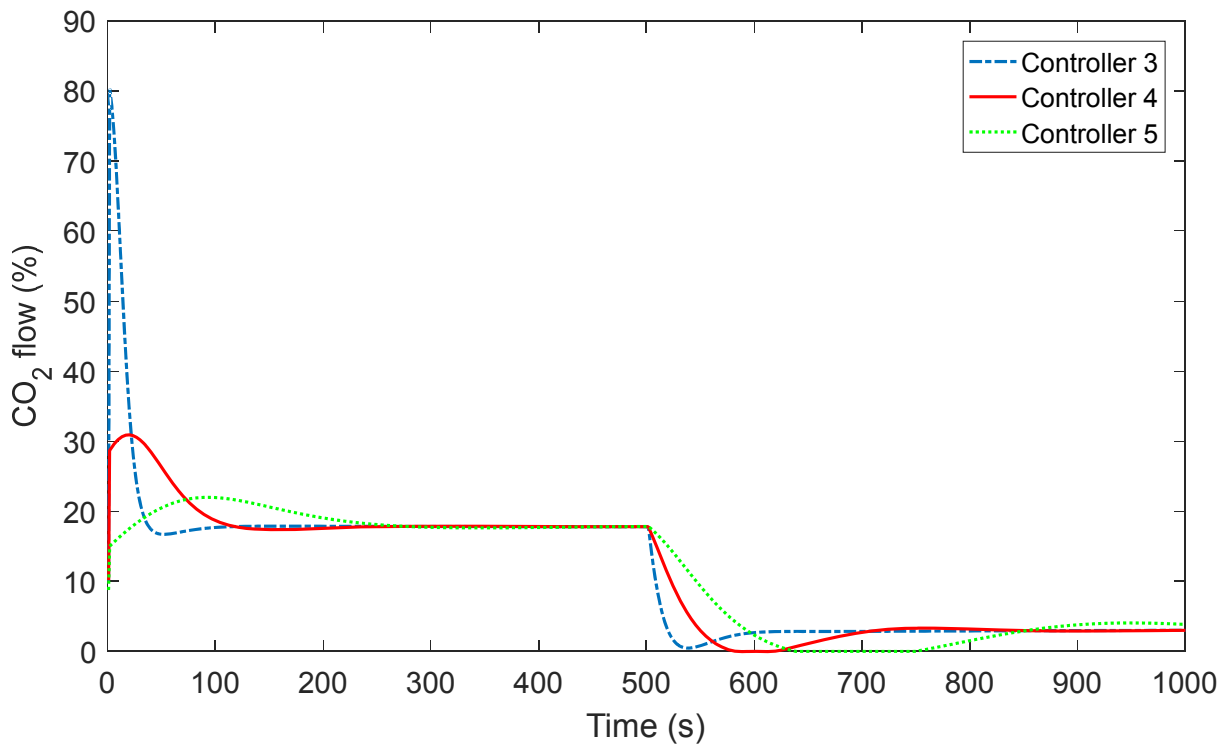


**Figure 5.11. Controller output as a result of a set point change and disturbance for Controller 3, Controller 4 and Controller 5**

As observed from Figure 5.11, in the time period of 0 to 500 seconds (associated with step point tracking), Controller 3 has the most aggressive usage. A smoother CO<sub>2</sub> usage is seen

for Controller 4. Controller 5 has the minimum input usage during this period. In the time period of 500 to 1000 seconds (associated with disturbance rejection), similar usage is observed for all three controllers.

To quantitatively compare the input performance of the controllers, TV is calculated for each controller (for both set point tracking and disturbance rejection) based on their CO<sub>2</sub> usage as presented in Figure 5.11. The calculated values are summarized in Table 5.5.

**Table 5.5. TV values for Controller 3, Controller 4 and Controller 5**

	TV		
	Overall	Set point tracking	Disturbance rejection
Controller 3	155	135	19.9
Controller 4	56.5	34.9	21.6
Controller 5	39.9	17.8	22.1

TV results as summarized in Table 5.5 are in line with qualitative comparison of CO<sub>2</sub> usage. That is, during the set point tracking period, Controller 3 has a significantly larger TV value in comparison to Controller 4 and Controller 5. During the disturbance rejection period, very close TV values are obtained for all three controllers.

To summarize, Controller 3, which was associated with the smallest  $\tau_c$  value, is advantageous regarding speed of response and results in tight control for both set point tracking and disturbance rejection. However, this controller results in aggressive CO<sub>2</sub> usage. On the other hand, Controller 5, which was associated with the largest  $\tau_c$  value, is advantageous regarding input usage and results in the smallest input changes, specifically during the set point change period, but has poor output performance and is very sluggish in maintaining the pressure set point. Therefore, based on the governing process conditions of the SFE process under investigation and the aim of control (set point tracking and disturbance rejection), Controller 4 ( $\tau_c$  value close to the open loop time constant) is chosen as the best (i.e. most operationally effective) controller among the three designed controllers, because of its acceptable output and input performance. Therefore, Controller 4 is applied in subsequent sections for comparison with other designed controllers in this chapter.

It should be emphasized that this section provided a guideline for designing model-based controllers for the SFE process under investigation in the IMC framework. Three different values for  $\tau_c$  were selected and the performance of the resulting controllers were compared. All three

controllers lead to successful control. Increasing the  $\tau_c$  value resulted in a smooth but sluggish response. Decreasing the  $\tau_c$  value resulted in a fast pressure response at the expense of excessive CO<sub>2</sub> usage. For safety reasons, this scenario should be avoided. Therefore, selecting a  $\tau_c$  value close to the time constant of the process ( $\tau_l$ ) was selected best (among the three cases) because it resulted in both acceptable input and output performance.

### 5.4.3 Controller performance comparison (manually tuned vs. model-based)

In this section, the performance of the manually tuned PI controller is compared with that of the model-based PI controller. This comparison is done through two routes. First, the two controllers are individually applied to the SFE hydrodynamic model and their performances are compared. The second route is comparing the performance of the controllers by applying them to the actual pilot scale SFE process. These two routes for comparing performance of controllers are presented in Subsections 5.4.3.1 and 5.4.3.2, respectively.

Controller 4 as designed in the previous section is chosen to be compared with the manually tuned controller (Controller 2). The parameters of the two controllers are summarized in Table 5.6.

**Table 5.6. Controller 2 and Controller 4 parameter comparison**

	Description	$K_c$ ( $\frac{\%}{MPa}$ )	$\tau_l$ (s)	$\tau_l$ (min)
Controller 2	manually tuned controller	8	18	0.3
Controller 4	model-based controller	9.24	36.8	0.61

In terms of controller gain, Controller 4 has a slightly higher gain than Controller 2 and in terms of controller time constant, Controller 4 has a time constant approximately two times that of Controller 2.

#### 5.4.3.1 Comparison via SFE hydrodynamic model

In this section, the performance of Controller 2 and Controller 4 are compared by individually applying the controllers to the hydrodynamic model of the SFE process. Similar to the previous section, both set point tracking and disturbance rejection are applied. The time span of 0 to 500 s is associated with a step change in pressure from 10 to 12 MPa. The time span of 500 to 1000 s is associated with disturbance rejection. Pressure responses as a result of individually applying each controller to the SFE system are depicted in Figure 5.12.

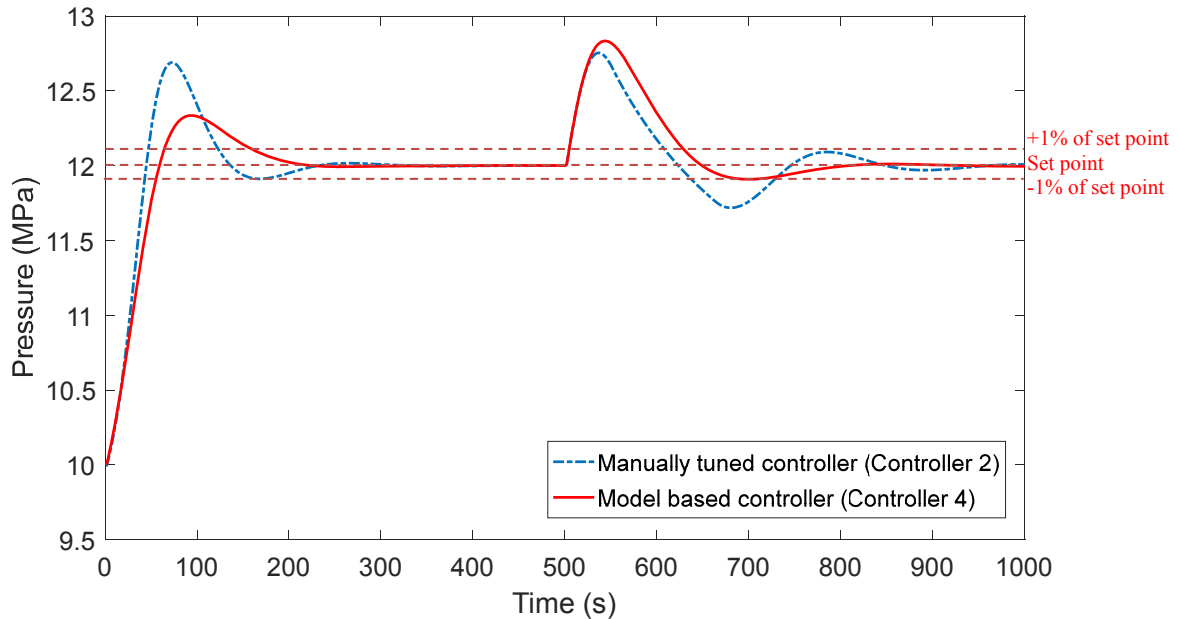


**Figure 5.12. Pressure response to a set point change and disturbance for manually tuned controller (Controller 2) and model-based controller (Controller 4)**

In comparing the pressure responses as in Figure 5.12, for set point tracking, a smoother response and smaller overshoot are observed for the model-based controller (Controller 4) in comparison to that of the manually tuned controller (Controller 2). The response times (within  $\pm 1\%$  of set point) for both controllers are relatively close.

For disturbance rejection, the pressure response of the model-based controller (Controller 4) has a slightly higher overshoot than that of the manually tuned controller (Controller 2). However, pressure response of the model-based controller (Controller 4) depicts a less oscillatory response.

To quantitatively compare performance of the two controllers, IAE values are calculated based on the pressure responses of the two controllers as presented in Figure 5.12.

**Table 5.7. IAE values for the manually tuned controller (Controller 2) and the model-based controller (Controller 4)**

	IAE		
	Overall	Set point tracking	Disturbance rejection
Controller 2	168	90.7	77.6
Controller 4	160	83.9	75.9

As seen in Table 5.7, slightly lower IAE values are calculated for the model-based

controller for both set point tracking and disturbance rejection. Overall, IAE values for the two controllers are very close indicating acceptable output performance for both controller types.

The CO<sub>2</sub> usage as a result of applying the two types of controllers is presented in Figure 5.13.

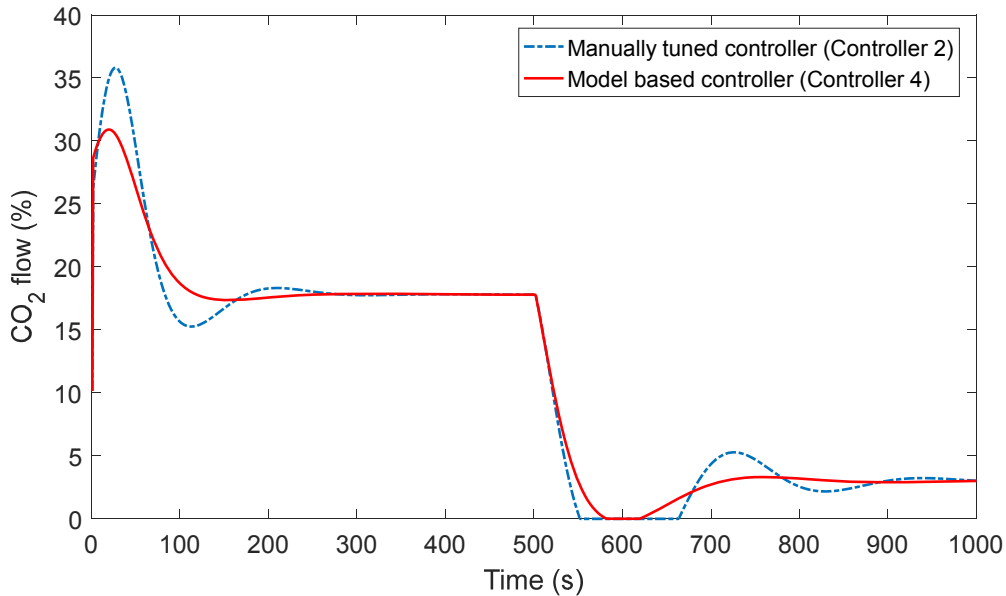


**Figure 5.13. Controller output as a result of a set point change and disturbance for the manually tuned controller (Controller 2) and the model-based controller (Controller 4)**

In terms of CO<sub>2</sub> usage, it is observed from Figure 5.13 that applying the model-based controller (Controller 4) results in less aggressive CO<sub>2</sub> consumption in comparison to the manually tuned controller (Controller 2) for both set point tracking and disturbance rejection. Overall, a less oscillatory response is observed for the model-based controller.

To quantitatively compare input performance of the controllers, TV is calculated for each controller based on their CO<sub>2</sub> usage for both set point tracking and disturbance rejection. The calculated values are summarized in Table 5.8.

**Table 5.8. TV values for the manually tuned controller (Controller 2) and the model-based controller (Controller 4)**

	TV		
	Overall	Set point tracking	Disturbance rejection
Controller 2	77.3	49.9	27.4
Controller 4	56.5	34.9	21.6

TV results as summarized in Table 5.8 are in line with qualitative comparison of CO<sub>2</sub> usage. For both set point tracking and disturbance rejection, a smaller TV value is calculated for the model-based controller.

Based on the qualitative and quantitative measures of both pressure responses (output performance) and CO<sub>2</sub> usage (input performance), it is concluded that performance of both controllers are quite similar and both controller types lead to successful control. It should be reminded that Controller 2 was tuned at a pressure below 7.4 MPa. However, it also depicts acceptable performance at higher pressures i.e. pressures above 7.4 MPa.

It should be noted that although the manually tuned controller leads to acceptable input performance and output performance, it was tuned based on a trial and error approach. Having a systematic approach i.e. designing a model-based controller in the IMC framework (as presented in Section 5.4.2) is potentially a more efficient approach in comparison to a trial and error approach for tuning the PI controller.

#### **5.4.3.2 Comparison via actual SFE process**

In this section, the performance of the manually tuned controller (Controller 2) and the model-based controller (Controller 4) are compared by individually applying the controllers to the actual SFE process. These results are associated with Run 81 as listed in Table 5.1.

Similar to the previous section, both set point tracking as well as disturbance rejection are considered. First, a set point change is applied from 10 to 12 MPa at time zero. Next, the metering valve position is decreased from 10% to 5% at 330 seconds. For both controllers, during set point change, the slurry flow was initially set to 17% but had to be increased to 19.5% to prevent emptying the extraction vessel. During the disturbance rejection period, slurry flow was constant at 19.5%. The pressure response as a result of individually applying each controller to the SFE process is depicted in Figure 5.14.

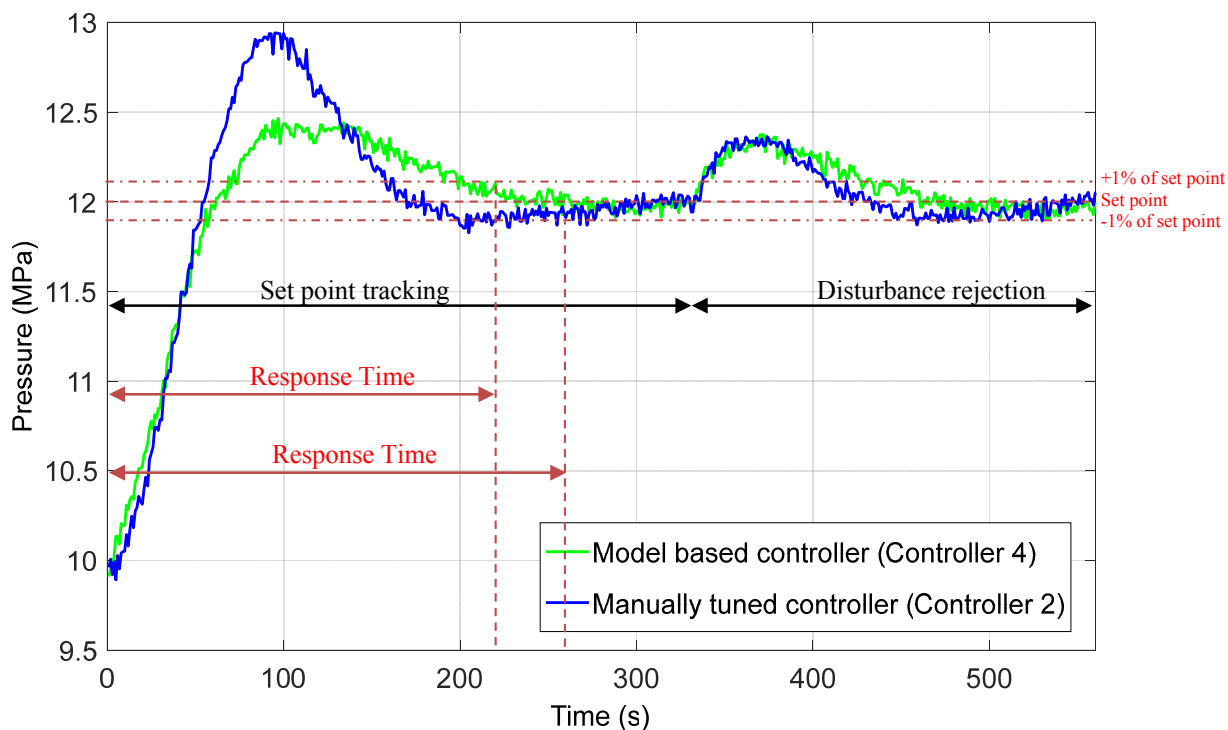


**Figure 5.14. Pressure response in the SFE process to a set point change and disturbance for the manually tuned controller (Controller 2) and the model-based controller (Controller 4)**

As can be seen in Figure 5.14, during the set point change period, the manually tuned controller has a higher overshoot (0.9 MPa) in comparison to the model-based controller (0.4 MPa). The response time (within  $\pm 1\%$  of set point) for the model-based controller is faster (200 seconds) in comparison to that of the manually tuned controller (240 seconds). For disturbance rejection, similar responses are obtained for both controllers.

To quantitatively compare the performance of the two controllers, IAE values are calculated based on the pressure response of the two controllers as presented in Figure 5.14 for both set point tracking and disturbance rejection. IAE values are presented in Table 5.9.

**Table 5.9. IAE values (based on actual SFE experiment) for the manually tuned controller (Controller 2) and the model-based controller (Controller 4)**

	IAE		
	Overall	Set point tracking	Disturbance rejection
Controller 2	160	132	28
Controller 4	136	107	29

As seen from Table 5.9, for set point tracking, a lower IAE value is calculated for the model-based controller. However, regarding disturbance rejection, very close IAE values are obtained. Overall, the response obtained from the model-based controller to both set point tracking and disturbance rejection result in a slightly lower IAE value. These results are in line with qualitative comparison of the pressure responses.

The CO<sub>2</sub> usage as a result of applying the two types of controllers is presented in Figure 5.15.

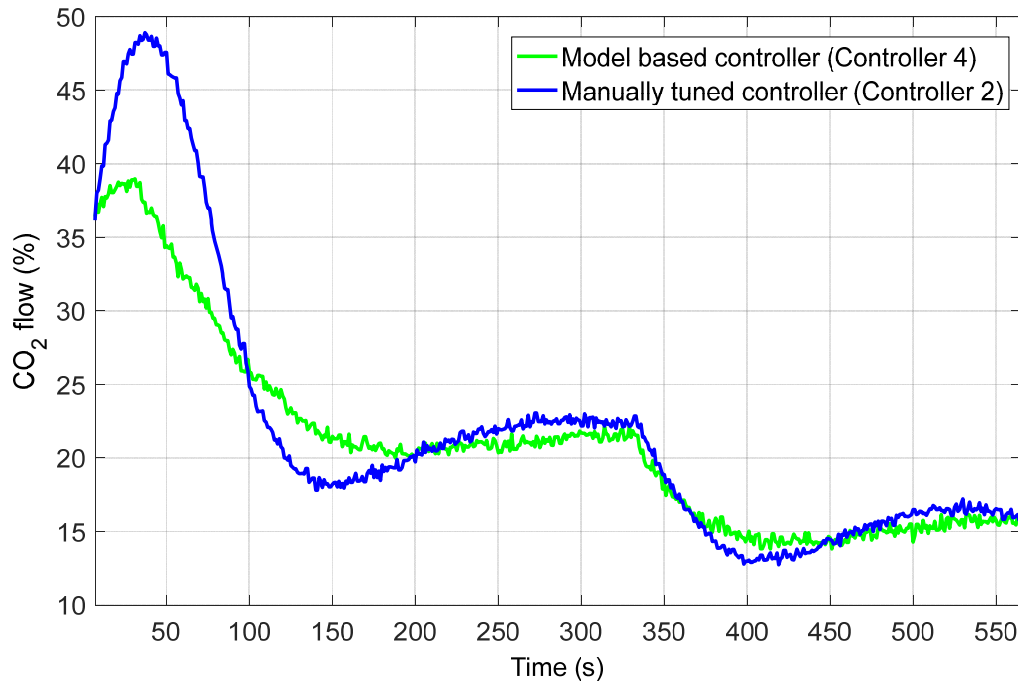


**Figure 5.15. Controller output in the SFE process as a result of a set point change and disturbance for the manually tuned controller (Controller 2) and the model-based controller (Controller 4)**

Figure 5.15 shows that applying the model-based controller results in a less aggressive usage in comparison to the manually tuned controller, specifically for set point tracking. For disturbance rejection, similar responses are obtained.

To quantitatively compare the input performance of the controllers, TV is calculated for each controller based on their CO<sub>2</sub> usage as presented in Figure 5.15 for both set point tracking and disturbance rejection. The calculated values are summarized in Table 5.10.

**Table 5.10. TV values (based on actual SFE experiment) for the manually tuned controller (Controller 2) and the model-based controller (Controller 4)**

	TV		
	Overall	Set point tracking	Disturbance rejection
Controller 2	177	123	54
Controller 4	179	106	73

Based on the results summarized in Table 5.10, for set point tracking a smaller TV value is calculated for the model-based controller (Controller 4). However, for disturbance rejection, a smaller TV value is calculated for the manually tuned controller (Controller 2). Overall, very close TV values is calculated for both controller types. Based on the qualitative comparison of the responses (Figure 5.15), a lower TV value is expected for Controller 4 for both set point tracking and disturbance rejection. However, a slightly lower TV value has been obtained for Controller 2 during the disturbance rejection period. Instrumentation noise is assumed to contribute to this error in calculating the TV value.

To conclude, based on qualitative and quantitative measurements from pressure responses and input usages, the two controller types have similar performance. These results are in line with the results obtained in the previous section i.e. comparison via applying the controllers to the hydrodynamic model of the SFE process (Section 5.4.3.1), therefore additionally confirming the validity of the hydrodynamic model.

#### **5.4.4 System identification via hydrodynamic model**

In this section, the same approach is followed as presented in Section 5.4.2 to design a model-based controller. However, instead of applying the step test to the pilot scale SFE process, the step test was applied to the hydrodynamic model (developed in Chapter 4) for obtaining a simple linear model which, in turn, is used for designing a model-based controller. Two operating conditions are explored for this purpose: pressures in the vicinity of 12 MPa (referred to as low operating pressure) and pressures in the vicinity of 17 MPa (referred to as high operating pressure).

##### **5.4.4.1 System identification at a low operating pressure**

A step change in CO<sub>2</sub> flow from 21.5% to 25% was applied to the hydrodynamic model, the same step change as applied in Section 5.4.2. The operating pressure is in the vicinity of 12

MPa. The pressure response as a result of this step change is illustrated in Figure 5.16 and compared to the pressure response that was obtained in Section 5.4.2. It should be noted that the slurry flow was constant at 15.5% for both scenarios.

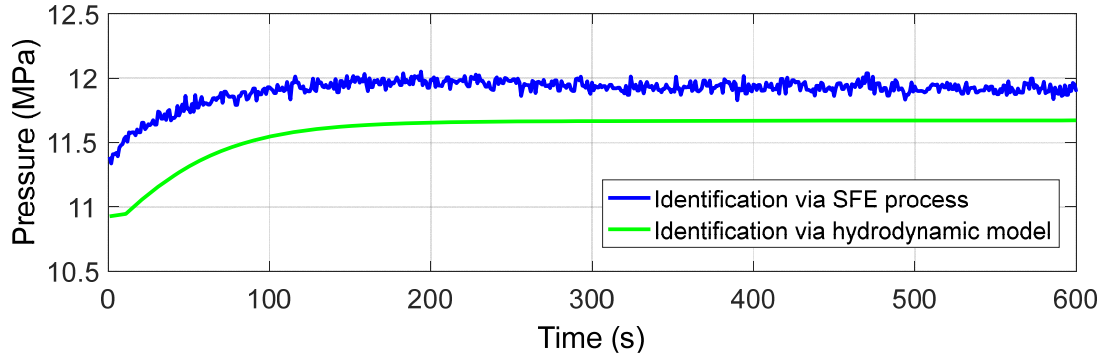


**Figure 5.16. Step test output (pressure) time variation for identification via SFE process and identification via hydrodynamic model**

As seen in Figure 5.16, similar responses are obtained for both scenarios. However, when using the hydrodynamic model for the step test, the pressure response starts at 11 MPa i.e. 0.4 MPa lower than the obtained pressure response when using the SFE process. One reason that contributes to this minor difference is the slurry level inside the extraction vessel which was not being controlled during the step test. As discussed in Chapter 4, slurry level inside the extraction vessel impacts pressure response.

Input-Output data obtained from applying the step test to the hydrodynamic model is imported to the system identification toolbox in MATLAB<sup>®</sup>. As a result, the following first order model is obtained:

$$G(s) = \frac{0.21e^{-1.7s}}{50.4s + 1} \quad (5.11)$$

Based on Equation 5.11, the process gain ( $k$ ) and dominant time constant ( $\tau_l$ ) are  $0.21 \frac{\text{MPa}}{\%}$  and 50.4 s, respectively. Process dead time is 1.7 s, which, as expected, is very small compared to the dominant time constant.

Similar to Section 5.4.2, simple analytical rules for PID control tuning in the IMC structure as presented by Skogestad (2003, 2004 and 2006) and Skogestad and Grimholt (2012) are applied. Therefore, Equation 5.7 and Equation 5.8 are used to calculate the PI controller parameters based on the obtained liner model (Equation 5.11) as follows:

$$K_c = \frac{240}{\tau_c + 1.7} \quad (5.12)$$

$$\tau_I = \min\{50.4, 4(\tau_c + 1.7)\} \quad (5.13)$$

Assuming  $\tau_c = \frac{2}{3}\tau_1$  (as discussed in Section 5.4.2), and based on Equation 5.12 and Equation 5.13, the PI controller (Controller 6) parameters are calculated as  $6.8 \frac{\%}{MPa}$  and 50.4 s respectively. These tuning parameters are compared with the PI controller tuning parameters presented in Section 5.4.2. This comparison is presented in Table 5.11.

**Table 5.11. Controller 4 and Controller 6 parameter comparison**

Description		$\tau_c$ (s)	$K_c$ ( $\frac{\%}{MPa}$ )	$\tau_I$ (s)	$\tau_I$ (min)
Controller 4	Identification via SFE process	24.5	9.24	36.8	0.61
Controller 6	Identification via hydrodynamic model	33.6	6.80	50.4	0.84

As seen in Table 5.11, Controller 6 has a slightly smaller gain and larger time constant in comparison to that of Controller 4. Therefore, by applying Controller 4, a tighter pressure response is expected at the price of excessive CO<sub>2</sub> usage. However, considering that both the gain and the time constant of the two controllers are close, similar controller performance is expected to be obtained by applying them to the pressure control loop. A summary of IAE and TV values obtained for Controller 4 and Controller 6 for set point tracking and disturbance rejection (similar to Section 5.4.2) is provided in Table 5.12.

**Table 5.12. Summary of IAE and TV values for Controller 4 and Controller 6**

	IAE			TV		
	Overall	Set point tracking	Disturbance rejection	Overall	Set point tracking	Disturbance rejection
Controller 4	160	83.9	75.9	56.5	34.9	21.6
Controller 6	241	109	132	43.9	23.4	20.5

It is mostly common to apply system identification techniques to actual physical processes and design model-based controllers based on real data. However, based on the controller parameters presented in Table 5.11 and the IAE and TV values obtained in Table 5.12, it can be concluded that having a reliable model at hand could also aid with the process of designing a model-based controller. This approach (i.e. system identification via hydrodynamic model) is valuable for future upgrades of the process in which a first estimation of controller

parameters is required. Therefore, instead of using trial and error to tune a controller with acceptable performance (as presented in Section 5.4.1), the approach presented in this section can also be applied to obtain initial parameters for the PI controller in the extraction vessel.

#### 5.4.4.2 System identification at a high operating pressure

In this subsection, a step test is applied to the hydrodynamic model to obtain a simple linear model for controller design (same approach as presented in Section 5.4.4.1). However, a different operating region is explored i.e. operating pressure in the vicinity of 17 MPa. Tuning parameters of the designed controller are compared with that of the previous section (Controller 6) to explore effect of changing operating conditions on model-based controller parameters.

To achieve a higher pressure in the extraction vessel, higher CO<sub>2</sub> and slurry flows must be applied. Therefore, the slurry flow was set to a constant value of 19% and a step change was applied to CO<sub>2</sub> flow from 37% to 40.5%. The pressure response as a result of this step change is illustrated in Figure 5.17.

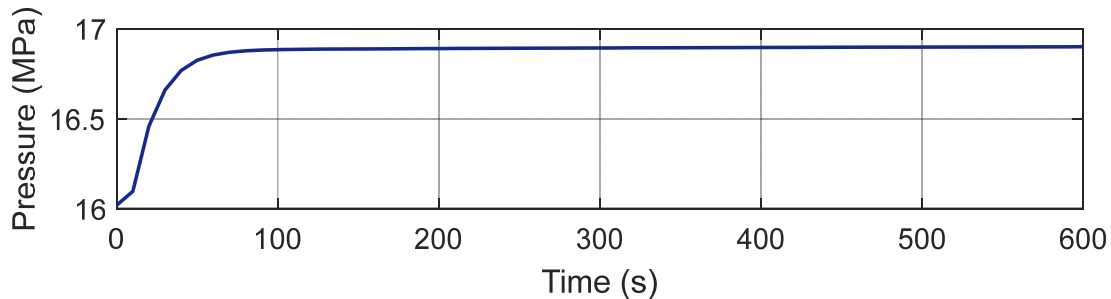


**Figure 5.17. Step test output (pressure) time variation for identification via hydrodynamic model at a high operation pressure**

Input-Output data obtained from applying the step test to the hydrodynamic model is imported to the system identification toolbox in MATLAB<sup>®</sup>. As a result, the following first order model is estimated:

$$G(s) = \frac{0.25e^{-0.1s}}{15.6s + 1} \quad (5.14)$$

First order model parameters obtained at high operating pressure are compared with those obtained in Section 5.4.4.1 (i.e. at low operating pressure). This comparison is presented in Table 5.13.

**Table 5.13. Model parameter comparison for system identification at a low operating pressure and a high operating pressure**

Description	k	$\tau_1$ (s)	$\theta$ (s)
Identified model at low operating pressure	0.21	50.4	1.7
Identified model at high operating pressure	0.25	15.6	0.1

As seen in Table 5.14, the two models have very close gains. However, the model identified at low operating pressure has a significantly larger time constant in comparison to the model identified at high operating pressure. In other words, the pressure response is achieved much faster at a higher operating pressure. This difference in process models at different operating conditions is expected due to process nonlinearity. In other words, the relationship between the controlled and manipulated variable changes at different operating conditions.

Following the same approach as in Section 5.4.4.1, the PI controller parameters based on the obtained liner model (Equation 5.14) are calculated as follows:

$$K_c = \frac{62.4}{\tau_c + 0.1} \quad (5.15)$$

$$\tau_I = \min\{15.6, 4(\tau_c + 0.1)\} \quad (5.16)$$

Assuming  $\tau_c = \frac{2}{3}\tau_1$  (as discussed in Section 5.4.2), and based on Equation 5.15 and Equation 5.16, the PI controller (Controller 7) gain and time constant are calculated as  $5.94 \frac{\%}{MPa}$  and 15.6 s respectively. These parameters are compared with that of the controller that was designed at low operating pressures (Controller 6). This comparison is provided in Table 5.14.

**Table 5.14. Controller 6 and Controller 7 parameter comparison**

Description	$\tau_c$ (s)	$K_c$ ( $\frac{\%}{MPa}$ )	$\tau_1$ (s)	$\tau_1$ (min)
Controller 6 Identification via model at low operating pressure	33.6	6.80	50.4	0.84
Controller 7 Identification via model at high operating pressure	10.4	5.94	15.6	0.26

As seen in Table 5.14, the  $\tau_c$  value obtained for Controller 6 is higher (approximately three times higher) than the  $\tau_c$  value obtained for Controller 7. In terms of controller parameters, Controller 7 has a slightly smaller gain in comparison to that of Controller 6. However, the

controller time constant of Controller 7 is significantly smaller. Therefore, a tighter pressure control is expected to be obtained by applying Controller 7 and a smoother response is expected to be obtained by applying Controller 6.

#### 5.4.4.3 Controller performance comparison (low operating pressure vs. high operating pressure)

In order to compare the performance of the controllers presented in Table 5.14, each controller is applied to the hydrodynamic model individually at two different operating conditions (i.e. low operating pressure and high operating pressure).

In the first simulation and for the purpose of exploring a low operating pressure, the initial pressure of the system is assumed to be at 10 MPa. At time zero, a step change is applied to the pressure set point from 10 to 12 MPa. Next, to simulate the occurrence of a disturbance in the process, the metering valve opening is decreased from 32% to 5% at 500 seconds. Figure 5.18 demonstrates the pressure response inside the extraction vessel for the two controllers as a result of the applied set point change and disturbance.

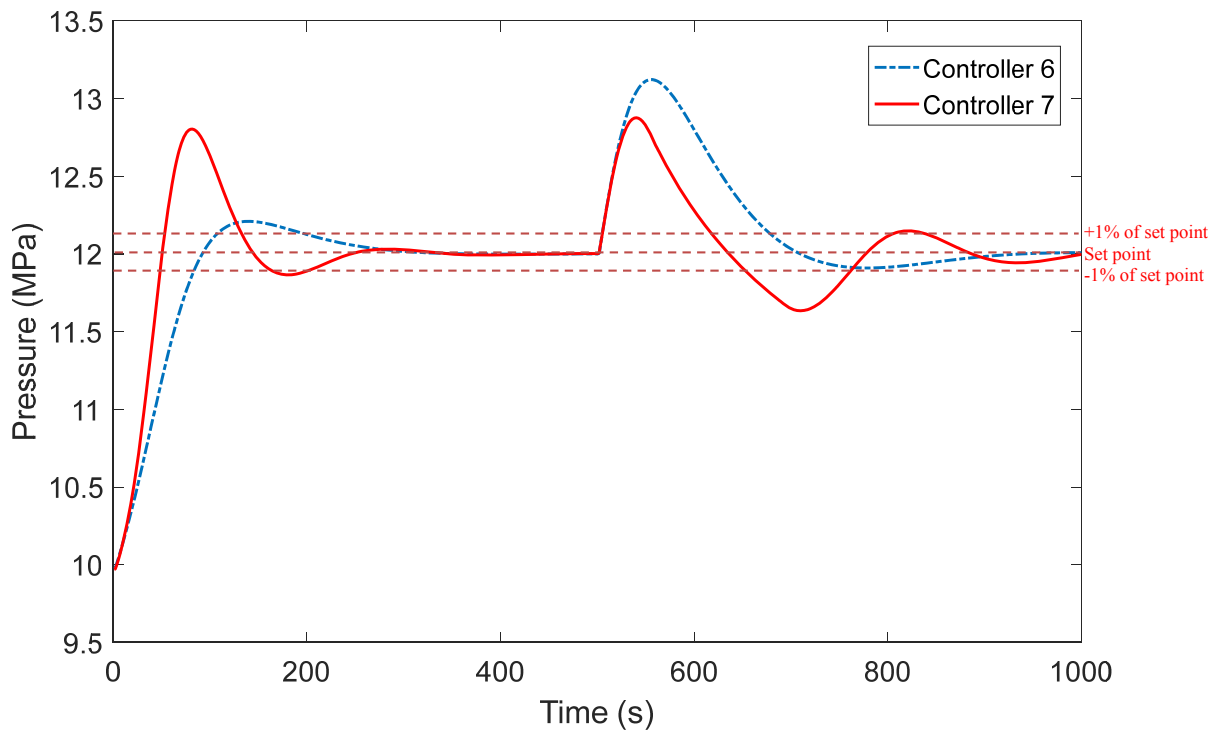


Figure 5.18. Pressure response to a set point change and disturbance for Controller 6 and Controller 7 at a low operating pressure

As seen in Figure 5.18, for both set point tracking and disturbance rejection, Controller 6 depicts a less oscillatory response and smoother response while Controller 7 depicts tighter control. For set point tracking, Controller 7 has a larger overshoot. However, for disturbance rejection, Controller 6 has a larger overshoot but a faster response time (within  $\pm 1\%$  of set point) in comparison to Controller 7.

To quantitatively compare output performance of the controllers, the IAE is calculated for the controllers based on their pressure responses presented in Figure 5.18 for both set point tracking and disturbance rejection. The calculated values are summarized in Table 5.15.

**Table 5.15. IAE values for Controller 6 and Controller 7 at a low operating pressure**

	IAE		
	Overall	Set point tracking	Disturbance rejection
Controller 6	241	109	132
Controller 7	219	112	107

As seen in Table 5.15, close IAE values are obtained for the set point tracking period. For disturbance rejection, a slightly lower value is obtained for Controller 7. Overall, both controllers depict close output performance. However, as expected, Controller 7 results in a tighter pressure control resulting in a slightly lower overall IAE value.

The CO<sub>2</sub> usage as a result of applying the two types of controllers is presented in Figure 5.19.

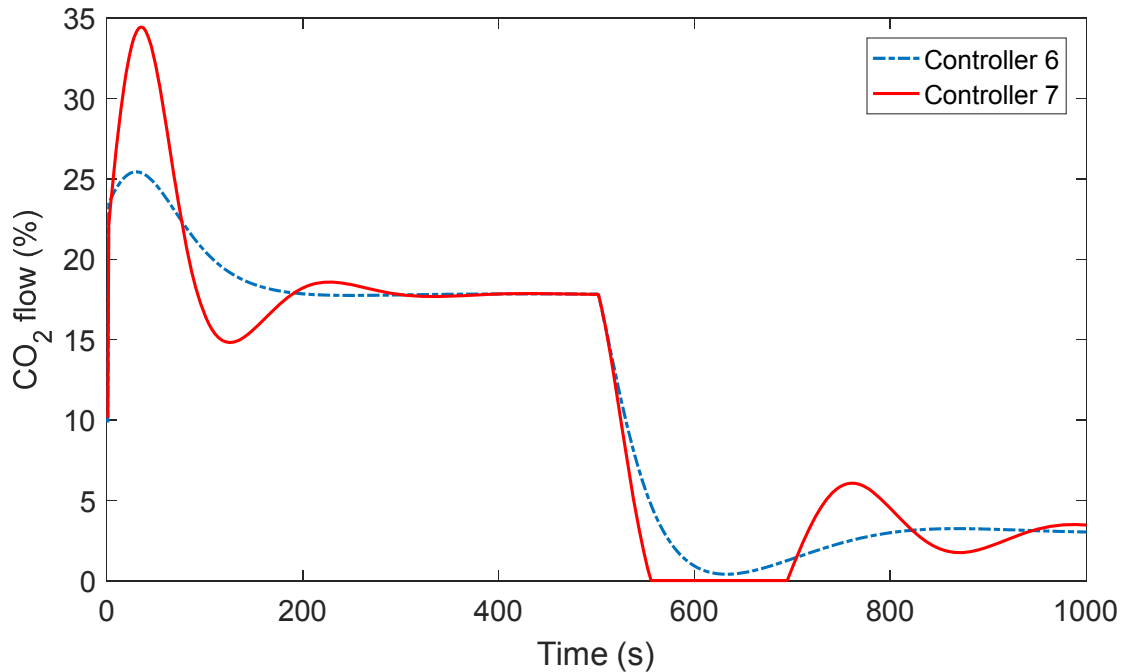


**Figure 5.19. Controller output as a result of a set point change and disturbance for Controller 6 and Controller 7 at a low operating pressure**

As seen from Figure 5.19 and as expected, a smoother response is obtained for Controller 6 in comparison to Controller 7, which has excessive CO<sub>2</sub> usage.

To quantitatively compare the input performance of the controllers, TV is calculated for each controller based on their CO<sub>2</sub> usage presented in Figure 5.19, for both set point tracking and disturbance rejection. The calculated values are summarized in Table 5.16.

**Table 5.16. TV values for Controller 6 and Controller 7 at a low operating pressure**

	TV		
	Overall	Set point tracking	Disturbance rejection
Controller 6	43.9	23.4	20.5
Controller 7	78.7	48.8	29.9

TV results as summarized in Table 5.16 are in line with the qualitative comparison of CO<sub>2</sub> usage. As expected, for both set point tracking and disturbance rejection, a smaller TV value is obtained for Controller 6, which corresponds to less aggressive CO<sub>2</sub> usage.

In the second simulation, and for the purpose of exploring a high operating pressure, the initial pressure of the system is assumed to be at 15 MPa. At time zero, a step change is applied to the pressure set point from 15 to 17 MPa. To simulate the occurrence of a disturbance in the

process, the metering valve opening is decreased from 32% to 5% at 500 seconds. Figure 5.20 demonstrates the pressure response inside the extraction vessel for the two controllers as a result of the applied set point change and disturbance.

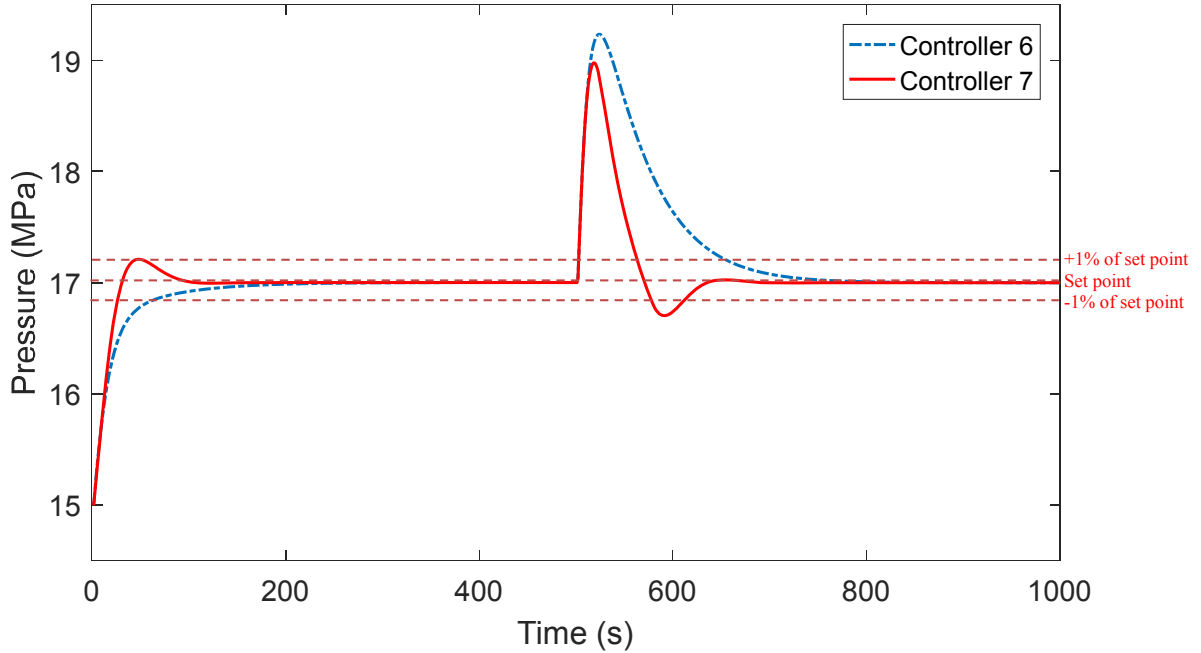


**Figure 5.20. Pressure response to a set point change and disturbance for Controller 6 and Controller 7 at a high operating pressure**

As seen in Figure 5.20, for both set point tracking and disturbance rejection, tighter control is obtained by applying Controller 7, while a smoother response is obtained for Controller 6. For set point tracking, Controller 6 has no overshoot. Relatively same response time is obtained for both controllers during this period. For disturbance rejection, Controller 6 does not oscillate. Controller 7 has a faster response time during this period.

To quantitatively compare the output performance of the controllers, the IAE is calculated for the controllers based on their pressure responses presented in Figure 5.20, for both set point tracking and disturbance rejection. The calculated values are summarized in Figure 5.17.

**Table 5.17. IAE values for Controller 6 and Controller 7 at a high operating pressure**

	IAE		
	Overall	Set point tracking	Disturbance rejection
Controller 6	218	46.6	171
Controller 7	115	32.9	82.1

As seen in Table 5.17, for both set point tracking and disturbance rejection, smaller IAE values are obtained for Controller 7.

The CO<sub>2</sub> usage as a result of applying the two controllers is presented in Figure 5.21.

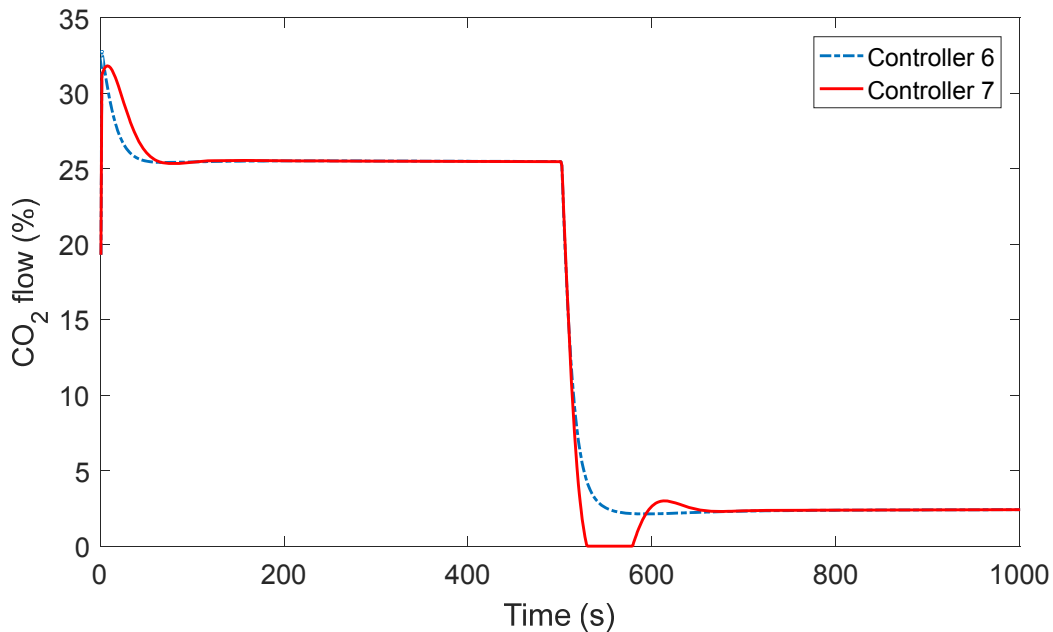


**Figure 5.21. Controller output as a result of a set point change and disturbance for Controller 6 and Controller 7 at a high operating pressure**

As seen from Figure 5.21, for set point tracking, a smoother response is obtained for Controller 7. However, for disturbance rejection, a smoother response is obtained for Controller 6. Overall, both controllers depict similar CO<sub>2</sub> usage especially during the set point tracking period.

To quantitatively compare input performance of the controllers, the TV is calculated for each controller based on their CO<sub>2</sub> usage presented in Figure 5.21, for both set point tracking and disturbance rejection. The calculated values are summarized in Table 5.18.

**Table 5.18. TV values for Controller 6 and Controller 7 at a high operating pressure**

	TV		
	Overall	Set point tracking	Disturbance rejection
Controller 6	44.7	21.1	23.6
Controller 7	48.6	19.3	29.3

TV results as summarized in Table 5.18 are in line with qualitative comparison of CO<sub>2</sub> usage. For set point tracking, a smaller TV value is obtained for Controller 7 while for disturbance rejection, a smaller TV value is obtained for Controller 6. Overall TV values are close for the two controllers.

To summarize, all quantitative results (IAE and TV values) obtained for Controllers 6 and 7 are presented in Table 5.19

**Table 5.19. Summary of IAE and TV values obtained for Controller 6 and Controller 7**

		IAE			TV		
		Overall	Set point tracking	Disturbance rejection	Overall	Set point tracking	Disturbance rejection
<i>Low pressure</i>	Controller 6	241	109	132	43.9	23.4	20.5
	Controller 7	219	112	107	78.7	48.8	29.9
<i>High pressure</i>	Controller 6	218	46.6	171	44.7	21.1	23.6
	Controller 7	115	32.9	82.1	48.6	19.3	29.3

Based on the summarized results presented in Table 5.19, for both operating conditions (low pressure and high pressure), Controller 7 results in a lower overall IAE value while Controller 6 results in a lower overall TV value. Lower IAE values for Controller 7 (in comparison to Controller 6) were expected based on the obtained controller parameters. However, for the low operating pressure condition, the difference between overall IAE value of Controller 6 and Controller 7 is less than the difference at the high operating pressure condition. The reason for this difference is that Controller 6 was designed based on a step test at a low operating pressure. Therefore, similar IAE values have been obtained for Controller 6 and Controller 7, especially for the set point tracking period. For the same reason, for the high operating pressure condition, the difference between obtained TV values of Controller 6 and 7 is less than the difference at the low operating pressure condition, the reason being that Controller 7 was designed based on a step test at a high operating pressure.

In summary, in both operating regions, Controller 7 results in better output performance and Controller 6 results in better input performance. However, taking into account both input and output performance, Controller 6 is best at the low operating pressure condition, while Controller 7 is best at the high operating pressure condition. This outcome was expected because of the operating regions that the step tests were conducted for designing the model-based controllers.

Based on the results obtained, it is concluded that changing operating conditions will impact controller performance. Therefore, based on the selected pressure set point of an experimental run, compatible PI parameters with that pressure will result in better controller performance in terms of both input performance and output performance. However, for the two operating conditions investigated in this section (i.e. 12 MPa and 17 MPa), both controllers (Controller 6 and Controller 7) depicted acceptable input and output performance. For higher operating pressures and depending on the extent of nonlinearity in the process, redesigning of the PI controller might be required.

## 5.5 Summary

Pressure control was successfully achieved by applying a feedback control loop with PI control to the pilot scale SFE process. Tuning of the PI controller was first done manually (Section 5.2.1). The tuned controller (Controller 2) was capable of controlling pressure with SC-CO<sub>2</sub> and water flowing countercurrently through the extraction vessel. Pressure control was achieved during both pressurization of the extraction vessel and during extraction, at different operating conditions (i.e. below supercritical pressure and above supercritical pressure). For a step change in pressure of 1 MPa, Controller 2 provided a non-oscillatory pressure response with a response time of less than 100 s (within  $\pm 2\%$  of set point) as well as a smooth CO<sub>2</sub> usage. Therefore, the first objective of this chapter (i.e. implementing and demonstrating pressure control in the extraction vessel) was achieved at pressures up to 11 MPa. The success in controlling pressure gives basis for pressure control in a full scale SFE process.

A systematic approach for designing a PI controller based on a model of the process, was presented (Section 5.2.2). The design was done in the IMC framework. For this purpose, initially, a first order model was derived for the process by applying a simple step test to the actual SFE process. Parameters of the first order model were used for designing PI controllers. Based on the aim of control (set point tracking and disturbance rejection) and simulation results which were obtained by applying the controllers to the hydrodynamic model of the SFE system, it was concluded that Controller 4 i.e. the PI controller with  $\tau_c$  (closed loop time constant) close to  $\tau_l$  (open loop time constant), resulted in both acceptable input and output performance. Applying Controller 4 resulted in a pressure response time of less than 200 s (within  $\pm 1\%$  of set point), an overshoot of less than 1 MPa and smooth CO<sub>2</sub> usage for both set point tracking (2 MPa

set point change) and disturbance rejection. This systematic approach of designing a model-based controller is more efficient in comparison to the previous approach (i.e. manual tuning of the controller), which was based on trial and error and could be relatively tedious. Having a systematic approach at hand is specifically important for future upgrades of the process in which different operating conditions will be required.

Performance of the manually tuned controller (Controller 2) was compared with that of the model-based controller i.e. Controller 4 (Section 5.4.3) at pressures in the vicinity of 12 MPa. This comparison was done by two routes i.e. applying them individually to the hydrodynamic model of the SFE process and to the actual SFE process. Results obtained from both of these routes were in line confirming that the hydrodynamic model is a good representation of the actual SFE process and reliable to be used for control studies and comparing performance of controllers. Both controller types, that is the manually tuned controller (Controller 2) and the model-based controller (Controller 4), resulted in acceptable input and output performance for both set point tracking and disturbance rejection, reinforcing the first objective i.e. successful pressure control in the SFE extraction vessel.

An alternative approach was investigated for designing a model-based controller (Controller 6), that is, the hydrodynamic model (rather than the actual SFE process) was applied for system identification and developing a simple linear model of the process (Section 5.4.4.1). Obtained results demonstrated the ability of the hydrodynamic model to be applied for system identification purposes and designing model-based controller. This approach proves valuable for pressure control of a full scale SFE process with regards to obtaining first estimates of the PI controller parameters.

The hydrodynamic model was applied to design model-based controllers (Controller 6 and Controller 7) at two different operating conditions i.e. extraction vessel pressure in the vicinity of 12 MPa and 17 MPa. The developed first order models were different, specifically with regards to their time constant (i.e. dominant time constant was faster at higher pressures), confirming the nonlinear nature of the SFE process. Both controllers (Controller 6 and Controller 7) proved successful control of pressure at both operating conditions. However, results indicated that each controller performs best at the operating conditions at which it was designed.

To conclude, pressure control was successfully achieved (considering both input performance and output performance) in the SFE process extraction vessel by applying a PI controller in a feedback loop. A manually tuned controller and a model-based controller were individually applied to the actual SFE process and both controller types lead to successful pressure control for both set point tracking and disturbance rejection. Overall, three different approaches were tested for tuning a PI controller in this chapter: manual tuning (trial and error), model-based controller design with identification based on real Input-Output data and model-based controller design with identification based on Input-Output data obtained from the hydrodynamic model. All three approaches led to successful pressure control.

## 6 Level Control in the Continuous Pilot Scale SFE Process

## 6.1 Introduction

Process control is an important part in demonstrating successful operation of the continuous pilot scale SFE process. Pressure and liquid level in the extraction vessel are the two key variables that are required to be controlled. As presented in Chapter 5, pressure can be successfully controlled in the extraction vessel of the continuous pilot scale SFE process. Control of pressure at a predefined set point ensures safe operation and contributes to consistent extraction. Controlling the slurry level in the extraction vessel is also important with regards to process safety and obtaining consistent extractions. Therefore, exploring slurry level control in the extraction vessel of the continuous pilot scale SFE process is the focus of this chapter.

In this continuous SFE process, the slurry phase enters the top of the extraction vessel and exits the bottom, while CO<sub>2</sub> enters the bottom of the extraction vessel and exits the top. From a safety perspective, emptying or overfilling the vessel with slurry must be minimized. The vessel becoming empty of slurry will result in CO<sub>2</sub> entering the slurry outlet line at the bottom of the extraction vessel. This scenario may lead to high CO<sub>2</sub> concentration in the lab and freezing of the slurry outlet line. Overfilling the vessel will result in slurry entering the CO<sub>2</sub> outlet line at the top of the extraction vessel. This scenario leads to an emergency shutdown of the process because of the operational complications caused such as freezing and clogging of the CO<sub>2</sub> outlet line. From an extraction perspective, the level of the slurry must be kept as low as possible to maximize the remaining extraction vessel volume for mass transfer between the slurry and CO<sub>2</sub>. Therefore, during the entire operation time of the continuous SFE process, a volume of slurry is required at the bottom of the extraction vessel, and the level of this volume must be low.

As demonstrated in Chapter 4, slurry level in the extraction vessel is a non-self regulating variable. In other words, if left uncontrolled, it will naturally tend to decrease or increase and it will not settle naturally at a steady state operating level at fixed conditions (Shinskey, 1979; Rice and Cooper, 2008). This non-self regulating character of the slurry level in the extraction vessel is not a desirable scenario for the SFE process and emphasizes the need to control this process variable.

In the majority of the runs that were conducted on the pilot scale SFE process, slurry level was maintained manually by system operators. Manual control of the slurry level in the extraction vessel was based on physical observations of the SFE process, in particular, using the

pressure gauge located on the slurry outlet line from the extraction vessel and the two CO<sub>2</sub> sensors (with monitors) located in the SFE lab. Rapid oscillation of the pressure gauge and/or an increase of the CO<sub>2</sub> concentration in the lab were an indication of CO<sub>2</sub> exiting along with the slurry and into the slurry receiving tank, and thus a low slurry level in the extraction vessel. In this scenario, the manual response was to increase the slurry flow (usually) in increments of 0.5% to increase the slurry level inside the extraction vessel and thus prevent CO<sub>2</sub> from exiting through the slurry outlet line located at the bottom of the extraction vessel. Once the rapid oscillation of the pressure gauge stopped and once the CO<sub>2</sub> concentration in the lab started to decrease, the slurry flow was decreased (usually) in increments of 0.5%. After each increment, both the pressure gauge and CO<sub>2</sub> concentration were monitored for a few minutes to ensure they remained stable before continuing to the next increment. Although manual control of the slurry level was successful in most cases (i.e. emptying or overfilling of the vessel did not occur in the majority of the runs), a consistent approach that would provide automated level control is necessary for the continued development of this technology.

To measure and control slurry level inside the extraction vessel of the SFE process, two on/off level sensors with different heights (5 cm and 16 cm) are installed from the bottom of the extraction vessel. The initial aim of control was defined as maintaining the slurry level between 5 and 16 cm. However, the level sensors are unstable. Therefore, a different approach must be devised for level measurement. The proposed approach in this chapter, referred to as the pulse test, is to use slurry pump pulses and measure the corresponding pressure response in the extraction vessel to measure the slurry level. Successful measurement of slurry level enables level control (i.e. maintaining slurry level within a desired range).

The overall objective of this chapter is to control slurry level in the extraction vessel of the SFE process within a modelling framework (i.e. via hydrodynamic model of the SFE process). For this purpose, first the pulse test approach is described and implemented for measuring slurry level in the extraction vessel. Second, slurry level control is demonstrated by applying the pulse test approach. The measures of success for slurry level control is first, reliably measuring slurry level at each pulse and second, maintaining the level within a range over a certain period of time. Although demonstration of slurry level control in the actual pilot scale SFE process is also desired, this objective is left to future work.

Section 6.2 is the methodology section in which the pulse test approach for slurry level measurement and control is described. In Section 6.3, results associated with applying the pulse test approach for measurement and control of the slurry level in the extraction vessel are presented. The impact of different factors on the pulse test approach are discussed via simulation with the hydrodynamic model. The application of the pulse test approach on the actual SFE process is briefly explored in Section 6.4. A summary is provided in Section 6.5.

## **6.2 Methodology**

The methodology for implementing the pulse test approach for slurry level measurement and slurry level control is presented in this section. For measuring the slurry level, a method for developing an equation to relate level ( $z$ ) to pulse generated pressure difference ( $\Delta P$ ) is presented. After the development of the  $\Delta P$ - $z$  relationship, the pulse test approach is applied to measure the slurry level in the extraction vessel. The measured level is then used towards slurry level control.

### **6.2.1 Level measurement**

Based on the physical characteristics of the SFE process, an increase of the slurry flow will result in an increase in the extraction vessel pressure. It should be remembered that the main source of pressure inside the vessel is the CO<sub>2</sub> flow i.e. pressure is controlled with the CO<sub>2</sub> flowrate. However, the slurry flow also impacts the pressure inside the extraction vessel. Depending on the level of the slurry, different pressure responses will be observed as a result of manipulating the slurry flow. In other words, at a higher slurry level in the extraction vessel, a larger magnitude of change is observed in the pressure (when manipulating the slurry flow) than at a lower slurry level in the extraction vessel. This concept is utilized to measure the slurry level through the pulse test approach. It should be noted that the produced pressure changes through the pulse test approach must be minor and they must not influence the overall performance of the SFE process in terms of pressure control.

To implement the pulse test approach for slurry level measurement, a relationship between  $\Delta P$  and  $z$  is required. The SFE process cannot be used for this purpose because actual level measurement does not exist in the extraction vessel. Therefore, the hydrodynamic model is applied for deriving a  $\Delta P$ - $z$  relationship. Via simulation with the hydrodynamic model, when

pressure has reached its set point in the extraction vessel (i.e. the pressure is controlled throughout the simulation), pulses are introduced in the slurry flow (by adjusting the flow of the slurry pump). As a result, the pressure in the extraction vessel also pulses/changes and a peak is expected in the pressure response. The difference between the pressure peak and pressure set point is calculated and referred to as  $\Delta P$ . A certain  $\Delta P$  corresponds to a certain slurry level  $z$  inside the extraction vessel. Therefore, a  $\Delta P$ - $z$  relationship can be developed.

The first simulation (referred to as Case 1) for applying the pulse test to develop a  $\Delta P$ - $z$  relationship was conducted with the following specifications:

- The applied pulses have an amplitude of 8%, width of 10 s and a frequency of 1/500 1/s i.e. a pulse applied every 500 s. These values were carefully chosen. Choosing the correct amplitude and width is a tradeoff between two factors. First, the pulses must be big enough so that a measurable difference between pressure responses is observed at different slurry levels. This measurable difference is essential in order to get reliable level measurements. Second, the pulses must be small enough so that the pressure in the extraction vessel is not significantly perturbed. The reason being that the pressure is also a key variable that needs to be maintained at a constant value throughout an SFE run. The pulse frequency must be chosen so that the pressure has enough time to return to the set point before the next pulse is applied. Pulse amplitude, width and frequency in Case 1 were chosen in an attempt to fulfill the stated criteria.
- The controller applied for controlling pressure is the PI controller designed in Chapter 5 in the IMC framework (i.e. Controller 4). The gain ( $K_c$ ) and integral time constant ( $\tau_I$ ) of Controller 4 are  $9.24 \frac{\%}{\text{MPa}}$  and 36.8 s, respectively.
- The operating pressure is 14 MPa. In other words, pressure set point is at 14 MPa throughout the simulation.

Results associated with developing the  $\Delta P$ - $z$  relationship, by applying the pulse test with the stated specifications (via simulation with the hydrodynamic model) are presented in Section 6.3.

## 6.2.2 Level control

To control the slurry level in the extraction vessel, the feedback control structure is applied. In order to implement a feedback loop, a level set point, level measurements and a controller are required. Based on the difference between the level set point and the level measurement (i.e. error), controller action is calculated and applied to the slurry flow.

As stated earlier, a volume of slurry is required at the bottom of the extraction vessel to prevent CO<sub>2</sub> from exiting the slurry outlet line. This volume of slurry should be kept as low as possible in order to maximize the remaining vessel volume for mass transfer between the two phases i.e. slurry and SC-CO<sub>2</sub>. Based on experience gained from operating the actual SFE process, it was concluded that the level of this slurry volume should be kept in the range of approximately 25 to 40 cm. In other words, the aim of slurry level control is keeping it within a certain range and it is not necessary to maintain it at an exact level. It should be noted that the initial reason for maintaining slurry level within a range was based on the anticipated two level sensors being operational in the extraction vessel. The idea of having two level sensors located at the bottom of the extraction vessel for slurry level control was adopted from Forsyth (2006). Therefore, in the feedback loop for controlling slurry level, a “range of level” is used for feedback instead of an exact value of the level. For this purpose, the extraction vessel height is divided into different regions and each region represents a Level state.

In the first attempt (i.e. Case 1) of conducting a simulation for slurry level control using the pulse test, the extraction vessel height was divided into five different regions in which each region represents a Level state. Table 6.1 provides defined states for slurry level in the extraction vessel. Level state 1 represents the desired region (i.e. set point) for control purposes.

**Table 6.1. Defined Level states in the extraction vessel for Case 1**

<i>Level state</i>	<i>Level range</i>
0	$z < 25$ cm
1	$25\text{cm} \leq z < 40$ cm
2	$40\text{ cm} \leq z < 100$ cm
3	$100\text{ cm} \leq z < 150$ cm
4	$z \geq 150$ cm

The controller applied in the feedback loop mimics operator behaviour when manually controlling the level. Based on the selected set point (i.e. Level state 1) and measured level

(therefore Level state), error is calculated. Slurry flow is increased or decreased in increments of 0.5% based on the calculated error. In other words, for Level state 0, slurry flow is increased 0.5%. For Level state 2, 3 and 4, slurry flow is decreased 0.5%, 1% and 1.5%, respectively.

To apply the pulse test approach for controlling level (based on the defined regions and the described controller action), the following steps take place in the simulation for Case 1:

1. The extraction vessel is pressurized to the desired set point (i.e. 14 MPa) by applying the same pressure controller applied when deriving/developing the  $\Delta P$ - $z$  relationship (i.e. Controller 4). During this period, the slurry level is not controlled and the slurry pump is set to a constant flow of 17%.
2. After the pressure reaches its set point of 14 MPa, the slurry pump pulses are started (i.e. at 1000 s) with a predefined amplitude of 8%, width of 10 s and frequency of 1/500 1/s. The pulse amplitude and width must be the same as when developing the  $\Delta P$ - $z$  relationship. The pulse frequency must be chosen so that the pressure has enough time to return to the set point before the next pulse is applied and enough time for the control action to have an impact.
3. With the introduction of each pulse, a response is observed in the extraction vessel pressure.
4. Based on the observed response,  $\Delta P$  is calculated as the difference between the maximum reached pressure and pressure set point (i.e. 14 MPa).
5. After each pulse is applied,  $z$  is calculated via the developed  $\Delta P$ - $z$  relationship (i.e.  $z=f(\Delta P)$ ).
6. The estimated  $z$  corresponds to a specific Level state (as defined in Table 6.1). The corresponding Level state is used for feedback to the controller.
7. The controller adjusts the slurry flow based on the calculated error (i.e. the difference between measured Level state and Level state set point). This action is applied 50 s after the pulse. This time span ensures sufficient time for the pressure peak to happen. Therefore, a more reliable  $\Delta P$  and therefore  $z$  is calculated.
8. Steps 3 to 7 are repeated with the introduction of each pulse which occur every 500 s.

Results associated with slurry level control by applying the pulse test (based on the specifications of Case 1) are presented in Section 6.3. For the purpose of additionally evaluating/exploring the pulse test approach and improving slurry level control, some factors were altered in subsequent simulations (i.e. other cases were explored). These cases and their main specifications are summarized in Table 6.2.

**Table 6.2. Simulation cases for evaluating and exploring the pulse test approach for slurry level measurement and slurry level control**

	Pulse specifications			Pressure control		Level control	
	Amplitude (%)	Width (s)	Frequency <sup>-1</sup> (s)*	Set point	Controller	Level state	Controller increments
Case 1	8	10	500 - 500	14	4	0-4	0.5%
Case 2	8	10	500 - 200	14	4	0-4	0.5%
Case 3	8	10	500 - 200	14	4	0-4	0.2%
Case 4	8	10	500 - 200	14	4	0-4	0.2% or 1%
Case 5	8	10	500 - 200	14	4	0-5	0.2% or 1%
Case 6	4	10	500 - N/A	14	4	N/A	N/A
Case 7	8	10	500 - 200	18	4	0-5	0.2% or 1%

\*The first frequency is associated with  $\Delta P$ -z relationship development. The second frequency is associated with slurry level control.

Results associated with the cases summarized in Table 6.2 are presented in Section 6.3.

## 6.3 Results and discussion

In this section, results associated with measurement and control of the slurry level in the extraction vessel are presented. First, results associated with Case 1 are presented and discussed. Next, results associated with altering some factors in the simulation (Case, 2, 3, 4, 5, 6 and 7) are presented and compared.

### 6.3.1 Case 1

As previously explained, first a  $\Delta P$ -z relationship needs to be developed. To develop a  $\Delta P$ -z relationship using the pulse test approach, the hydrodynamic model is applied. In the simulation, after the pressure reaches the desired set point inside the vessel, pulses are introduced in the slurry flow. Figure 6.1 illustrates simulation results for the pulse test. Applied pulses (also depicted in Figure 6.1) have an amplitude of 8%, a width of 10 s and a frequency of 1/500 1/s.

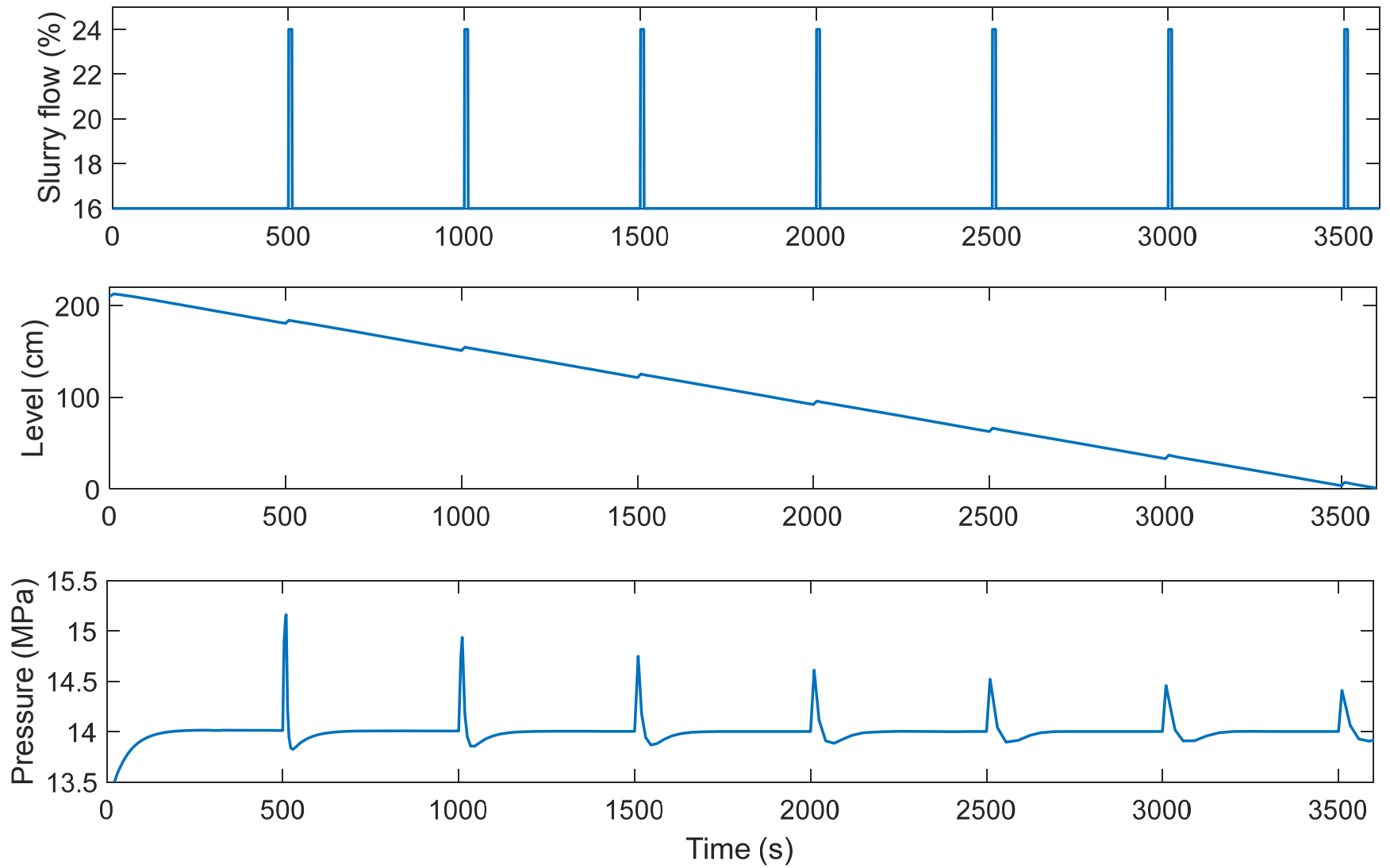


**Figure 6.1. Applied pulses in slurry flow (pulse amplitude = 8%, width = 10 s and frequency = 1/500 1/s) and obtained slurry level and pressure responses for Case 1**

As seen in Figure 6.1,  $\Delta P$  decreases with each pulse as the slurry level decreases in the extraction vessel. The pulses applied to the slurry flow are also seen in Figure 6.1. Data points for deriving a  $\Delta P$ - $z$  relationship are extracted from Figure 6.1 at each pulse (i.e. every 500 s). These data points are provided in Table 6.3.

**Table 6.3. Slurry levels and corresponding pressure differences as a result of applying the pulse test in Case 1**

<i>Level (cm)</i>	<i><math>\Delta P</math> (MPa)</i>
3.41	0.409
33.0	0.456
62.5	0.520
92.0	0.601
121.5	0.748
151.1	0.935
180.7	1.160

Next, a polynomial is fitted to the data provided in Table 6.3 (in Figure 6.2).

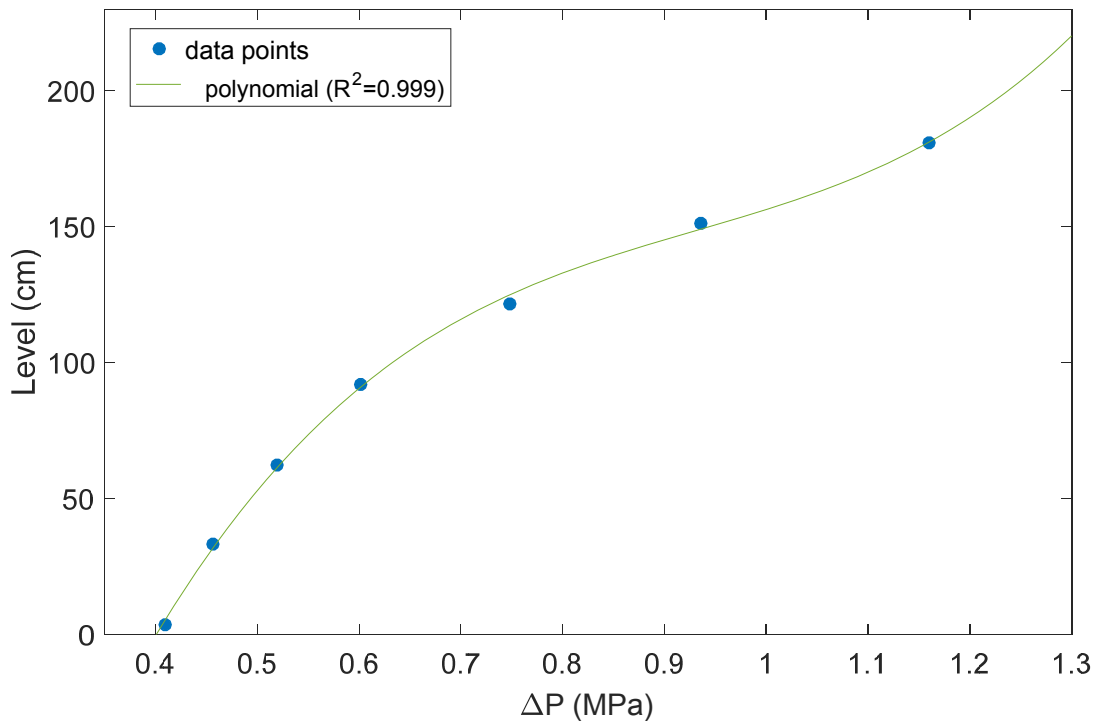


**Figure 6.2. Fitted polynomial to data obtained from the pulse test (pulse amplitude = 8%, pulse width = 10 s) in Case 1**

The equation of the polynomial represents the relationship between pressure difference ( $\Delta P$ ) and slurry level ( $z$ ) in the extraction vessel at a pressure set point of 14 MPa and based on

pulses of 8% amplitude and 10 s width. The polynomial equation is as follows:

$$z = 614.92(\Delta P)^3 - 1714.1(\Delta P)^2 + 1701.7(\Delta P) - 446.28 \quad ( 6.1 )$$

There are several factors that impact the  $\Delta P$ - $z$  relationship described in Equation 6.1:

- Pulse specifications: different pulse specifications (i.e. amplitude and width) impact pressure response differently. Therefore, level measurement is also impacted by pulse specifications.
- Pressure controller parameters: controller parameters directly impact controller performance. In other words, pressure responses with different characteristics (e.g. overshoot, response time) are observed for controllers with different parameters. Because the level measurement is based on the pressure response, controller parameters will also impact level measurement.
- Pressure set point in the extraction vessel: operating pressure impacts pressure response as a result of a slurry pulse. Therefore, level measurement is also impacted by operating pressure.

Now that an equation has been developed representing a relationship between  $\Delta P$  and  $z$ , the equation can be used in a simulation for slurry level measurement and control.

Responses associated with the slurry flow, slurry level, measured slurry level, Level state and pressure are presented in Figure 6.3. It should be noted that the slurry flow response is a result of the controller action and applied pulses. As stated earlier, pulses start at 1000 s. Also, the controller action is applied 50 s after the initiation of a pulse (i.e. 40 s after the pulse has ended because the width of a pulse is 10 s).

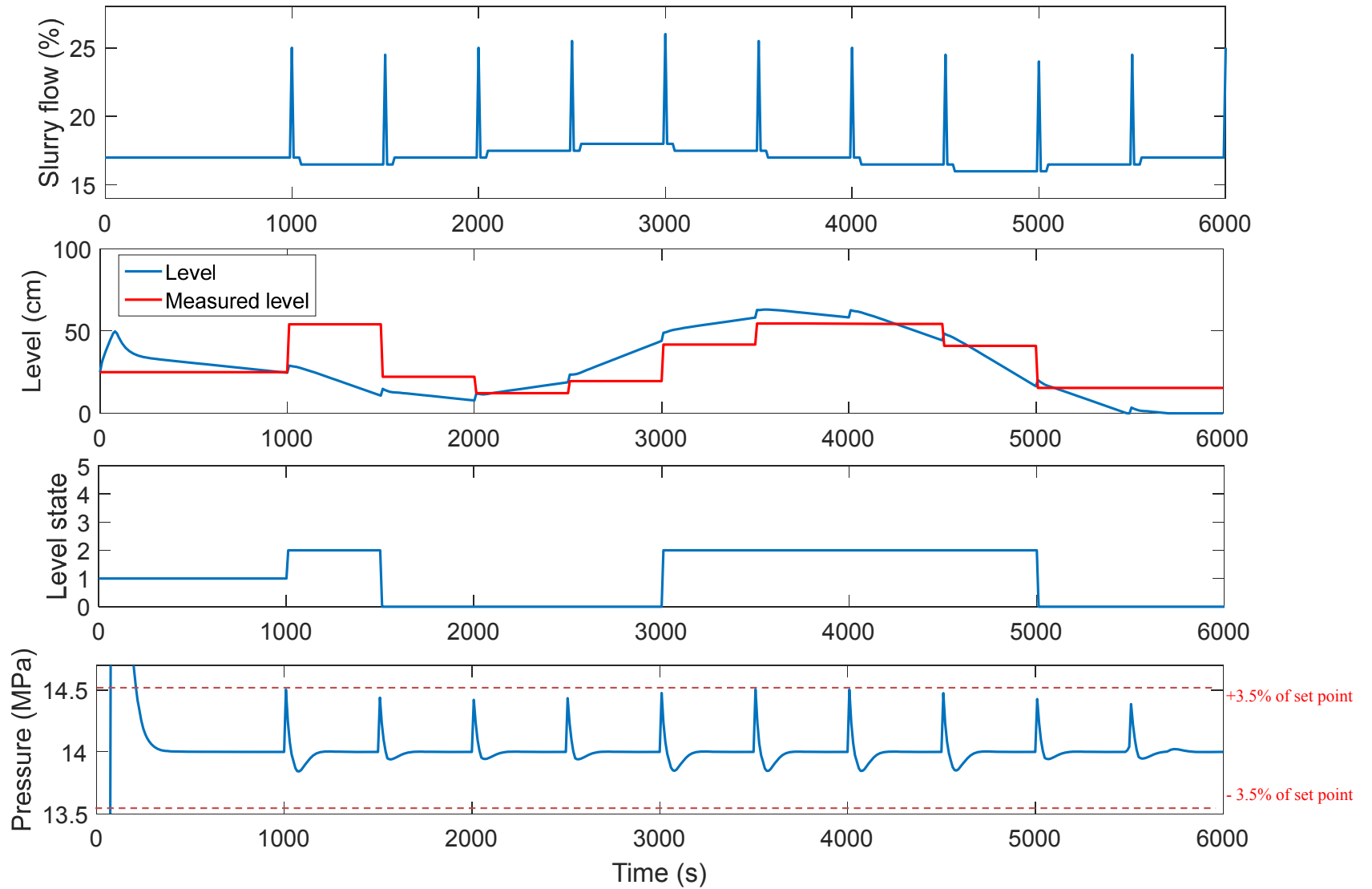


**Figure 6.3. Responses associated with slurry flow (controller action and pulse), slurry level, measured slurry level, Level state and pressure in Case 1**

In comparing the level and measured level responses (as seen in Figure 6.3), there is a large error at the first pulse (i.e. at 1000 s). However, the following measurements are quite accurate and it is concluded that the measured level is capable of following the correct trend of slurry level in the extraction vessel. The reason for the error associated with the first pulse is unknown but it may be due to a numerical error or programming error in the simulation.

The simulation time as presented in Figure 6.3 is 6000 s. During this period, the Level state changes between 0 and 2. The highest and lowest slurry level reached during the simulation time is 63 cm and 0 cm, respectively. At 2000 s, the level reaches a low value of 7.8 cm and the controller is able to recover the slurry level by increasing the slurry flowrate. However, at 5500 s, the level is again low at 0.5 cm, in which the controller is not able to recover the low level and the extraction vessel becomes empty of slurry (i.e. the slurry level becomes 0 cm). Conclusively, the control approach is not successful when slurry level is very low. More frequent pulses might be required to improve control action.

Based on the pressure response in Figure 6.3, it is concluded that the chosen pulse specifications (amplitude and width) fulfil the required criteria stated in Section 6.2.1. That is, a measurable difference between pressure responses is observed at different slurry levels and the pressure response in the extraction vessel is not significantly perturbed at each pulse (i.e. the pressure response is within  $\pm 3.5\%$  of the set point). In addition, the  $1/500$  1/s pulse frequency, allows sufficient time for the pressure to return to set point and the controller action to have an impact before the next pulse is applied.

In the pressure response after the last pulse (at 5500 s), a small bump is observed. The reason for this unusual pressure response is that once the level becomes 0 cm, the hydrodynamic model can no longer describe the SFE process reliably and some anomalies might happen past that point.

### **6.3.2 Case 2**

Based on the results obtained from Case 1, it was decided to introduce pulses more frequently (i.e. every 200 s). Other simulation conditions remained unchanged i.e. pulse amplitude and width, controller action, pressure controller parameters and operating pressure. Responses associated with the slurry flow, slurry level, measured slurry level, Level state and pressure for Case 2 are presented in Figure 6.4.

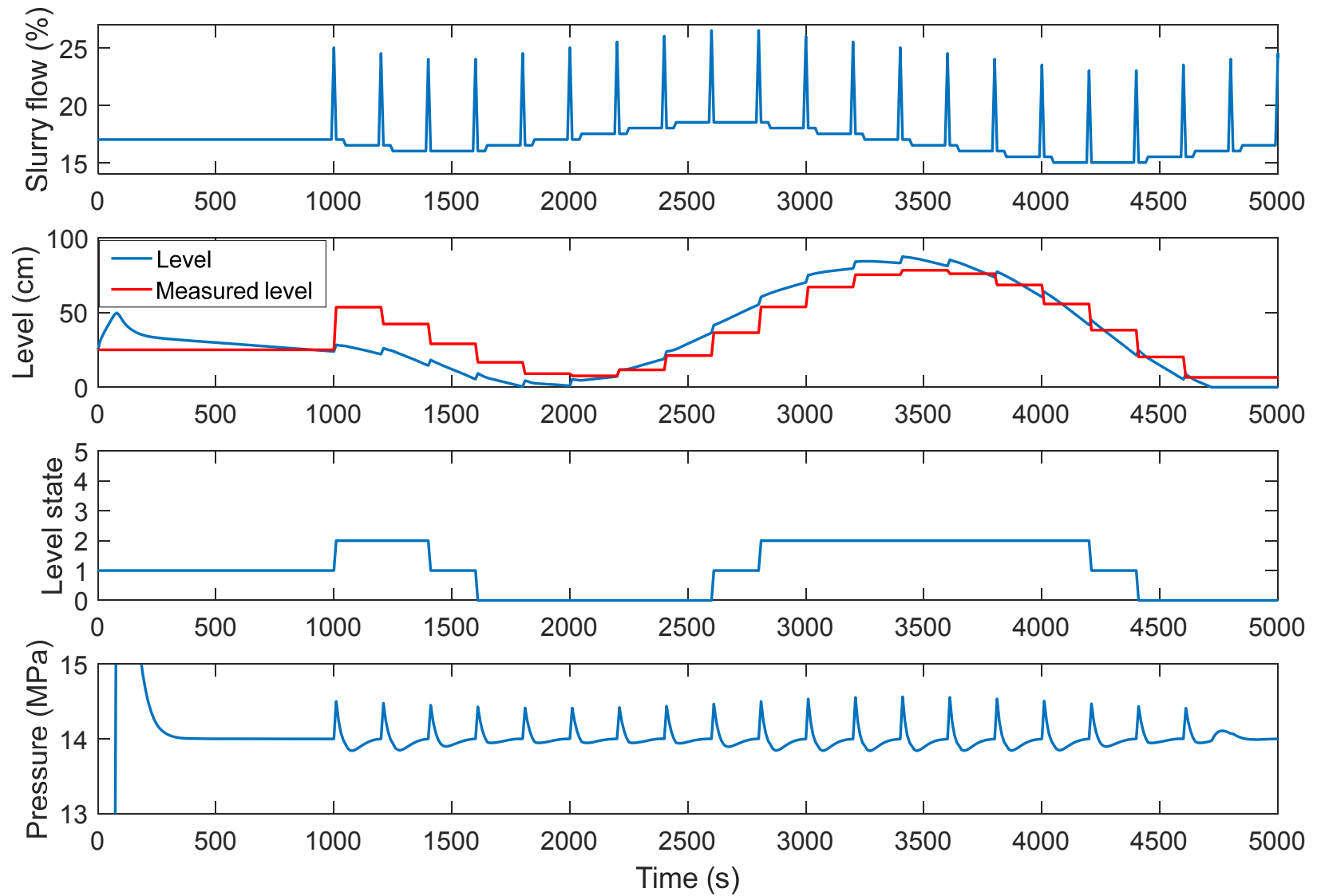


**Figure 6.4. Responses associated with slurry flow (controller action and pulse), slurry level, measured slurry level, Level state and pressure in Case 2**

In comparing the level and measured level responses (as seen in Figure 6.4), there is a large error at the first, second and third pulses at 1000 s, 1200 s and 1400 s, respectively. However, the following measurements are quite accurate and similar to the previous case (i.e. Case 1) therefore it is concluded that the measured level is capable of following the correct trend of slurry level in the extraction vessel.

The simulation time as presented in Figure 6.4 is 5000 s. During this period, the Level state is changing between 0, 1 and 2. The highest and lowest slurry level reached during the simulation time is 87 cm and 0 cm, respectively. At 2000 s, the level reaches a low value of 1 cm and the controller is able to recover the slurry level by increasing the slurry flowrate. However, at 4600 s, the level is again low at 5 cm, in which the controller is not able to recover the level and the extraction vessel becomes empty of slurry before the next pulse is applied at 4800 s. Conclusively, similar to Case 1 the control approach is not successful in the presented scenario. Although the more frequent pulses are useful in terms of having a measurement every 200 s and therefore applying the correct control action more frequently, the controller action must be further enhanced to prevent the extraction vessel from becoming empty.

As seen in Figure 6.4, the pressure in the extraction vessel has enough time to return to set point (i.e. 14 MPa) before the next pulse is applied every 200 s.

### **6.3.3 Case 3**

Based on the results obtained in Case 2, it was decided to relax the controller action. Therefore, the controller action was changed from increments of 0.5% to 0.2% to prevent rapid changes of level in the extraction vessel. It seems like the 0.5% increment change of the controller action is too big and results in a fast level change in the extraction vessel specifically when the slurry level is low. Other simulation conditions remained unchanged i.e. pulse amplitude, pulse width, pulse frequency, pressure controller parameters and operating pressure.

Responses associated with the slurry flow, slurry level, measured slurry level, Level state and pressure for Case 3 are presented in Figure 6.5.

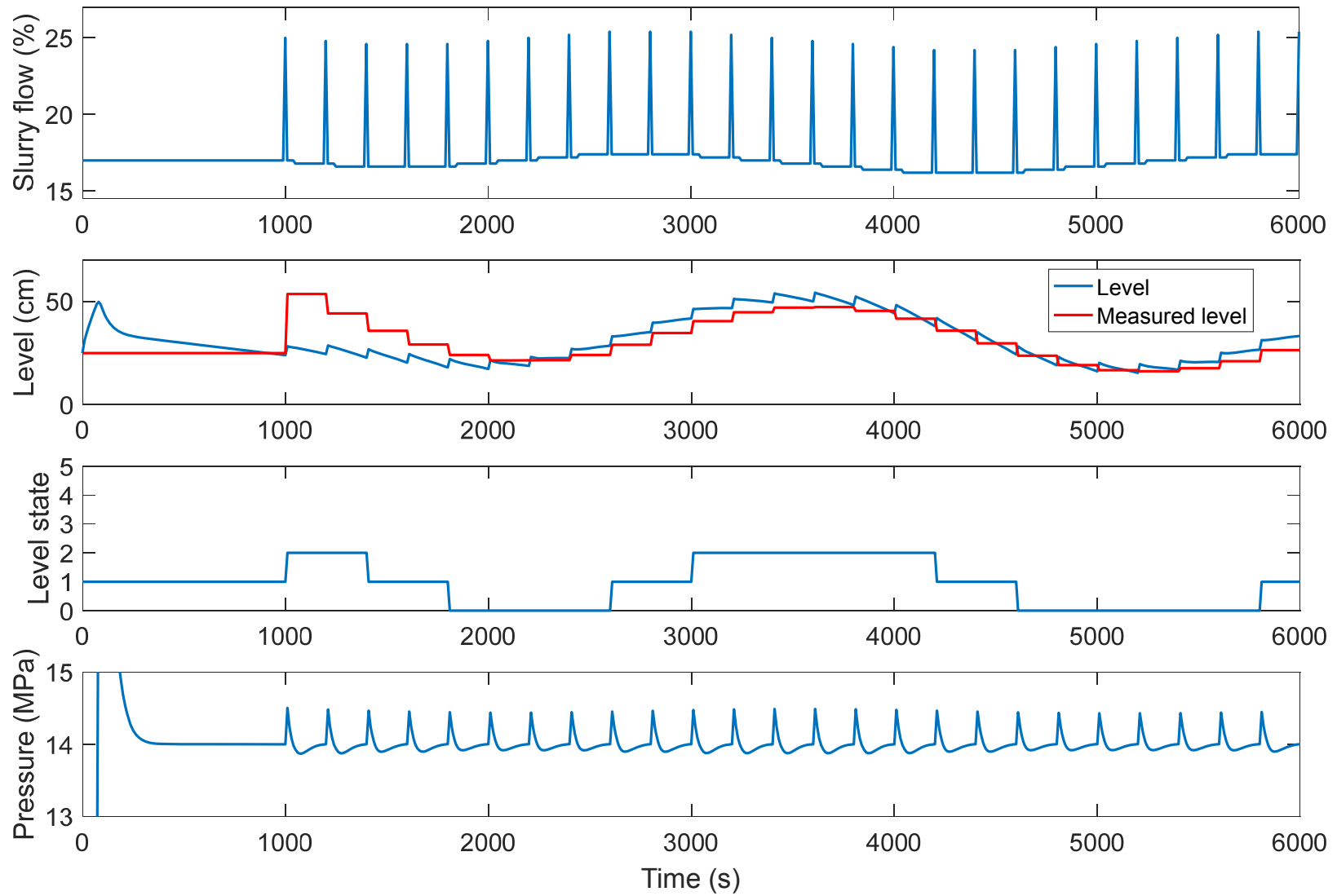


**Figure 6.5. Responses associated with slurry flow (controller action and pulse), slurry level, measured slurry level, Level state and pressure in Case 3**

In comparing the level and measured level responses (as seen in Figure 6.5), similar to Case 2 there is a large error at the first, second and third pulses. However, the following measurements are quite accurate and it is concluded that the measured level is capable of following the correct trend of slurry level in the extraction vessel.

The simulation time as presented in Figure 6.5 is 6000 s. During this period, the Level state is changing between 0, 1 and 2. The highest and lowest slurry level reached during the simulation time is 54 cm and 15 cm, respectively. Because of the relaxed control action (i.e. changes in increments of 0.2%), slurry level doesn't become too low that the controller action does not have a chance to recover. Conclusively, the enhanced controller action is successful in the presented scenario in terms of preventing the extraction vessel from becoming empty or full of slurry. It should be noted that the presented scenario is a typical scenario of an SFE run (at an operating pressure of 14 MPa) in which the initial slurry level in the extraction vessel and the initial slurry flowrate are in the vicinity of 20 cm and 17%, respectively.

To further explore the pulse test as demonstrated in Case 3, another scenario is simulated in which the initial slurry level in the extraction vessel is high (i.e. in the vicinity of 150 cm). This scenario might occur in the extraction vessel as result of a process disturbance.

Responses associated with the slurry flow, slurry level, measured slurry level, Level state and pressure for this scenario (i.e. Case 3 with initial high slurry level in the extraction vessel) are presented in Figure 6.6.

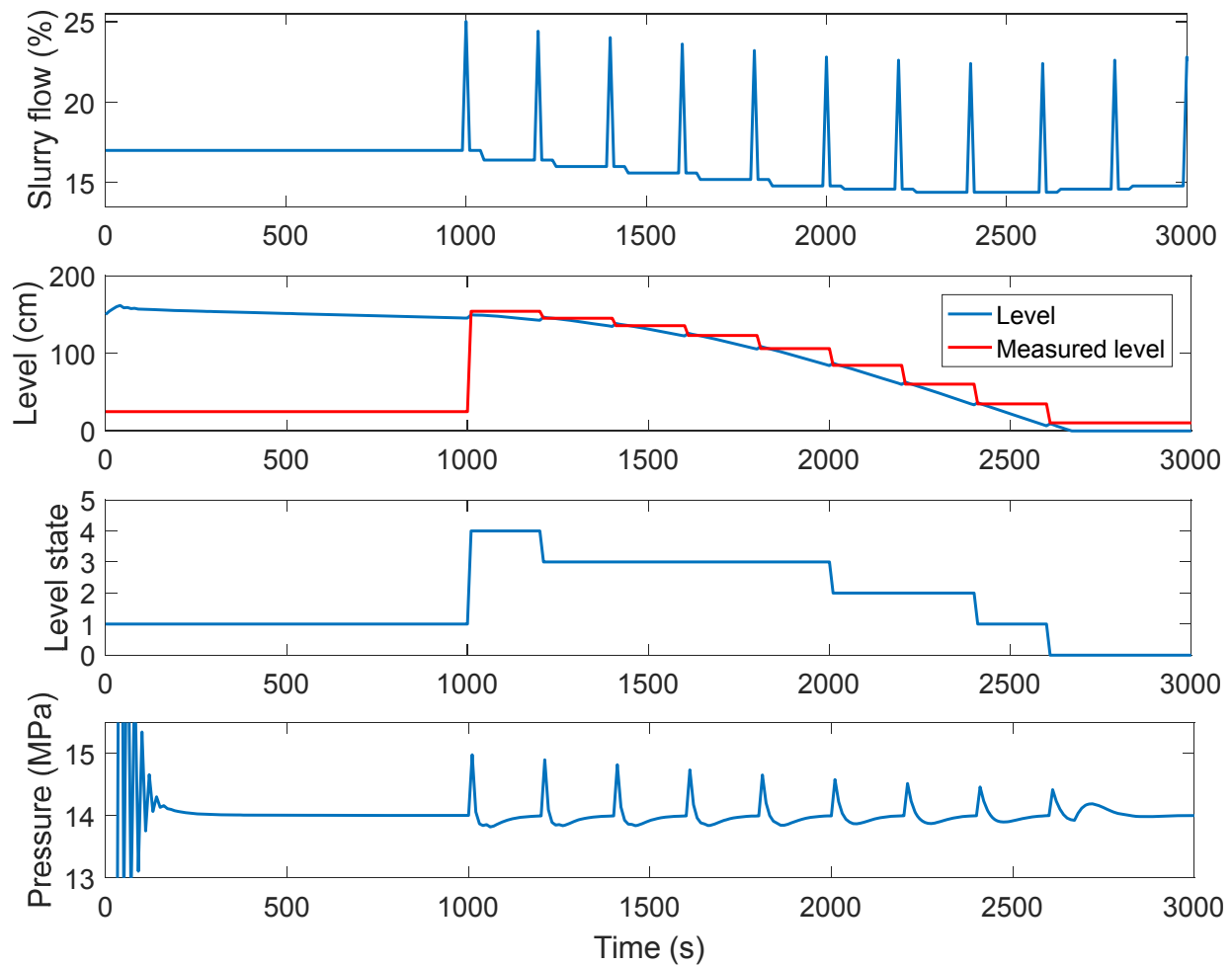


**Figure 6.6. Responses associated with slurry flow (controller action and pulse), slurry level, measured slurry level, Level state and pressure in Case 3 (with initial high slurry level)**

In comparing the level and measured level responses (as seen in Figure 6.6), accurate level measurements are obtained for all pulses.

In terms of slurry level control, because the initial slurry level is very high (in the vicinity of 150 cm), slurry flowrate is decreased after each pulse. However, by the time the slurry level reaches the desired state (i.e. Level state 1), the slurry flowrate is relatively low and the controller cannot recover the slurry level fast enough to prevent the vessel from becoming empty. Conclusively, the proposed controller action for Case 3 is unsuccessful in this scenario (i.e. high initial slurry level). Therefore, another control strategy must be adapted with a more aggressive controller action when slurry level is low (i.e. in Level state 0).

### 6.3.4 Case 4

Based on the results obtained for Case 3 for the scenario of a high initial slurry level, it was decided to have a more aggressive controller action when the slurry level is low (i.e. Level state 0). Therefore, based on the selected set point (Level state 1) and measured slurry level, error is calculated. Depending on the calculated error, the slurry flow is decreased in increments of 0.2% when Level state is 2, 3 or 4 or increased in increments of 1% when Level state is 0. In other words, for a Level state of 0, slurry flow is increased 1% (rather than 0.2%) to prevent the extraction vessel from becoming completely empty of slurry. Other simulation conditions remained unchanged i.e. pulse specifications (amplitude and width), pulse frequency, pressure controller parameters and operating pressure.

Responses associated with slurry flow, slurry level, measured slurry level, Level state and pressure are presented in Figure 6.7.

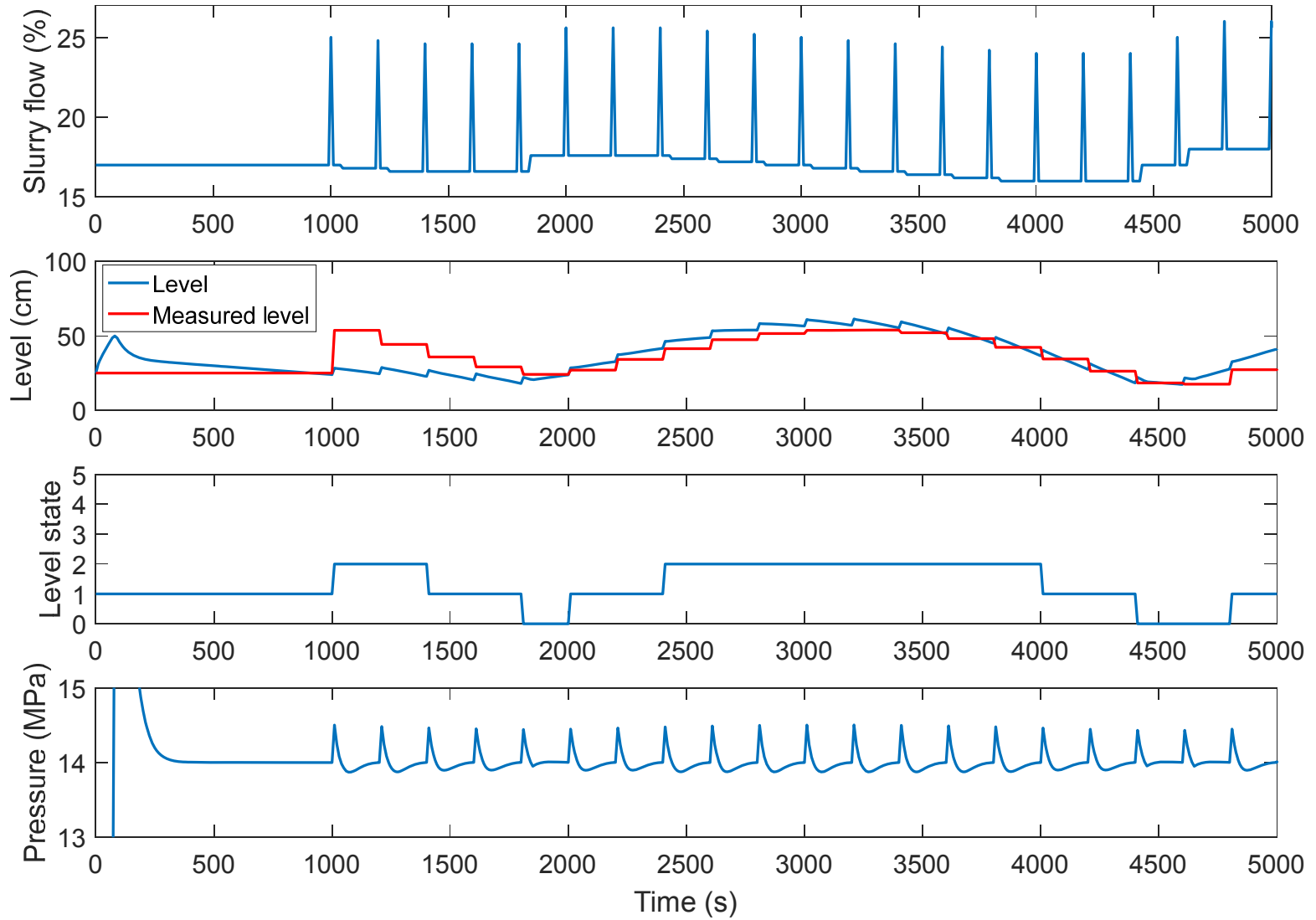


**Figure 6.7. Responses associated with slurry flow (controller action and pulse), slurry level, measured slurry level, Level state and pressure in Case 4**

Slurry flowrate response is presented in Figure 6.7. Based on the obtained Level state at each pulse, controller action results in a slurry flowrate decrease in increments of 0.2% or a slurry flowrate increase in increments of 1% (i.e. at 1800 s, 4400 s and 4600 s).

As seen in Figure 6.7, the measured level is capable of following the correct trend of the actual level inside the extraction vessel.

There are two time instances (1800 s and 4600 s) in which the slurry level is very low (at approximately 18 cm). As seen in Figure 6.7, the control strategy is capable of recovering slurry level in the extraction vessel and exiting Level state 0 in a timely manner. Conclusively, the adapted controller action is successful in the presented scenario in terms of preventing the extraction vessel from becoming empty or full of slurry.

Case 4 was also tested for the scenario in which the initial level of slurry inside the extraction vessel is high (i.e. in the vicinity of 150 cm).

Responses associated with slurry flow, slurry level, estimated slurry level, Level state and pressure for this scenario of Case 4 (i.e. initial high slurry level) are presented in Figure 6.8.

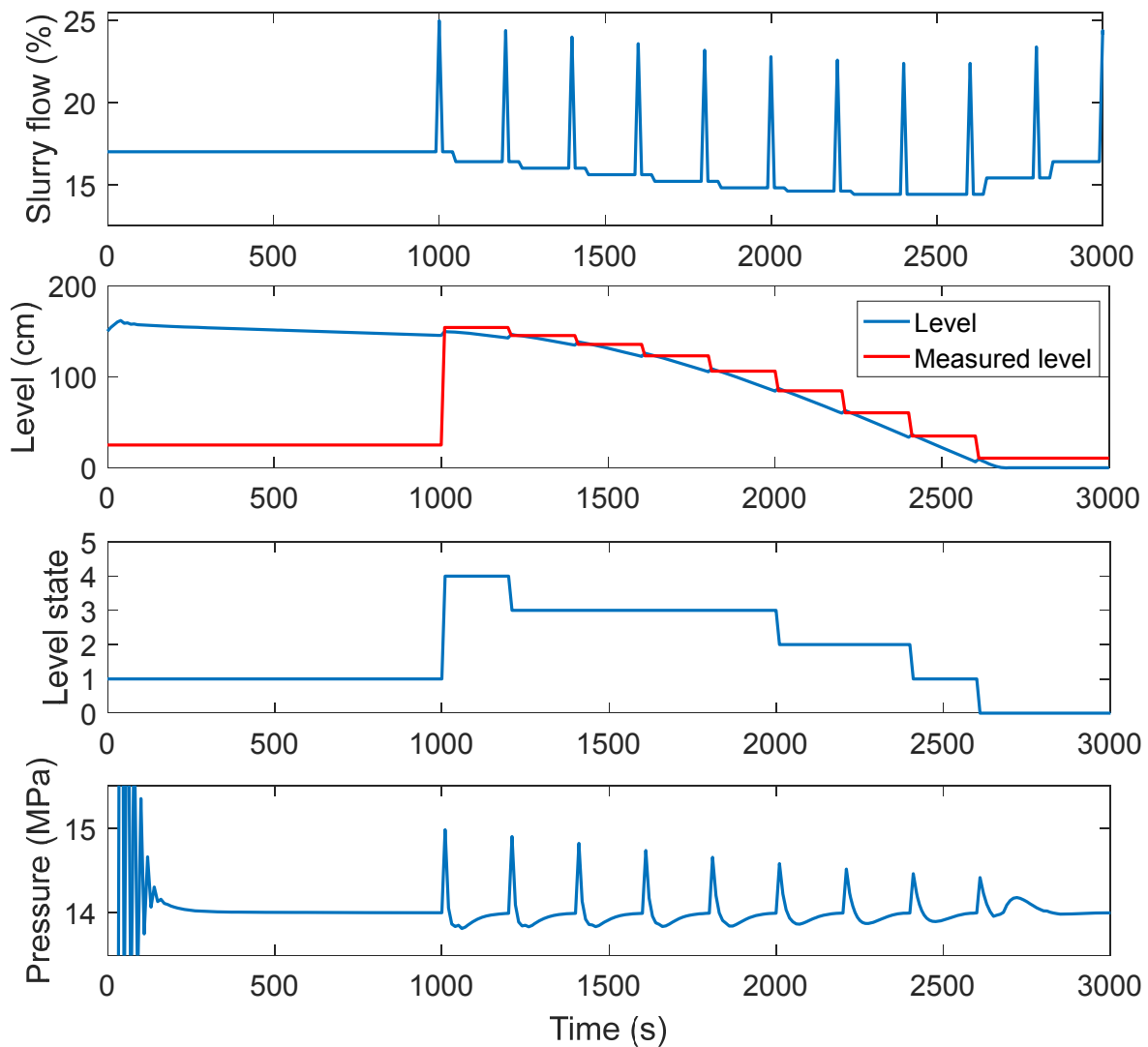


**Figure 6.8. Responses associated with slurry flow (controller action and pulse), slurry level, measured slurry level, Level state and pressure in Case 4 (initial high slurry level)**

In comparing the level and measured level responses (as seen in Figure 6.8), accurate level measurements are obtained for all pulses.

In terms of slurry level control, because the initial slurry level is very high (in the vicinity of 150 cm), slurry flowrate is decreased after each pulse. Similar to Case 3, by the time the slurry level reaches the desired state (i.e. Level state 1), the slurry flowrate is relatively low and the controller cannot recover the slurry level fast enough to prevent the vessel from becoming empty. Conclusively, the proposed controller action for Case 4 is also unsuccessful in this scenario. Therefore, the control strategy must be further enhanced.

### 6.3.5 Case 5

Case 5 is a modified version of Case 4 in an effort to enhance controller action when slurry level is low in the extraction vessel. In the enhanced control strategy in Case 5, the extraction vessel height was divided into six different regions. Table 6.4 provides defined states for slurry level in the extraction vessel applied in Case 5. Level state 2 represents the desired region (i.e. set point) for control purposes.

**Table 6.4. Defined Level states in the extraction vessel for Case 5**

<i>Level state</i>	<i>Level Range</i>
0	$z < 10 \text{ cm}$
1	$10\text{cm} \leq z < 25 \text{ cm}$
2	$25\text{cm} \leq z < 40 \text{ cm}$
3	$40 \text{ cm} \leq z < 100 \text{ cm}$
4	$100 \text{ cm} \leq z < 150 \text{ cm}$
5	$z \geq 150 \text{ cm}$

Based on the selected set point (Level state 2) and measured level (therefore Level state), error is calculated. Depending on the calculated error, slurry flow is decreased in increments of 0.2% when the Level state is 3, 4 or 5 or increased in increments of 1% when the Level state is 0 or 1. Therefore, for a Level state of 0 and 1, slurry flow is increased 2% and 1%, respectively and for a Level state of 3, 4 and 5, slurry flow is decreased 0.2%, 0.4% and 0.6%, respectively.

Responses associated with slurry flow, slurry level, measured slurry level, Level state and pressure are presented in Figure 6.9.

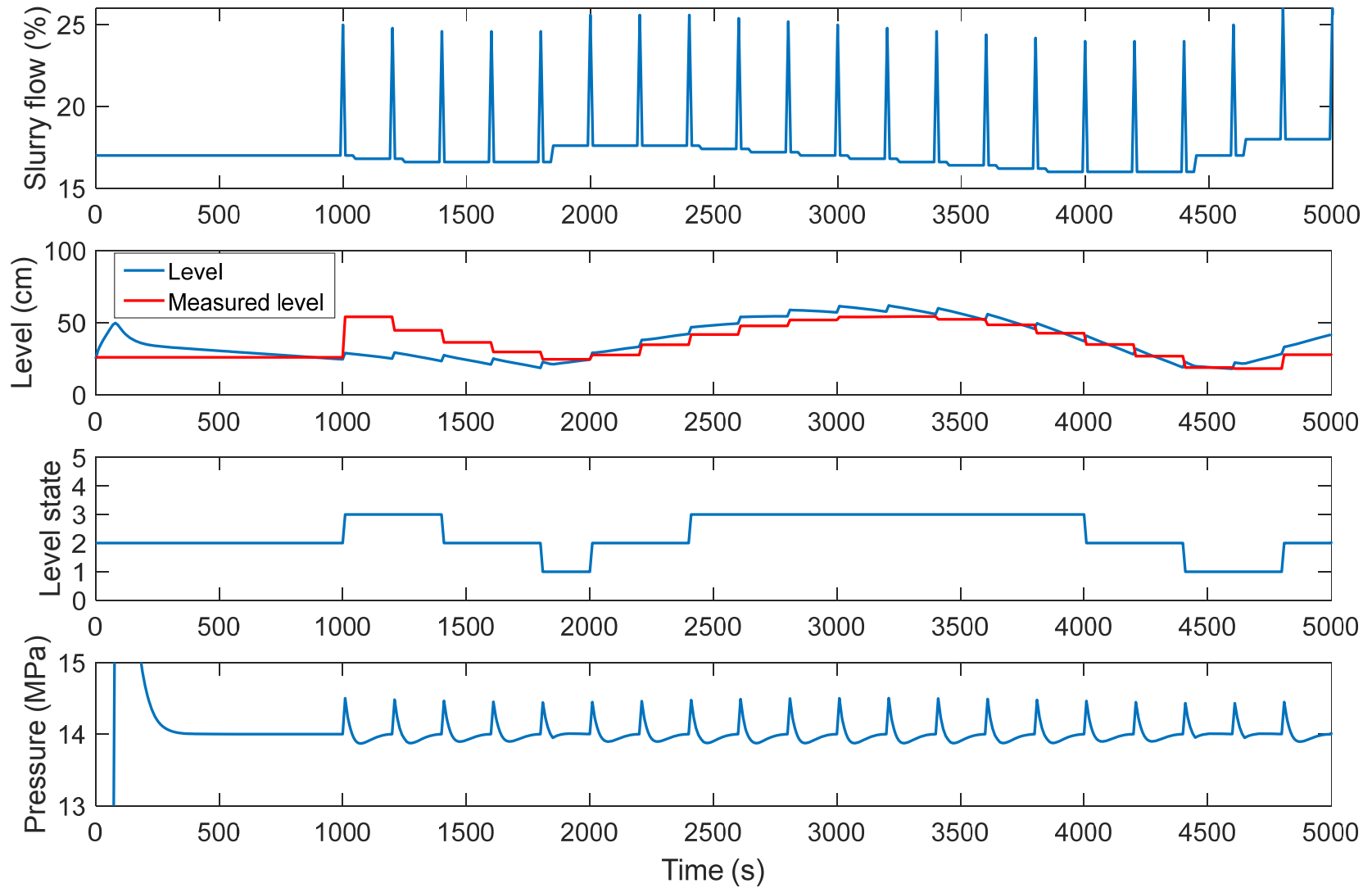


**Figure 6.9. Responses associated with slurry flow (controller action and pulse), slurry level, measured slurry level, Level state and pressure for Case 5**

As seen in Figure 6.9, the measured level is capable of following the correct trend of the actual level inside the extraction vessel. Obtained results are similar to that of Case 4 (i.e. Figure 6.7).

Case 5 was also tested for the scenario in which the initial level of slurry inside the extraction vessel is high (i.e. in the vicinity of 150 cm). Responses associated with slurry flow, slurry level, measured slurry level, Level state and pressure for this scenario of Case 5 (i.e. initial high slurry level) are presented in Figure 6.10.

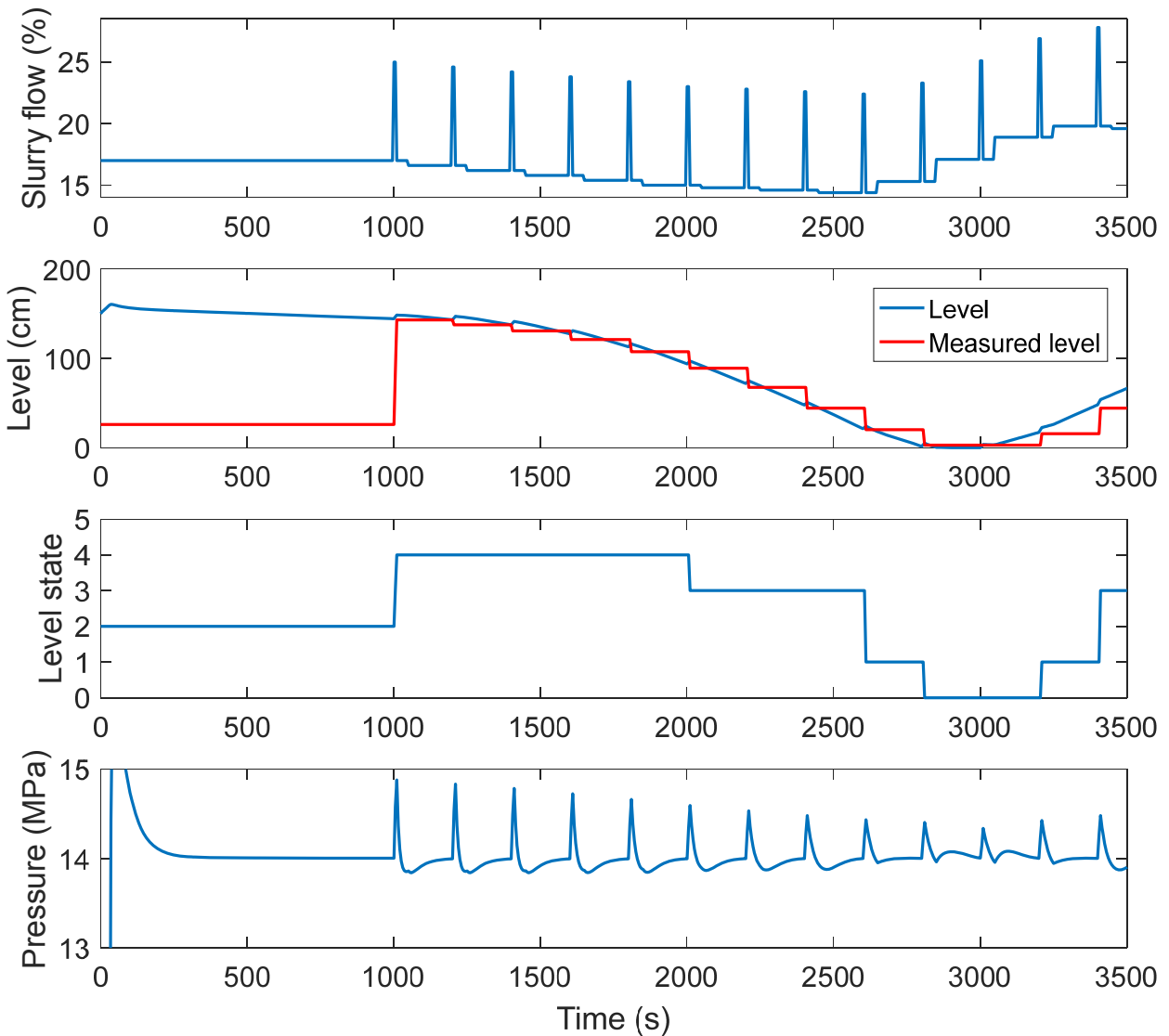


**Figure 6.10. Responses associated with slurry flow (controller action and pulse), slurry level, measured slurry level, Level state and pressure for Case 5 (initial high slurry level)**

As seen in Figure 6.10, the enhanced controller action is capable of preventing the extraction vessel from becoming empty just before slurry level becomes 0 cm.

To summarize and based on the obtained results in Case 5, the pulse test approach proves promising in measuring and controlling the slurry level in the extraction vessel for the two presented scenarios: initial low slurry level (i.e. in the vicinity of 25 cm) in the extraction vessel and initial high slurry level (in the vicinity of 150 cm) in the extraction vessel. The first scenario is a typical scenario observed in the actual SFE process. The second scenario is not typical in the SFE process but might occur due to disturbances during an experimental run.

### **6.3.6 Case 6**

Case 6 is presented for the purpose of additionally exploring the pulse test approach for slurry level measurement and control. As previously stated, pulse specifications must be carefully chosen so that a measurable difference between pressure responses is observed at different slurry levels and at the same time avoid significantly perturbing the pressure response in the extraction vessel. Therefore, in Case 6, pulses with different specifications i.e. 4% amplitude and 10 s width are applied and results are compared with pulses in the previous cases which had an amplitude of 8% and width of 10 s.

First and similar to Case 1, a  $\Delta P$ - $z$  relationship needs to be developed. To develop a  $\Delta P$ - $z$  relationship using the pulse test approach, the hydrodynamic model is applied. In the simulation, after pressure reaches 14 MPa inside the extraction vessel, pulses are introduced in the slurry flow. Figure 6.11 illustrates simulation results for the pulse test at a pressure set point of 14 MPa. Applied pulses (also depicted in Figure 6.11) have an amplitude of 4%, a width of 10 s and a frequency of 1/500 1/s.

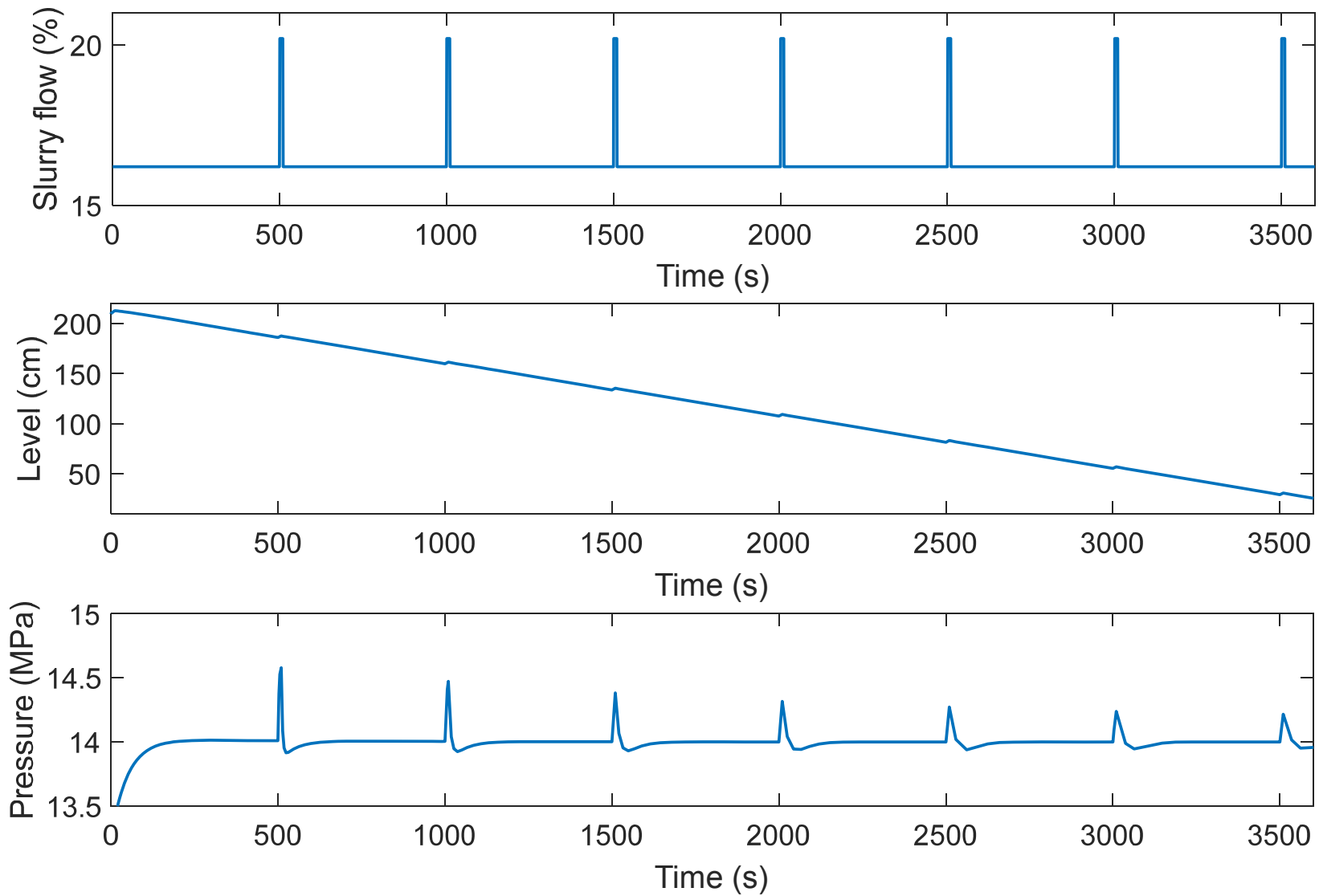
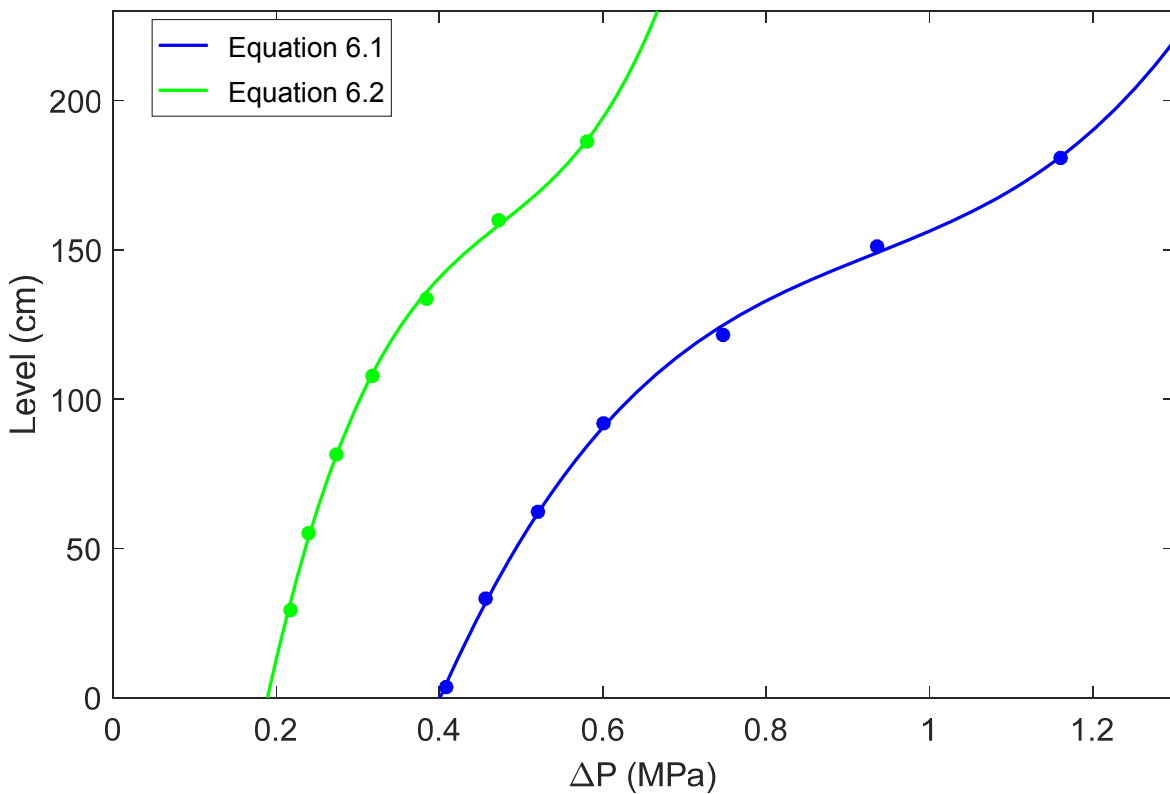


Figure 6.11. Applied pulses in slurry flow (pulse amplitude = 4%, width =10 s and frequency = 1/500 1/s) and obtained slurry level and pressure responses for Case 6

Data points for deriving a  $\Delta P$ - $z$  relationship are extracted from Figure 6.11. Next, a polynomial is fitted to the extracted data. The equation of the polynomial represents the relationship between  $\Delta P$  and  $z$  in the extraction vessel at a pressure set point of 14 MPa and based on pulses of 4% amplitude and 10 s width. The polynomial equation is as follows:

$$z = 4150.1(\Delta P)^3 - 5913.1(\Delta P)^2 + 3026.3(\Delta P) - 389.26 \quad ( 6.2 )$$

The polynomial of Equation 6.2 (associated with pulses of 4% amplitude and 10 s width) is compared with that of Equation 6.1 (associated with pulses of 8% amplitude and 10 s width). This comparison is depicted in Figure 6.12.



**Figure 6.12. Comparison between the polynomial associated with Equation 6.1 and the polynomial associated with Equation 6.2**

As seen in Figure 6.12, there is a significant difference between the two polynomials and there is no overlap in any region. For the polynomial associated with Equation 6.1,  $\Delta P$  changes from 0.4 MPa to 1.3 MPa (over the length of the extraction vessel). While for the polynomial associated with Equation 6.2,  $\Delta P$  only changes from 0.2 to 0.7 (over the length of the extraction vessel).

In an actual SFE run, there are several factors that influence the pressure response in the extraction vessel. A typical example is the measurement noise associated with the pressure sensors in the extraction vessel. As presented in Chapter 5, the noise associated with the pressure sensor at the top of the extraction vessel is in the order of  $\pm 2\%$  of set point. And the noise associated with the pressure sensor at the bottom of the extraction vessel is in the order of  $\pm 0.5\%$  to  $\pm 1\%$  of set point (depending on the magnitude of the set point). Other factors such as clogging or freezing of lines might also occur during a run and impact the pressure response in the extraction vessel to some extent. Therefore, having a wider range associated with  $\Delta P$  over the length of the extraction vessel, is likely to give more reliable level measurements when the pulse test is being applied for slurry level measurement and control. Conclusively, Equation 6.1 is preferable from this perspective in comparison to Equation 6.2.

With regards to the magnitude of change in the pressure response at each pulse, the pulses associated with Equation 6.2 have a smaller amplitude (i.e. 4%) in comparison to the pulses associated with Equation 6.1 (i.e. 8%). Therefore, smaller  $\Delta P$  measurements will be obtained via Equation 6.2. However, as presented in Case 1 to Case 5 (in the simulations associated with the typical scenario of the SFE process), by applying the pulse test approach via Equation 6.1, pressure response in the extraction vessel remains within  $\pm 3.5\%$  of the set point. It should be remembered that the performance of the designed model-based controllers in Chapter 5 were evaluated based on a  $\pm 1\%$  deviation from the set point. Therefore, a  $\pm 3.5\%$  deviation from the set point at each pulse (e.g. at every 200 s) is considered acceptable and it is not expected to influence the overall performance of the SFE run in terms of pressure control in the extraction vessel.

Conclusively, Equation 6.1 fulfills both criteria associated with the pressure response and therefore the corresponding pulse specifications (i.e. amplitude of 8% and width of 10 s) are considered as an appropriate choice for the pulse test approach in measuring and controlling slurry level in the extraction vessel.

### **6.3.7 Case 7**

Case 7 is presented for the purpose of additionally exploring the pulse test approach for slurry level measurement and control. In this case, the impact of operating pressure (i.e. pressure set point) on the pulse test approach is investigated. Therefore, conditions of Case 5 are applied

(i.e. pulse specifications, pulse frequency, pressure controller parameters and control strategy) with the exception of operating pressure which is assumed to be at 18 MPa in Case 7. For this purpose, in applying the pulse test approach for slurry level measurement and control, pressure set point is set to 18 MPa (rather than 14 MPa) via simulation with the hydrodynamic model.

Responses associated with slurry flow, slurry level, measured slurry level, Level state and pressure for Case 7 are presented in Figure 6.13.

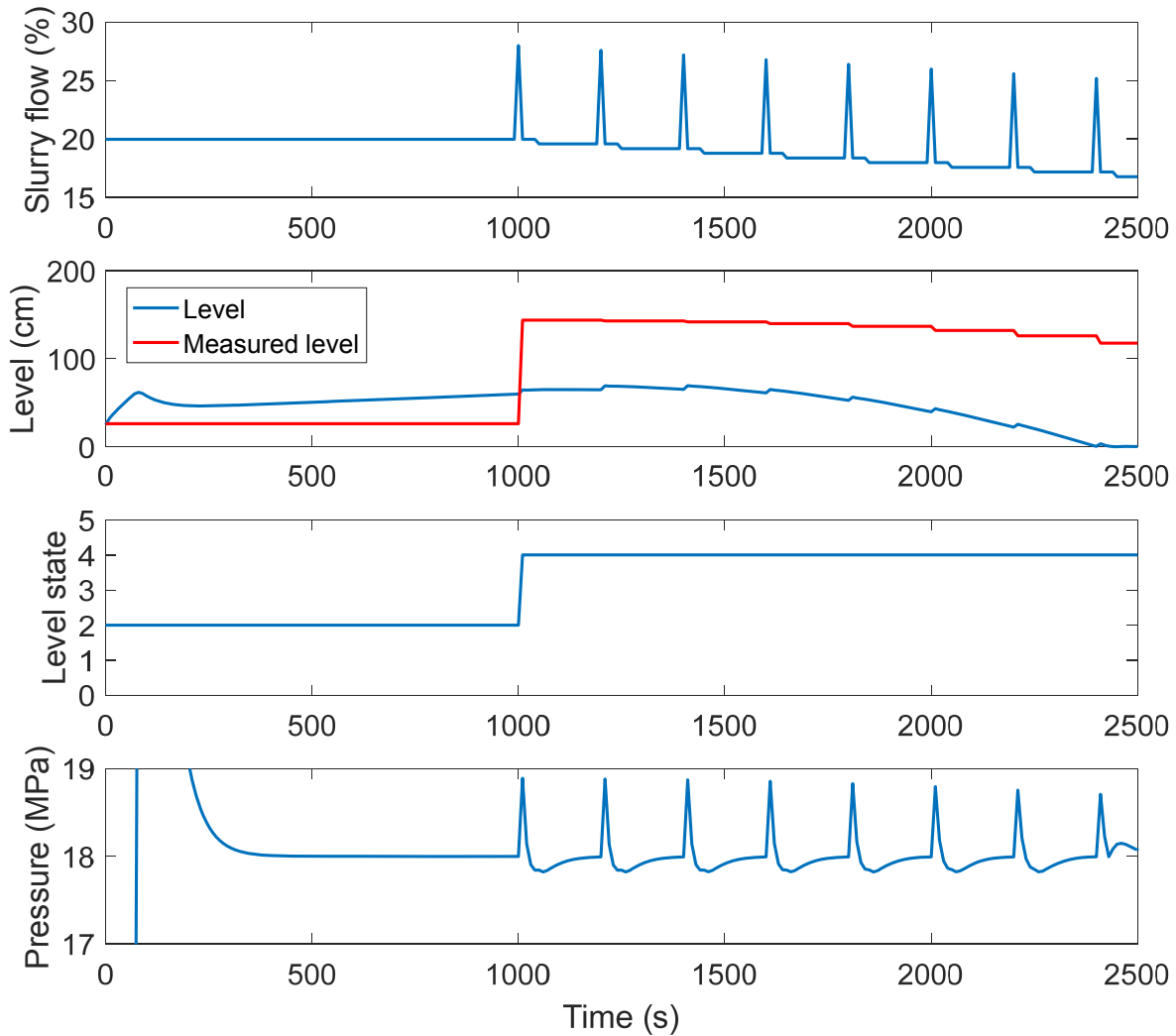


**Figure 6.13. Responses associated with slurry flow (controller action and pulse), slurry level, measured slurry level, Level state and pressure for Case 7**

As seen in Figure 6.13, as soon as the pulses start at 1000 s, there is large error (between slurry level and measured slurry level) and the error is sustained until the end. As a result, an incorrect controller action is applied and the vessel eventually becomes empty of slurry (i.e.

slurry level becomes 0 cm). This demonstrates the impact of operating pressure on the pulse test approach. In conclusion, Equation 6.1 results in a reliable level measurement for an operating pressure of 14 MPa. With an increase of the operating pressure of the SFE process, the reliability of slurry level measurements decreases (via Equation 6.1). For best results, other  $\Delta P$ - $z$  relationship must be developed at the desired operating pressure and applied for slurry level measurement and control (using the pulse test approach). Developing a  $\Delta P$ - $z$  relationship which takes into account process pressure functionality will be of value.

## **6.4 Application of the pulse test to the pilot scale SFE process**

Promising results were obtained in Section 6.3 with regards to applying the pulse test approach for slurry level measurement and control via simulation with the hydrodynamic model. The next step, is applying the proposed approach to the actual SFE process.

The pulse test approach is currently programmed in the control system of the pilot scale SFE process and a few experiments have been conducted to troubleshoot and test the approach for the purpose of controlling slurry level in the extraction vessel during a countercurrent run of the SFE process. These runs (Run 72, 73, 74 and 75 – with the objective of level measurement and Runs 76, 77, 79, 80 and 82 – with the objective of level control) were not completely successful from several perspectives. It was evident that a number of issues were active, especially programming errors with regards to level control. It was clear that the runs did not represent a fair assessment of the proposed level measurement and control. A conclusion could not be drawn whether the pulse test approach is successful for slurry level control of the actual SFE process. Further experiments are required.

As discussed in Section 6.3, the developed polynomial as presented in Equation 6.1 and the control strategy in Case 5, depicted better results (compared to other cases) for slurry level measurement and control. Therefore, the next step is applying Equation 6.1 and simulation specifications of Case 5 for measurement and control of the slurry level in the extraction vessel of the actual SFE process.

## 6.5 Summary

An approach was proposed for measuring and controlling slurry level in the extraction vessel of the SFE process in the absence of a continuous level sensor. This approach, referred to as the pulse test, uses pulses in the slurry flow to perturb the pressure in the extraction vessel. Changes in the pressure are used to measure slurry level in the extraction vessel. The hydrodynamic model of the SFE process was applied to implement and evaluate the capability of the pulse test for slurry level measurement and control.

In applying the pulse test approach to the hydrodynamic model, some factors namely controller action and pulse frequency, were altered in the demonstrated cases to improve slurry level measurement and control. Ultimately, Case 5 resulted in better control performance (in comparison to previous cases) in applying the pulse test approach. Results obtained for Case 5 demonstrate reliable slurry level measurement (with the exception of the first pulses due to numerical/program error). In addition, in the two scenarios that were explored, controller action was capable of maintaining the level within an acceptable range over a certain period of time.

Case 5 was associated with pulses with an amplitude of 8%, width of 10 s and frequency of 1/200 1/s. The Control strategy applied in Case 5 was based on the extraction vessel divided into 6 Level states in which Level state 2 was the set point (representing slurry level between 25 cm to 40 cm). Therefore, the slurry flow was increased in increments of 1% for Level states below the set point and decreased in increments of 0.2% for Level states above the set point.

To conclude, promising results were obtained via simulation in applying the pulse test approach for the purpose of slurry level control in the extraction vessel. The next step is applying the pulse test approach (with the obtained specifications in Case 5) to the pilot scale SFE process. Success of the proposed approach in the pilot scale SFE process enables automated slurry level control which is essential for the continued development of this technology.

## 7 Conclusions and Recommendations

## 7.1 Conclusions

This thesis set out to investigate the feasibility and operation of a continuous pilot scale SFE process for the treatment of drill cuttings. Therefore, a fully continuous pilot scale SFE process was developed, characterized with a hydrodynamic model and controlled.

The main contributions of this thesis are summarized as follows:

1. A pilot scale continuous SFE process for treatment of drill cuttings was successfully designed, built, commissioned and operated.

Design of the SFE process was completed. Building of the SFE process was also completed despite the challenges in procuring equipment for a novel process of this scale. Commissioning and safe operation of the SFE process resulted in 82 experimental runs conducted for the purpose of troubleshooting the process and gathering data for mass transfer and process control studies.

The continuous SFE process proved functional over a wide range of operating conditions. Pressures and temperatures up to 17.9 MPa and 45.4 °C, respectively, were reached in the extraction vessel. The SFE process operated safely and it was capable of extracting oil from a slurried solid phase.

The developed pilot scale continuous SFE process for treatment of slurried solids is the first of its kind and it has not been previously developed. The present study is expected to facilitate the subsequent steps towards full scale operation for the treatment of drill cuttings on an offshore drilling platform or in a fixed facility onshore. The technology might also be applied to continuous extraction of oil/hydrocarbons from other types of slurried solids.

2. A hydrodynamic model characterizing the pilot scale SFE process was successfully developed, implemented, verified and validated.

The hydrodynamic model has been developed based on first principle equations and it is capable of demonstrating pressure and slurry level response in the extraction vessel at different CO<sub>2</sub> and slurry flowrates. Based on a validation test and its replicate, the metering valve opening and manifold length values were adjusted to reconcile model responses with actual SFE process responses. The adjusted model proved capable of accurately predicting steady state pressure response in another trial of a validation test and its replicate. The adjusted model also provided

consistency with the final slurry level in the extraction vessel.

The adjusted hydrodynamic model proved valuable for pressure and slurry level control studies, specifically for comparing performance of different controllers, designing model-based controllers and exploring different control strategies. The adjusted hydrodynamic model will also prove valuable in process operation (e.g. start-up, shutdown, exploring different operating conditions) and in the development of a full scale SFE process for treatment of drill cuttings. The hydrodynamic model also has the potential to be adapted for similar continuous SFE processes which use SC-CO<sub>2</sub> as the solvent.

3. Pressure control was successfully achieved in the extraction vessel of the pilot scale SFE process.

Three approaches were explored and compared for tuning/designing a PI controller in a feedback loop for controlling pressure in the extraction vessel. All three approaches led to successful pressure control for set point tracking and disturbance rejection. In the first approach, the PI controller was tuned manually. In the second approach, the IMC framework was applied to design a model-based controller. In this approach, process identification was conducted on the actual SFE process to obtain Input-Output data. In the third approach, again the IMC framework was applied. However, the hydrodynamic model was utilized to conduct process identification and obtain Input-Output data for the purpose of designing a model-based controller. Successful pressure control in the extraction vessel of the continuous pilot scale SFE process provides basis for pressure control in a full scale process.

4. An approach was explored (in the modelling framework) for slurry level measurement and control in the extraction vessel of the SFE process.

An approach, referred to as the pulse test, was explored for measuring and controlling slurry level in the extraction vessel (in the absence of a functional level sensor). This approach used a slurry pump pulse and measured the corresponding pressure response in the extraction vessel to quantify the slurry level. The slurry level measurements were then utilized towards controlling slurry level in a feedback control loop. Promising results were obtained by applying the pulse test approach through the hydrodynamic model, which paves the way for testing the approach with the obtained specifications on the actual pilot scale continuous SFE process. The capability of this approach to measure and control slurry level in the extraction vessel of the pilot

scale SFE process provides the basis for automated slurry level control in the extraction vessel of the SFE process and ultimately in a full scale process.

Overall, demonstrating automated control of pressure and slurry level in the SFE process is a key part in demonstrating operability of the SFE process under investigation.

## **7.2 Recommendations**

Recommendations for future work regarding development of the pilot scale continuous SFE process are as follows:

1. Sourcing a continuous level sensor to install in the extraction vessel, compatible with high pressures and other operational conditions of the SFE process. Although promising results were obtained by applying the pulse test approach for slurry level measurement and control, the existence of a continuous level sensor in the extraction vessel may be useful for future upgrades of the SFE process.
2. Expanding the range of conditions tested for the process i.e. temperature and pressure, slurry flowrate, CO<sub>2</sub> flowrate and slurry solids content, and evaluating the performance of the SFE process at these conditions.
3. Testing the technology for extraction of oil from other type of solid slurries.

Recommendations for future work regarding hydrodynamic modelling of the continuous SFE process are as follows:

1. Conducting additional experimental runs on the continuous SFE process at other operating conditions specifically higher pressures e.g. 18 MPa and comparing the results with the predictions of the hydrodynamic model.
2. Conducting the pulse test approach during a validation test to measure slurry level in the extraction vessel at different intervals (rather than just having the end point slurry level). This approach will help with additional validation of the slurry level response in the extraction vessel.
3. Adding the separator to the hydrodynamic model to predict the pressure and temperature in the separator at different operating conditions of the SFE process. The predictions are valuable with regards to preventing freezing of lines in the separator

and potentially controlling temperature in the separator in future upgrades of the process.

Recommendations for future work regarding pressure control in the extraction vessel are as follows:

1. Designing two independent controllers i.e. one specifically for system pressurization (i.e. set point tracking) and the other specifically for the optimum extraction period of the process (i.e. disturbance rejection). Comparing this approach with the current approach in which only one controller is used during the entire duration of the SFE experimental run is of value in terms of pressure control performance for future upgrades of the SFE process. Designing a controller for the purpose of only set point tracking or disturbance rejection, will result in a more operationally effective controller in each phase.
2. Conducting step tests with different amplitudes to check the degree of proportionality of the output (i.e. pressure) to the input (CO<sub>2</sub> flow). These tests will determine the degree of process non-linearity at operating conditions outside of those tested in this thesis. Therefore, if the process were to be operated at pressures greater than 17 MPa, decisions can be made with regards to designing a new pressure controller or applying controllers designed at pressures explored in this thesis.

Recommendations for future work regarding level control in the extraction vessel are as follows:

1. Developing a  $\Delta P$ - $z$  relationship which takes into account process pressure functionality to be used at any operating pressure set point.
2. Conducting further experimental runs on the pilot scale SFE process to explore the capability of the pulse test approach for slurry level measurement and control.
3. Designing a PI/PID controller based on system identification techniques (for non-self-regulating processes) to apply with the pulse test (for controlling slurry level in the extraction vessel) and comparing the results with the current approach (i.e. feedback control based on level state).
4. Exploring control strategies (other than the pulse test approach) for slurry level

control in the extraction vessel. Although the pulse test approach demonstrated promising results, availability of a continuous level sensor in the extraction vessel may facilitate slurry level control.

## References

Akgerman, A. 1993. Supercritical Fluid Extraction of Contamination from Environmental Matrices. *Waste Management*, Vol. 13, P. 403-415.

Alloy Digest. 2012. Data on World Wide Metals and Alloys. ASM International. Retrieved August 2015. Available online at: <http://app.knovel.com>

Astrom, K.J. & Hagglund, T. 1995. *PID Controllers: Theory, Design and Tuning*. Second Edition. Instrument Society of America.

Astrom, K.J. & Murray, R.M. 2010. *Feedback Systems: An introduction for Scientists and Engineers*. Princeton University Press.

Autoclave Engineers. 2012. Technical Information for Electric Flow Control Valve. Available online at: [http://www.autoclave.com/aefc\\_pdfs/VA\\_Elec\\_FlowCont\\_Valve.pdf](http://www.autoclave.com/aefc_pdfs/VA_Elec_FlowCont_Valve.pdf)

Bender, E. 1970. Equation of State Exactly Representing the Phase Behaviour of Pure Substances. Proceedings of the 5<sup>th</sup> symposium on Thermophysics Properties. ASME. New York.

Birchfield, G.S. 2002. *Advanced Process Control, Optimization and Information Technology in the Hydrocarbon Processing Industries - The Past, Present and Future*. Birchfield Consulting, LLC, FOREWORD, AspenTech.

Bright, F.V. & McNally, M.E.P. 1992. *Supercritical Fluid Technology: Theoretical and Applied Approaches to Analytical Chemistry*. American Chemical Society. Washington, DC.

Brunner, G. 2010. Applications of Supercritical Fluids. *Annual Reviews: Chem. Biomol. Eng.*, P. 321-342.

Brunner, G. 2012. *Supercritical Fluids for Effective Separation Processes*. Institute for Thermal Separation Processes, Hamburg University of Technology.

Bruno, T.J. & Ely, J.F. 1991. *Supercritical Fluid Technology: Reviews in Modern Theory and Applications*. Boca Raton, FL, USA: CRC Press.

Camel, V. 2013. *Environmental Applications: Supercritical Fluids*. AgroParisTech. Elsevier Inc. Available online at: <http://dx.doi.org/10.1016/B978-0-12-409547-2.04735-1>

Canadian Association of Oilwell Drilling Contractors (CAODC). 2016. Forecast Overview. Accessed online at: <http://www.caodc.ca/caodc-forecast-2016>

Canadian Association of Petroleum Producers (CAPP). 2001. *Offshore Drilling Waste Management Review*. Technical Report.

Canadian Association of Petroleum Producers (CAPP). 2014. *Statistical Handbook for Canada's*

Upstream Petroleum Industry. Technical Report.

Canadian Centre for Energy Information (CCEI). 2004. Canada's Evolving Offshore Oil and Gas Industry. Available online at: <http://www.centreforenergy.com>

Cat Pumps. 2008. Pump Catalogue: 8 Frame Block-Style Stainless Steel Plunger Pump, Model 781 and 781K. Available online at: [http://www.catpumps.com/products/pdfs/781\\_D.pdf](http://www.catpumps.com/products/pdfs/781_D.pdf)

Cesari, G., Fermeglia, M., Kikic, I. & Policastro, M. 1989. A Computer Program for the Dynamic Simulation of a Semi-Batch Supercritical Fluid Extraction Process. *Comput. Chem. Eng.*, Vol. 13, P. 1175-1181.

Chrastil, J. 1982. Solubility of Solids and Liquids in Supercritical Gases. *J. Phys. Chem.*, Vol. 86, P. 3016-3021.

Cocero, M.J., Alonso, E. & Lucas, S. 2000. Pilot Plant for Soil Remediation with Supercritical CO<sub>2</sub> under Quasi-Isobaric Conditions. *Industrial & Eng. Chem. Research*, Vol. 39, P. 4597-4602.

Cohen, G.H. & Coon, G.A. 1953. Theoretical Consideration of Retarded Control Trans. *ASME*. 75, P. 827-834.

Coughanowr, D.R. 1991. *Process System Analysis and Control*. Second edition. McGraw-Hill, Inc.

Cygnarowicz, M.L. & Seider, W.D. 1990. Design and Control of a Process to Extract  $\beta$ -Carotene with Supercritical Carbon Dioxide. *Biotechnol. Prog.*, Vol. 6, P. 82-91.

Diaz, M.S. & Brignole, E.A. 2009. Modeling and Optimization of Supercritical Fluid Processes. *J. Supercrit. Fluids*, Vol. 47, P. 611-618.

Eldridge, R.B. 1996. Oil Contaminant Removal from Drill Cuttings by Supercritical Extraction. *Ind. Eng. Chem. Res.*, Vol. 35, P. 1901-1905.

Eppig, C.P., Putnam, B.M. & De Filippi, R.P. 1984. Apparatus for Removing Organic Contaminants from Inorganic-Rich Mineral Solids. United States Patent No. 4434028.

Fernandes, J., Ruivo, R. & Simões, P. 2007a. Dynamic Model of a Supercritical Fluid Extraction Plant. *AIChE Journal*, Vol. 53, P. 825-837.

Fernandes, J., Ruivo, R., Mota, J.P.B. & Simões, P. 2007b. Non-isothermal Dynamic Model of a Supercritical Fluid Extraction Packed Column. *J. Supercrit. Fluids*, Vol. 41, P. 20-30.

Fernandes, J.B., Lisboa, P.F., Mota, J.P.B. & Simões, P.C. 2011. Modelling and Simulation of a Complete Supercritical Fluid Extraction Plant with Countercurrent Fractionation Column. *Sep.*

Sci. Tech., Vol. 46, P. 2088-2098.

Forsyth, V.C. 2006. Fully-Continuous Supercritical Fluid Extraction of PAHs from Soil Slurries. M.Sc. Thesis, School of Engineering, University of Guelph, Guelph, Ontario, Canada.

Fortin, M.M. 2003. Fully-Continuous Supercritical Fluid Extraction of Naphthalene from Soil Slurries. M.Sc. Thesis, School of Engineering, University of Guelph, Guelph, Ontario, Canada.

Garcia, C.E. & Morari, M. 1982. Internal Model Control. 1. A Unifying Review and Some New Results. *Ind. Eng. Chem. Process Des. Dev.* Vol. 21 (2).

Goodwin, C.G., Graebe, S.F. & Salgado, M.E. 2000. *Control System Design*. Prentice Hall.

Huang, B., Qi, Y. & Monjur Murshed, A.K.M. 2013. *Dynamic Modeling and Predictive Control in Solid Oxide Fuel Cells: First Principle and Data-based Approaches*. John Wiley & Sons.

Hvala, N., Strmcnik, S., Sel, D., Milanic, S. & Banko, B. 2005. Influence of Model Validation on Proper Selection of Process Models – an industrial case study. *Computers and Chemical Engineering*, Vol. 29, 1507-1522.

International Association of Oil & Gas Producers (OGP). 2003. *Environmental Aspects of the Use and Disposal of Non Aqueous Drilling Fluids Associated with Offshore Oil and Gas Operations*. Report No: 342.

Jones, C.R. 2010. Treatment of Oily Drill Cuttings Slurries Using Supercritical Carbon Dioxide. M.Sc. Thesis, Department of Civil and Environmental Engineering, University of Alberta, Edmonton, Alberta, Canada.

Kano, M. & Ogawa, M. 2009. The State of the Art in Advanced Chemical Process Control in Japan. *IFAC Symposium on Advanced Control of Chemical Processes*. Istanbul, Turkey.

Kleijnen, J.P.C. 1995. Verification and Validation of Simulation Models. *European Journal of Operational Research*, Vol. 82, 145-162.

Knez, Z., Markocic, E., Leitgeb, M., Primožic, M., Knez Hrncic, M. & Skerget, M. 2014. Industrial Applications of Supercritical Fluids: A Review. *Energy*, Vol. 77, P. 235-243.

Kozak, S. 2014. State-of-the-art in Control Engineering. *Journal of Electrical Systems and Information Technology*, Vol. 1 (2014), P. 1-9.

Kozak, S. 2016. From PID to MPC: Control Engineering Methods Development and Applications. *Proceedings of the 28<sup>th</sup> International Conference Cybernetics and Informatics*. February 2 – 5, 2016, Slovakia.

Laitinen, A., Michaux, A. & Aaltonen, O. 1994. Soil Cleaning by Carbon Dioxide Extraction: A Review. *Environmental Technology.*, Vol. 15, P. 715-727.

Linstrom, P.J. & Mallard, W.G. Eds. NIST Chemistry WebBook, NIST Standard Reference Database Number 69, National Institute of Standards and Technology, Gaithersburg MD, 20899. Retrieved August 2015. Available online at: <http://webbook.nist.gov>

Lopez-Gomez, J.J. 2004. The Use of Supercritical Fluid Extraction for the Treatment of Oil Contaminated Drilling Waste. M.Sc. Thesis, Department of Civil and Environmental Engineering, University of Alberta, Edmonton, Alberta, Canada.

Luyben, W.L. 1996. *Process Modelling, Simulation and, Control for Chemical Engineers.* McGraw Hill.

Luyben, W.L & Luyben, M.L. 1997. *Essentials of Process Control.* McGraw-Hill.

Machado, B.A.S, Pereira, C.G, Nunes, S.B., Padilha, F.F. & Umsza-Guez, M.A. 2013. Supercritical Fluid Extraction Using CO<sub>2</sub>: Main Applications and Future Perspectives. *Separation Science and Technology.*, Vol. 48, P. 2741–2760.

Madras, G., Thiabaud, C., Erkey, C. & Akgerman, A. 1994. Modelling of Supercritical Extraction of Organics from Solid Matrices. *AIChE Journal*, Vol. 5, P. 777-785.

Malhotra, R., Singh, N. & Singh, Y. 2011. Soft Computing Techniques for Process Control Applications. *International Journal on Soft Computing.*, Vol. 2 (3), P. 32-44.

Marr, R. & Gamse, T. 2000. Use of Supercritical Fluids for Different Processes Including New Developments - A Review. *Chemical Engineering and Processing.*, Vol. 39, P. 19-28.

Mathworks®. 2015. Documentation. Retrieved November 2015. Available online at: <http://www.mathworks.com/help/simulink/gui/solver-pane.html>

McHugh, M.A. & Krukoni, V.J. 1994. *Supercritical Fluid Extraction: Principles and Practice.* Second Edition, Butterworth-Heinemann, Boston.

Melton, H.R., Smith, J.P., Martin, C.R., Nedwed, T.J., Mairs, H.L. & Raught, D.L. 2000. Offshore Discharge of Drilling Fluids and Cuttings – A Scientific Perspective on Public Policy. Rio Oil and Gas Conference. Rio de Janeiro.

Moody, L.F. 1944. *Trans. A.S.M.E.*, 66, 671.

National Energy Board (NEB), Canada-Newfoundland and Labrador Offshore Petroleum Board (CNLOPB) and Canada-Nova Scotia Offshore Petroleum Board (CNSOPB). 2010. *Offshore Waste Treatment Guidelines.* ISBN #: 978-1-100-17491-4.

NIST Chemistry WebBook. 2015. Retrieved August 2015. Available online at: <http://webbook.nist.gov>

Odusanya, O.O. 2004. Supercritical Carbon Dioxide Treatment of Oil Contaminated Drill Cuttings, M.Sc. Thesis, Department of Civil and Environmental Engineering, University of Alberta, Edmonton, Alberta, Canada.

OMEGA Engineering Inc. 2015. Products. Retrieved May 2015. Available online at: <http://www.omega.com/pptst/HTWAT.html>

Pajonk, O. 2009. Overview of System Identification with Focus on Inverse Modelling: Literature Review. Institute of Scientific Computing, Technical University Braunschweig. Available online at: <http://www.digibib.tu-bs.de/?docid=00030245>

Peters, M.S. & Timmerhaus, K.D. 1991. Plant Design and Economics for Chemical Engineers. Fourth Edition, Mc-Graw-Hill Inc.

Phelps, C.L., Smart, N.G. & Wai, C.M. 1996. Past, Present, and Possible Future Applications of Supercritical Fluid Extraction Technology. Journal of Chemical Education. Vol. 73, P. 1163-1168.

Potter, M.C. & Wiggert, D.C. 2002. Mechanics of Fluids. Prentice-Hall Inc.

Price-Schonstrom Inc. 2009. Technical Drawing: 40 MPa Extraction Vessel.

Ray, W.H. 1989. Advanced Process Control. Mc-Graw-Hill Book Company.

Ramchandran. B., Riggs, J.B. & Heichelheim, H.R. 1992a. Nonlinear Plant-Wide Control: Application to a Supercritical Fluid Extraction Process. Ind. Eng. Chem. Res., Vol. 31, P. 290-300.

Ramchandran. B., Riggs, J.B., Heichelheim, H.R., Seibert, A.F. & Fair J.R. 1992b. Dynamic Simulation of a Supercritical Fluid Extraction Process. Ind. Eng. Chem. Res., Vol. 31, P. 281-290.

Rice, R. & Cooper, D.J. 2008. Improve Control of Liquid Level Loops. Chemical Engineering Progress, 104, 54.

Rivera, D.E., Morari, M. & Skogestad, S. 1986. Internal Model Control 4 PID Controller Design. Ind. Eng. Chem. Res., Vol. 25 (1), P. 252-265.

Riverol, C. & Cooney, J. 2005. Assessing Control Strategies for the Supercritical Extraction from Coffee Beans: Process-Based Control Versus Proportional Integral Derivative. Journal of Food Process Eng., Vol. 28, P. 494-505.

- Roffel, B. & Betlem, B.H. 2003. *Advanced Practical Process Control*. Springer.
- Rosenthal, A. 2012. *Safe Design of a Continuous Supercritical Extraction System for the Extraction of Drilling Fluid from Drill Cuttings*. M.Sc. These, Department of Engineering, University of Guelph, Guelph, Ontario, Canada.
- Ruivo, R., Paiva, A., Mota, J.P.B. & Simões, P. 2004. Dynamic Model of a Countercurrent Packed Column Operating at High Pressure Conditions. *J. Supercrit. Fluids.*, Vol. 32, P. 183-192.
- Saintpere, S. & Morillon-Jeanmaire, A. 2000. *Supercritical CO<sub>2</sub> Extraction Applied to Oily Drill Cuttings*. Presented at SPE Annual Technical Conference and Exhibition, Dallas, USA, October 1–4.
- Samyudia, Y., Lee, P. & Cameron, I. 1996. Control Strategies for a Supercritical Fluid Extraction Process. *Chem. Eng. Sci.*, Vol. 51, P. 769-787.
- Schmal, J.P. 2013. *Dynamic Chemical Process Modelling and Validation: Theory and Application to Industrial and Literature Case Study*. Dissertation, Department of Chemical Engineering, Delft University of Technology.
- Shinskey, F.G. 1979. *Process Control Systems: Application, Design and Tuning*. McGraw-Hill Book Company.
- Skogestad, S. 2003. Simple Analytic Rules for Model Reduction and PID Controller Tuning. *Journal of Process Control.*, Vol. 13, P. 291-309.
- Skogestad, S. 2004. Simple Analytic Rules for Model Reduction and PID Controller Tuning. *Modeling, Identification and Control.*, Vol. 2 (2), P. 85-120.
- Skogestad, S. 2006. Tuning for Smooth PID Control with Acceptable Disturbance Rejection. *Ind. Eng. Chem. Res.*, Vol. (45), P. 7817-7822.
- Skogestad, S. & Grimholt, C. 2012. *The SIMC Method for Smooth PID Controller Tuning*.
- Skogestad, S. and Postlethwaite, I. 2005. *Multivariable Feedback Control: Analysis and Design*. John Wiley & Sons.
- Smith, C.L. 2009. *Practical Process Control: Tuning and Troubleshooting*. Wiley.
- Soderstrom, T. & Stoica, P. 2001. *System Identification*. Prentice Hall.
- Span, R. & Wagner, W. 1996. A New Equation of State for Carbon Dioxide Covering the Fluid Region from the Triple-Point Temperature to 1100 K at Pressures up to 800 MPa. *J. of Phys.*

Chem. Ref. Data., Vol. 25 (6), P. 1509-1596.

Stantec – Jacques Whitford Stantec Limited. 2009. Cuttings Treatment Technology Evaluation. Environmental Studies Research Funds. Report No. 166. ISBN 978-1-926750-05-7.

Stephanopoulos, G. 1984. Chemical Process Control: An Introduction to Theory and Practice. Prentice Hall International Series.

Street, C.G. 2008. Extraction of Hydrocarbons from Drilling Waste Using Supercritical Carbon Dioxide. M.Sc. Thesis, Department of Civil and Environmental Engineering, University of Alberta, Edmonton, Alberta, Canada.

Swagelok. 2015. Product Catalogue: Stainless Steel Seamless Tubing.

Swamee, P.K., Jain, A.K. 1976. Explicit Equations for Pipe-Flow Problems. Journal of the Hydraulics Division (ASCE), Vol. 102 (5), P. 657-664.

Temelli, F. 2009. Perspectives on Supercritical Fluid Processing of Fats and Oils. J. of Supercritical Fluids., Vol. 47, P. 583-590.

Tunncliffe, I. & Joy, R.Mt. 2004. Cleaning of Hydrocarbon-Containing Materials with Critical and Supercritical Solvents. United States Patent No. 0065353.

U.S. Environmental Protection Agency (EPA). 2000. Profile of the Oil and Gas Extraction Industry. EPA Office of Compliance Sector Notebook Project. Available online at: <http://www.epa.gov/oeca/sector>

Vanwasen, U., Swaid, I. & Schneider, G.M. 1980. Physicochemical Principles and Applications of Supercritical Fluid Chromatography (SFC). Angewandte Chemie-International Edition in English, Vol. 19 (8), P. 575-587.

Veil, J.A., SPE, Argonne National Laboratory. 2002. Drilling Waste Management: Past, Present, and Future. SPE Annual Technical Conference and Exhibition. San Antonio, Texas.

Vilanova, R. & Visioli, A. PID Control in the Third Millennium, Advances in Industrial Control (Chapter 5). Springer-Verlag London.

Ziegler, J.G. & Nichols, N.B. 1942. Optimum Settings for Automatic Controllers. Transactions of the ASME, Vol. 64, P. 759–768.

# Appendices

## Appendix A1: Line specifications

**Table A1. Line specification in the SFE process**

Item	Drawing reference	Description	Supplier	Service	Material
½" flexible hose	LN-2001	Connected directly after the CO <sub>2</sub> tank	Swagelok	CO <sub>2</sub>	Plastic
¾" tubing (.109 wall thickness)	LN-2002	CO <sub>2</sub> tank to CO <sub>2</sub> pump rigid line	Pinacle/ Swagelok	CO <sub>2</sub>	SS
¾" tube	LN-2003	Cauldron brass tubing	Swagelok	CO <sub>2</sub>	Brass
½" flexible hose	LN-2004	Coming out of the cauldron	Swagelok	CO <sub>2</sub>	Plastic
¼" tubing (0.065 wall thickness)	LN-2005	CO <sub>2</sub> pump to extraction vessel main line	Pinacle/ Swagelok	CO <sub>2</sub>	SS
1/8" tubing (0.028 wall thickness)	LN-2006	Extended CO <sub>2</sub> inlet line in to the extraction vessel	Pinacle/ Swagelok	CO <sub>2</sub>	SS
¼" tubing (0.065 wall thickness)	LN-2007	Extraction vessel by-pass line	Pinacle/ Swagelok	CO <sub>2</sub>	SS
2" flexible hose	LN-3001	Outlet of slurry tank FT-3601	Mcmaster-Carr	Slurry	Plastic
2" flexible hose	LN-3002	Outlet of slurry tank FT-3602	Mcmaster-Carr	Slurry	Plastic
2" flexible hose	LN-3003	Outlet of water tank FT-3603	Mcmaster-Carr	Slurry	Plastic
2" nipples, elbows and tees	LN-3004	Rigid line after FT-3602	Pinacle	Slurry	SS
2" nipples, elbows and tees	LN-3005	Rigid line after FT-3601	Pinacle	Slurry	SS
2" nipples, elbows and tees	LN-3006	Rigid line after FT-3603	Pinacle	Slurry	SS
2" nipples, elbows and tees	LN-3007	Rigid joint line after FT-3601 and FT-3602	Pinacle	Slurry	SS
2" nipples, elbows and tees	LN-3008	Slurry pump inlet	Pinacle	Slurry	SS
¾" tubing (.109 wall thickness)	LN-3009	Slurry pump outlet	Pinacle/ Swagelok	Slurry	SS
¾" tubing (.109 wall thickness)	LN-3010	Slurry/water tank by-pass line	Pinacle/ Swagelok	Slurry	SS
3/8" flexible hose	LN-3011	Flexible line at the end of ¾" slurry line (LN-3009)	Swagelok	Slurry	Plastic
¼" tubing (0.065 wall thickness)	LN-3012	Slurry inlet to extraction vessel	Pinacle/ Swagelok	Slurry	SS
¼" tubing (0.065 wall thickness)	LN-4001	CO <sub>2</sub> outlet from extraction vessel	Pinacle/ Swagelok	CO <sub>2</sub> /Oil	SS
¼" tubing (0.065 wall thickness)	LN-4002	CO <sub>2</sub> line after bypass and into separator	Pinacle/ Swagelok	CO <sub>2</sub> /Oil	SS
3/8" tubing	LN-4003	High pressure line in and out of the metering valve (MV-4303)	Zimco	CO <sub>2</sub> /Oil	SS
1/8" tubing (0.028 wall thickness)	LN-4004	CO <sub>2</sub> inlet extended tubing into separator	Swagelok	CO <sub>2</sub> /Oil	SS

<b>Item</b>	<b>Drawing reference</b>	<b>Description</b>	<b>Supplier</b>	<b>Service</b>	<b>Material</b>
1/8" tubing (0.028 wall thickness)	LN-4005	Product out extended tubing from separator	Swagelok	Oil	SS
1/4" tubing (0.065 wall thickness)	LN-4006	Product main line out from separator	Pinacle/ Swagelok	Oil	SS
3/8" flexible and removable hose	LN-4007	Required for pumping out oil from separator	Fisher	Oil	Plastic
1/4" tubing (0.065 wall thickness)	LN-4008	CO <sub>2</sub> outlet line from separator	Pinacle/ Swagelok	CO <sub>2</sub>	SS
1/4" tubing (0.065 wall thickness)	LN-4009	Separator by-pass line	Pinacle/ Swagelok	CO <sub>2</sub> /Oil	SS
1/4" tubing (0.065 wall thickness)	LN-4010	CO <sub>2</sub> line to fume hood	Pinacle/ Swagelok	CO <sub>2</sub> /Oil	SS
1/8" tubing (0.028 wall thickness)	LN-5001	Manifold	Pinacle/ Swagelok	Slurry/CO <sub>2</sub>	SS
1/4" tubing (0.065 wall thickness)	LN-5002	Extraction vessel to LN-5003	Pinacle/ Swagelok	Slurry/CO <sub>2</sub>	SS
3/4" tubing (.109 wall thickness)	LN-5003	LN-5002 to slurry tanks	Pinacle/ Swagelok	Slurry/CO <sub>2</sub>	SS

## Appendix A2: Valve specifications

**Table A2. Valve specification in the SFE process**

Item	Drawing reference	Location	Function	Service	Supplier
¼" relief valve	RV-1301	Extraction vessel (top)	Pressure relief	CO <sub>2</sub> /Slurry	Swagelok
¼" relief valve	RV-1302	Extraction vessel (bottom)	Pressure relief	CO <sub>2</sub> /Slurry	Swagelok
¾" check valve	CV-2301	LN-2002	Flow direction	CO <sub>2</sub>	Swagelok
¼" check valve	CV-2302	LN-2005	Flow direction	CO <sub>2</sub>	Swagelok
¼" relief valve	RV-2303	LN-2005	Pressure relief	CO <sub>2</sub>	Swagelok
¼" ball valve	BV-2304	LN-2005	Isolation	CO <sub>2</sub>	Swagelok
¼" ball valve	BV-2305	LN-2007	Isolation	CO <sub>2</sub>	Swagelok
¾" ball valve	BV-2306	LN-2002	Isolation	CO <sub>2</sub>	Swagelok
¾" relief valve	RV-2307	LN-2002	Pressure relief	CO <sub>2</sub>	Praxair
¾" relief valve	RV-2308	CO <sub>2</sub> pump	Pressure relief	CO <sub>2</sub>	Cat pumps
¾" ball valve	BV-2309	LN-2002	Drain	CO <sub>2</sub>	Swagelok
¼" ball valve	BV-2310a	LN-2005	Drain	CO <sub>2</sub>	Swagelok
¼" three-way ball valve	BV-2310b	LN-2005	Back pressure prevention	CO <sub>2</sub>	Swagelok
2" ball valve	BV-3301	LN-3005	Isolation	Slurry	Pinacle
2" ball valve	BV-3302	LN-3004	Isolation	Slurry	Pinacle
¾" relief valve	RV-3304	LN-3009	Relief of pressure	Slurry	Pumps and pressure
¾" check valve	CV-3305	LN-3009	Flow direction	Slurry	Western Gauge and Instruments Ltd.
¾" ball valve	BV-3306	LN-3009	Isolation	Slurry	Swagelok
¾" ball valve	BV-3307	LN-3010	Isolation	Slurry	Pinacle
¾" ball valve	BV-3308	LN-3010	Isolation	Slurry	Swagelok
2" ball valve	BV-3309	LN-3006	Isolation	Slurry	Pinacle
¾" ball valve	BV-3310	LN-3010	Isolation	Slurry	Swagelok
¾" ball valve	BV-3311	LN-5003	Isolation	Slurry/CO <sub>2</sub>	Swagelok
¾" ball valve	BV-3312	LN-3010	Isolation	Slurry	Swagelok
¾" ball valve	BV-3313	LN-5003	Isolation	Slurry/CO <sub>2</sub>	Swagelok
2" check valve	CV-3314	LN-3006	Flow direction	Slurry	Pinacle
2" ball valve	CV-3315	LN-3005	Flow direction	Slurry	Pinacle
2" ball valve	CV-3316	LN-3004	Flow direction	Slurry	Pinacle
¼" ball valve	BV-3317	LN-3012	Isolation	Slurry	Swagelok
2" ball valve	BV-3318	LN-3008	Drain	Slurry	Pinacle
¾" ball valve	BV-3319	LN-3009	Drain	Slurry	Pinacle
2" plastic ball valve	BV-3320	FT-3601	Isolation	Slurry	McMaster-Carr
2" plastic ball valve	BV-3321	FT-3602	Isolation	Slurry	McMaster-Carr
2" plastic ball valve	BV-3322	FT-3603	Isolation	Slurry	McMaster-Carr
¼" ball valve	BV-4301	LN-4001	Isolation	CO <sub>2</sub>	Swagelok
¼" ball valve	BV-4302	LN-4009	Isolation	CO <sub>2</sub>	Swagelok
3/8" metering valve	MV-4303	LN-4003	Metering	CO <sub>2</sub>	Autoclave
¼" relief valve	RV-4304	Separator	Pressure relief	CO <sub>2</sub>	Swagelok
¼" ball valve	BV-4305	LN-4006	Isolation	CO <sub>2</sub>	Swagelok

<b>Item</b>	<b>Drawing reference</b>	<b>Location</b>	<b>Function</b>	<b>Service</b>	<b>Supplier</b>
¼" ball valve	BV-4306	LN-4002	Isolation	CO <sub>2</sub>	Swagelok
¼" ball valve	BV-4307	LN-4008	Isolation	CO <sub>2</sub>	Swagelok
¼" ball valve	BV-5301	LN-5001	Isolation	Slurry/CO <sub>2</sub>	Swagelok
¼" ball valve	BV-5302a	LN-5002	Manifold	Slurry/CO <sub>2</sub>	Swagelok
¼" ball valve	BV-5302b	LN-5002	Manifold	Slurry/CO <sub>2</sub>	Swagelok
¼" ball valve	BV-5302c	LN-5002	Manifold	Slurry/CO <sub>2</sub>	Swagelok
¼" ball valve	BV-5303	LN-5001	Drain	Slurry/CO <sub>2</sub>	Swagelok

## Appendix A3: Instrumentation specifications

**Table A3. Instrumentation specification in SFE process**

Item	Drawing reference	Location	Function	Supplier	Temperature rating (°C)	Pressure rating
Level sensor	LI-1401	Extraction vessel	IRC (on/off)	Corr Instruments	0 to 100	6500 psig
Pressure sensor	PI-1402	Extraction vessel	IRC	Digikey	-40 to 125	5000 psig
Temperature sensor	TI-1403	Extraction vessel	IRC	Omega	J type	N/A
Pressure sensor	PI-1404	Extraction vessel	IRC	Omega	15 to 70	5000 psig
Level sensor	LI-1405	Extraction vessel	IRC (on/off)	Corr Instruments	0 to 100	6500 psig
Level sensor	LI-1406	Extraction vessel	RC (on/off)	Corr Instruments	0 to 100	6500 psig
Temperature gauge	TI-1407	Extraction vessel	I	McMaster-Carr	0 to 100	N/A
Temperature gauge	TI-1408	Extraction vessel	I	McMaster-Carr	0 to 100	N/A
Temperature gauge	TI-1409	Extraction vessel	I	McMaster-Carr	0 to 100	N/A
Temperature sensor	TI-1410	Extraction vessel	IR	Omega	J type	N/A
Heating tape	HX-1411	Extraction vessel (bottom)	C (on/off)	Omega	232 (max)	N/A
Pressure sensor	PI-2403	CO <sub>2</sub> pump	I	Cat pumps	N/A	10000 psi
Temperature sensor	TI-2404	LN-2002	IR	Omega	J type	N/A
Pressure sensor	PI-2405	LN-2002	IR	Digikey	-40 to 125	5000 psig
Pressure sensor	PI-2406	LN-2005	IRC	Wika	0 to 50	5000 psi
Temperature sensor	TI-2407	LN-2005	IR	Omega	J type	N/A
Temperature sensor	TI-2408	LN-2005	IR	Omega	J type	N/A
Chiller	HX-2409	CO <sub>2</sub> pump	IC	Cole-Parmer	-35 to 100	N/A
Cauldron (dry ice)	HX-2410	LN-2003	C	N/A	Optional based on amount of dry ice used	N/A
Temperature sensor	TI-3401	FT-3601	IR	Omega	J type	N/A
Temperature sensor	TI-3402	FT-3602	IR	Omega	J type	N/A
Level switch	LI-3403	FT-3601	IR (on/off)	Omega	N/A	N/A
Level switch	LI-3404	FT-3602	IR	Omega	N/A	N/A

Item	Drawing reference	Location	Function	Supplier	Temperature rating (°C)	Pressure rating
			(on/off)			
Pressure sensor	PI-3405	LN-3008	IR	Omega	15 to 70	5000 psig
Pressure sensor	PI-3406	LN-3009	IRC	Omega	15 to 70	5000 psig
Flow meter	FI-3407	LN-3008	IRC	Simark Controls	-20 to 80	0.1 – 3 MPa
Temperature sensor	TI-3407	LN-3008	IR	Omega	J type	N/A
Level switch	LI-3408	FT-3603	IR (on/off)	Omega	N/A	N/A
Temperature sensor	TI-3410	LN-3009	IR	Omega	J type	N/A
Temperature sensor	TI-3411	FT-3603	IR	Omega	J type	N/A
Pressure sensor	PI-4402	Separator	IRC	Digikey	-40 to 125	5000 psig
Temperature sensor	TI-4403	Separator	IR	Omega	J type	N/A
Pressure sensor	PI-4406	LN-4002	I	Swagelok	N/A	5000 psi
Heating tape	HX-4407	MV-4303	C (on/off)	Omega	N/A	N/A
Heating tape	HX-4408	LN-4002	C	Omega	232 (max)	N/A
Temperature sensor	TI-5401	LN-5003	IR	Omega	J type	N/A
Pressure sensor	PI-5403	LN-5003	IR	Omega	15 to 70	5000 psig
Pressure sensor	PI-5404	LN-5001	I	Swagelok	N/A	1000 psi

I=indicator; C=controller; R=recorder

## Appendix A4: List of Priority 1, 2, 3 and 4 alarms

Table A4. List of Priority 1, 2, 3 and 4 alarms in the SFE process

Alarm ID	Condition	Action	Related to
<i>Priority 1 alarm</i>			
EAH1-CO <sub>2</sub>	CO <sub>2</sub> Level > 9,500 ppm	System is interlocked to shut down and the control system to operate in Emergency mode. (Kill switch should be used if automated shutdown fails.)	The Lab
<i>Priority 2 alarms</i>			
PAH2-1402	27 MPa < PI-1402	System is interlocked to shut down and the control system to operate in Emergency mode. (Kill switch should be used if automated shutdown fails.)	Extraction vessel
PAH2-2406	27 MPa < PI-2406	System is interlocked to shut down and the control system to operate in Emergency mode. (Kill switch should be used if automated shutdown fails.)	CO <sub>2</sub> Pump Outlet
PAH2-3406	27 MPa < PI-3406	System is interlocked to shut down and the control system to operate in Emergency mode. (Kill switch should be used if automated shutdown fails.)	Slurry Pump Outlet
PAH2-4402	20 MPa < PI-4402	System is interlocked to shut down and the control system to operate in Emergency mode. (Kill switch should be used if automated shutdown fails.)	Separator
TAH2-1403	85 °C < TI-1403	System is interlocked to shut down and the control system to operate in Emergency mode. (Kill switch should be used if automated shutdown fails.)	Extraction Vessel
LAH2-1401	LI-1401 activated	System is interlocked to shut down and the control system to operate in Emergency mode. (Kill switch should be used if automated shutdown fails.)	Extraction Vessel
<i>Priority 3 alarms</i>			
PAH3-1402	22 MPa < PI-1402	Troubleshoot for blockages or other failures. Shutdown if there is evidence of a blockage or unable to correct condition. Correct pressure if no evidence of blockage or other failure: change pressure set-point, open BV-4303 to relieve pressure, switch restrictor	Extraction vessel
PAH3-2405	3.1 MPa < PI-2405	Shutdown (because relief valve is not working correctly)	CO <sub>2</sub> Pump Inlet
PAL3-2405	PI-2405 < 2.5 MPa	Shutdown immediately and ensure sufficient CO <sub>2</sub> available.	CO <sub>2</sub> Pump Inlet
PAH3-2406	22 MPa < PI-2406	Troubleshoot for blockages or other failures. Shutdown if there is evidence of a blockage or unable to correct condition. Correct pressure if no evidence of blockage or other failure: change pressure set-point, open BV-4303 to relieve pressure, switch restrictor	CO <sub>2</sub> Pump Outlet
TAL3-1410	TI-2407 < 31 °C	Check related cooling and heating facilities. Shutdown if abnormal condition is not corrected or if temperature decreases.	CO <sub>2</sub> Pump Outlet
TAH3-2407	60 °C < TI-2407	Check related cooling and heating facilities. Shutdown if abnormal condition is not corrected or if temperature increases. If no failure is found and extraction vessel temperature is safe and stable, the experiment may continue.	CO <sub>2</sub> Pump Outlet
PAH3-3406	22 MPa < PI-3406	Troubleshoot for blockages or other failures.	Slurry Pump

Alarm ID	Condition	Action	Related to
		Shutdown if there is evidence of a blockage or unable to correct condition. Correct pressure if no evidence of blockage or other failure: change pressure set-point, open BV-4303 to relieve pressure, switch restrictor	Outlet
TAH3-3410	60 °C < TI-3410	Check related cooling and heating facilities. Shutdown immediately if abnormal condition is not corrected or if temperature increases above 85 °C. If no failure is found and extraction vessel temperature is safe and stable, the experiment may continue.	Slurry Pump Outlet
PAH3-4402	8 MPa < PI-4402	Troubleshoot for blockages or other failures. Shutdown if there is evidence of a blockage or unable to correct condition. Correct pressure if no evidence of blockage or other failure: change pressure set-point, open BV-4303 to relieve pressure.	Separator
TAL3-4403	TI-4403 < 0 °C	Increase temperature of heating jacket on metering valve. Shutdown if abnormal condition is not corrected or if temperature decreases.	Separator
LAL3-3408	LI-3408 on in water tank	Shutdown. Or quickly add some water to the water tank.	Slurry Pump Inlet
TAH3-1403	60 °C < TI-1403	Shutdown if abnormal condition is not corrected or if temperature approaches 85 °C. If no failure is found and extraction vessel temperature is safe and stable, the experiment may continue.	Extraction vessel
PAL3-4402	PI-4402 < 1 MPa	Shut down if abnormal condition is not corrected or if pressure is still decreasing during normal operations	Separator
<i>Priority 4 alarms</i>			
PAL4-1402	PI-1402 < 6 MPa	Troubleshoot for blockages, leaks or other failures. Shutdown if there is evidence of a blockage or unable to correct condition. Correct pressure if no evidence of blockage or other failure: change pressure set-point, change setting of BV-4303 to increase pressure, ensure adequate CO <sub>2</sub> supply available	Extraction vessel
LAH4-1405	LI-1405 is on (i.e. level past 16 cm)	Ensure the system is responding correctly: slurry exit flow should be greater than delivery flow. Troubleshoot for evidence of blockages or leaks. Shutdown if level does not decrease or if slurry exit flow is less than delivery flow.	Extraction vessel
LAL4-1406	LI-1406 is off (i.e. level is below 5 cm)	Ensure the system is responding correctly: slurry exit flow should be less than delivery flow. Troubleshoot for evidence of blockages or leaks. Shutdown if level does not increase or if slurry exit flow is greater than delivery flow or if CO <sub>2</sub> continuously escapes from slurry return line.	Extraction vessel
FAHL4-3407	FI-3407 (mass flow) is: (+/- 30%) of flow indicated by slurry pump RPM	Watch slurry level and pump RPM. Verify the sensors are working correctly. Ensure the system is responding correctly to extraction vessel pressure and slurry level.	Slurry Pump Inlet